

MCNP4B MODELING OF PEBBLE-BED REACTORS

By

Julian Robert Lebenhaft

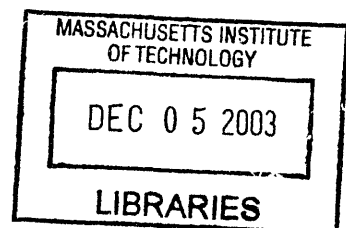
B.Sc. (Chemistry with Physics) 1977
M.Sc. (Chemical Physics) 1978

Ph.D. (Chemical Physics) 1982
University of Toronto

Submitted to the Department of Nuclear Engineering in partial fulfillment of
the requirements for the degree of

Nuclear Engineer
and Master of Science in Nuclear Engineering

at the
Massachusetts Institute of Technology
[February 2002]
October 2001



© 2001 Julian R. Lebenhaft. All rights reserved.

V.1

The author hereby grants to MIT permission to reproduce and distribute publicly paper
and electronic copies of this thesis document in whole or in part.

Signature of Author: _____
U. Department of Nuclear Engineering
October 15, 2001

Certified by: _____ Michael J. Driscoll
Professor Emeritus of Nuclear Engineering
Thesis Supervisor

Certified by: _____ Pavel Hejzlar
Program Director, Center for Advanced Nuclear Energy Systems
Reader

Accepted by: _____ Jeffrey A. Coderre
Assistant Professor of Nuclear Engineering
Chairman, Department Committee on Graduate Students

ARCHIVES

MCNP4B MODELING OF PEBBLE-BED REACTORS

By

Julian Robert Lebenhaft

Submitted to the Department of Nuclear Engineering on October 15, 2001
in partial fulfillment of the requirements for the Degrees of
Nuclear Engineer and Master of Science in Nuclear Engineering

ABSTRACT

The applicability of the Monte Carlo code MCNP4B to the neutronic modeling of pebble-bed reactors was investigated. A modeling methodology was developed based on an analysis of critical experiments carried out at the HTR-PROTEUS and ASTRA facilities, and the critical loading of the HTR-10 reactor. A body-centred cubic lattice of spheres with a specified packing fraction approximates the pebble bed, and exclusion zones offset the contribution of partial spheres generated by the geometry routines in MCNP4B at the core boundaries. The coated fuel particles are modeled in detail and are distributed over the fuelled region of the fuel sphere using a simple cubic lattice. This method predicted the critical core loading accurately in all cases. The calculation of control-rod worths in the more decoupled tall annular ASTRA core gave results within 10% compared to the reported experiments.

An approximate method was also developed for the MCNP4B modeling of pebble-bed reactors with burnup. The nuclide densities of homogenized layers in the VSOP94 reactor model are transferred to the corresponding MCNP4B model with the lattice of spheres represented explicitly. The method was demonstrated on the PBMR equilibrium core, and used for a parallel study of burnup k_{∞} and isotopics on a single pebble.

Finally, a study was carried out of the proliferation potential of a modular pebble-bed reactor for both normal and off-normal operation. VSOP94 analysis showed that spent fuel from pebble-bed reactors is proliferation resistant at high discharge burnup, because of its unfavourable plutonium isotopic composition and the need to divert ~157,000 pebbles to accumulate sufficient ^{239}Pu for a nuclear weapon. The isotopics of first-pass fuel pebbles are more favourable, but even more pebbles (~258,000) would be needed. However, a supercell MOCUP model was used to demonstrate that ~20,000 pebbles would be needed if loaded with depleted uranium. But the associated reactivity loss would necessitate a compensatory increase in core height of approximately 50 cm. Such a change in core loading, as well as the properties of the special pebbles, would be noticed in a safeguarded facility.

Thesis Supervisor: Michael J. Driscoll

Title: Professor Emeritus of Nuclear Engineering

ACKNOWLEDGEMENTS

I would like to express my deepest gratitude to Professor Michael J. Driscoll, who helped guide this thesis research through numerous conversations and “back of the envelope” calculations. His prompt comments were particularly useful during the writing of this report. I would also like to thank Prof. Driscoll for generously funding my trips to South Africa and Europe, which proved to be crucial for both my research and career prospects.

Thanks are also due to Professors Andrew C. Kadak and Ronald G. Ballinger, the Principal Investigators of the Advanced Modular Pebble Bed Reactor Project. Prof. Kadak’s constructive comments during his review of the thesis were much appreciated. Funding for this research was provided by the Idaho National Engineering and Environmental Laboratory (INEEL) under the Strategic INEEL/MIT Nuclear Research Collaboration Program for Sustainable Nuclear Energy. It has been my pleasure to collaborate with Hans D. Gouger, Kevan D. Weaver and J. Steven Herring of the INEEL.

My colleagues at ESKOM in South Africa deserve special mention for their technical assistance during the course of this research. Dr. Eben J. Mulder provided key PBMR related physics data, including the VSOP94 model and engineering drawings of the reference core, and Diana Naidoo supplied the ASTRA documentation. The hospitality of the entire PBMR staff during my visits to Centurion is gratefully acknowledged.

Finally, I would like to thank Dr. Walter Y. Kato for his assistance in obtaining a variety of unpublished reports through his numerous international contacts, and for his friendship and valuable advice throughout my stay at MIT.

TABLE OF CONTENTS

1.	INTRODUCTION	13
1.1	Scope and Objectives	13
1.2	Gas-Cooled Reactors	14
1.3	Overview of Research	21
2.	PEBBLE BED REACTOR PHYSICS	26
2.1	Diffusion Theory	26
2.1.1	Resonance Absorption	27
2.1.2	Neutron Streaming	31
2.1.3	Thermalization in Graphite	34
2.1.4	The VSOP94 Code	35
2.2	The Monte Carlo Method	39
2.2.1	The Boltzmann Equation	40
2.2.2	The MCNP Code	44
2.3	Summary	46
3.	MCNP4B MODELING OF PEBBLE-BED REACTORS	47
3.1	Regular Lattices	47
3.2	Edge Effects in MCNP4B	49
3.3	Double Heterogeneity	51
3.4	Conclusions	53
4.	HTR-PROTEUS FACILITY	54
4.1	Description of the PROTEUS Facility	53
4.2	Fuel and Moderator Spheres	56
4.3	The Stochastic Cores	58
4.4	The MCNP4B Model	60
4.5	Summary	63
5.	THE HTR-10 REACTOR	64
5.1	Description of the HTR-10 Reactor	65
5.2	Physics Benchmark Problems	69
5.3	Reference Core Physics Model	70
5.4	MCNP4B Model of HTR-10	70

5.4.1	Reactor Structure	75
5.4.2	Control Absorbers	76
5.4.3	Core	77
5.4.4	Boron Content	81
5.5	MCNP4B Calculations	81
5.6	Discussion	84
5.7	Summary	87
6.	ASTRA	88
6.1	Description of the ASTRA Facility	88
6.2	Description of the Experiments Performed at the ASTRA Facility	91
6.3	MCNP4B Model of the ASTRA Facility	96
6.3.1	Structural Components	97
6.3.2	Core	101
6.4	Results of MCNP4B Analysis	107
6.5	Discussion	110
6.6	Summary	113
7.	MCNP4B MODELLING OF PEBBLE BED CORES WITH BURNUP	114
7.1	The Pebble Bed Modular Reactor	114
7.2	The VSOP94 Model of the PBMR	118
7.3	Link Between VSOP94 and MCNP4B	121
7.3.1	Modifications to VSOP94	122
7.3.2	Program MCARDS	122
7.4	MCNP4B Model of the PBMR	123
7.5	MCNP4B/VSOP94 Results	127
7.6	Discussion	130
7.7	Summary	132
8.	PLUTONIUM PRODUCTION IN PEBBLE BED REACTORS	135
8.1	Modelling Methods	135
8.1.1	Supercell Model	136
8.1.2	Production Pebbles	137
8.2	Analysis and Results	138
8.2.1	Regular Fuel Pebbles	138

8.2.2 Supercell Analysis of Production Pebbles	140
8.3 Discussion	141
9. CONCLUSIONS AND FUTURE DIRECTIONS	145
10. REFERENCES	152
<u>APPENDIX A MCNP4B Models of the HTR-PROTEUS Facility</u>	171
APPENDIX A.1: MCNP4B model of HTR-PROTEUS Core 4.1	172
APPENDIX A.2: MCNP4B model of HTR-PROTEUS Core 4.2	177
APPENDIX A.3: MCNP4B model of HTR-PROTEUS Core 4.3	181
<u>APPENDIX B MCNP4B Models of HTR-10</u>	185
APPENDIX B-1: MCNP4B model of HTR-10 Benchmark Problem B1	186
APPENDIX B-2: MCNP4B model of HTR-10 Benchmark Problem B2.1	201
<u>APPENDIX C MCNP4B Models of ASTRA Facility</u>	217
APPENDIX C.1: MCNP4B model of ASTRA, ‘super’ cell core representation	218
APPENDIX C.2: Infinite ASTRA lattice using exact ‘super’ cell model	236
APPENDIX C.3: Infinite ASTRA lattice using borated fuel shell	241
APPENDIX C.4: MCNP4B model of ASTRA using BCC core representation	244
<u>APPENDIX D MCNP4B/VSOP94 Models of PBMR</u>	260
APPENDIX D.1—VSOP94 input file for reference PBMR core	261
APPENDIX D.2: MCNP4B model of PBMR	272
APPENDIX D.3: Modified subroutine VORSHU	330
APPENDIX D.4: Program MCARDS	345

APPENDIX E Plutonium Production in a Modular Pebble Bed Reactor	349
APPENDIX E.1: MOCUP Supercell model of production pebble	350
APPENDIX E.2: Excel analysis of VSOP94 equilibrium core results	358

TABLES

Table 1-1. Typical parameters of British Magnox Reactors	15
Table 1-2. Typical parameters of AGRs	16
Table 1-3. Main characteristics of HTGR prototypes	18
Table 1-4. Main characteristics of MHTGRs	20
Table 3-1. Properties of regular lattices	47
Table 4-1. Atom densities in PROTEUS graphite reflector	56
Table 4-2. LEU-HTR fuel and moderator sphere data	57
Table 4-3. Atom densities in HTR-PROTEUS fuel spheres	58
Table 4-4. Atom densities in HTR-PROTEUS moderator spheres	58
Table 4-5. HTR-PROTEUS experimental core configurations	59
Table 4-6. Experimental results for HTR-PROTEUS stochastic cores	59
Table 4-7. Lattice parameters for MCNP4B model of HTR-PROTEUS cores	62
Table 4-8. HTR-PROTEUS criticality analysis	62
Table 5-1. HTR-10 reactor core parameters	68
Table 5-2. Homogenized nuclide densities in HTR-10 reflector zones	72
Table 5-3. Composition of HTR-10 control-rod stainless steel	77
Table 5-4. HTR-10 control rod geometry and material specifications	77
Table 5-5. HTR-10 model pebble-bed geometry specifications	80

Table 5-6.	Material compositions of HTR-10 pebble-bed core	80
Table 5-7.	MCNP4B simulation results for HTR-10	83
Table 5-8.	Calculated differential reactivity worth of HTR-10 control rod	84
Table 5-9.	Diffusion code benchmark results by other CRP-5 participants	85
Table 5-10.	MCNP benchmark results for other CRP-5 participants and MIT	86
Table 6-1.	ASTRA core specifications	89
Table 6-2.	ASTRA spherical elements	90
Table 6-3.	ASTRA regulating rod material specification	90
Table 6-4.	Basic critical configuration of ASTRA facility	96
Table 6-5.	ASTRA core lattice parameters	102
Table 6-6.	Individual control rod worths in ASTRA facility	108
Table 6-7.	Reactivity worth of two-rod combinations in ASTRA	108
Table 6-8.	Reactivity worth of three-rod combinations in ASTRA	108
Table 6-9.	Differential worth of ASTRA control rod CR5	109
Table 6-10.	Dependence of ASTRA control rod worth on distance from core	110
Table 6-11.	Interference coefficients for ASTRA rod combinations	112
Table 7-1.	PBMR reference core specifications	116
Table 7-2.	Reference specifications for PBMR fuel elements	116
Table 7-3.	Fission product chain 44 in VSOP94	120
Table 7-4.	Modified VSOP94 Card V21	124
Table 7-5.	Temperature reactivity coefficients in the PBMR	129
Table 8-1.	Plutonium Isotopic Composition of PBMR Spent Fuel	139
Table 8-2.	Plutonium isotopic composition of PBMR first-pass fuel	139

Table 8-3.	Neutron fluxes calculated with supercell MCNP4B model	140
Table 8-4.	Pu-239 production calculated with supercell MCNP4B model	141
Table 8-5.	Isotopic composition of plutonium in irradiated solid UO ₂ target	141
Table 9-1.	Summary of key MCNP4B criticality calculations	145

FIGURES

Figure 2-1. TRISO coated fuel particle	28
Figure 2-2. Neutron escape probabilities in a pebble-bed core	29
Figure 2-3. Packing density of $\frac{1}{8}$ " spheres in a 65 mm-OD cylinder	32
Figure 2-4. Packing density of $\frac{1}{8}$ " spheres in infinite cylinders of varying diameter	32
Figure 2-5. The graphite lattice	35
Figure 2-6. Structure of the VSOP94 code	37
Figure 2-7. Overlay of VSOP94 and CITATION meshes	38
Figure 2-8. Relation between vectors	40
Figure 3-1. Body centred cubic structures	48
Figure 3-2. Partial spheres generated by MCNP4B	50
Figure 3-3. The sphere exclusion zone	51
Figure 3-4. MCNP4B model of a coated fuel particle	52
Figure 3-5. MCNP4B model of a fuel pebble	52
Figure 3-6. MCNP4B model of a pebble-bed core	53
Figure 4-1. Top view of HTR-PROTEUS facility	55
Figure 4-2. A schematic representation of the HTR-PROTEUS facility	56
Figure 4-3. Vertical view of MCNP4B model of HTR-PROTEUS	61
Figure 4-4. Horizontal view of MCNP4B model of HTR-PROTEUS	61
Figure 5-1. Vertical cross section of the HTR-10 reactor	66
Figure 5-2. Horizontal cross section of the HTR-10 reactor	67
Figure 5-3. Reference core physics calculation model	71

Figure 5-4. Structure of the HTR-10 control rod	73
Figure 5-5. Vertical cross section of the MCNP4B model of HTR-10	74
Figure 5-6. Horizontal cross section of the MCNP4B model of HTR-10	75
Figure 5-7. MCNP4B model of HTR-10 control rod	76
Figure 5-8. Calculated differential reactivity worth of a control rod	84
Figure 6-1. Horizontal cross section of ASTRA facility	92
Figure 6-2. Vertical cross section of ASTRA facility	93
Figure 6-3. Engineering drawing of an ASTRA control rod	94
Figure 6-4. Engineering drawing of the ASTRA manual regulating rod	95
Figure 6-5. MCNP4B model of ASTRA facility—Horizontal view	97
Figure 6-6. Bottom of ASTRA control rod—Vertical view	98
Figure 6-7. Joint between two halves of an ASTRA control rod	98
Figure 6-8. Lower pin holder in an ASTRA control rod-Horizontal view	99
Figure 6-9. Air-filled sections of pins in an ASTRA control rod—Horizontal view	99
Figure 6-10. Absorber sections of pins in an ASTRA control rod—Horizontal View	100
Figure 6-11. Upper pin holder in an ASTRA control rod—Horizontal View	100
Figure 6-12. Spider at top of ASTRA control-rod assembly	101
Figure 6-13. ASTRA super cell MCNP4B model—Horizontal view 1	103
Figure 6-14. ASTRA super cell MCNP4B model—Horizontal view 2	104
Figure 6-15. ASTRA super cell MCNP4B model—Vertical view	104
Figure 6-16. Approximate MCNP4B Model of ASTRA Facility—Vertical	

View	106
Figure 6-17. Approximate MCNP4B Model of ASTRA Facility—Horizontal View	106
Figure 6-18. Differential worth of ASTRA control rod CR5	109
Figure 7-1. A vertical view of the PBMR	117
Figure 7-2. A horizontal view of the PBMR core	118
Figure 7-3. VSOP94 model of the PBMR	119
Figure 7-4. MCNP4B model of the PBMR— Vertical View	125
Figure 7-5. MCNP4B model of the PBMR—Horizontal View	126
Figure 7-6. Channel for small absorber balls in MCNP4B model of PBMR	126
Figure 7-7. Power density in PBMR equilibrium core	127
Figure 7-8. Fast neutron flux in PBMR equilibrium core	128
Figure 7-9. Thermal neutron flux in PBMR equilibrium core	128
Figure 7-10. Proposed MCNP-based code system for pebble-bed reactors with burnup	134
Figure 8-1. Supercell MCNP4B model of plutonium production sphere	137
Figure 8-2. Different configurations of plutonium production pebbles: (a) solid core; (b) shells; (c) dense BISO	138
Figure 9-1. Six-cell BCC model used in the plutonium production study	146

1. INTRODUCTION

Although high-temperature gas-cooled reactors (HTGRs) exist today only as pilot-scale facilities, the growing recognition of their unique characteristics makes them leading candidates for the future electricity generating market. These characteristics include inherent safety, simplicity of design and expected low capital cost, fuel-cycle flexibility and high thermal efficiency. HTGRs are graphite-moderated and -reflected reactors, which are loaded with a unique type of fuel and are cooled by helium gas. Two types of HTGRs exist, which differ in the shape of their fuel elements—prismatic and spherical. The focus of this thesis is on the physics aspects of the latter type of reactor, the pebble-bed reactor.

After a statement of the thesis scope and objectives, this chapter will provide a historical overview of HTGR development, and a summary of the research reported here.

1.1 Scope and Objectives

From the 1960s until the present, the neutronic design of pebble-bed reactors has been carried out using diffusion-theory codes. These include the German VSOP¹ suite of codes [1-1], the modern Dutch code PANTHERMIX [1-2, 1-3], and PEBBED that is currently under development at the INEEL [1-4]. The VSOP code, as well as the unique features of pebble-bed reactor physics, will be described briefly below. However, the subject of this thesis is the neutronic modeling of pebble-bed cores using the Monte-Carlo code MCNP4B [1-5]. Prior to the research reported here, MCNP (Versions 4A and 4B) modeling of pebble-bed cores has been limited to the analysis of HTR-PROTEUS critical

¹ Very Special Old Programs.

experiments involving regular lattices [1-6]. Randomly packed cores had only been investigated using MCNP-BALL, which is a version of MCNP3B that was modified to include a stochastic geometry feature [1-7]. The goal of the research undertaken at MIT was to determine whether randomly packed cores could be described with sufficient accuracy by regular lattices, an approximation that is imposed by the use the repeated-geometry feature in MCNP4B. Such a methodology was developed and validated against several critical experiments, including the stochastic HTR-PROTEUS cores, the HTR-10 start-up core and the ASTRA criticals.

1.2 Gas Cooled Reactors

The history of gas-cooled reactors dates back to the plutonium-production piles built in the US at Hanford in the 1940s, and in the UK at Windscale in the 1950s. In the US, gas cooling of nuclear reactors was subsequently rejected in part because of anticipated difficulties with the procurement of blowers and pressure vessels. However, a different route was followed in the UK, where the first power reactors were natural-uranium fueled, graphite-moderated and utilized atmospheric air-cooling. This choice of reactor was initially dictated by the availability of nuclear materials, but the inherent safety features of gas-cooled reactors were soon recognized.

The early gas-cooled reactors were the British Magnox reactors, which were CO₂ cooled, graphite moderated, and used metallic natural uranium clad with a magnesium-aluminium alloy. Because the operating temperature of this reactor is limited to 500°C to prevent CO₂ oxidation of the cladding, the maximum coolant temperature achieved is 365°C. The power density is very low (approximately 0.5 MW/m³) and, even with on-

line refueling, the discharge burnup of fuel in Magnox reactors is about 6 MWd/kgU. The first Magnox reactor began operating at Calder Hall in 1956, and the last of these first-generation reactors will be shut down by 2010. Typical parameters of the British Magnox reactors are given in Table 1-1.

Table 1-1
Typical Parameters of British Magnox Reactors [1-8]

Item	Calder Hall	Hinkley Point A	Oldbury	Wylfa
First power	1956	1965	1968	1971
Net power [MW(e)]	35	250	300	590
Net design efficiency (%)	19	25	33.6	31.5
Active core:				
Length (m)	6.4	7.6	9.6	9.15
Diameter (m)	9.45	14.9	13	17.35
Power density (MW/m ³)	0.5	0.74	0.65	0.87
Specific power (kW/kg ²³⁵ U)	190	360	400	450
Maximum burnup (MWd/kgU)	2.7	≥ 3	4.5	≥ 3
Number of fuel channels	1696	4500	3308	6150
Fuel channel diameter (mm)	54	96	97	96.5
Elements per channel	6	8	8	8
Fuel element:				
Diameter (mm)	29	28.5	28	28
Length (mm)	1015	900	960	1050
Max cladding temperature (°C)	418	430	472	451
Coolant:				
Pressure (MPa)	0.8	1.36	2.55	2.7
Temperature (°C)	140-336	180-375	245-410	247-414
Power per circulator (MW)	1.4	5.5	5.2	14
Steam (Inlet/Outlet):				
Pressures (MPa)	1.5/0.4	4.7/1.3	10/5	4.8
Temperatures (°C)	314/182	363/350	400/393	396
Pressure vessel type	Steel	Steel	PCRV	PCRV
Thickness (mm)	50.8	75	4600- 6700	3350
Length (m)	21.65	20	18.3	29.3
Diameter (m)	11.25	20	23.6	29.3

The Advanced Gas Reactor (AGR) represents an evolutionary improvement over the Magnox reactor. The use of 2.5% enriched uranium oxide fuel and stainless steel cladding permits a higher gas temperature (560°C), increases fuel discharge burnup to

Table 1-2
Typical Parameters of AGRs [1-8]

<i>Item</i>	<i>WAGR</i>	<i>Hinkley Point B</i>	<i>Dungeness B</i>	<i>Heysham 2</i>
First power	1963	1976	1982	1987
Net power [MW(e)]	28-33	625	600	620
Net design efficiency (%)	28-31	41.5	41.5	40
Active core:				
Length (m)	4.2	8.3	8.2	8.3
Diameter (m)	4.5	9.5	9.4	9.45
Power density (MW/m ³)	1.43	2.55	2.5	2.65
Specific power (kW/kg ²³⁵ U)	350	~600	~500	~600
Maximum burnup (MWd/kgU)	10-20	~20	18-20	18
Fuel enrichment (% ²³⁵ U)	2.5	1.4-2.6	1.5-2.5	2.11-2.77
Number of fuel channels	210	310	410	332
Graphite sleeve ID (mm)	130	190	178	190
Elements per channel	8	8	8	8
Fuel element:				
Number of rods	21	36	36	36
Rod diameter (mm)	10.2	14.5	14.5	14.5
Rod length (mm)	510	1040	1040	1040
Max cladding temperature (°C)	650-750	825	835	—
Coolant:				
Pressure (MPa)	1.9	4.2	3.45	4.35
Temperature (°C)	250-560	290-670	320-675	335-635
Power per circulator (MW)	1.4	4.3	10.9	5.3
Circulator pressure rise (MPa)	0.1	0.24	0.32	0.29
Steam:				
Pressures (MPa)	4.6	16.3	16.3	16
Temperatures (°C)	454	538	565	538
Reheat (MPa/°C)	None	4.4/538	3.9/565	3.9/538
Pressure vessel type	Steel	PCRV	PCRV	PCRV
Thickness (mm)	44.5-111.1	4900-7300	3800-6400	5800
Length (m)	16	19.4	17.7	21.9
Diameter (m)	6.3	18.9	20	20.2

20 MWd/kgU, and decreases the size of the core. The first AGR began operation at Windscale in 1963 and fourteen such reactors were subsequently built and operated. Typical parameters of the British Magnox reactors are given in Table 1-2.

The design of the high temperature gas-cooled reactor (HTGR) was initiated in the UK at the same time as the AGR. The goal of this program was an all-ceramic, helium-cooled and graphite moderated reactor utilizing the thorium fuel cycle. The first such reactor, the 20 MW(t) DRAGON High Temperature Reactor, achieved criticality at Winfrith in August 1964, and was soon followed by two other prototypes: the 40 MW(e) Peach Bottom Unit 1 in March 1966 in the US, and the 15 MW(e) AVR in August 1967 in West Germany.

Both DRAGON and Peach Bottom utilized fuel assemblies that contained coated fuel particles uniformly dispersed throughout annular graphite compacts. The original fuel particles were composed of 93% enriched uranium and thorium carbide surrounded by a single pyrolytic carbon coating. This primitive coating proved inadequate, and BISO fuel particles were introduced that were coated with a double layer of pyrolytic carbon. BISO fuel was used successfully in Peach Bottom, where very low activity levels were subsequently experienced in the primary cooling system. Fuel was irradiated successfully in DRAGON to burnups exceeding 100 MWd/kgU. The main characteristics of HTGRs are given in Table 1-3.

A key feature of the HTGR is the use of coated fuel particles that are dispersed in a graphite matrix. The purpose of this design is to avoid corrosion to the fuel element and to enhance the retention of fission products with the graphite. However, this basic

concept can be satisfied by several fuel geometries. The British and US reactors relied on the traditional rod geometry, either hexagonal (DRAGON) or cylindrical (Peach Bottom). A completely different approach was followed in Germany, where the development of spherical fuel elements led to the design of the pebble-bed reactor. The fuel spheres are loaded from the top and discharged from the bottom of the reactor core. This is a particularly attractive concept because of its apparent simplicity and flexibility.

Table 1-3
Main Characteristics of HTGR Prototypes [1-8]

<i>Item</i>	<i>Dragon</i>	<i>Peach Bottom</i>	<i>AVR</i>
Country	UK	USA	Germany
Thermal power (MW)	20	115	49
Net electrical power (MW)	—	40	15
First power operation	1965	1967	1968
Helium pressure (MPa)	2	2.25	2.25
Helium temperatures [†]	350/750	345/725	200/850
Active core:			
Diameter (m)	1.07	2.8	3.0
Height (m)	1.6	2.3	3.5
Core power density (MW/m ³)	14	8.3	2.3
Fuel element:			
Design	Hex rods	Cylinders	Spheres
Number	37 × 7	804	100,000
Diameter (mm)	72	89	60
Length (mm)	2540	3660	—
Max fuel burnup (MWd/kgU)	≥ 100	~75	160
Steam conditions (MPa/°C) [†]	—	10/538	7.2/504
Net cycle efficiency (%)	—	35	30

[†]Inlet/Outlet

The first prototype pebble-bed reactor was the Arbeitsgemeinschaft Versuchsreaktor (AVR), which was started up at Jülich, West Germany, in August 1967. The AVR was a helium-cooled, graphite-moderated, high-temperature reactor with a thermal power rating of 46 MW and an electric power output of 15 MW. The core, the steam generator and the two helium circulators were contained in a double-walled pressure vessel. With the

exception of a water ingress accident from a leak in the steam generator in 1978, the AVR operated successfully for 21 years. During these years, the AVR was used to test a variety of fuels and to demonstrate the inherent safety of the pebble-bed reactor.

These prototype HTGRs were followed in 1974 by the following third-generation gas-cooled reactors: the General Atomics 330 MW(e) nuclear power station at Fort St. Vrain, USA, which utilized hexagonal graphite fuel elements with TRISO coated fuel particles; and the Thorium High Temperature Reactor (THTR), a 300 MW(e) pebble-bed reactor that was built in Schmehausen, West Germany, between 1971 and 1983. Both reactors used a PCRV to enclose the core and primary cooling system. The Fort St. Vrain reactor was shut down prematurely because of numerous mechanical problems, while the THTR was shutdown because of both mechanical problems and an unfavourable political climate in Germany after the Chernobyl accident.

Interest is being expressed once again in HTGRs because of their inherent safety, simplicity and potential for competing economically with other forms of electricity generation. Several countries are actively pursuing the development of HTGRs for a variety of applications. These include two prismatic reactors: the 30 MW(t) High Temperature Engineering Test Reactor (HTTR), which is currently undergoing commissioning tests at the Oarai Research Establishment in Japan, and the General Atomics GT-MHR intended for the disposition of excess weapons-grade plutonium. A small pebble-bed reactor, the HTR-10, was recently constructed in China, and the Pebble Bed Modular Reactor (PBMR) project is at an advanced design stage in South Africa. Details of the HTR-10 and PBMR appear elsewhere in this report. Table 1-4 summarizes

the main characteristics of the fourth-generation modular HTGRs. Numerous paper studies are underway elsewhere, including the Dutch conceptual design of a small (40 MWt) pebble-bed type HTGR [1-9, 1-10].

**Table 1-4
Main Characteristics of MHTGRs**

<i>Item</i>	<i>HTTR</i>	<i>HTR-10</i>	<i>GT-MHR</i>	<i>PBMR</i>
Country	Japan	China	USA/ Russia	South Africa
Thermal power (MW)	30	10	600	268
Net electrical power (MW)		—	284	110
Helium pressure (MPa)	4	3	7	7
Helium temperatures	395/950	250/700	490/850	491/850
Active core:				
Diameter (m)	2.3	1.8		3.5
Height (m)	2.9	1.97		8.5
Core power density (MW/m ³)	2.5	2.0		3.27
Fuel element:				
Design	UO ₂	UO ₂	PuO ₂	UO ₂
Enrichment (% ²³⁵ U)	Prismatic	Spherical	Prismatic	Spherical
Number	3-10	17		8
Diameter (mm)	150	27,000	1020	285,000
Length (mm)	360 [†]	60	360	60
Max fuel burnup (MWd/kgHM)	580	—	800	80,000
		80,000		80,000

[†] Flat-to-flat distance.

The work described in this report is part of a larger effort at MIT on the development of an advanced modular pebble-bed reactor [1-11]. The objective of this project is to develop a conceptual design for a 110 MWe helium-cooled, gas turbine powered nuclear power plant that will be competitive with natural gas. Funded by the Idaho National Engineering and Environmental Laboratory (INEEL), the project has focused on fuel performance modeling, reactor physics, safety analysis, balance of plant design, and the application of modularity to the construction of the plant. The design features an

intermediate heat exchanger that decouples the gas turbine from the primary cooling system.

1.3 Overview of Research

The remainder of this thesis is organized as follows. Chapter 2 covers pebble-bed reactor physics, treating in detail the unique features associated with neutron transport in such reactors and the computer codes used to perform this research (VSOP94 and MCNP4B). The discussion includes both diffusion theory and Monte Carlo methods.

The application of diffusion theory to core physics calculations requires the preparation of few-group cross sections and diffusion coefficients [1-12]. These parameters are obtained by the homogenization of fine-group cross sections, which are generated from detailed calculations in a large number of energy groups with a coarser spatial dependence. An important part of this spectrum calculation is the accurate determination of resonance absorption of neutrons in ^{238}U . The collision probability form of the transport equation is used for this calculation, which requires the determination of the Dancoff factor appearing in the expression for the probability that a neutron experiences its next collision in the moderator. The Dancoff factor is the moderator escape probability [1-12]. Use of coated fuel particles creates a double heterogeneity on both the microscopic and macroscopic levels (the coated particle and the pebble) that complicates the calculation of the Dancoff factor. An additional peculiarity of pebble-bed reactor physics is the need to introduce a streaming correction to the calculation of the diffusion coefficient because of the effect of voids between pebbles on neutron leakage.

Use of the Monte Carlo method in conjunction with a point-wise cross-section library eliminates the need to prepare few-group parameters or to calculate the Dancoff and diffusion streaming corrections. The Monte Carlo method is an effective numerical tool for solving the Boltzmann transport equation [1-13], and its implementation in codes such as MCNP is becoming increasingly the method of choice for the analysis of light water and liquid metal reactors. Its application to HTGRs has been limited until recently to the analysis of homogenized cores [1-14], the HTR-PROTEUS critical experiments involving regularly packed pebble beds [1-6, 1-15, 1-16], and the prismatic Very High Temperature Reactor Critical assembly in Japan [1-17]. Significant progress was made last decade in Japan, where a new sampling method was developed for irregularly distributed fuel elements [1-7]. In this approach, the location of the modeled fuel element is generated probabilistically along the flight path of the neutron by sampling from nearest-neighbour distribution functions for the fuel spheres and the coated fuel particles.

The MCNP4B modeling methodology is described in Chapter 3. In common with all full-core MCNP4B models, the pebble-bed reactor structure can be modeled in detail. The challenge lies in the representation of the randomly packed core, which must be approximated by a regular lattice of spheres. Of several possible types of packing, the body-centred cubic (or body-centred tetragonal) was found to be accurate and convenient. The large number of fuel and moderator spheres in such reactors precludes the explicit specification of the core geometry, and regular lattices of spheres are used instead. Analysis of several critical experiments showed that MCNP4B can be used for accurate criticality calculations of pebble-bed cores using appropriately modeled regular lattices to approximate the random loading [1-18].

Analyzing three sets of critical experiments validated this modeling methodology. The HTR-PROTEUS experiments [1-19] are discussed in Chapter 4. MCNP4B analysis of three stochastic cores showed the need for a peripheral buffer zone to compensate for partial fuel spheres at the reflector interface. These partial spheres, which are introduced into the model by the repeated-structure feature of code, have the effect of adding extra fuel into the core. The same approach was then applied successfully to the prediction of the initial critical loading of the HTR-10 reactor (a total sphere loading of 16,830 calculated *versus* 16,890 measured). This analysis was part of a larger IAEA physics benchmark problem [1-20], which is the subject of Chapter 5. A single zone and two types of spheres (fuel and moderator) characterize both the HTR-PROTEUS and the HTR-10 cores. A considerably more complicated pebble-bed core geometry was assembled for the ASTRA experiments [1-21]. This configuration constituted a scaled mock-up of the PBMR annular core, with an inner reflector zone, an outer fuel zone and an intermediate mixing zone. Moreover, a small number of absorber spheres were added to the fuelled zones. The polygonal shape of the ASTRA core vessel precluded the use of an explicit exclusion zone, because a distribution of partial spheres of all sizes does not occur in this case. However, the equivalent reduction in the amount of fuel was achieved by using a reduced packing fraction. The presence of an absorber and the more neutronically decoupled core resulted in poorer agreement with experiments. The MCNP4B modeling of the ASTRA experiments is discussed in Chapter 6.

The ultimate goal of the MCNP4B methodology described here is the modeling of a large pebble-bed core such as that of the Pebble Bed Modular Reactor [1-22]. Although not

investigated in this report, the approach used to model the ASTRA criticals is directly applicable to the PBMR start-up core. More important is the ability to analyze a pebble-bed reactor with a representative equilibrium burnup distribution. The composition of depleted fuel can be readily determined in a static core, but a key feature of pebble-bed reactors is the continuous recycling of fuel spheres [1-23]. In theory, the stochastic nature of such cores lends itself to direct Monte Carlo simulation. However, the large number of pebbles found in a typical core (for example, there are approximately 370,000 pebbles in the PBMR) renders the direct simulation of three-dimensional pebble flow impractical at this time. An alternative procedure is to perform the fuel management study using a diffusion theory-burnup code and to transfer the equilibrium fuel compositions to the detailed MCNP4B model. Chapter 7 describes one such approach, which involves a semi-automated link between VSOP94 and MCNP4B. The method is demonstrated in principle on the PBMR equilibrium core using the reference VSOP model of the reactor and an equivalent MCNP4B model.

The final topic covered in Chapter 8 is a preliminary investigation of the proliferation potential of the reference PBMR fuel cycle performed in collaboration with the INEEL. Four physics codes were used to estimate the production of plutonium in the reactor, including VSOP94, MCNP4B, ORIGEN2 [1-24] and MOCUP [1-25]. The Monte Carlo analysis was carried out at the INEEL using a simple-cell model representing an infinite lattice of pebbles [1-26], and at MIT using a supercell model consisting of a single production pebble in the center of a driver core representative of the PBMR. The ^{239}Pu production was estimated from a tally of the $^{238}\text{U}(\text{n},\gamma)^{239}\text{U}$ reaction rate for an MCNP4B snapshot simulation, and by tracking the isotopic composition of the production pebble in

a MOCUP depletion calculation. The results were compared with VSOP94 predictions for the composition of discharged fuel. The analysis confirmed that spent fuel from pebble-bed reactors is proliferation resistant at high discharge burnups (≥ 80 MWd/kgU), because of its unfavourable plutonium isotopic composition and the large number of pebbles that would have to be diverted—about half a core load. The isotopes of first-pass fuel pebbles are more favourable, but an even larger number would be needed to accumulate 6 kg of ^{239}Pu . However, the analysis also showed that it is possible to produce a significant quantity of plutonium in a pebble-bed reactor by inserting special pebbles with a high loading of depleted uranium. Only 20,000 pebbles would have to be diverted over a minimum period of 1.5 years, in the unlikely event that the associated loss in reactivity can be compensated undetected by raising the core height or other means.

The thesis concludes with a discussion of the results and recommendations for future research in Chapter 9. All models and computer programs developed during the course of this thesis research are documented in the Appendices.

2. PEBBLE BED REACTOR PHYSICS

The physics analysis of pebble-bed reactors shares much in common with other thermal reactors. With the exception of early KENO analysis of homogenized cores [2-1], the neutronic design of pebble-bed reactors has been carried out exclusively using S_N and diffusion-theory codes, whose few-group parameters are generated by averaging fine-group cross sections [2-2, 2-3]. The fine-group parameters are obtained from a detailed spectrum calculation using a large number of energy groups with a coarse spatial dependence. However, the calculations are complicated by some features of pebble-bed reactors, including the use of spherical fuel elements, the double heterogeneity associated with the embedded coated fuel particles, and the irregular packing of fuel spheres in the core. Of particular interest are resonance absorptions and neutron streaming in pebble beds. These special features are discussed in this chapter both because of their general importance and as motivation for the use of Monte Carlo methods, which offer an alternative and often-simpler route for pebble-bed reactor physics calculations.

2.1 Diffusion Theory [2-2, 2-3]

In common with all HTGRs, pebble-bed reactors are graphite-moderated and -reflected. While graphite has a relatively high atomic weight for a moderator, its very low absorption cross-section makes it inferior only to heavy water and beryllium as a moderator. The nature of this moderator dictates the slowing down process and the choice of energy structure for few-group reactor calculations. The upper bound of the thermal group is chosen such that the probability for a neutron gaining energy in a collision becomes negligible. For HTGRs, this occurs at approximately 2 eV, and the range above

the thermal group is usually subdivided into three energy groups that contain the resolved resonances, the unresolved resonances, and higher energies where the resonance structure of the heavy metal cross-sections is unimportant. The group boundaries used in the VSOP94 model of the PBMR are 1.86 eV, 29 eV and 100 keV.

2.1.1 Resonance Absorption

Fission neutrons are born with an average energy of approximately 2 MeV, and are rapidly slowed down through collisions with carbon atoms. In order to sustain the chain reaction, a sufficient number of neutrons must be thermalized without being absorbed in the large resonances of ^{238}U . Moreover, as burnup proceeds, the ^{240}Pu isotope also becomes an important resonance absorber. These resonance absorptions have a significant effect on the physics of HTGRs, especially on core reactivity, plutonium breeding and burnup. Because of the heterogeneous fuel geometry and the large changes in cross section exhibited by resonance materials, resonance absorptions are often treated using collision probability methods for solving the integral Boltzmann equation. The resonances of ^{238}U are distinct (resolved) up to about 1-4 keV. Above this energy, the resonance cross-sections are calculated using statistical distribution laws for the widths and separations of the unresolved resonances.

The spherical fuel element used in pebble-bed reactors is a 6 cm-diameter graphite ball with a (nominal) 5 cm-diameter inner-fuelled zone. The fuel typically is contained in coated particles that are randomly embedded in the graphite matrix. The TRISO coated fuel particle consists of a 500 μm -diameter UO_2 kernel surrounded by an inner low-density carbon buffer layer (9 μm thick), an inner high-density pyrolytic carbon layer (7

μm), a silicon carbide layer ($6 \mu\text{m}$) and an outer pyrolytic carbon layer ($6 \mu\text{m}$). The function of these layers is to retain fission products, while the graphite matrix further protects the fuel against corrosion and moderates neutrons. See Figure 2-1.

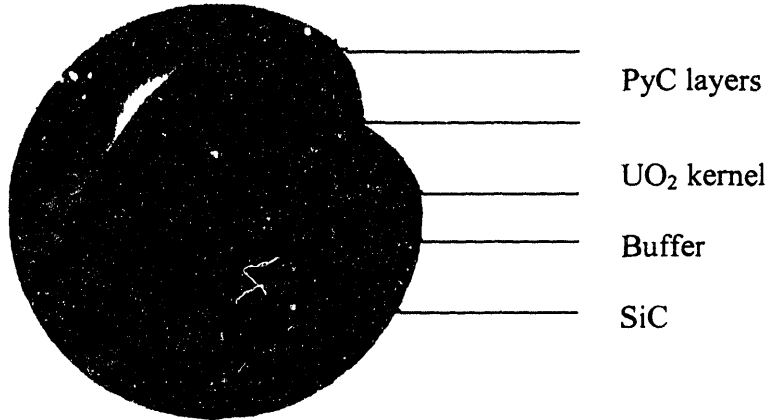


Figure 2-1. TRISO coated fuel particle (General Atomics, San Diego).

The combination of TRISO coated fuel particles and fuel spheres creates a double-heterogeneity on the microscopic and macroscopic levels, which must be factored into the expressions for fuel escape probabilities that appear in the resonance absorption calculations. This is usually achieved via the calculation of the Dancoff correction, γ , defined as the factor by which the fuel escape probability is reduced in a collection of fuel lumps relative to that for an isolated fuel lump [2-4]. Thus, the Nordheim geometric escape probability is given by [2-5]

$$P(E) = \frac{P_0(E) \cdot [1 - \gamma]}{1 - [1 - \bar{l}_0 \Sigma_a(E) P_0(E)] \gamma}, \quad (2-1)$$

where $P_0(E)$ is the probability that a neutron escapes the fuel lump where it is born, \bar{l}_0 is the mean penetration chord length and $\Sigma_a(E)$ is the macroscopic absorption cross section.

However, the Nordheim treatment does not apply directly to the double heterogeneity found in pebble-bed reactors, because the small size of the fuel kernel results in $P_0(E) \approx 1$. Teuchert and Breitbarth calculated an alternative escape probability by following the path of a neutron in coated particles and fuel spheres [2-6]. The possible path is subdivided into parts for which the traversing probability can be evaluated numerically, and is expressed in terms of eight collision probabilities as follows:

$$P(E) = W_1 + W_2(W_3 + W_4) + W_2W_5 \frac{W_6 + W_7}{1 - W_8}, \quad (2-2)$$

where the W_i are the collision probabilities in region I (see Figure 2-2). The first term gives the probability that a neutron born in a fuel kernel undergoes its next collision in the same kernel; the second gives the probability that the neutron leaves the kernel uncollided and suffers its next collision in the graphite matrix of the originating sphere (in either the fuelled zone or shell); while the third gives the probability that the neutron leaves the sphere, penetrates any number of other spheres without collision and suffers its next collision in graphite. This expression was implemented in the VSOP code [2-7].

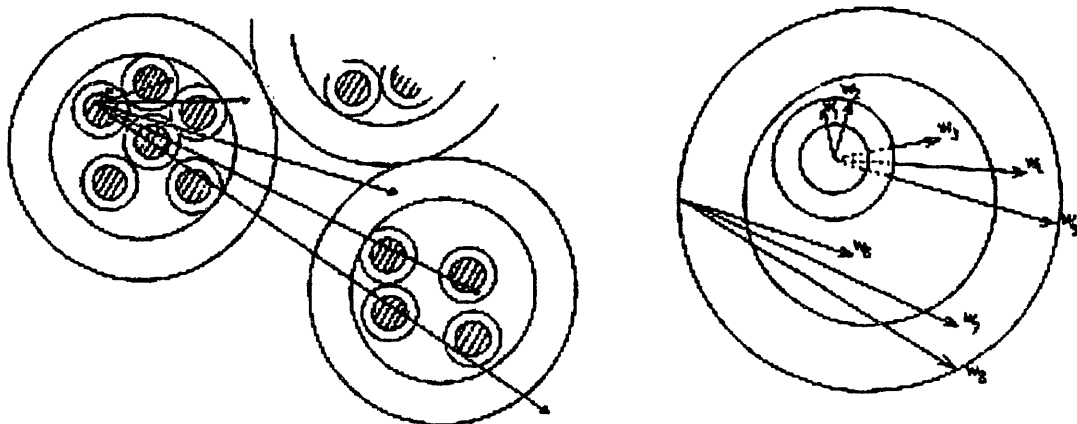


Figure 2-2. Neutron escape probabilities in a pebble-bed core [2-7].

Resonance absorptions are often treated using an equivalence relation, which transforms the complicated heterogeneous calculation into an equivalent one for a homogeneous medium. This is done by defining an energy-independent lattice escape cross section Σ_e , such that [2-4]

$$P_0(E) = \frac{\Sigma_0(E)}{\Sigma_0(E) + \Sigma_e}, \quad (2-3)$$

where $\Sigma_0(E)$ is the macroscopic total cross section for the fuel at energy E . Segev derived the following accurate formula for Σ_e [2-8]:

$$\Sigma_e = \frac{\frac{1}{\bar{l}_0}}{\frac{1}{a} + \frac{1}{\gamma_{eff}} - 1}, \quad (2-4)$$

where \bar{l}_0 is the mean penetration chord length in the fuel lump, a is a user selected Bell factor, and γ_{eff} is an effective Dancoff factor for the lattice:

$$\gamma_{eff} = \frac{1}{1 + \left(\frac{1}{\gamma} - 1\right)\beta},$$

and

$$\beta = (1 - \bar{l}_c \Sigma_L) \frac{1 + \frac{1}{3} \bar{l}_c \Sigma_1 \frac{V_1}{V_c}}{1 + \frac{1}{3} l_c \Sigma_1 \frac{V_1}{V_c} + \frac{\Sigma_L}{\Sigma_1} \frac{V_c}{V_1}}. \quad (2-5)$$

Here, \bar{l}_c is the mean penetration chord length, Σ_l the moderator cross-section, V_l the volume of the moderator, and V_c is the volume of the nominal cell. The equivalent cross section of the outer (pebble-bed) lattice is given by

$$\Sigma_L = \frac{\frac{1}{L}}{\frac{1}{A} + \frac{1}{\Gamma} - 1}, \quad (2-6)$$

where L is the mean penetration chord length, Γ is the Dancoff factor and A is the Bell factor for the outer lattice. Because these equations assume the general form programmed for the escape cross-section in the (two-dimensional) WIMS lattice code [2-9], the above theoretical development defines an alternative calculational route for pebble-bed reactors. An approach of this type is used in the Dutch OCTOPUS reactor physics analysis code system [2-10].

2.1.2 Neutron Streaming

Numerous researchers have investigated the random packing of same-sized spheres in three dimensions since early in the 20th century [2-11]. Scott carried out a series of experiments, which involved the filling of cylindrical tubes with $\frac{1}{8}$ in. steel ball bearings [2-12]. The manner of filling the tubes determined the type of packing. When the tubes were filled by pouring and then shaken for several minutes, the resulting packing was termed “dense random packing.” The tubes were then tipped horizontally, rotated slowly about the longitudinal axis, and gradually returned to the upright position. The resulting packing was termed “loose random packing.” The experiments were carried out in four rigid cylinders with different diameters, and the packing densities in cylinders of infinite

length were determined from extrapolations as in Figure 2-3, plotted against reciprocals of diameters as in Figure 2-4. As $\frac{1}{D} \rightarrow 0$, the limiting packing densities are 0.60 for loose random packing and 0.63 for dense random packing.

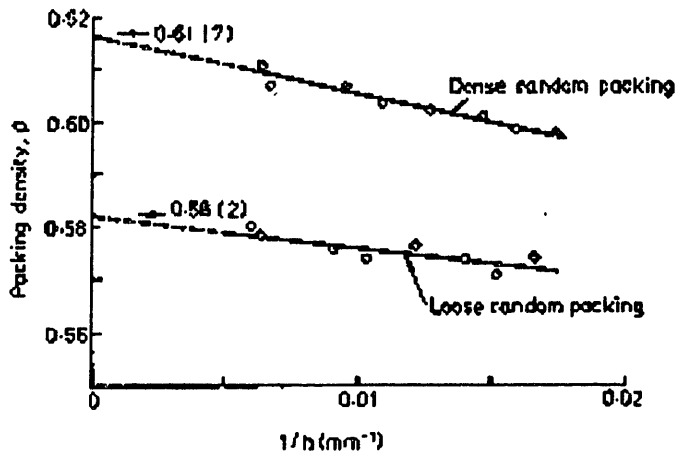


Figure 2-3. Packing density of $\frac{1}{8}$ " spheres in a 65mm-OD cylinder [2-11]

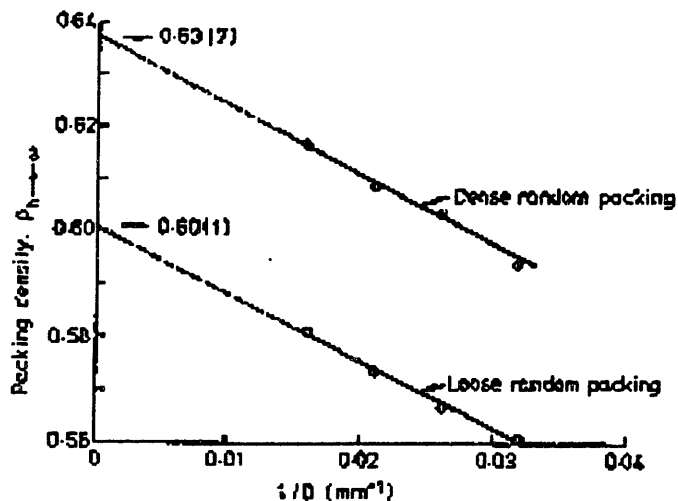


Figure 2-4. Packing density of $\frac{1}{8}$ " spheres in infinite cylinders of varying diameter [2-11].

The coordination number is defined as the number of spheres in contact with any given sphere. The coordination number can be used as a means for quantifying the arrangement of three-dimensional arrays of spheres. Only even coordination numbers are possible in regularly arranged three-dimensional cubic lattices, although odd coordination numbers are possible in hexagonal and random arrangements of spheres. Wadsworth investigated the distribution of coordination numbers for smooth hard spheres using $\frac{1}{4}$ in.-diameter steel ball bearings [2-13]. He made three important conclusions:

- a) In random packing, the void fraction is only a function of the sphere-to-container diameter ratio and is insensitive to the method of stacking.
- b) The random packing in flat-bottomed cylinders tends towards rhombohedral (hexagonal) close packing and the degree of incompleteness is random.
- c) A critical diameter exists for forcing complete rhombohedral packing at the flat bottom of a container. This value was estimated to be 20 sphere diameters radially and axially.

The loading of spheres in pebble-bed reactors is usually assumed to be loose random packing with a 0.61 density, with regular configurations appearing only near the walls and on the bottom of the core. Neutron leakage, and hence criticality, is affected by the shape and distribution of cavities in the pebble bed. The core may be homogenized if the cavities are evenly distributed and are small relative to the neutron mean free path. However, this approximation no longer applies for larger cavities. Lieberoth and Stojadinović derived a theoretical expression for the neutron diffusion constant D , which was verified using a Monte Carlo analysis of a system with 3000 spheres [2-14]. Thus,

assuming that no correlation exists between the passage lengths in the cavities and in the spheres,

$$\frac{D}{D_H} = 1 + \frac{\phi^2}{(1+\phi)^2} \left\{ \frac{2}{3} \Sigma_{tot} Q R + \frac{4}{3} \Sigma_{tot} R , \right. \\ \left. \times \left[\frac{2 \Sigma_{tot}^2 R^2}{2 \Sigma_{tot}^2 R^2 - 1 + (1 + 2 \Sigma_{tot} R) \exp(-2 \Sigma_{tot} R)} - 1 \right] - 1 \right\}, \quad (2-7)$$

where

$$Q = \frac{\langle h^2 \rangle}{\langle h \rangle^2}, \quad (2-8)$$

and

$$\phi = \frac{\langle h \rangle}{\langle t \rangle}. \quad (2-9)$$

Here, Σ_{tot} is the total macroscopic cross section in the homogeneous model, R is the radius of a sphere, h is the chord length in a cavity and t is the escape chord length in a sphere (the angular brackets denote an average).

Spectrum and diffusion calculations in heterogeneous reactors are often performed on a homogenized core. In this approach, which is used in the VSOP94 physics code, the cross sections are multiplied by energy dependent self-shielding factors, while the diffusion constant for the homogeneous model is scaled as shown in Equation 2-7.

2.1.3 Thermalization in Graphite

The fission neutrons are slowed down through collisions with the carbon atoms until they equilibrate with the thermal motion of the graphite. The energies of the thermalized

neutrons are distributed about the neutron temperature (which is slightly higher than the moderator temperature because of leakage and absorption hardening) according to the Maxwellian distribution. Thermalized neutrons can gain energy in a collision with a carbon atom. Because the carbon atoms are part of a graphite lattice (see Figure 2.5), the exchange of energy is restricted to the quanta of the crystal vibrational energy (phonons). The interaction between the thermal neutrons and the carbon atoms is given by a double differential cross section, which is commonly expressed in terms of a measured scattering law $S(\alpha,\beta)$, where α and β are dimensionless exchanges of momentum and energy. This scattering law can be related to the frequency distribution of phonons in the graphite, which can be calculated theoretically. The VSOP94 code implements the graphite phonon calculation by Young and Koppel [2-15].

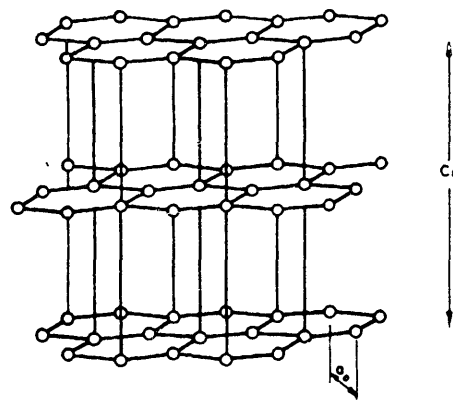


Figure 2-5. The graphite lattice [2-16].

2.1.4 The VSOP94 Code [2-7]

VSOP94 is a computer code system for reactor physics and fuel cycle simulation, which is the main physics code for the neutronic design of pebble-bed reactors. It comprises neutron cross-section libraries and routines for the following neutronic calculations:

nuclear data processing and preparation of temperature-dependent few-group parameters; repeated neutron spectrum evaluation; two- and three-dimensional diffusion calculations based on neutron flux synthesis with fuel depletion and shutdown features; fuel management including pebble recycling; fuel cycle cost analysis; and quasi-static thermal hydraulics. VSOP94 is a general-purpose code, which has also been applied successfully to light- and heavy-water reactors.

The structure of the code is shown in Figure 2-6. The ZUT-DGL code is used to generate the fast spectrum involving resonances in both the resolved and unresolved ranges [2-17]. The corresponding few-group parameters are prepared by the GAM-I code in the P_1 approximation, which accounts for leakage and anisotropic scattering [2-18]. The required fast and epithermal data, which are provided in a GAM library with 68 energy groups ranging from 10 MeV to 0.414 eV, were extracted from the ENDF/B-IV, ENDF/B-V and JEF-I evaluations. In the thermal range, the spectrum calculations are carried out with the THERMOS code, which is based on the integral form of the Boltzmann transport equation [2-19]. The THERMOS library is given in 30 energy groups ranging from 0 to 2.05 eV, and is prepared by the THERMALIZATION code (which is a precursor of the GATHER code [2-20]) from a 96-group library taking into account the specific design of the fuel elements and reactor [2-21]. Both the ZUT-DGL and THERMOS codes have been modified to allow for the double-heterogeneity present in the pebble-bed reactor [2-22]. The graphite scattering matrices are based on the Young phonon spectrum in graphite [2-15].

Several auxiliary codes are used to prepare the geometrical data needed by the main routines. The DATA-2 code prepares the fuel element input data from its geometry specification [2-23]. The auxiliary code BIRGIT prepares a two-dimensional (R-Z) geometric design of the core, which specifies a pebble flow pattern of pebbles in finite

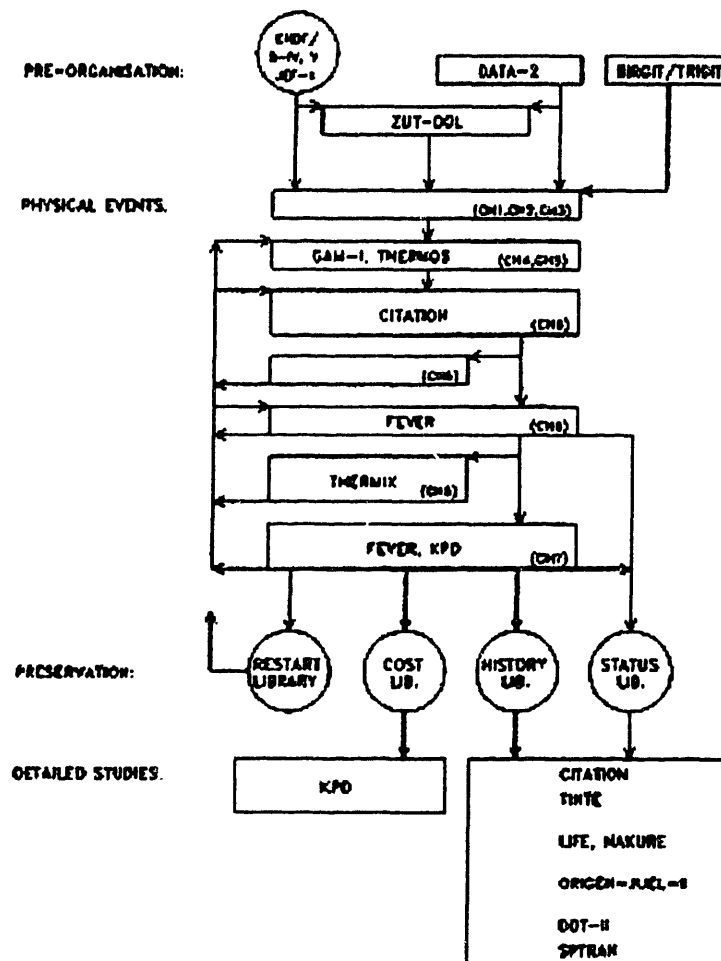
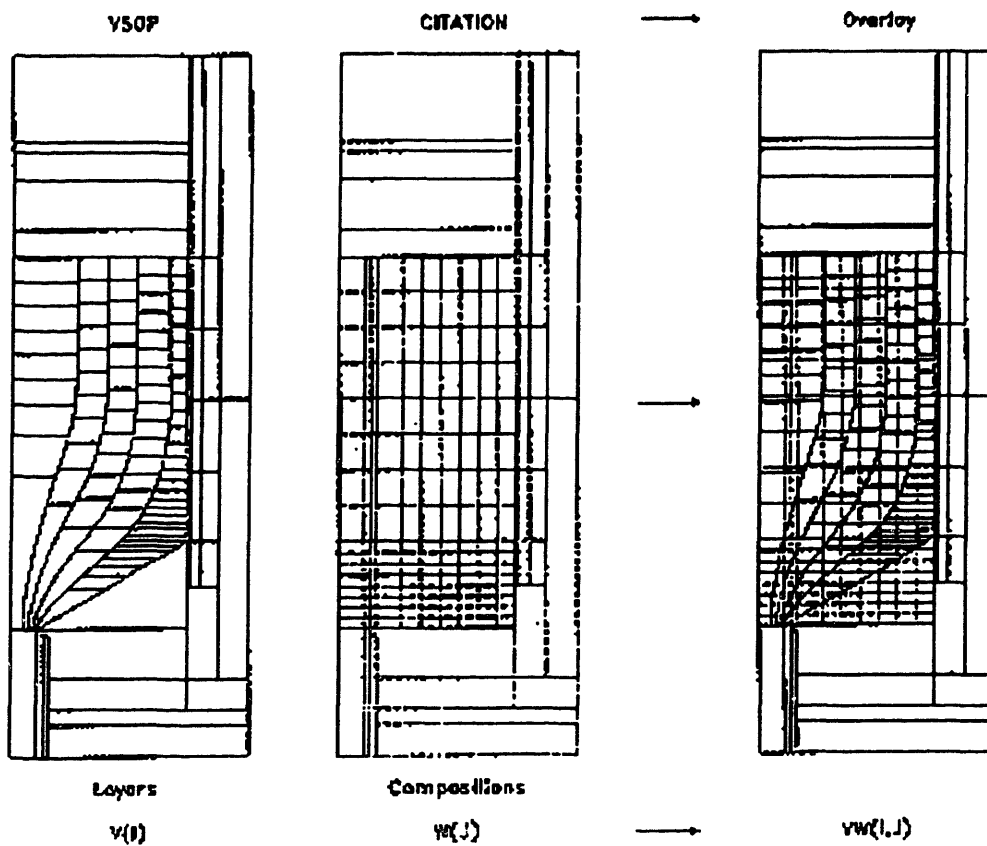


Figure 2-6. Structure of the VSOP94 code [2-7].

batches grouped into layers in different flow channels (see Figure 2-7). The batches are used to represent fuel spheres that have traversed the core a given number of times and hence have a specific burnup. The layers and flow channels allow for axial and radial burnup variations in the core. The material compositions are homogenized within each batch. Burnup is modeled by depleting the fuel in each homogenized batch by the specified time step, then shuffling its contents to the next layer in each channel. Batches at the bottom of the core are either discarded or recycled depending on the burnup.



File 2-7. Overlay of VSOP94 and CITATION meshes [2-7]

A two- or three-dimensional neutron flux map is generated with the CITATION diffusion code in several energy groups (usually four groups are chosen) [2-24]. This is utilized in a burn-up calculation for up to 200 different core regions using a scheme developed from the FEVER code, which follows explicitly the build-up history of 40 fission products in each region [2-25]. The diffusion calculation is repeated for short burn-up intervals, while the neutron spectrum is recalculated at larger time intervals. Because the diffusion calculation is carried out on a regular grid pattern, a matrix transformation (and its inverse) is provided between the VSOP flow pattern and the CITATION mesh for the macroscopic cross sections and neutron fluxes.

The THERMIX code is included in VSOP94 to perform both static and time-dependent thermal hydraulic calculations for pebble-bed reactors [2-26]. The temperatures of the fuel and moderator regions are fed back to the spectrum evaluations for subsequent core neutronic calculations. The fuel management and cost module KPD performs the in-core and out-of-pile fuel shuffling, as well as general evaluations of the reactor and fuel element irradiation history [2-27].

2.2 The Monte Carlo Method

The Monte Carlo method consists of simulating a large number of neutron (and/or photon) histories by using a random number generator to sample appropriate probability distribution functions for track lengths between collisions, scattering angles, type of interaction, *etc.* In this fashion, each neutron is followed from birth throughout its life to its removal from the system through absorption or leakage. When a large number of such

histories are followed, the neutron distribution becomes known and quantities of interest such as the neutron flux can be tallied. [2-28, 2-29]

2.2.1 The Boltzmann Equation

The Monte Carlo method is ideally suited for the calculation of integrals. For example, consider the simple integral

$$I = \int_a^b f(x) dx \approx \frac{(b-a)}{N} \sum_{i=1}^N f(x_i). \quad (2-10)$$

The x_i are chosen randomly instead of at regular intervals, and the purely statistical error is inversely proportional to \sqrt{N} independently of the dimension of the integral. Because the Boltzmann transport equation can be cast in integral form, it is clear that the Monte Carlo method is ideally suited for simulating neutron and photon transport in nuclear reactors. The following brief description of the Monte Carlo sampling of the Boltzmann equation is based on the discussion in Reference 2-30.

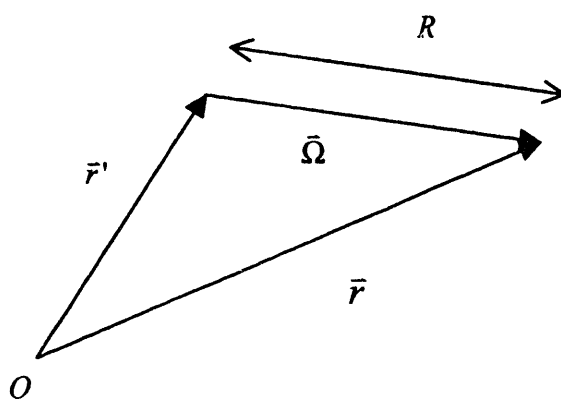


Figure 2-8. Relation between vectors [2-30].

The steady-state Boltzmann equation for the directional flux density $\phi(\vec{r}, \bar{\Omega}, E)$ is as follows:

$$\bar{\Omega} \cdot \bar{\nabla} \phi(\vec{r}, \bar{\Omega}, E) + \Sigma_t(\vec{r}, \bar{\Omega}, E) \phi(\vec{r}, \bar{\Omega}, E) = \int dE' \Sigma_s(\vec{r}, \bar{\Omega}' \rightarrow \bar{\Omega}, E' \rightarrow E) \phi(\vec{r}, \bar{\Omega}', E') + S(\vec{r}, \bar{\Omega}, E), \quad (2-11)$$

The first term on the left-hand side of the equation denotes the leakage of neutrons traveling in direction $\bar{\Omega}$, and the second term gives the rate of neutron loss by absorption and scattering. On the right-hand side, $\Sigma_s(\vec{r}, \bar{\Omega}' \rightarrow \bar{\Omega}, E' \rightarrow E) dE'$ is the differential scattering cross section from energy E' and direction $\bar{\Omega}'$ into the interval $dE d\bar{\Omega}$, and the first term represents the rate at which neutrons appear at position \vec{r} with energy E due to scattering. The term $S(\vec{r}, \bar{\Omega}, E)$ denotes the rate at which neutrons appear at \vec{r} with energy E and moving in direction $\bar{\Omega}$, with contributions from both fission and extraneous sources.

This integro-differential equation can be converted into the following integral form of the Boltzmann equation:

$$\begin{aligned} \phi(\vec{r}, \bar{\Omega}, E) &= \int_0^\infty dR \cdot \exp \left(- \int_0^R \Sigma_t(\vec{r} - R' \bar{\Omega}, E) dR' \right) \\ &\times \left[\int \int d\bar{\Omega}' dE' \Sigma_s(\vec{r}, \bar{\Omega}' \rightarrow \bar{\Omega}, E' \rightarrow E) \phi(\vec{r}, \bar{\Omega}', E') + S(\vec{r}, \bar{\Omega}, E) \right], \end{aligned} \quad (2-12)$$

where \vec{r}' is related to \vec{r} and $\bar{\Omega}$ via $\vec{r}' = \vec{r} - R \bar{\Omega}$, and $R = |\bar{\Omega}|$ (see Figure 2-8). This equation is next expressed in operator form as

$$\psi(\vec{r}, \bar{\Omega}, E) = \int d\vec{r}' T(\vec{r}', \vec{r} | \bar{\Omega}, E) \chi(\vec{r}', \bar{\Omega}, E) \quad (2-13)$$

and

$$\chi(\bar{r}, \bar{\Omega}, E) = S(\bar{r}, \bar{\Omega}, E) + \iint d\bar{\Omega}' dE' C(\bar{\Omega}', E', \bar{\Omega}, E | \bar{r}) \psi(\bar{r}, \bar{\Omega}', E'), \quad (2-14)$$

where the collision density ψ is defined as

$$\psi(\bar{r}, \bar{\Omega}, E) = \int d\bar{r}' T(\bar{r}', \bar{r} | \bar{\Omega}, E) \quad (2-15)$$

and the density χ of collided particles leaving position \bar{r} ,

$$\chi(\bar{r}, \bar{\Omega}, E) = \iint d\bar{\Omega}' dE' \Sigma_s(\bar{r}, \bar{\Omega}' \rightarrow \bar{\Omega}, E' \rightarrow E) \phi(\bar{r}, \bar{\Omega}, E') + S(\bar{r}, \bar{\Omega}, E). \quad (2-16)$$

The transport and collision operators are defined respectively as follows:

$$T(\bar{r}', \bar{r} | \bar{\Omega}, E) = \Sigma_t(\bar{r}, E) \exp \left(- \int_{\bar{r}' \rightarrow \bar{r}} \Sigma_t(\bar{r}'', E) ds \right) \frac{\delta \left(\bar{\Omega}' \cdot \frac{\bar{r} - \bar{r}'}{|\bar{r} - \bar{r}'|} - 1 \right)}{|\bar{r} - \bar{r}'|^2} \quad (2-17)$$

and

$$C(\bar{\Omega}', E', \bar{\Omega}, E | \bar{r}) = \frac{\Sigma_s(\bar{r}, \bar{\Omega}' \rightarrow \bar{\Omega}, E' \rightarrow E)}{\Sigma_t(\bar{r}, \bar{\Omega}', E')} . \quad (2-18)$$

The propagation of neutrons is modeled in a recursive manner. Starting with a source term $S(\bar{r}', \bar{\Omega}', E')$,

$$\chi_0(\bar{r}', \bar{\Omega}', E') = S(\bar{r}', \bar{\Omega}', E'), \quad (2-19)$$

$$\psi_0(\bar{r}, \bar{\Omega}', E') = \int d\bar{r}' T(\bar{r}', \bar{r} | \bar{\Omega}', E') \chi_0(\bar{r}', \bar{\Omega}', E') \quad (2-20)$$

and

$$\chi_1(\bar{r}, \bar{\Omega}, E) = \iint d\bar{\Omega}' dE' C(\bar{\Omega}', E' \rightarrow \bar{\Omega}, E | \bar{r}) \psi_0(\bar{r}, \bar{\Omega}', E'). \quad (2-21)$$

Subsequent steps are given by

$$\psi_n(\bar{r}, \bar{\Omega}', E') = \int d\bar{r}' T(\bar{r}', \bar{r} | \bar{\Omega}', E') \chi_n(\bar{r}', \bar{\Omega}', E') \quad (2-22)$$

and

$$\chi_n(\bar{r}, \bar{\Omega}, E) = \iint d\bar{\Omega}' dE' C(\bar{\Omega}', E' \rightarrow \bar{\Omega}, E | \bar{r}) \psi_n(\bar{r}, \bar{\Omega}', E'). \quad (2-23)$$

The transport operator T propagates the neutron from \bar{r}' to \bar{r} by sampling over the interval $(0, R)$ according to Equation 2-22. If \bar{r} is outside the boundaries of the reactor model, the neutron has escaped and the history is terminated; otherwise, an interaction takes place. The collision operator, which describes this interaction via Equation 2-23, may be rewritten as

$$\begin{aligned} C(\bar{\Omega}', E' \rightarrow \bar{\Omega}, E | \bar{r}) &= \frac{\Sigma_s(\bar{r}, \bar{\Omega}, E)}{\Sigma_s(\bar{r}, \bar{\Omega}, E)} \cdot \frac{\Sigma_s(\bar{\Omega}', E' \rightarrow \bar{\Omega}, E | \bar{r})}{\Sigma_s(\bar{r}, \bar{\Omega}, E)} \\ &= P_s(\bar{r}, \bar{\Omega}, E) \cdot C_s((\bar{\Omega}', E' \rightarrow \bar{\Omega}, E | \bar{r})), \end{aligned} \quad (2-24)$$

which expresses the collision operator in terms of a scattering kernel multiplied by a correction factor for absorption. The scattering kernel may be further written as follows:

$$\begin{aligned} C_s(\bar{\Omega}', E' \rightarrow \bar{\Omega}, E | \bar{r}) &= \frac{\Sigma_s(\bar{\Omega}', E' \rightarrow \bar{\Omega}, E | \bar{r})}{\Sigma_s(\bar{r}, \bar{\Omega}, E)} \\ &= \left[\frac{N_A(\bar{r}) \sum_j \sigma_{Aj}(\bar{\Omega}', E')} {\Sigma_s(\bar{r}, \bar{\Omega}', E')} \right] \left[\frac{\sigma_{Aj}(\bar{\Omega}', E')}{\sum_j \sigma_{Aj}(\bar{\Omega}', E')} \right] f_{Aj}(\bar{\Omega}', E' \rightarrow \bar{\Omega}, E), \end{aligned} \quad (2-25)$$

where N_A is the atomic number density for nuclide A, and σ_{ij} is the microscopic cross section for reaction type j . By sampling randomly in the interval (0,1), the bracketed terms are used to determine the interacting nuclide and the type of reaction, and the normalized scattering function f_{Aj} is used to generate the scattering angle, $\mu = \cos \theta$. The particle energy E is determined from $E = E(\mu, E')$ and $\bar{\Omega}$ is calculated so as to satisfy the relation $\mu = \bar{\Omega} \cdot \bar{\Omega}'$. The neutron history is terminated if E is below the energy cutoff, otherwise \bar{r}' and E' are reset to \bar{r} and E .

Monte Carlo codes such as MCNP do not require explicit treatment of the slowing-down process when continuous-energy cross-sections are used, because the values of cross sections can be looked up directly at any energy level. The cross sections for each reaction are given on one energy grid, which is sufficiently dense to permit the reproduction of the evaluated cross sections within a 1% error. For example, for the ENDF/B-V evaluation, the energy grid for ^1H contains approximately 250 points, while ^{197}Au uses approximately 22,500. [2-31]

The Monte Carlo method offers further simplifications over the analogous diffusion-theory approach. For example, the ability to specify the exact geometry of the reactor precludes the need for neutron-streaming corrections, which are needed when a homogenized representation of the core is used.

2.2.2 The MCNP Code

MCNP (Monte Carlo N-Particle) is a general-purpose, continuous-energy, generalized-geometry, time-dependent, coupled neutron-photon-electron, Monte-Carlo transport code

system [2-31]. The calculations reported in this thesis were performed with version 4B2 of the code, although a later version (4C) is now available. The generalized geometry capability of MCNP4B, combined with the use of continuous cross-section data, make it possible to model nuclear reactors with great accuracy. The goal of the research reported here was to investigate the applicability of MCNP4B to pebble-bed reactors with randomly packed cores.

MCNP can model an arbitrary three-dimensional configuration of materials arranged in geometric cells, which are bounded by first- and second-degree surfaces and some special fourth-degree surfaces. Point-wise, continuous-energy cross-section libraries are typically used. However, multigroup data may also be used for fixed-source adjoint calculations. The cross-section evaluation accounted for all neutron interactions, and both free gas and $S(\alpha, \beta)$ thermal treatments are used. Fission sources as well as fixed and surface sources are available. For photons, the code takes account of incoherent and coherent scattering with and without electron binding effects, the possibility of fluorescent emission following photoelectric absorption, and absorption in pair production with local emission of annihilation radiation. A very general source and tally structure is available. The tallies have extensive statistical analysis of convergence, and rapid convergence is enabled by a wide variety of variance reduction methods. Normal energy ranges are 0-20 MeV for neutrons and 1 keV - 1 GeV for photons and electrons.

The large number of randomly situated fuel and moderator spheres, and the large number of fuel particles per sphere (approximately 10^4), in pebble-bed reactors precludes the explicit specification of the core geometry, and regular lattices of spheres are used

instead. The repeated-structure feature of MCNP4B permits the definition of an array consisting of hexahedral or hexagonal unit cells. This can be used to approximate the randomly packed pebble-bed core.

2.3 Summary

An overview of pebble-bed reactor physics was presented in this chapter. The double-heterogeneity of the pebble-bed core, which is related to the presence of small fuel grains embedded in graphite spheres, requires the correct treatment of mutual shielding between grains. For diffusion-theory core calculations, the effect of this shielding is embodied in the Dancoff correction for resonance absorptions. Although complicated, this procedure is fully automated in codes like VSOP94. The Monte Carlo code MCNP4B offers an alternative approach by relying on a point-wise representation of nuclear reaction cross sections, in which a large number of energy points are used to describe accurately the resonance curve. Therefore, the effect of mutual shielding between the fuel grains is included automatically. This feature of MCNP4B, as well as its ability to model reactor geometry in detail, is explored in this report.

3. MCNP4B MODELLING OF PEBBLE-BED REACTORS

Constructing an MCNP4B model consists of establishing the geometry of the reactor from engineering drawings, representing each subsystem by a cell whose boundaries are defined mathematically by a logical combination of surfaces, and specifying the density and composition of each such cell [3-1]. In the case of pebble-bed reactors, the structure of the reactor can be modeled as accurately as is required by the application. The challenge lies in modeling the randomly packed pebble-bed core, which must be approximated by a regular lattice of spheres.

3.1 Regular Lattices

Several lattices are available including simple cubic (SC), body-centred cubic (BCC) or tetragonal (BCT), face-centred cubic (FCC), simple hexagonal (SH), and hexagonal close packed (HCP) [3-2]. These lattices differ in the number of spheres present in the unit cell and the maximum packing fraction (see Table 3-1).

Table 3-1
Properties of Regular Lattices

Type of Lattice	Number of Spheres in Unit Cell	Coordination Number	Maximum Packing Fraction
SC	1	6	0.52
BCC or BCT	2	8	0.68
FCC	4	12	0.74
SH	6	5	0.60
HCP	6	12	0.74

The simple cubic and simple (point-on-point) hexagonal lattices can be eliminated for most cores, because of their leakiness and low packing densities. The choice among the

remaining lattices depends on their ability to represent specific sphere combinations, since the packing fraction can be achieved by adjusting the cell size; the size of the unit cell a is related to the radius of the sphere R and the packing fraction f as follows:

$$a = \left(\frac{8\pi}{3f} \right)^{\frac{1}{3}} R . \quad (3-1)$$

For example, a core characterized by a 1:1 fuel-to-moderator sphere ratio is modeled most easily by a BCC or BCT lattice because their unit cell contains two spheres (see Figure 3-1). All spheres contained within the FCC and HCP lattices are positioned along the bounding planes of the unit cell, making it impossible to model more complicated mixtures of spheres (such as the combination of moderator, fuel and absorber spheres encountered in the ASTRA critical experiments) because adjacent spheres overlap incorrectly. Therefore, although the packing of spheres in pebble beds is expected to approximate a rhombohedral lattice (see Section 2.1.2), a loose HCP lattice may not be a proper choice.

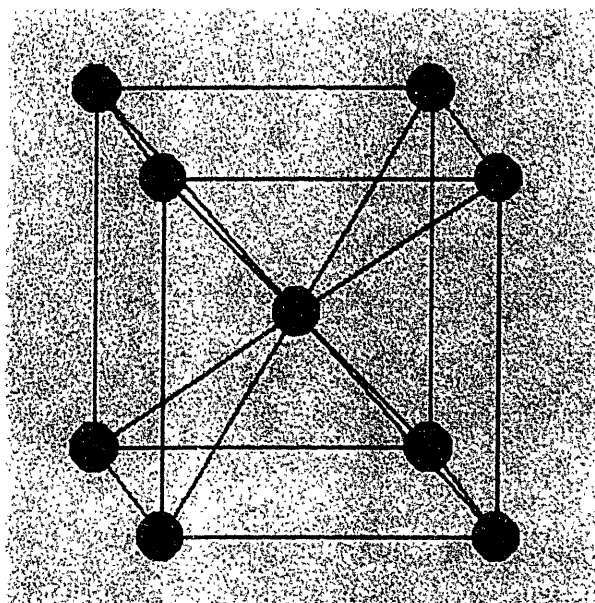


Figure 3-1. Body Centred Cubic Structure

As the subsequent chapters show, the BCC lattice was found to work well for the loose packing typically encountered in pebble-bed reactors.

The effect that the choice of packing arrangement has on neutron streaming was investigated in Reference 3-3. Criticality calculations were performed for both BCT and HCP lattices, using a spherical core (with a radius of 140 cm) packed with spheres; both reflected and unreflected configurations were considered. The results of the analysis showed that the k_{eff} is not very sensitive to the specific sphere arrangement for reflected systems for which leakage effects are less important.

Sphere mixtures other than the 1:1 fuel-to-moderator ratio present a problem. Reducing the size or density of the moderator sphere can approximate a small deviation, such as the 57:43 percent ratio used for the HTR-10 start-up core. Alternatively, a repeating cell may be constructed from several BCC (or BCT) unit cells such that the exact combination of spheres can be defined. For example, ten layers of five BCC unit cells (for a total of 100 spheres) can be used to model the HTR-10 core. More complicated core loadings may also be modeled in this fashion, although the results are sensitive to the (ideally stochastic) manner in which the spheres are distributed throughout the repeating cell.

3.2 Edge Effects in MCNP4B

A side effect associated with the repeated-structure feature in MCNP4B is the appearance of partial spheres at the core boundary (Figure 3-2), because this adds extra fuel to the core. Murata first identified this problem during the development of MCNP-BALL [3-4]. A correction had to be made to the sampling algorithm for spherical fuel spheres in order

to reproduce the specified packing fraction. This was achieved by generating a nearest neighbour distribution function for a slightly higher packing fraction, f' :

$$f' = f \frac{V}{V - \Delta V} \leq 0.636, \quad (3-1)$$

where f is the actual packing fraction, V is the core volume, and ΔV is the volume of an exclusion zone of thickness R (the radius of a fuel sphere in a one-zone core). Sampled fuel spheres that overlapped the core boundary were rejected.

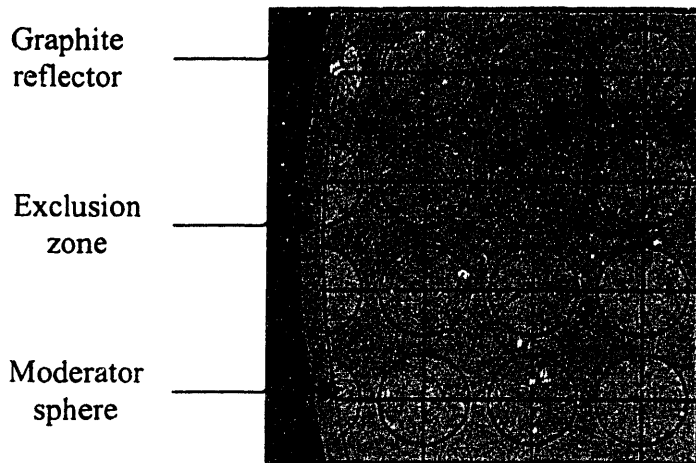


Figure 3-2. Partial spheres generated by MCNP4B

A more direct approach was chosen for the MCNP4B modeling of circular pebble-bed cores in the present work. An exclusion zone was introduced at the boundaries of the core, which effectively reduced the size of the sphere fill volume by ΔV . The size of this exclusion zone was the radius of a sphere, scaled by the ratio of the number of fuel spheres to the total number of spheres in the unit cell. Thus, for the 57:43 percent sphere ratio specified for the HTR-10 reactor, this corresponded to $3 \times \frac{57}{57 + 43} = 1.71$ cm.

Because there is a distribution of differently sized partial spheres around the core edge, deleted portions of physically realizable spheres are made up by leftover portions of physically unrealizable spheres (see Figure 3-3). This procedure does not work for the ASTRA facility with its polygonal core, because such a cancellation does not occur on average. Therefore, a reduced packing fraction was used instead in order to eliminate partial spheres.

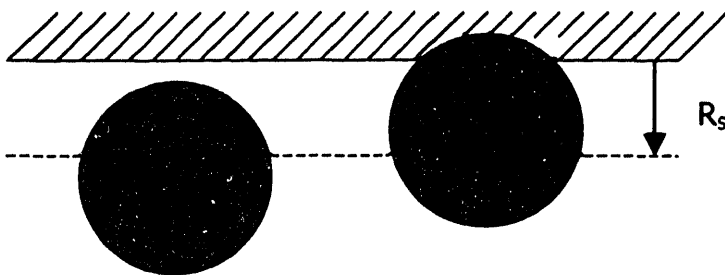


Figure 3-3. The sphere exclusion zone

3.3 Double Heterogeneity

For a high-fidelity MCNP model of a pebble-bed reactor, the double heterogeneity of the core must also be reproduced accurately. The coated fuel particles were modeled exactly (Figure 3-4), and the random distribution of these fuel particles in the fuel sphere was approximated using a simple-cubic regular array without an exclusion zone (Figure 3-5). Figure 3-6 shows a slice through the BCC core representation.

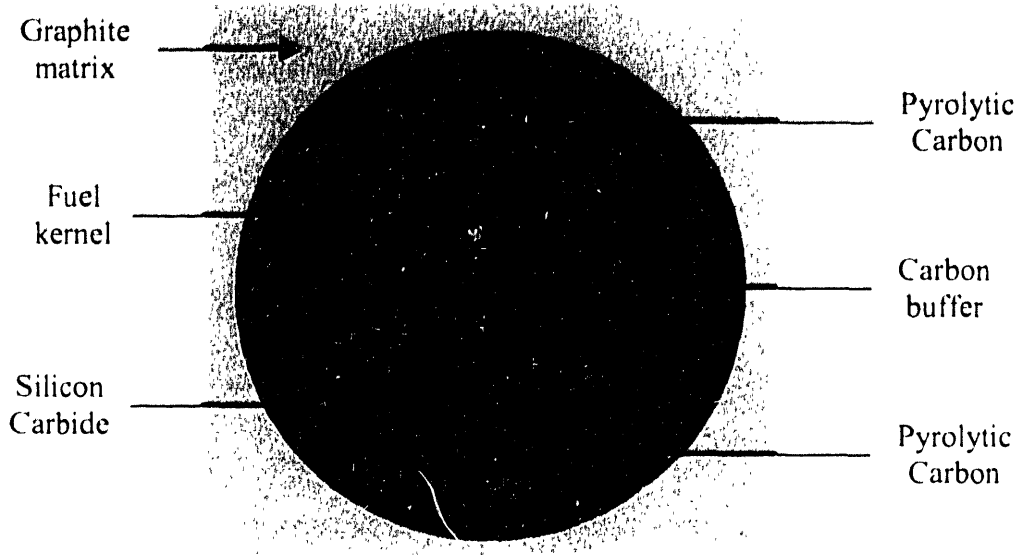


Figure 3-4. MCNP4B Model of a Coated Fuel Particle.

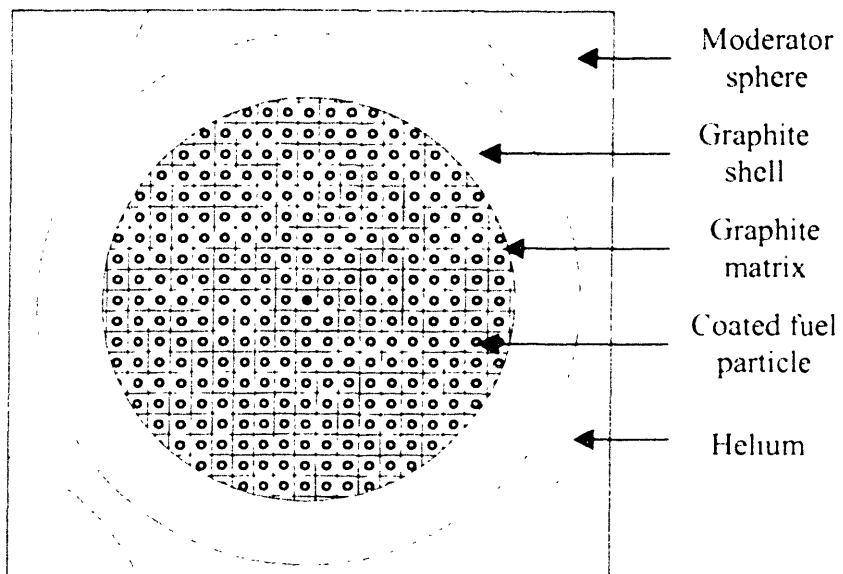


Figure 3-5. MCNP4B Model of a Fuel Pebble

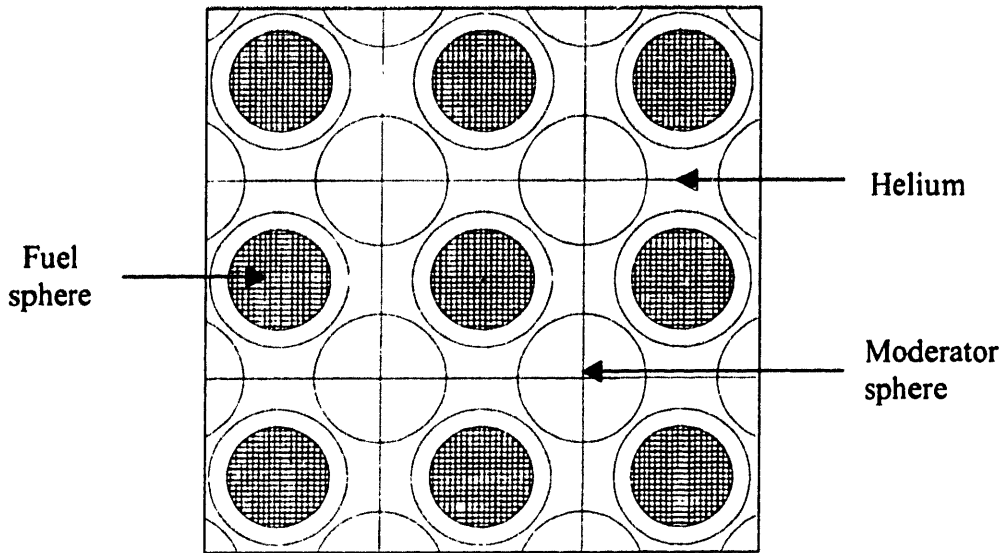


Figure 3-6. MCNP4B Model of a Pebble-Bed Core

3.4 Conclusions

The BCC lattice is a convenient, and a neutronically accurate, representation of a randomly packed, reflected pebble-bed core. It is characterized by the size of the cubic unit cell, which is determined from the specified packing fraction and the detailed design of the component spheres. Complicated mixtures of different spheres can be assembled by combining BCC unit cells into larger repeating cells. Use of the repeated-structure feature of MCNP4B generates partial spheres at the core boundaries, whose effect can be minimized by either introducing an exclusion zone or by reducing the packing fraction.

4. THE HTR-PROTEUS FACILITY

The PROTEUS zero-power experimental facility is located at the Paul Scherrer Institute in Switzerland. The facility has been used for a variety of critical experiments involving both light-water and gas-cooled reactor cores. The various critical assemblies are usually configured in PROTEUS as a subcritical test zone in the centre of an annular thermal driver zone. However, for the LEU-HTR experiments, the facility was set up as a critical pebble-bed core surrounded radially and axially by a graphite reflector. PROTEUS was initially prepared for the HTR experiments between January and August 1980, but was subsequently reconfigured to accommodate advanced light-water reactor experiments. The facility was rebuilt for the LEU-HTR tests in 1991 [4-1], and the experimental program continued until 1996. [4-2]

4.1 Description of the PROTEUS Facility

The HTR-PROTEUS facility consists of a graphite cylinder with a central cavity. The height of the cylinder is 3304 mm and its radius is 3262 mm. The cavity starts 780 mm above the bottom of the lower axial reflector, and is a 22-sided polygon with a flat-to-flat separation distance of 1250 mm. The removable upper axial reflector is a 780 mm-high graphite cylinder inside an aluminium tank, which fits onto an aluminium safety ring located 1764 mm above the floor of the cavity. An air gap is present between the upper reflector and the pebble-bed core. [4-3, 4-4]

The radial reflector has numerous channels, which accommodate absorber rods and instrumentation. The facility uses eight shutoff rods located on a radius of 689 mm, four

control rods on a radius of 789 mm or 906 mm, and one servo-driven regulating rod at a distance of 900 mm from the core centre. The shutoff rods are made of 35 mm-diameter borated-steel (5 wt%) rod sections enclosed in stainless-steel tubes with an outer diameter of 40 mm. For the first core, the control rods were the Zebra-type made of aluminium with cadmium shutters. However, these were replaced with standard stainless-steel control rods for all subsequent cores. A photograph showing a top view of the HTR-PROTEUS facility appears in Figure 4-1, while Figure 4-2 provides a schematic side view

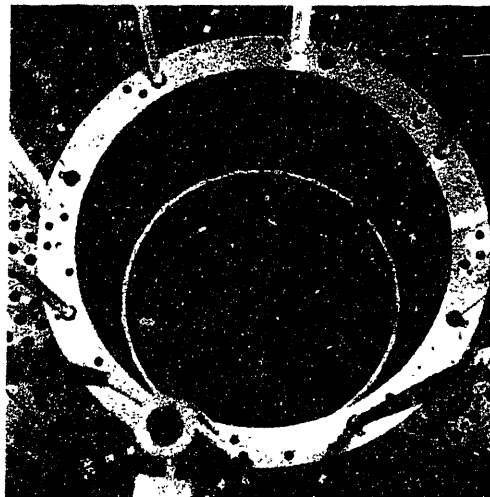


Figure 4-1. Top View of HTR-PROTEUS Facility

The reflector consists of graphite of various ages and moisture content. Table 4-1 gives the atom densities for the reflector used in the MCNP models of the facility. These values were later revised to incorporate a higher concentration of impurities (expressed as an equivalent natural boron content) resulting in a 2200 m/s cross-section of 4.09 mbarn. An average value of 1.763 g/cm^3 was recommended for the density of the graphite.

Table 4-1
Atom Densities in PROTEUS Graphite Reflector

<i>Nuclide</i>	<i>nuclei/barn-cm</i>	
	<i>Axial Reflectors</i>	<i>Radial Reflector</i>
^{10}B	9.00e-09	9.20e-09
^{11}B	3.60e-08	3.70e-08
Carbon	8.61e-02	8.84e-02

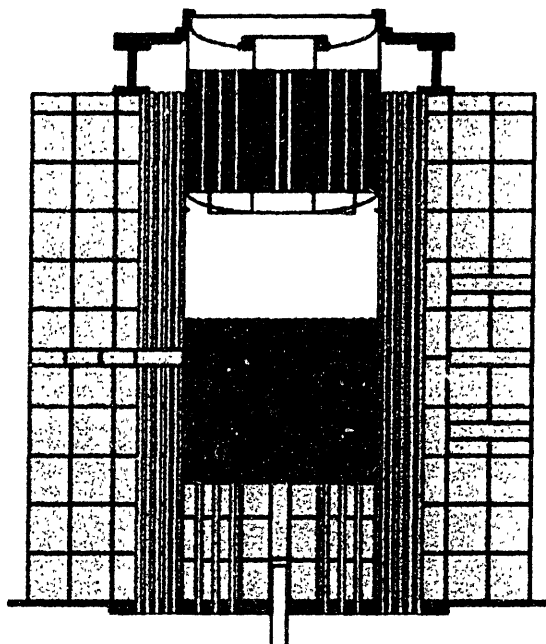


Figure 4-2. A schematic Representation of the HTR-PROTEUS Facility

4.2 Fuel and Moderator Spheres

The geometry and mass specifications of the LEU-HTR fuel spheres and moderator spheres are summarized in Table 4-2. The 6 cm-diameter fuel spheres contain TRISO coated fuel particles, with 16.7 wt% enriched UO_2 , embedded in a graphite matrix. The atom densities in the fuel and moderator spheres are given in Tables 4-3 and 4-4, respectively. The presence of impurities in the graphite is approximated by a boron

content that results in an effective 2200 m/s absorption cross section of 4.79 mbarn. The presence of moisture in the spheres is ignored in these specifications, because the moisture content was shown to be less than 0.01 wt%. The diameter and mass of the fuel pebbles was measured at the beginning and end of the experiments to address concerns regarding the potential erosion of the graphite during loading and unloading operations. No change in mass occurred, although some surface indentation was observed. [4-4]

Table 4-2
LEU-HTR Fuel and Moderator Sphere Data

<i>Property</i>	<i>Value</i>
Mass of uranium per fuel pebble	5.966 g
^{235}U mass per fuel pebble	1.000 g
Mass of carbon per fuel pebble	193.1 g
Radius of fuel pebble fuelled zone	2.5 cm
Radius of fuel/moderator pebble	3.0 cm
Radius of UO_2 fuel kernel	0.02510 cm
Thickness of carbon buffer coating	0.00915 cm
Thickness of inner PyC coating	0.00399 cm
Thickness of SiC coating	0.00353 cm
Thickness of outer PyC coating	0.00400 cm
Density of UO_2 fuel	10.88 g/cm^3
Density of carbon buffer coating	1.100 g/cm^3
Density of inner PyC coating	1.900 g/cm^3
Density of SiC coating	3.200 g/cm^3
Density of outer PyC coating	1.890 g/cm^3
Number of CFPs per fuel sphere	9393
Mass of carbon in moderator sphere	189.1 g
Radius of moderator sphere	3.0 cm

Table 4-3
Atom Densities in HTR-PROTEUS Fuel Spheres

<i>Nuclide</i>	<i>Atom Density (nuclei/barn-cm)</i>		
	<i>UO₂ kernel</i>	<i>Graphite Matrix</i>	<i>Graphite Shell</i>
¹⁰ B	0.0	2.45968e-08	2.47855e-08
¹¹ B	0.0	9.96296e-08	1.00394e-07
Carbon	0.0	8.57982e-02	8.64563e-02
Oxygen	4.86157e-02	0.0	0.0
Silicon	0.0	4.94711e-04	0.0
²³⁵ U	4.11729e-03	0.0	0.0
²³⁸ U	2.01906e-02	0.0	0.0

Table 4-4
Atom Densities in HTR-PROTEUS Moderator Spheres

<i>Nuclide</i>	<i>Atom Density (nuclei/barn-cm)</i>
¹⁰ B	2.40326e-08
¹¹ B	9.73442e-08
Carbon	8.38302e-02

4.3 The Stochastic Cores

As summarized in Table 4-5, a total of eleven cores were investigated during the HTR-PROTEUS experimental program. The majority of the cores utilized deterministic sphere arrangements, which facilitated the studying of effects such as neutron streaming, moderation and water ingress (simulated with polyethylene rods) because of the easy access to the core. Moreover, because k_{∞} and the related spectral indices are independent of the pebble-bed geometry, it was possible to use the deterministic cores for the zero-leakage neutron balance measurement. [4-5]

However, criticality measurements were also carried out on three stochastic cores (4.1, 4.2 and 4.3), which used a 1:1 fuel-to-moderator (F/M) sphere ratio to achieve criticality

at a reasonable core height. The experimental results for these cores are summarized in Table 4-6 (the control-rod reactivity worths were also measured but are not reported here) [4-2]. The reported k_{eff} are on the order of 1.013, because of corrections for various experimental effects and control-rod insertions needed to maintain criticality [4-6].

**Table 4-5
HTR-PROTEUS Experimental Core Configurations**

Core	F/M	Packing	Prominent Feature
1	2:1	HCP [†]	Used Zebra Cd/Al shutters instead of control rods.
1A	2:1	HCP	
2	2:1	HCP	Investigated influence of upper reactor cavity.
3	2:1	HCP	Water ingress using 8.9 mm OD polyethylene rods.
4	1:1	Random	Stochastic cores.
5	2:1	POP [‡]	
6	2:1	POP	Simulated water ingress with polyethylene/copper rods.
7	2:1	POP	Water ingress using 8.3 mm OD polyethylene rods.
8	2:1	POP	Partial water ingress using 15 cm-long polyethylene rods.
9	1:1	POP	
10	1:1	POP	Water ingress using 6.5 mm OD polyethylene rods.

[†] Hexagonal Close Packed; [‡] Point-on-Point (column hexagonal).

**Table 4-6
Experimental Results for HTR-PROTEUS Stochastic Cores**

Parameter	Core 4.1	Core 4.2	Core 4.3
k_{eff}^{\dagger}	1.0134 ± 0.0011	1.0129 ± 0.0010	1.0132 ± 0.0010
Critical loading (F, M)	5020, 5020	4940, 4940	4900, 4900
Critical height	1.58 ± 0.01 m	1.52 ± 0.01 m	1.50 ± 0.01 m
Neutron flux	5×10^7 n/cm ² /s	5×10^7 n/cm ² /s	5×10^7 n/cm ² /s
Air temperature	19.8°C	19.6°C	21.2°C
Air pressure	975 mbar	980 mbar	980 mbar
Humidity	44%	50%	50%

[†] Corrected for the presence of control rods in the radial reflector.

The packing fractions of the three cores differed because the spheres were loaded differently [4-7]. Core 4.1 was prepared by clamping the fuel and moderator sphere delivery tubes together in parallel, and each sphere was allowed to fall into the core from its respective tube. To avoid any unwanted ordering effects, a second method was used to load cores 4.2 and 4.3 for which the fuel and moderator sphere channels were combined by means of a simple funnel arrangement. The pebble bed was lightly flattened after each loading step, and its height was determined by measuring the average distance from the safety ring to the bottom of a rod placed horizontally on top of the core. A 1 cm error is associated with this procedure at the 1σ confidence interval.

4.4 The MCNP4B Model

A detailed MCNP4B model of the HTR-PROTEUS facility was prepared based on the calculational benchmark specifications given in Reference 4-4. This physics benchmark was part of the IAEA Coordinated Research Program (CRP) on the “Validation of Safety Related Reactor Physics Calculations for Low-Enriched HTGRs.” To simplify the modeling task, details of the channels in the reflector tank and the absorber rods were not included in the specifications. Moreover, an equivalent core radius was provided, which proved crucial for defining a sphere exclusion zone. However, the removable upper axial reflector was modeled accurately. Figures 4-3 and 4-4 are vertical and horizontal plan views of the MCNP4B model, and further generic details of the core region appear in Chapter 3. Table 4-7 summarizes the pebble-bed lattice parameters.

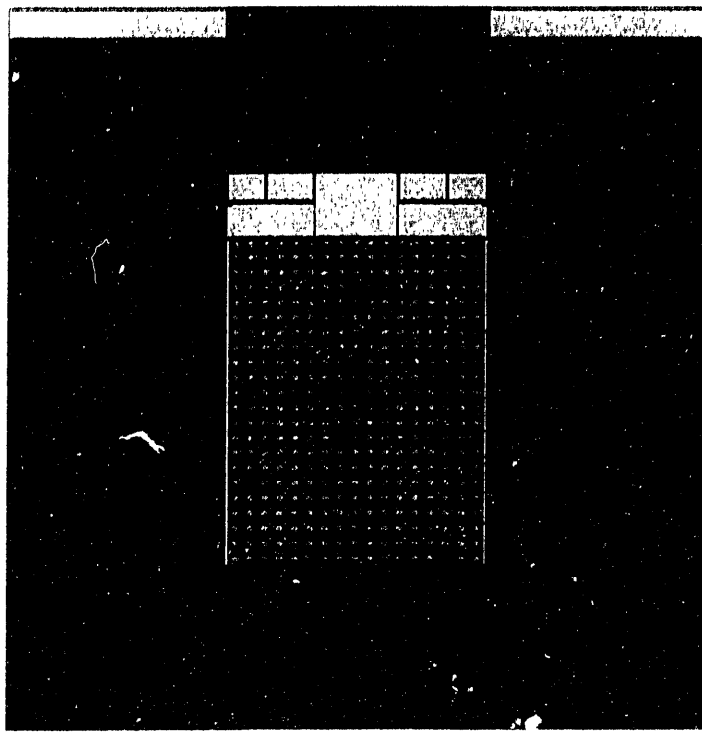


Figure 4-3. Vertical View of MCNP4B Model of HTR-PROTEUS

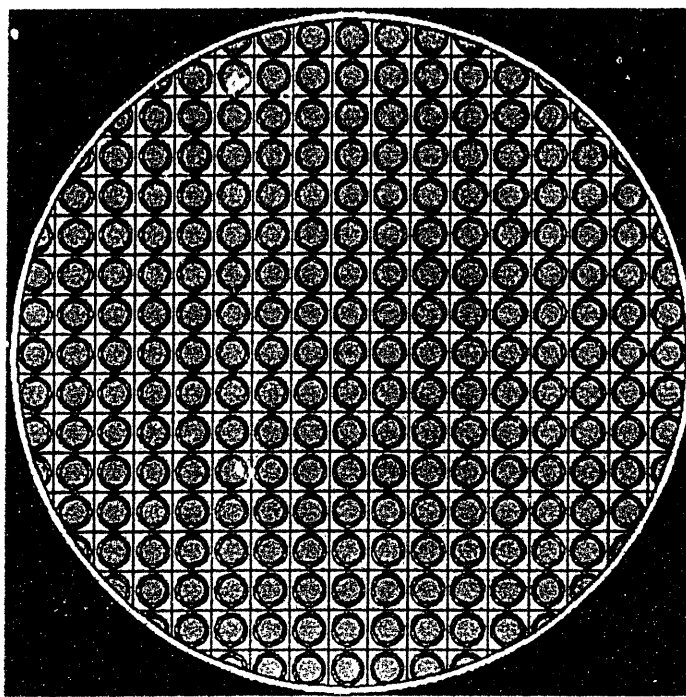


Figure 4-4. Horizontal View of MCNP4B Model of HTR-PROTEUS

A 1.5 cm sphere exclusion zone was used to compensate for the presence of partial spheres (with a 1:1 fuel-to-moderator sphere ratio) around the core periphery. The three MCNP4B models for cores 4.1 through 4.3 are included as Appendices A-1, -2 and -3.

**Table 4-7
Lattice Parameters for MCNP4B Model of
Stochastic HTR-PROTEUS Cores**

<i>Core</i>	<i>Packing Fraction</i>	<i>Cell Size (cm)</i>
4.1	0.60	7.223988
4.2	0.615	7.164773
4.3	0.618	7.153160

The results of the MCNP4B criticality analyses are summarized in Table 4-8, along with the measured k_{eff} and the results of an MCNP-BALL analysis carried out by Murata [4-7]. The two sets of calculations are seen to be in excellent agreement, although the cores are predicted to be more reactive than measured. The over-estimation of the calculated k_{eff} has been attributed to the specified composition of the graphite reflector [4-6].

**Table 4-8
HTR-PROTEUS Criticality Analysis**

<i>Core</i>	<i>Critical Height (cm)</i>	<i>Packing Fraction</i>	<i>Effective Multiplication Constant</i>		
			<i>Experiment</i>	<i>MCNP4B[†]</i>	<i>MCNP-BALL^[6]</i>
4.1	158	0.600	1.0134 ± 0.0011	1.0208 ± 0.0011	1.0206 ± 0.0011
4.2	152	0.615	1.0129 ± 0.0008	1.0172 ± 0.0010	1.0168 ± 0.0011
4.3	150	0.618	1.0132 ± 0.0007	1.0176 ± 0.0011	1.0172 ± 0.0011

[†] Using ENDF/B-VI cross-section data evaluated at 300 K; 0.5 million neutron histories.

4.5 Summary

The HTR-PROTEUS experiments involving stochastic cores were modeled successfully using a BCC lattice and a 1.5 cm exclusion zone. The calculated critical heights of the three experiments agreed closely with the predictions MCNP-BALL, a Japanese code that models the irregularly packed pebble-bed cores exactly. Because the model was based on incorrect PSI specifications of the impurity content in the reflector, the resulting effective multiplication constants were larger than those measured by approximately 0.7% $\Delta k/k$. The correct equivalent boron concentrations were not available. The success of this modeling methodology justified its application to the analysis of the HTR-10 reactor described in Chapter 5.

5. THE HTR-10 REACTOR

The HTR-10 is an experimental 10 MW(t) pebble-bed reactor recently constructed at the Institute of Nuclear Energy Technology (INET), Beijing. The main objectives of this high-temperature gas-cooled reactor project are as follows [5-1]:

- to acquire technical expertise in the design, construction and operation of pebble-bed reactors;
- to provide an experimental facility for the testing of spherical fuel elements;
- to demonstrate the inherent safety features of the modular pebble-bed reactor;
- to develop cogeneration and closed-cycle gas-turbine technology; and
- to investigate high-temperature process heat applications.

The safe operation of the reactor requires the ability to calculate accurately its neutron physics parameters using computer codes. These codes are typically validated using data from critical experiments performed both in zero-power research reactors and during the commissioning of the actual reactor. To facilitate this validation process for HTGRs, the International Atomic Energy Agency (IAEA) sponsored two benchmark problems in two separate Coordinated Research Programs (CRPs). The first was already discussed in Chapter 4. The second, which is entitled "Evaluation of High-Temperature Gas-Cooled Reactor Performance," is related to the commissioning of the HTR-10 reactor and is the subject of this Chapter [5-2].

5.1 Description of the HTR-10 Reactor

The HTR-10 is a pebble-bed reactor that uses spherical fuel elements with embedded coated fuel particles. The fuel particles contain kernels with low-enriched uranium (17% ^{235}U) whose design burnup is 80,000 MWd/t. Detailed specifications of the graphite fuel elements are given in Table 5-1. The full core consists of approximately 27,000 fuel elements randomly packed in a cylindrical cavity with a mean height of 1.97 m, a diameter of 1.8 m and a volume of 5.0 m³. The core is surrounded by a structure consisting of a graphite reflector and a borated carbon shield. The radial reflector, which is 100 cm thick, contains penetrations for ten control rods, seven absorber ball units, three irradiation sites and twenty coolant channels. Helium gas flows up these coolant channels before reversing direction at the top of the core and flowing downward into the pebble bed. The core inlet and outlet coolant temperatures are 250°C and 700°C, respectively, at a pressure of 3.0 MPa. Vertical and horizontal cross sections of the core are shown in Figures 5-1 and 5-2.

The initial approach to critical was achieved on December 1, 2000. The discharge tube and the cone at the bottom of the core was filled with moderator pebbles, then a mixture of fuel and moderator pebbles was added randomly until the critical height was reached with the control rods fully withdrawn. The ratio of fuel balls to moderator pebbles used was 57% to 43%, and the initial loading was carried out at room temperature (15°C) and in atmospheric air. The critical loading was 9627 fuel spheres and 7263 moderator spheres for a total of 16,890 spheres [5-3].

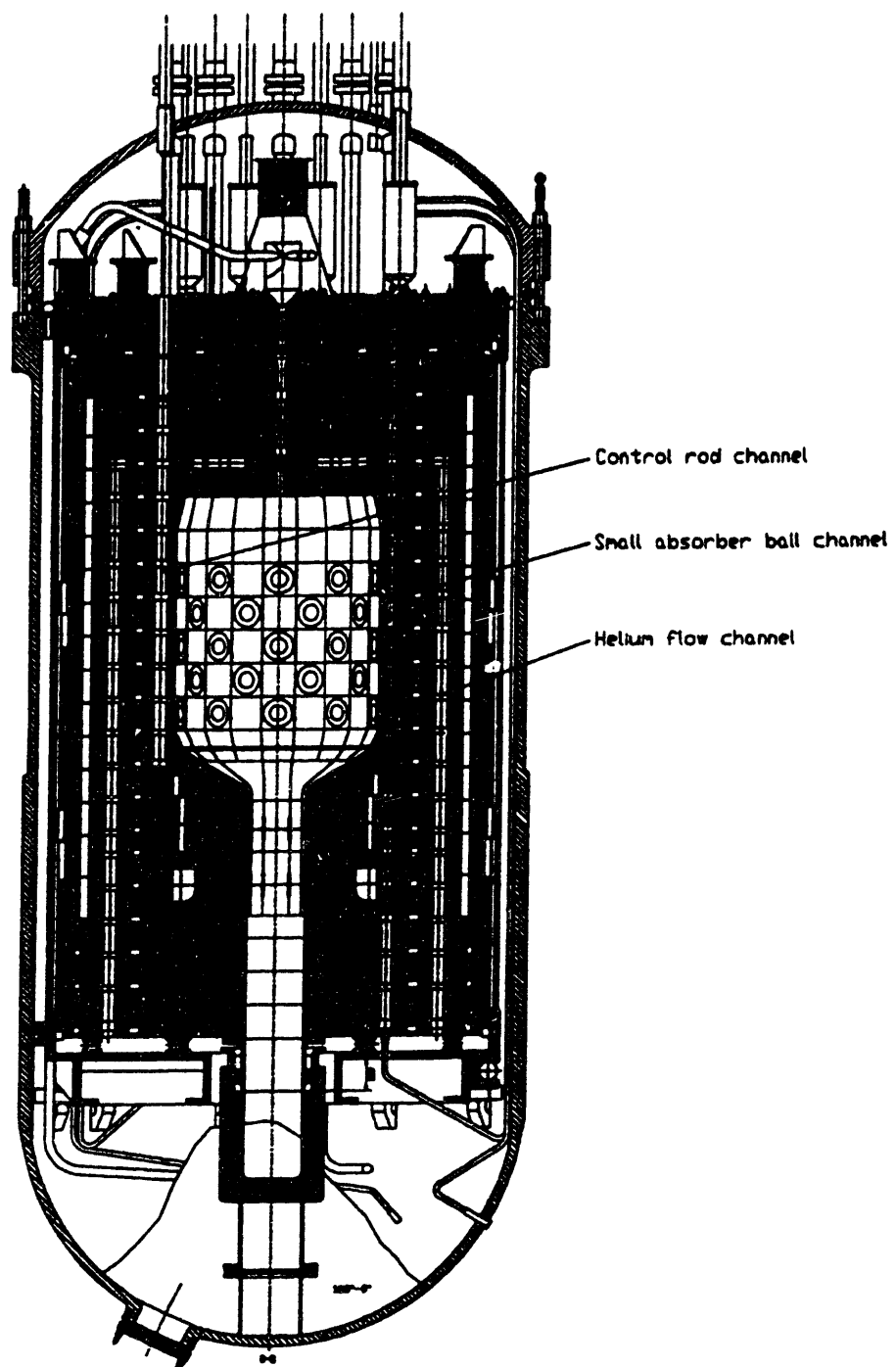


Figure 5-1. Vertical Cross Section of the HTR-10 Reactor [5-2]

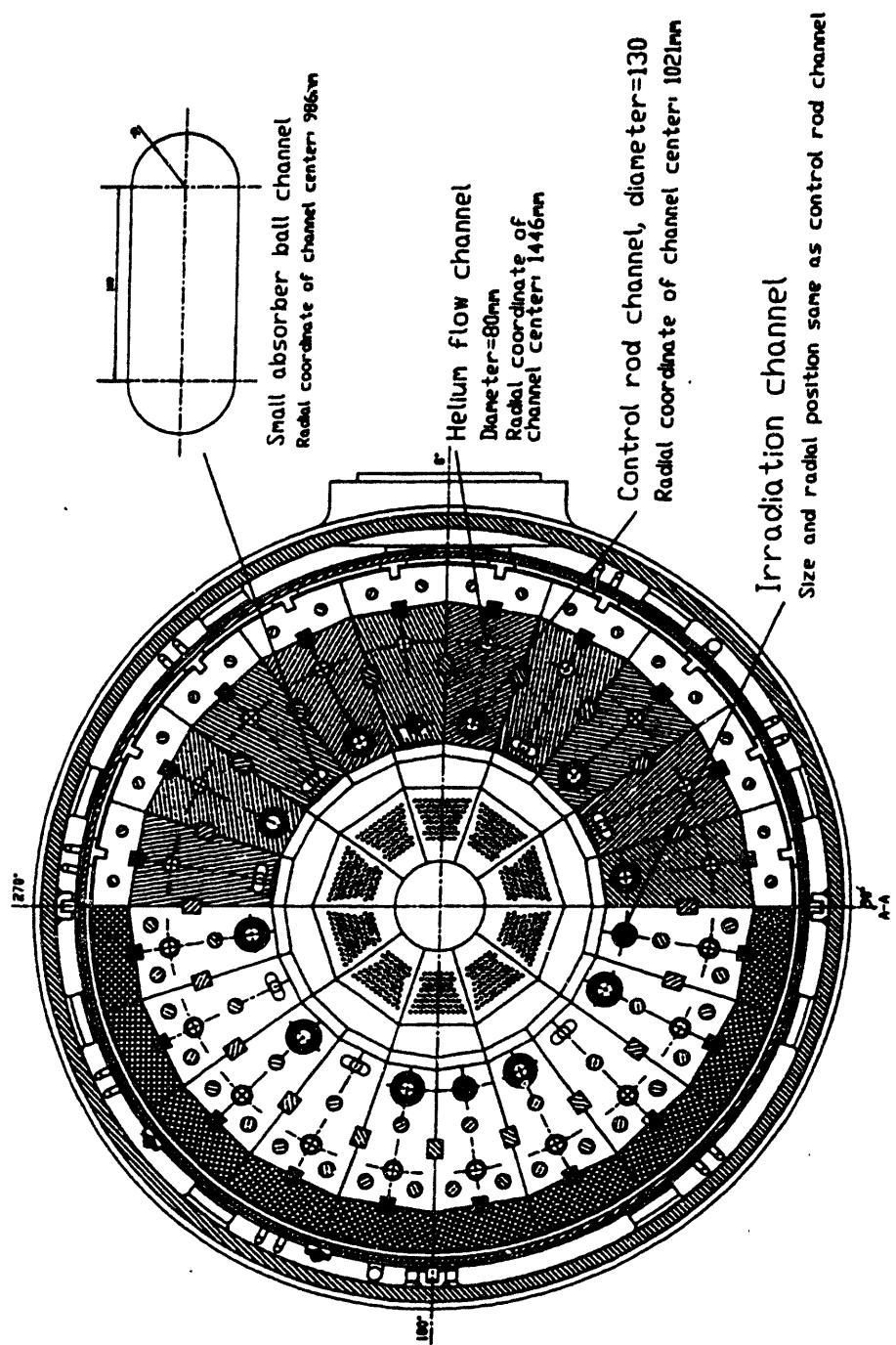


Figure 5-2. Horizontal Cross Section of the HTR-10 Reactor [5-2]

Table 5-1
HTR-10 Reactor Core Parameters

Parameter	Value	Units
<i>Structure</i>		
Density of reflector graphite	1.76	g/cm ³
Equivalent boron content of reflector graphite impurities	4.8366	ppm
Density of borated carbon brick (including B ₄ C)	1.59	g/cm ³
Weight ratio of B ₄ C in borated carbon brick	5	%
<i>Moderator Pebbles</i>		
Diameter of moderator pebble	6.0	cm
Density of graphite	1.84	g/cm ³
Equivalent natural boron content of impurities in graphite	0.125	ppm
<i>Fuel Pebbles</i>		
Diameter of fuel pebble	6.0	cm
Diameter of fuel zone	5.0	cm
Density of graphite in matrix and outer shell	1.73	g/cm ³
Uranium loading per fuel pebble	5.0	g
Enrichment of ²³⁵ U	17.0	wt. %
Equivalent natural boron content of impurities in uranium	4	ppm
Equivalent natural boron content of impurities in graphite	1.3	ppm
Volumetric filling fraction of balls in the core	0.61	
<i>Coated Fuel Particle</i>		
Radius of fuel kernel	0.025	cm
UO ₂ density	10.4	g/cm ³
Thickness of first pyrolytic carbon coating	0.009	cm
Thickness of second pyrolytic coating	0.004	cm
Thickness of silicon-carbide coating	0.0035	cm
Thickness of third pyrolytic carbon coating	0.004	cm
Density of first pyrolytic coating	1.1	g/cm ³
Density of second pyrolytic coating	1.9	g/cm ³
Density of silicon-carbide coating	3.18	g/cm ³
Density of third pyrolytic coating	1.9	g/cm ³

With the control rods inserted, the core will then be pressurized and completely filled using the same mixture of fuel and moderator balls. The initial critical core height was chosen so as to limit the maximum excess reactivity held down by the control absorber

rods to the amount required to provide sufficient xenon override. The excess reactivity margin will be controlled subsequently by the continuous refuelling of the reactor.

5.2 Physics Benchmark Problems

INET proposed the following benchmark problems for the HTR-10 to test the accuracy of physics codes in calculating the effective multiplication factor for various pebble-bed reactor configurations [5-2]. These are designated B1, B2, B3 and B4:

- a) **Problem B1.** Predict the initial cold critical loading ($k_{\text{eff}} = 1.0$), either in terms of the number of pebbles or the height of the pebble bed, with the control absorbers fully withdrawn. Assume a core temperature of 15°C and atmospheric air.
- b) **Problem B2.** Calculate the effective multiplication factor, k_{eff} , of the core filled completely to a height of 1.97 m under a helium pressure of 3.0 MPa and at the following core temperatures: 20°C (B21), 120°C (B22) and 250°C (B23). Assume that all control absorbers are fully withdrawn.
- c) **Problem B3.** Calculate the total reactivity worth of the ten control rods (B31) and of one control rod (B32) for a full core at a temperature of 20°C and a helium pressure of 3.0 MPa.
- d) **Problem B4.** Calculate the total reactivity worth of the ten control rods (B41) and the differential reactivity worth of one control rod (B42) for a core loading height of 126 cm at a temperature of 20°C and a helium pressure of 3.0 MPa.

These calculations are to be performed for the specified fuel-to-moderator pebble ratio of 57% to 43%. The given core temperatures assume a uniform temperature profile throughout the reactor, including the fuel pebbles and the surrounding graphite structure. The height of the core refers to the fuelled portion only, *i.e.*, excluding the conus filled with moderator pebbles. The accuracy of the codes was to be determined by comparing the code predictions with measurements during the initial approach to critical and low-power physics commissioning tests at the HTR-10 facility.

5.3 Reference Core Physics Model

A simplified reactor description was included in the physics benchmark specification to provide a common starting point for the modeling of the HTR-10 with a variety of codes. Figure 5-3 shows the recommended two-dimensional model of the reactor with zone identification numbers, and Table 5-2 gives the corresponding spatially homogenized material compositions of the reactor structure.

Benchmark problems B3 and B4 require the explicit modeling of the control rods. The design of the control rod is depicted in Figure 5-4, and its geometry and material specifications are summarized in Table 5-3. Boron carbide (B_4C) is used as the neutron absorber. Each control rod contains five B_4C annular segments with outer stainless-steel sleeves, and which are joined together by stainless steel joints.

5.4 MCNP4B Model of HTR-10

The HTR-10 physics benchmark problem was specified in a manner suitable for both diffusion-theory and Monte Carlo codes. The resultant simplification of the reactor

model (see Section 5-3) reduces the accuracy with which MCNP4B can reproduce experimental measurements. Moreover, the specification of a fuel-to-moderator pebble ratio of 57% to 43% further reduces the accuracy with which the repeated-structure

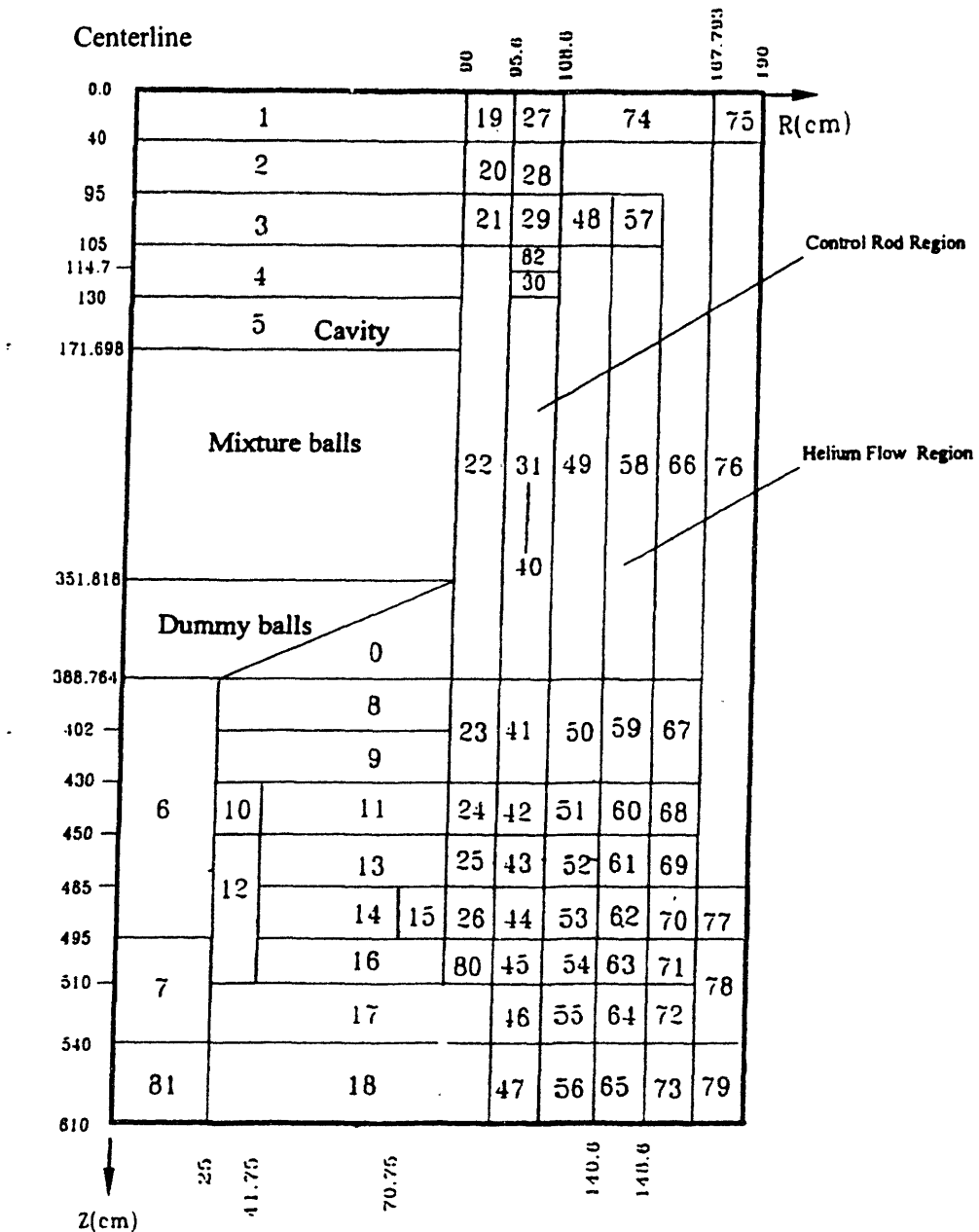


Figure 5-3. Reference Core Physics Calculation Model [5-2]

Table 5-2
Homogenized Nuclide Densities in Reflector Zones (nuclei/barn-cm)

<i>Zone</i>	<i>Carbon</i>	<i>Boron</i>	<i>Description</i>
0	8.51047E-02	4.56926E-07	Bottom reflector with hot helium flow borings
1	7.29410E-02	3.29811E-03	Borated carbon bricks
2	8.51462E-02	4.57148E-07	Top graphite reflector
3	1.45350E-02	7.80384E-08	Cold helium chamber
4	8.02916E-02	4.31084E-07	Top reflector
5	0.00000E+00	0.00000E+00	Top core cavity (helium filled)
6, 7	5.38275E-02	2.88999E-07	Dummy balls (= graphite with reduced density)
8	7.81408E-02	4.19537E-07	Bottom reflector structure
9	8.23751E-02	4.42271E-07	Bottom reflector structure
10	8.43647E-02	2.98504E-04	Bottom reflector structure
11	8.17101E-02	1.56416E-04	Bottom reflector structure
12	8.50790E-02	2.09092E-04	Bottom reflector structure
13	8.19167E-02	3.58529E-05	Bottom reflector structure
14	5.41118E-02	5.77456E-05	Bottom reflector structure
15	3.32110E-02	1.78309E-07	Bottom reflector structure
16	8.81811E-02	3.58866E-05	Bottom reflector structure
17, 55, 72, 74, 75, 76, 78, 79	7.65984E-02	3.46349E-03	Borated carbon bricks
18, 56, 73	7.97184E-02	0.00000E+00	Carbon bricks
19	7.61157E-02	3.44166E-03	Borated carbon bricks
20	8.78374E-02	4.71597E-07	Bottom reflector structure
21	5.79696E-02	3.11238E-07	Bottom reflector structure
22, 3, 25, 49 50, 52, 54, 66, 67, 69, 71, 80	8.82418E-02	4.73769E-07	Bottom reflector structure
24, 51, 68	8.79541E-02	1.68369E-04	Bottom reflector structure
26	8.46754E-02	4.54621E-07	Bottom reflector structure
27	5.89319E-02	2.66468E-03	Borated carbon bricks
	(8.18911E-02) ¹	(3.70281E-03)	
28, 82	6.78899E-02	1.40000E-05	Bottom reflector structure
	(9.43390E-02)	(1.94542E-05)	
29	4.03794E-02	1.40000E-05	Bottom reflector structure
	(5.61108E-02)	(1.94542E-05)	
30	6.78899E-02	3.64500E-07	Bottom reflector structure
	(9.43390E-02)	(5.06505E-07)	
31-40	6.34459E-02	3.40640E-07	Graphite reflector with control rod holes
	(8.81637E-02)	(4.73350E-07)	
41a	6.78899E-02	3.64500E-07	Bottom reflector structure
	(9.43390E-02)	(5.06505E-07)	
41b	6.78899E-02	3.64500E-07	Bottom reflector structure
42	6.76758E-02	1.25331E-04	Bottom reflector structure
43, 45	8.61476E-02	4.62525E-07	Bottom reflector structure
44	8.29066E-02	4.45124E-07	Bottom reflector structure
46	7.47805E-02	3.38129E-03	Borated carbon bricks
47	7.78265E-02	0.00000E+00	Carbon bricks
48	5.82699E-02	3.12850E-07	Bottom reflector structure
53	8.55860E-02	4.59510E-07	Bottom reflector structure
57	7.28262E-02	3.91003E-06	Bottom reflector structure
58, 59, 61, 63	7.60368E-02	4.08240E-07	Graphite reflector, cold helium flow region
60	7.57889E-02	1.45082E-04	Graphite reflector, cold helium flow region
62	7.37484E-02	3.95954E-07	Graphite reflector, cold helium flow region
64	6.60039E-02	2.98444E-03	Borated carbon bricks
65	6.86924E-02	0.00000E+00	Carbon bricks
70	8.61500E-02	4.62538E-07	Graphite reflector structure
77	7.49927E-02	3.39088E-03	Borated carbon bricks
81	7.97184E-02	0.00000E+00	Dummy balls (modeled as carbon bricks)

¹ Values in brackets are atom densities adjusted to account for channels in the graphite structure.

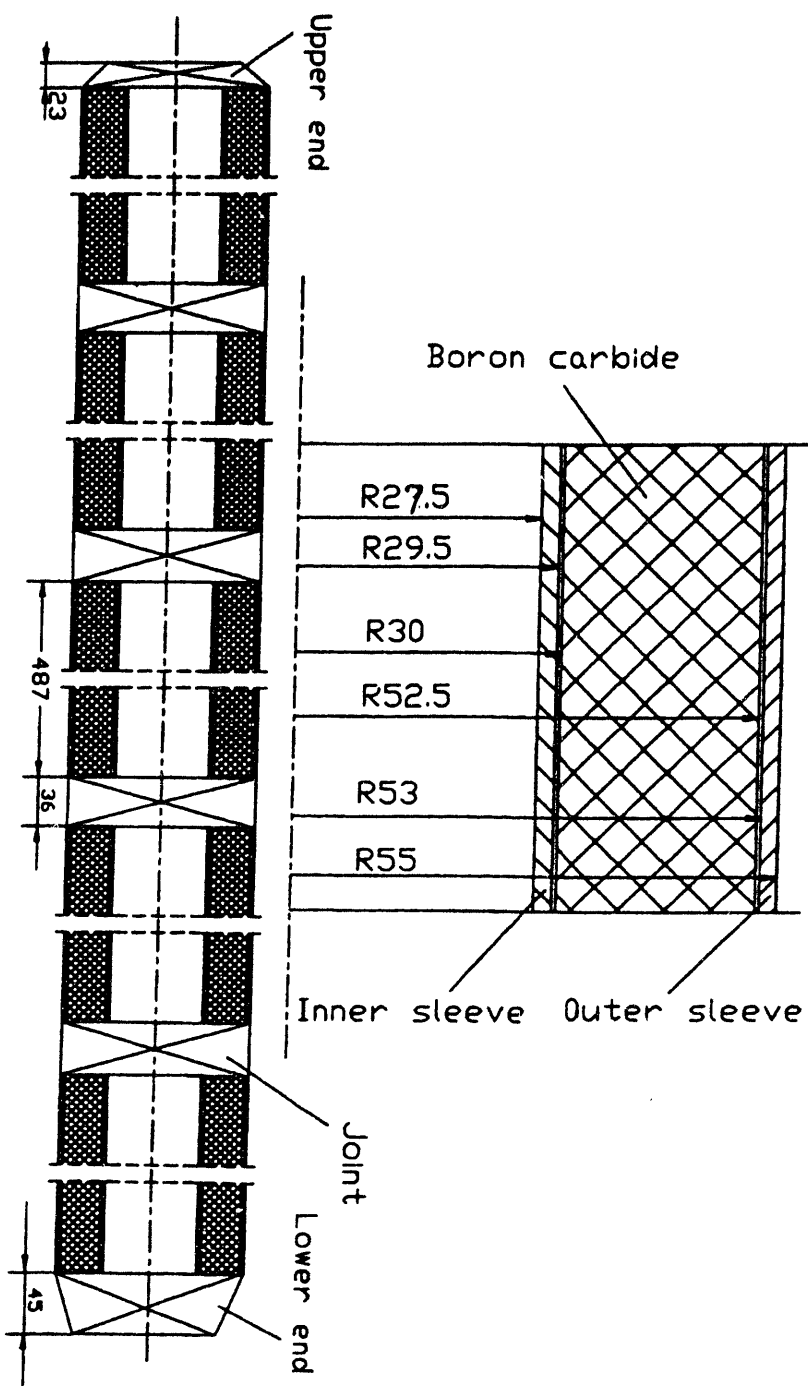


Figure 5-4. Structure of the HTR-10 Control Rod [5-2]

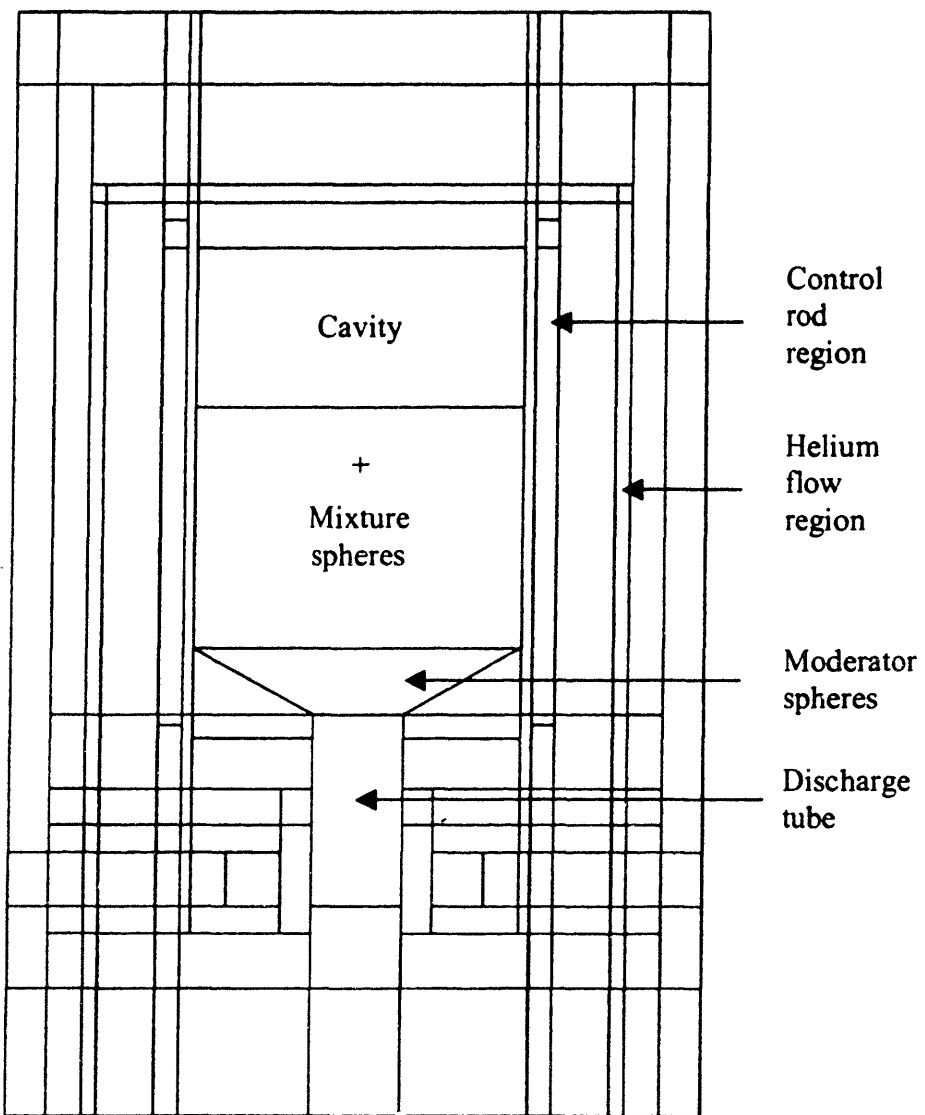


Figure 5-5. Vertical Cross Section of the MCNP Model of HTR-10

feature in MCNP4B can model the pebble-bed core, because all regular packings of mono-sized spheres except for simple-hexagonal have even coordination numbers [5-4]. This fuel-to-moderator sphere ratio was selected by INET to ensure criticality of the full core.

5.4.1 Reactor Structure

The MCNP model consists of the reactor structure, which includes the graphite reflector and the borated carbon bricks that surround the reflector, and the pebble-bed core. A vertical cross-sectional view of the modeled structure is shown in Figure 5-5. This model is identical to Figure 5-3 (including the zone numbers) except for the presence of control, irradiation and coolant channels. These channels are shown in the horizontal cross-sectional view of the reactor (Figure 5-6).

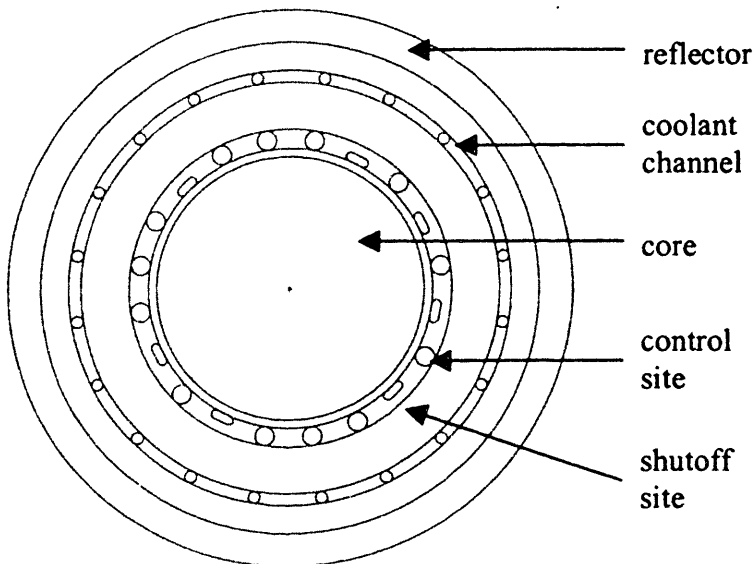


Figure 5-6. Horizontal Cross Section of the MCNP Model of HTR-10

5.4.2 Control Absorbers

Details regarding the stainless-steel joints between the control absorber segments were not included in the benchmark problem definition. The model was prepared assuming that the joints preserve the annular geometry of the absorber segments to allow coolant flow. The composition of the stainless steel is given in Table 5-3, and the geometry of the control-rod channels is otherwise modeled as specified in Table 5-4. The MCNP4B model of a control rod is shown in Figure 5-7. The vertical position of each control rod can be changed individually.

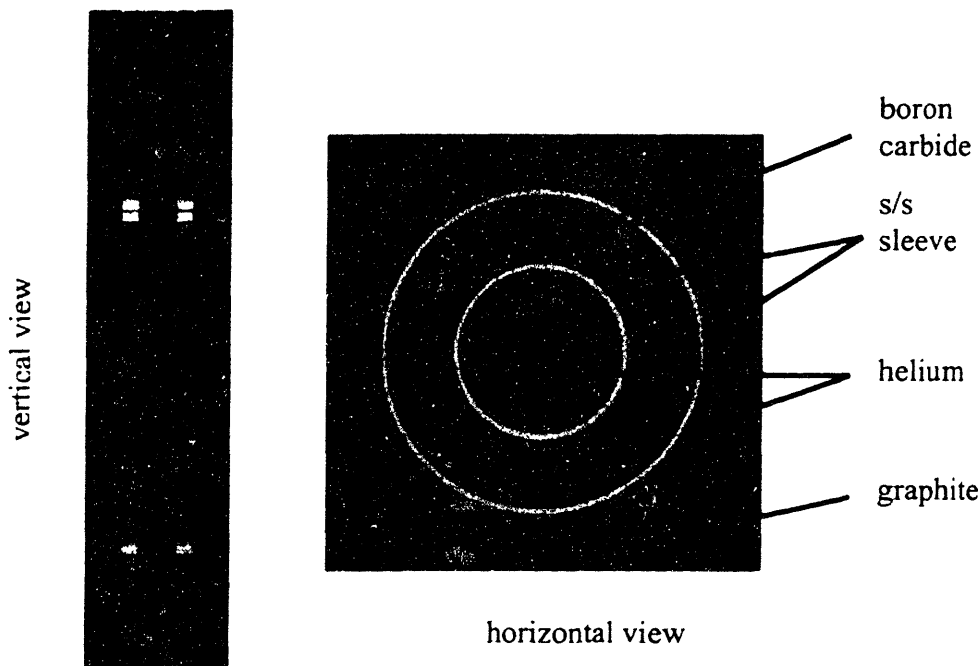


Figure 5-7. MCNP4B model of HTR-10 control rod

Since information about the control-rod drive shafts was also not provided, the control rods were modeled without such components. The absorber-ball and irradiation channels

were assumed to be empty (helium filled). The atom densities of the spatially homogenized zones that contain the various channels were corrected for the presence of these holes (shown in Table 5-2 in brackets).

Table 5-3
HTR-10 Composition of Control-Rod Stainless Steel
(density = 7.9 g/cm³)

<i>Element</i>	<i>Wt%</i>
Cr	18
Fe	68.1
Ni	10
Si	1
Mn	2
C	0.1
Ti	0.8

Table 5-4
HTR-10 Control Rod Geometry and Material Specifications

Description	Value	Units
Control rod channel radius	6.5	cm
Radial position of channel centre	102.1	cm
Length of B ₄ C segment	48.7	cm
Length of bottom metallic end	4.5	cm
Length of metallic joints	3.6	cm
Length of top metallic end	2.3	cm
Inside radius of inner stainless-steel sleeve	2.75	cm
Thickness of stainless-steel sleeve	0.2	cm
Thickness of gap between sleeve and B ₄ C	0.05	cm
Thickness of B ₄ C annulus	2.25	cm
Density of B ₄ C	1.7	g/cm ³
Length of control rod	264.7	cm

5.4.3 Core

The specification of a 57:43 fuel-to-moderator pebble percent ratio for the initial HTR-10 core loading complicates the modeling of the core using the repeated-structure feature of

MCNP4B. Except for the simple (point-on-point) hexagonal packing, regular lattices constructed of simple unit cells with equal-sized spheres are characterized by even coordination numbers and, therefore, cannot be used to model an uneven fuel-to-moderator ratio while preserving the original geometry of the pebbles. As discussed in Chapter 3, three approaches are available. If a single BCC unit cell is used, then either the size or the density of the graphite moderator sphere can be reduced in a manner that reproduces the specified fuel-to-moderator sphere ratio. Alternatively, a ‘super’ unit cell can be used containing a total of 100 spheres, which permits the explicit loading of 57 fuel spheres and 43 moderator spheres.

In the first method, the radius of the moderator sphere is reduced from 3 cm to 2.731 cm, and the size of the unit cell must be reduced from 7.1843 cm to 6.8772 cm in order to preserve the packing fraction ($f = 0.61$). This procedure assures that the fuel loading, the mass of heavy metal per unit core volume, is the same as for the 57:43 percent random packing. The two-sphere content of the BCC unit cell minimizes the size adjustment for the moderator pebbles. The original size of the fuel sphere was maintained to preserve the effect of the single heterogeneity on the ^{238}U resonance escape probability, which is expected to dominate reactivity effects, while minimizing the perturbation due to the double heterogeneity of the lattice. This method was used for the analysis presented in this report. In the second method, which has not been attempted to date, the graphite density would have to be reduced to $\frac{43}{50} \times 1.84 = 1.58 \text{ g/cm}^3$.

The super unit cell was constructed from $2 \times 5 \times 5 = 50$ unit BCC cells, with $a = 7.1843$ cm. Therefore, the repeating cell spans the following ranges: $-17.96075 \leq x \leq 17.96075$,

$-7.1843 \leq y \leq 7.1843$ and $-17.96075 \leq z \leq 17.96075$. Because each BCC unit cell contains two spheres, the large repeating cell holds 100 spheres in total. The 57 fuel and 43 moderator spheres were distributed deterministically but evenly among the cell lattice points. The calculated k_{eff} of the core was essentially identical to the unit BCC model (1.00081 ± 0.00080 at a core height of 128.0 cm vs. 1.00050 ± 0.00089 at 127.5 cm), although the execution time of the super cell model was nearly an order of magnitude longer. Because the results were generally found to be sensitive to the pattern used to distribute the spheres (see discussion in Chapter 6), the primitive unit cell approach is recommended. Details of the model may be found in the MCNP4B input file included in Appendix B.

A sphere exclusion zone was used around the sides and at the top of the core (see Chapter 3). The dimensions of the exclusion zone are $3 \times \frac{57}{100} = 1.71$ cm. An exclusion zone was not required at the bottom of the fuelled portion of the core, because the conus was filled entirely with moderator spheres. Thus, fuel spheres could be positioned such that only moderator spheres overlapped the bottom boundary of the fuelled core.

The individual TRISO coated fuel particles, which were modeled, were distributed in the fuelled region of the fuel pebbles using a simple-cubic lattice explicitly. The dimensions of the SC unit cell were chosen to reproduce the specified uranium loading of 5 g per fuel pebble. Table 5-5 summarizes the geometry specifications of the pebble-bed core as modeled with MCNP4B. Details of the MCNP4B model appear in Chapter 3.

Table 5-5
HTR-10 Model Pebble-Bed Geometry Specifications

Parameter	Value	Units
Fuel-to-moderator pebble volume ratio	1.3256	—
Radius of fuel pebble	3.0	cm
Radius of fueled region	2.5	cm
Packing fraction	0.61	—
Moderator pebble radius	2.7310	cm
BCC unit cell size	6.8773	cm
SC unit cell size	0.19876	cm

The material compositions of the fuel kernels and the graphite moderator that were used in the MCNP model are given in Table 5-6. The compositions of the pyrolytic carbon and silicon carbide layers in the TRISO coating of the fuel kernels are as specified in the benchmark problem specification (Table 5-1).

Table 5-6
Material Compositions of HTR-10 Pebble-Bed Core

<i>Isotope</i>	<i>Atom Density (1/b-cm)</i>
<i>Graphite moderator:</i>	
C	8.674169E-02
¹⁰ B	2.244010E-08
¹¹ B	9.032424E-08
total	8.674180E-02
<i>Fuel kernel:</i>	
²³⁵ U	3.992067E-03
²³⁸ U	1.924449E-02
O	4.647329E-02
¹⁰ B	1.849637E-08
¹¹ B	7.445022E-08
total	6.970994E-02

5.4.4 Boron Content

Impurities in graphite and uranium are specified in the benchmark problem definition in terms of equivalent concentrations of natural boron. The absolute isotopic abundance of ^{10}B is not given and the nominal value of 19.9% was used. This is a significant source of modeling uncertainty, since a natural variation in ^{10}B from 19.1% to 20.3% has been measured [5-5].

5.5. MCNP4B Calculations

The HTR-10 physics benchmark problems comprise a set of criticality calculations, in which the effective multiplication factor (k_{eff}) is determined for several core configurations. These configurations are achieved by varying the height of the pebble bed, adjusting the position of the control rods, or changing isothermally the temperature of the core.

Determination of the initial critical loading is subject to the uncertainty associated with the partial fuel spheres at the core boundaries. Moderator spheres play no role in the determination of the exclusion zone next to a graphite reflector. It was possible to set up the lower level of the fuelled region precisely, because the bottom of the core is filled with moderator spheres only. However, a separate correction is still required at the top of the core because of the overlapping of spheres in the BCC lattice. The critical loading is calculated using the reduced core volume, but the top exclusion distance should not be used when determining the critical height.

The total reactivity worth of the ten control rods is derived from k_{eff} values with the control rods first fully inserted and then fully withdrawn; similarly for a single control rod. The differential reactivity worth of a single control rod is determined by calculating the k_{eff} for different insertion depths. The temperature-dependent MCNP calculations in this study (benchmark problems B21, B22 and B23) did not include the reactivity effect due to the isothermal expansion of the reflector.

Benchmark problems B1, B3 and B4 were analyzed using the standard ENDF/B-VI cross-section data processed at 300 K. Benchmark problems B22 and B23, which correspond to 393.15 K (120°C) and 523.15 K (250°C) respectively, were estimated using temperature-dependent cross sections prepared at the University of Texas at Austin [5-6]. Benchmark problem B21 was analyzed using both libraries. All the cross-section libraries were originally evaluated using the NJOY nuclear data processing system [5-7].

The University of Texas cross-section libraries (UTXS) are only available at 300 K, 450 K and 558 K in the temperature range of interest. The predictions for benchmark problems B21, B22 and B23 were therefore obtained by interpolation using a polynomial fit of the k_{eff} values determined at the UTXS temperatures. Problem B21 was calculated using both the standard ENDF/B-VI and UTXS libraries in order to determine the bias associated with the different nuclear data evaluations.

In addition, the UTXS libraries do not include all the nuclides in the stainless steel used in the control rods. Instead, the UTXS cases (B21, B22 and B23) used iron with a reduced density of 5 g/cm³ as was specified in the earlier version of the benchmark

problem definition [5-8]. The associated bias was determined by running problem B41 with the iron control rods for both the ENDF/B-VI and UTXS cross-section libraries.

The results for these cases are presented in Tables 5-7 and 5-8, and the differential reactivity worth of a single control rod appears in Figure 5-7. The results are based on 1 million (active) neutron histories per case, which reduced the estimated $1-\sigma$ statistical uncertainties to $\sim 0.1\%$. Twenty non-active cycles, with 5000 neutrons per cycle, were used to establish a uniform source distribution.

**Table 5-7
MCNP4B Simulation Results for HTR-10**

Case	Critical Height (h) / k_{eff} (k)	Cross Sections	Comments
B1	$h = 127.5 \text{ cm}$ $k = 1.00050 \pm 0.00089$	ENDF/B-VI	300 K; air $\sim 16,841$ spheres [†]
	$h = 128.0 \text{ cm}$ $k = 0.99964 \pm 0.00084$	ENDF/B-VI	He, 3 MPa $\sim 16,907$ spheres [†]
B2	$k = 1.12744 \pm 0.00082$ $k = 1.12605 \pm 0.00083$ $k = 1.12249 \pm 0.00087$ $k = 1.11892 \pm 0.00096$	ENDF/B-VI UTXS UTXS UTXS	300 K 300 K 450 K 558 K
B21	$k = 1.12806$	UTXS	293.15 K; polynomial fit [†]
B22	$k = 1.12446$	UTXS	393.15 K; polynomial fit
B23	$k = 1.12005$	UTXS	523.15 K; polynomial fit
B31	$k = 0.96028 \pm 0.00090$	ENDF/B-VI	$\Delta\rho_{\text{rods}} = 154.4 \text{ mk}; 300 \text{ K}$
B32	$k = 1.10588 \pm 0.00091$	ENDF/B-VI	$\Delta\rho_{\text{one}} = 14.9 \text{ mk}; 300 \text{ K}$
B41	$k = 0.85300 \pm 0.00086$ $k = 0.84764 \pm 0.00089$ $k = 0.85119 \pm 0.00090$	ENDF/B-VI ENDF/B-VI UTXS	$\Delta\rho_{\text{rods}} = 172.8 \text{ mk}; \text{s/s CR}$ Equivalent iron CRs Equivalent iron CRs

[†] $k(T) = 1.13965 + 4.22152\text{E-}05*T + 9.08699\text{E-}09*T^2$, (T in $^{\circ}\text{K}$); error not calculated.

[‡] Actual initial critical loading was 16,890 (fuel and moderator) spheres [5-3].

Table 5-8
Calculated Differential Reactivity Worth of HTR-10 Control Rod

Insertion Depth (cm)	k_{eff}	$\Delta\rho$ (mk) [†]
0.000	1.01195 ± 0.00091	0.00
111.118	1.00895 ± 0.00089	-2.94
159.818	1.00429 ± 0.00094	-7.54
163.418	1.00390 ± 0.00085	-7.92
212.118	0.99704 ± 0.00081	-14.78
213.918	0.99724 ± 0.00086	-14.58
215.718	0.99611 ± 0.00087	-15.71
217.518	0.99565 ± 0.00085	-16.18
264.418	0.99497 ± 0.00087	-16.86

[†] $\text{mk} = 1000 \times \Delta k/k$

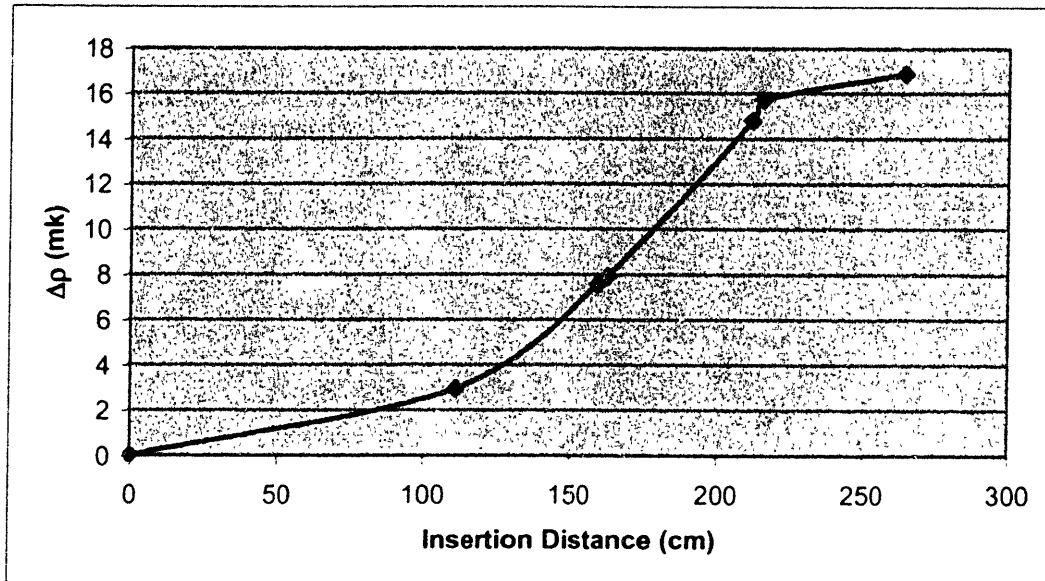


Figure 5-8. Calculated Differential Reactivity Worth of a Control Rod

5.6. Discussion

Tables 5-9 and 5-10 summarize the preliminary HTR-10 physics benchmark results reported at the IAEA Research Coordination Meeting for the Coordinated Research Project on the "Evaluation of High Temperature Gas-Cooled Reactor Performance," held

October 18-22, 1999, in Beijing [5-1]. Both diffusion-code and MCNP results calculated by several international organizations are shown.

There is considerable uncertainty in the prediction of the initial critical loading with MCNP4B, because of the approximations needed to account for the partial spheres at core boundaries. The approach followed at MIT has been to model the pebble bed as accurately as possible within the limitations of the regular lattice representation of the irregularly packed core. However, the randomness of the core also leads to the cancellation of errors, which allows coarser approximations. For example, the MCNP4A model developed at INET uses a simple hexagonal lattice and ignores partial spheres; the smaller packing fraction and the more leaky core appear to compensate for the additional fuel.

Table 5-9
Diffusion Code Benchmark Results by Other CRP-5 Participants

Case	China ¹	Indonesia/Japan ²	Russia ³	Comments
B1	125.81 cm	107.0 cm	179.6 cm	Critical height
B21	1.1197	1.2193	1.0290	k-eff 20°C
B22	1.1104	1.1983	1.0112	k-eff 120°C
B23	1.0956	1.1748	0.9938	k-eff 250°C
B31	152.4 mk	—	146.6 mk	All CRs - full core
B32	—	—	—	CR1 - full core
B41	182.7 mk	—	—	All CRs - 126 cm
B42	16.2 mk	—	—	CR1 - 126 cm

¹VSOP [5-9]; ²DELIGHT/CITATION-1000VP [5-10, 5-11]; ³WIMS-D4/JAR [5-12]

Table 5-10
MCNP Benchmark Results for Other Participants and MIT

Case	China ¹	Russia ²	MIT ³	Comments
B1	126.116 cm 16,821	164.6 cm —	127.5 cm 16,890	Critical height Critical loading
B21	—	1.0364 ± 0.0008	1.1261 ± 0.0008 ⁽⁴⁾	k-eff 20°C
B22	—	1.0198 ± 0.0008	1.1225 ± 0.0009 ⁽⁴⁾	k-eff 120°C
B23	—	1.0005 ± 0.0009	1.1189 ± 0.0010 ⁽⁴⁾	k-eff 250°C
B31	165.6 mk	167.1 mk	155.9 mk	All CRs - full core
B32	14.1 mk	—	—	CR1 - full core
B41	193.6 mk	—	181.2 mk	All CRs - 126 cm
B42	17.9 mk	—	16.9 mk	CR1 - 126 cm

¹MCNP4A and ENDF/B-V; ²MCNP4A and ENDF/B-VI; ³MCNP4B and ENDF/B-VI (⁴UTXS).

There is clearly large variation in the overall benchmark results. Nevertheless, there is excellent agreement between the MIT criticality calculations using MCNP4B and the VSOP predictions at INET. This lends credibility to the MIT modeling approach because VSOP had been previously validated through usage at the AVR and THTR. However, the absence of planned flux measurements in the HTR-10 reflector precludes the opportunity to test the ability of MCNP4B to model deep neutron penetration in graphite.

The analysis of the HTR-10 initial core using MCNP has identified several deficiencies in the definition of the physics benchmark problem. The isotopic composition of natural boron in the graphite moderator and reflector has not been specified. Similar uncertainty is believed to be the main reason for the inaccurate prediction of initial criticality in the Japanese HTTR reactor. Insufficient information is provided on the design of the control rods, specifically the stainless-steel joints and the drive shaft. The presence of the control rods is completely ignored in the INET reference model, because the all-rods-out case is simulated in VSOP using a region with low density (homogenized graphite plus void).

An increase in the temperature of the reflector is expected to reduce the reactivity of the core, because the decrease in the graphite density would reduce the number of thermal neutrons scattered back into to the core. This effect was investigated for benchmark problem B23 by assuming a uniform expansion of the graphite reflector corresponding to an increase in temperature from 27°C to 285°C. The resulting decrease in reactivity of approximately 0.1% $\Delta k/k$ is inconsequential.

Finally, criticality calculations using the University of Texas at Austin cross-section library (UTXS) were found to differ from the corresponding results obtained with standard ENDF/B-VI data. The UTXS-derived results are approximately 0.14 to 0.49 % $\Delta k/k$ more reactive, with the worst agreement (0.49% $\Delta k/k$) observed for benchmark problem B41 in which all ten control-rods were fully inserted. The use of reduced-density iron instead of stainless steel for the control-rod sleeves appears to be an acceptable approximation, the reactivity difference being less than 0.1% $\Delta k/k$.

5.7 **Summary**

The MCNP4B modelling methodology described in the previous chapters was applied successfully to the HTR-10 start-up core. This work was performed at MIT as part of the US contribution to the IAEA Coordinated Research Program on the evaluation of HTGR performance. The predicted initial critical loading agreed with the actual loading within 0.3% (16,841 total spheres *versus* 16,890 measured). Measured control-rod reactivity worths were not available at this report's writing time; however, the values calculated with MCNP4B agree well with VSOP predictions reported by INET.

6. THE ASTRA CRITICAL FACILITY

A single fuelled zone, a binary mix of fuel and moderator spheres, and a circular core characterized the core configurations analyzed in the previous two chapters. A much more complicated situation is encountered in the core design of the Pebble Bed Modular Reactor (PBMR), which includes an inner reflector region made of moderator spheres and a transition zone between the pure moderator and fuel zones [6-1]. Because this represents a significant departure from other pebble-bed core designs, a set of critical experiments were commissioned by PBMR (Pty) Limited in the ASTRA facility at the Russian Research Centre–Kurchatov Institute, Moscow, on a mock-up of the annular PBMR core [6-2]. The MCNP4B analysis of these experiments is the subject of this chapter.

6.1 Description of the ASTRA Facility

The ASTRA facility consists of a graphite cylinder with an outer diameter of 380 cm and a height of 460 cm [6-3]. This graphite structure, which serves as both the radial and lower reflectors, surrounds an octagonal core that is located 40 cm above the bottom and with an equivalent outer diameter of 181 cm. The core was loaded stochastically with fuel, moderator and absorber spheres. A special rig was used to ensure a clear separation between an inner reflector zone, a mixed fuel and moderator zone, and an outer fuel zone [6-4]. The procedure used to fill the core resulted in random dense loading with a packing fraction of 0.636. Experiments were performed both with and without an upper reflector. The unreflected critical core height was determined to be 269 cm, which yields a height-

to-radius ratio of 3. A horizontal cross-sectional view of the facility is shown in Figure 6-1, while a vertical cross-sectional view appears in Figure 6-2.

Absorber spheres were added to fuel spheres in the ratio of 5 to 95 to compensate for the relatively high uranium enrichment (21% ^{235}U) used in the fuel spheres. The absorber spheres consisted of boron-carbide kernels embedded in a graphite matrix. Thus, the transition zone contained a 50:47.5:2.5 mixture of moderator spheres (MS), fuel spheres (FS) and absorber spheres (AS) spheres. The impurities in the graphite of the spherical elements were specified by an equivalent natural-boron content of 1 ppm (by weight). Details on the core loading and the various types of spheres appear in Tables 6-1 and 6-2 [6-3].

Table 6-1
ASTRA Core Specifications

<i>Item</i>	<i>Value (cm)</i>
Inside radius of inner reflector zone	5.25
Outside radius of inner reflector zone	36.25
Outside radius of mixed zone	52.75
Corner points of core octagon	(87.5, 37.5), (37.5, 87.5), (-37.5, 87.5) (-87.5, 37.5), (-87.5, -37.5), (-37.5, -87.5) (37.5, -87.5), (87.5, -37.5)
Average packing fraction	0.636
Relative amounts of fuel and absorber spheres in fuel zone	95/5
Relative amounts of moderator, fuel and absorber spheres in mixed zone	50/47.5/27.5

The facility has a large number of channels to accommodate control and shutoff absorbers, instruments and sources. The radial reflector consists of individual graphite blocks (25 cm \times 25 cm \times 460 cm) each with a 5.7 cm-radius axial channel, which can be

sealed using a graphite plug. There are five steel-clad boron-carbide control rods, eight similar shutoff rods and one aluminum regulating-rod.

**Table 6-2
ASTRA Spherical Elements**

<i>Sphere Type</i>	<i>Outer Radius (cm)</i>	<i>Fill Radius (cm)</i>	<i>Density of Graphite (g/cm³)</i>	<i>Loading (g/sphere)</i>
MS	3.0	—	1.68	—
FS	3.0	2.5	1.85	2.44 U
AS	3.0	2.5	1.75	0.1 B

The Kurchatov Institute has to date provided only limited details on the geometry of these absorber rods. The control and shutoff rods consist of two sets of 15 half-height (187.5 cm) steel tubes arranged in a circle (7.6 cm radius) and held together by a spider (see Figure 6-3). The tubes contain boron carbide (B_4C) powder whose density is 1.53 g/cm³. The overall height of the control-rod assembly is 389.9 cm. A hollow aluminum cylinder serves as the manual regulating-rod (see Figure 6-4). Specifications for the control and shutoff rods appear in Reference 6-3. The composition of the regulating rod appears in Table 6-3.

**Table 6-3
ASTRA Regulating Rod Material Specification**

<i>Element</i>	<i>Wt. %</i>
Cu	0.1 – 0.5
Zn	≥ 0.2
Si	0.5 – 1.2
Cr	0.25
Mn	0.15 – 0.35
Fe	0.5
Al	Remainder

There are six vertical experimental tubes that extend the entire height of the core: a large aluminum tube in the centre of the reflector with an inner radius of 5 cm; and five small aluminum tubes, with an inner radius of 0.5 cm, which are located in line radially 5.5 cm, 25 cm, 45 cm, 65 cm and 80 cm from the centre of the core. Four additional small experimental channels are located in the reflector along the same radial line as the in-pile tubes.

6.2 Description of Experiments Performed at ASTRA Facility

A large number of experiments were carried out on the annular pebble-bed core in the ASTRA critical facility. The goal of these experiments was to generate data suitable for the validation of computer codes used for the neutronic design of pebble-bed reactors.

These experiments included the following:

- Determination of the critical height for a given core loading.
- Investigation of the total reactivity worth of control rods:
 - individual control rods,
 - dependence of rod worth on radial position in the reflector,
 - interference between control rods.
- Determination of the differential reactivity worth of a control rod.
- Investigation of the effect of varying the core height on control-rod worth with and without an upper reflector.
- Measurement of the spatial distribution of relative reaction rates in the core.
- Measurement of the reactivity worth of core components.

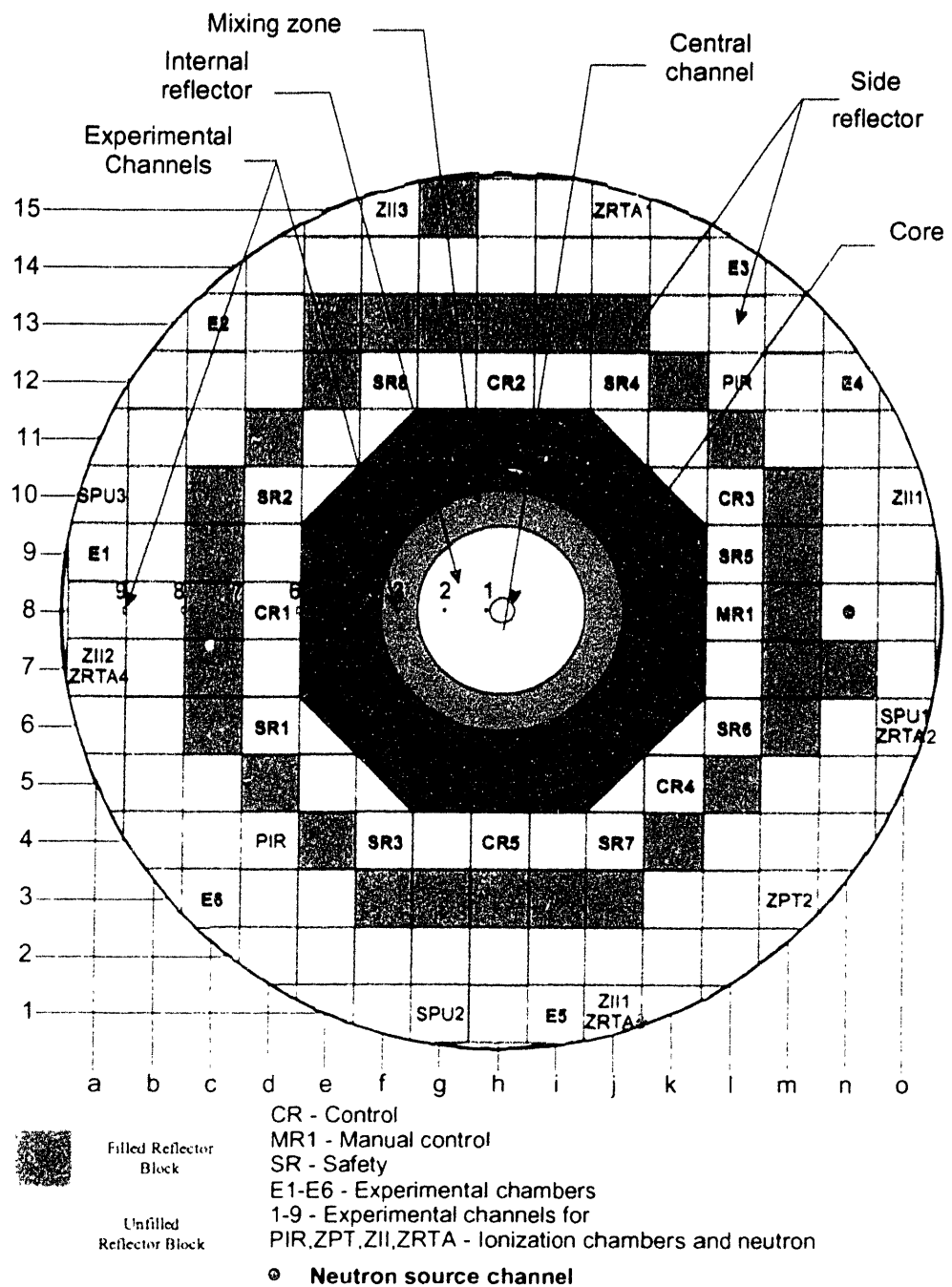


Figure 6-1. Horizontal Cross-Sectional View of ASTRA Facility [6-3]

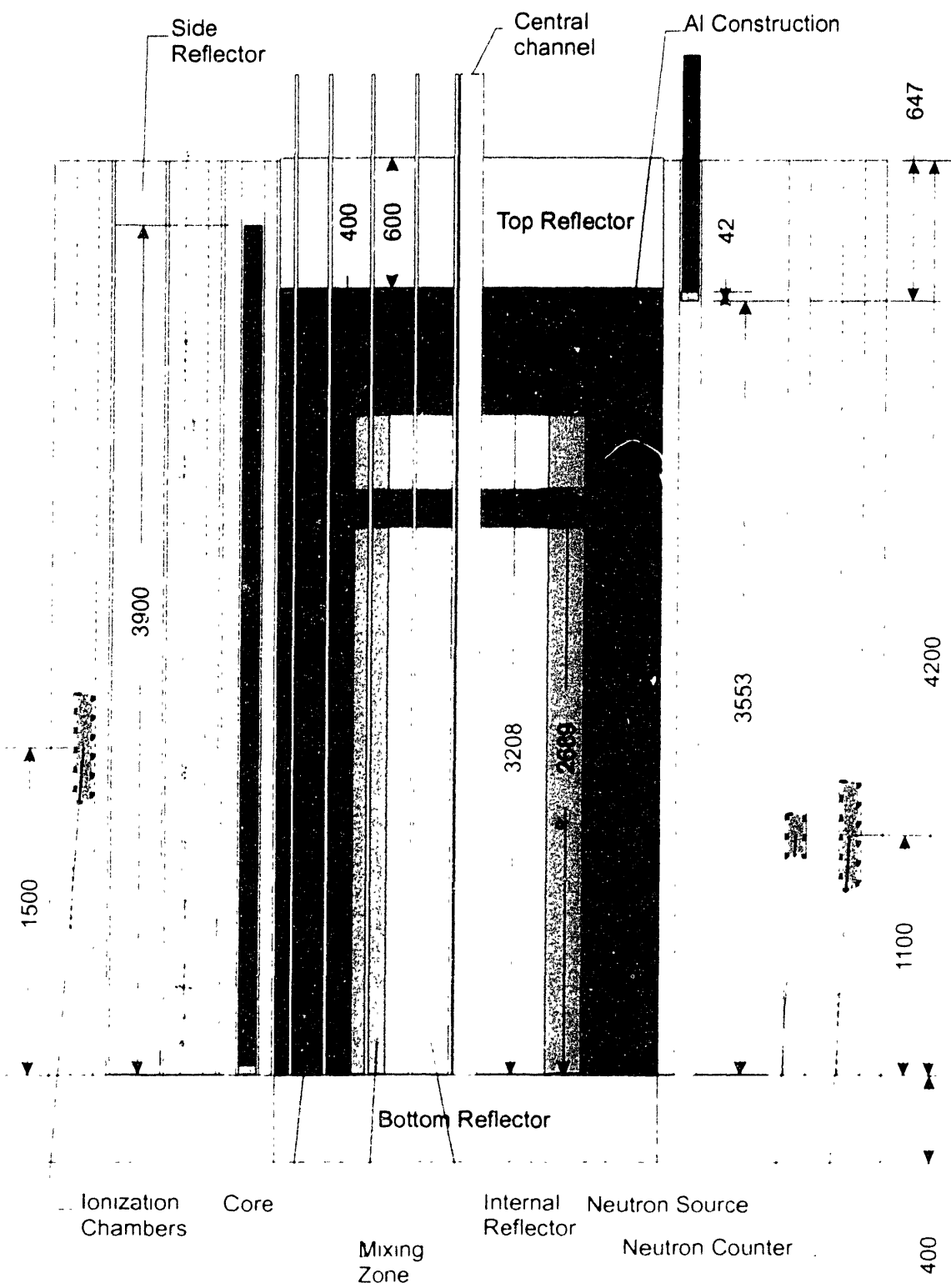


Figure 6-2 Vertical Cross-sectional View of ASTRA Facility [6-3]

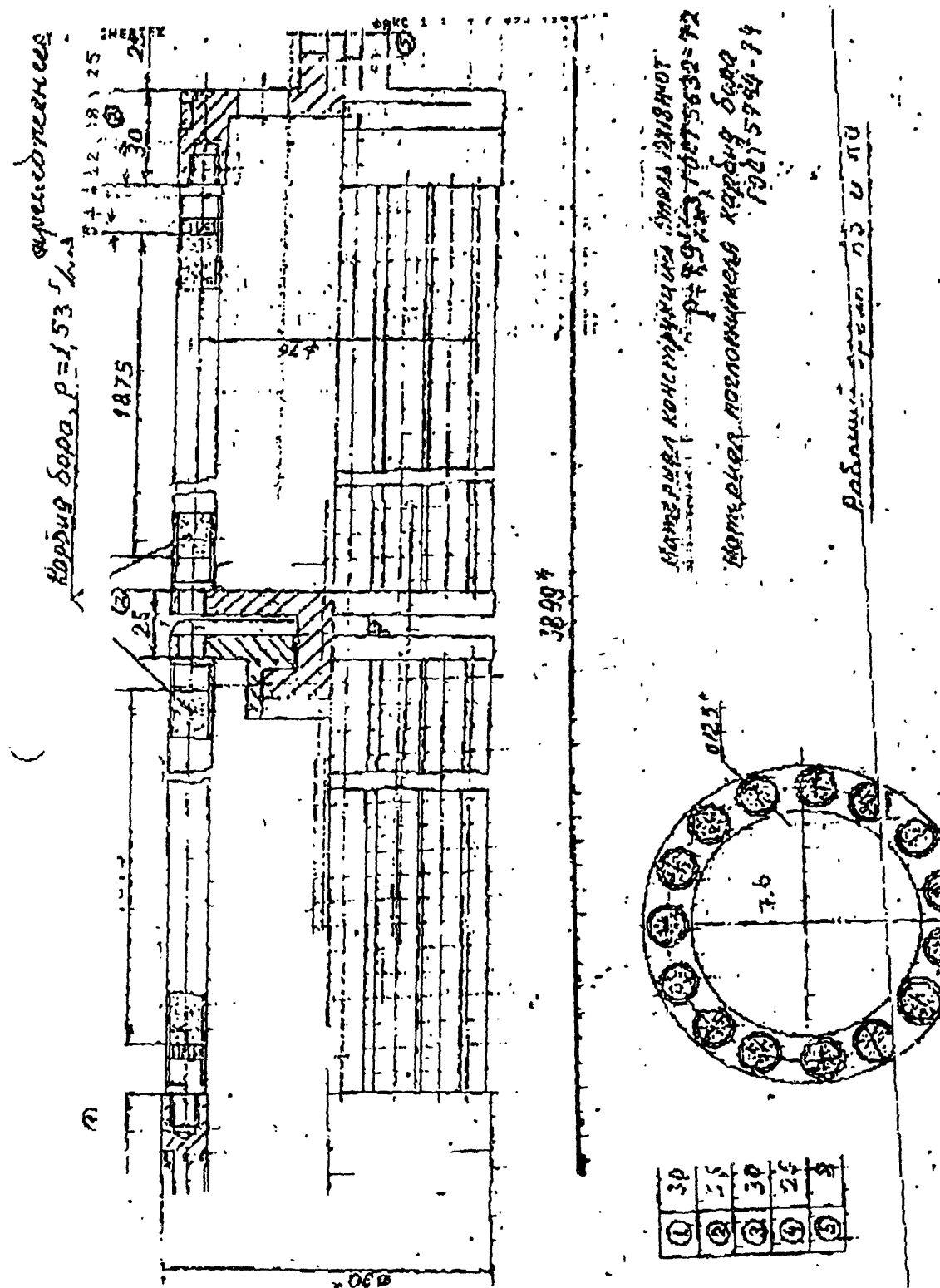


Figure 6-3. Engineering Drawing of ASTRA Control Rod

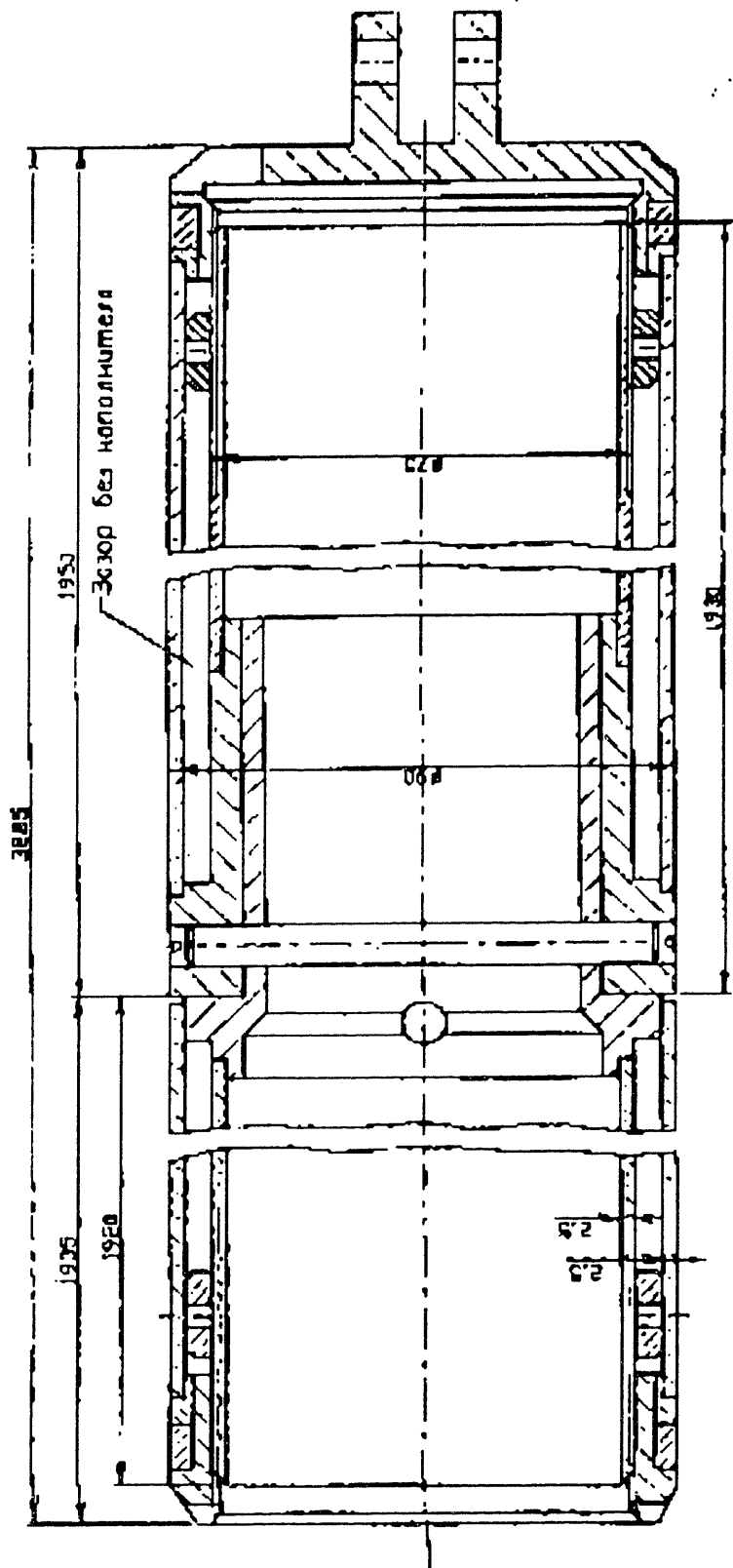


Figure 6-4. Engineering Drawing of ASTRA Manual Regulating Rod

Full details of the preliminary results of measurements and calculations may be found in References 6-4 and 6-5. As was the case for the analysis of the HTR-PROTEUS and HTR-10 in previous chapters, only experiments related to the determination of control-rod reactivity worths in the reference core are considered below [6-6]. The reactivity worths were measured using a reactivity meter based on the solution of the inverse point-kinetics equations; the accuracy of the reactivity measurement was within 0.5% β_{eff} [6-4]. Table 6-4 summarizes the basic critical configuration investigated at the ASTRA facility, which corresponds to a total of 38,584 spheres loaded according to the specifications given in Table 6-1 and without the top reflector.

**Table 6-4
Basic Critical Configuration of ASTRA Facility**

<i>Item</i>	<i>Value</i>
Number of spheres (FE/ME/AE/Total)	27,477 / 9,659 / 1,448 / 38,584
Average height of pebble bed (cm)	268.9
Position of all control rods	Fully withdrawn
Position of all shutoff rods	Fully withdrawn
Position of manual regulating rod (cm)	326.5 ± 26
Measured k-eff	1.000

6.3 MCNP4B Model of the ASTRA Facility

This section describes the model of the ASTRA facility that was developed using MCNP4B. It was possible to model the structural components of the facility very accurately, although assumptions had to be made regarding the engineering design of the control-rod assemblies. However, most of the modelling effort focused on the representation of the core. Both ‘super’ cell and simple BCC lattices were investigated.

6.3.1 Structural Components

A very detailed MCNP4B model of the ASTRA facility has been prepared, which reproduces accurately the structural components of the critical assembly (see Figure 6-5). Because documentation provided by the Kurchatov Institute did not include a complete description of the control-rod support structure, the model incorporates a hypothetical design of the assembly that holds the boron-carbide tubes (see Figures 6-6 to 6-12). In addition, no information was available on air humidity during the experiments. Therefore, the HTR-PROTEUS conditions were assumed to apply (see Chapter 4). Details of the MCNP4B model may be found in the input file in Appendix C.

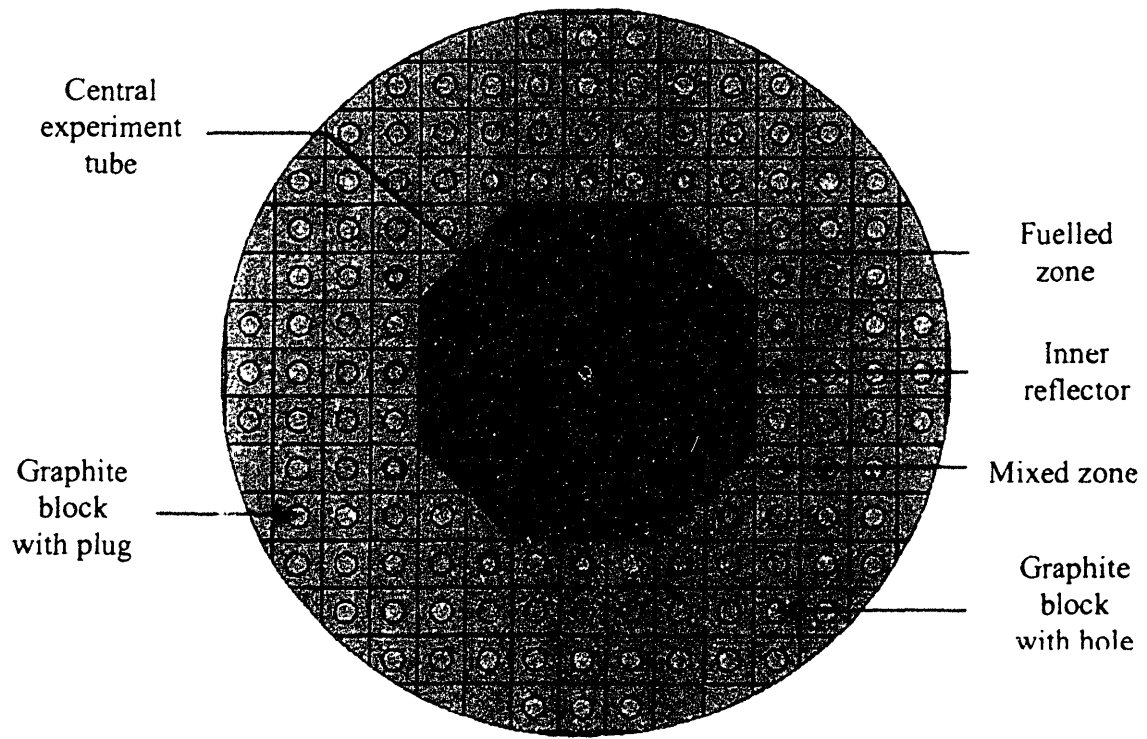


Figure 6-5. MCNP4B Model of ASTRA Facility—Horizontal View



Figure 6-6. Bottom of ASTRA Control Rod---Vertical View

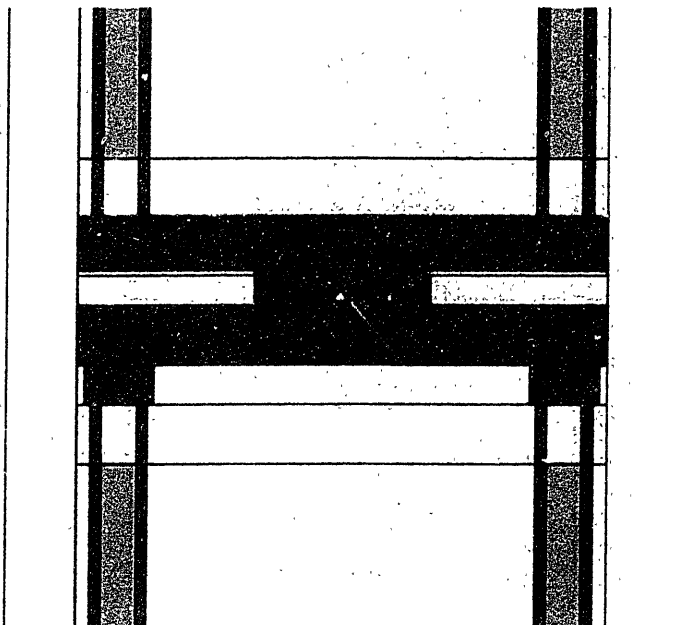


Figure 6-7. Joint Between Two Halves of ASTRA Control Rod—Vertical View

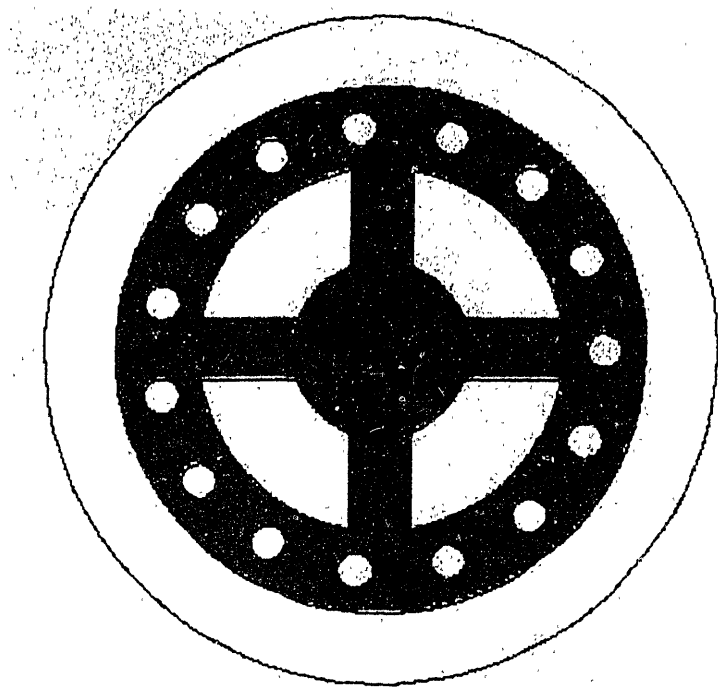


Figure 6-8. Lower Pin Holder in ASTRA Control Rod—Horizontal View

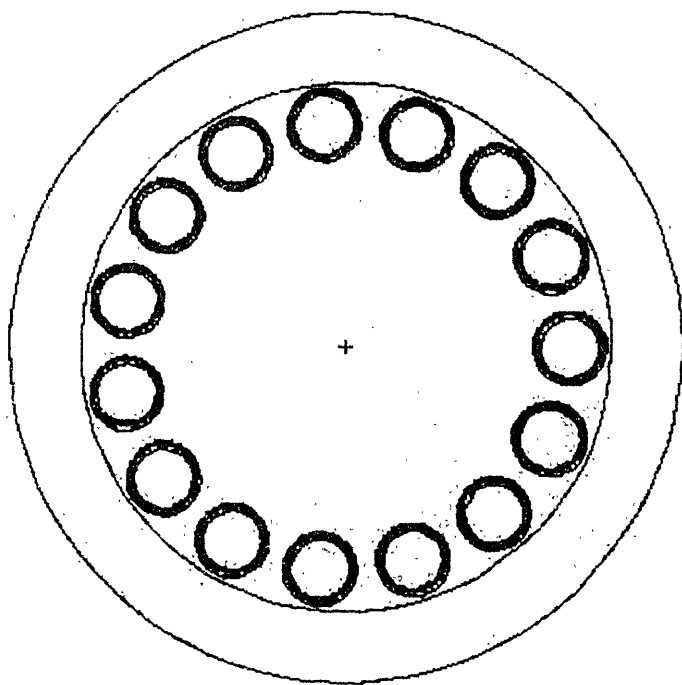


Figure 6-9. Air-Filled Section of Pins in ASTRA Control Rod--Horizontal View

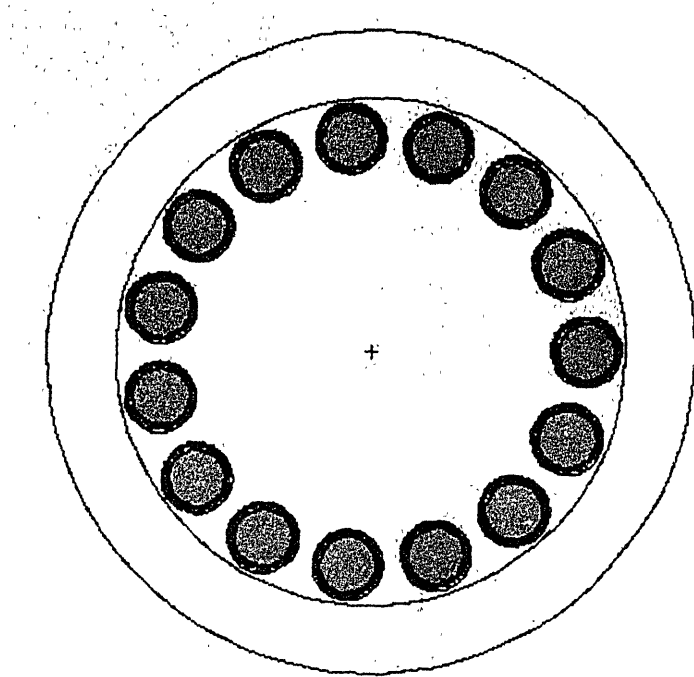


Figure 6-10. Absorber Sections of Pins in ASTRA Control Rod—Horizontal View

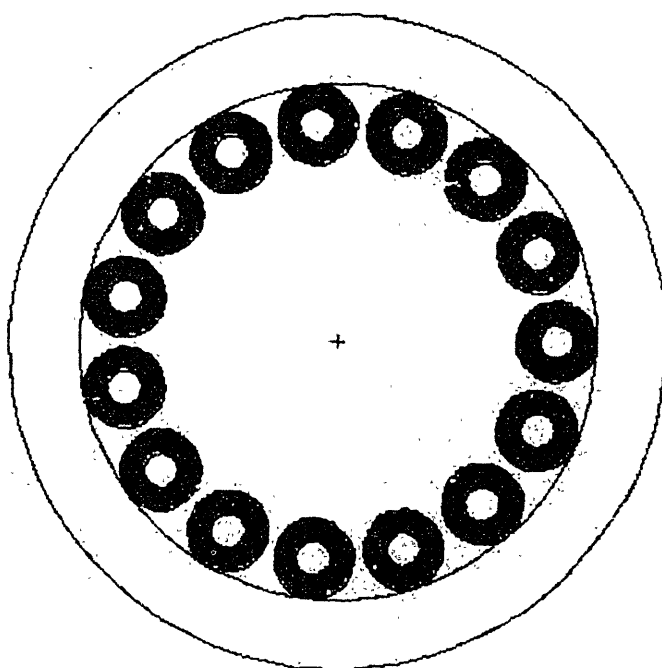


Figure 6-11. Upper Pin Holder in ASTRA Control Rod—Horizontal View

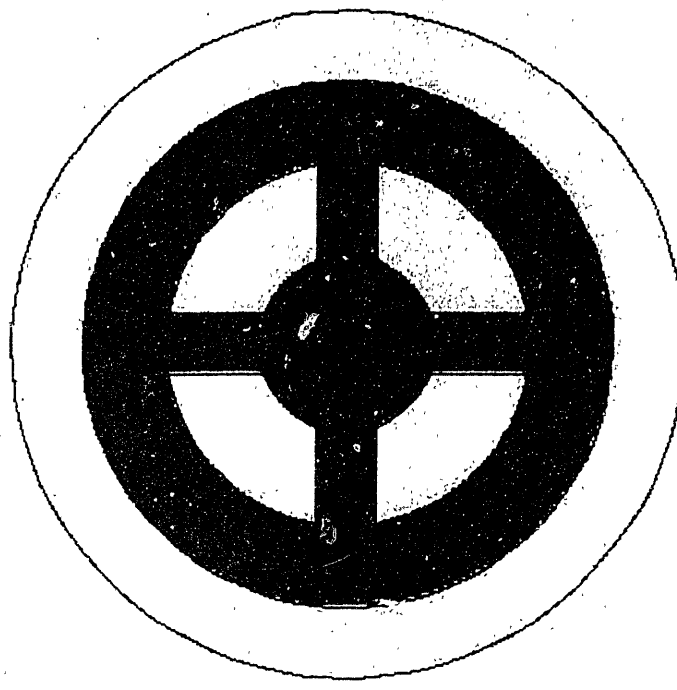


Figure 6-12. Spider at Top of ASTRA Control-Rod Assembly

6.3.2 Core

Three aspects of the ASTRA annular core must be addressed when developing the MCNP4B model. First, a regular lattice representation of the randomly packed core must be chosen that applies evenly across the three zones. The model is complicated by the presence of absorber spheres, which preclude the use of a simple BCC lattice if an exact model of these spheres is required. Second, provisions should be made for the partial spheres that arise at the periphery of the core when using the repeated-structure feature of the code. Third, the overlapping of fuel and absorber spheres at the interfaces between zones must be approximated.

The only direct representation of the mixture of moderator, fuel and absorber spheres possible is a ‘super’ cell containing 40 spheres. Such a repeating cell was constructed from $4 \times 5 = 20$ unit BCC cells, among which the three types of spheres were distributed. Other unit cells were also investigated, including hexagonal close packed (HCP) and body-centred tetragonal (BCT) lattices. A cell based on an HCP lattice proved to be too complex for the MCNP4B geometry routines. Moreover, because all the spheres in the HCP unit cell are located along the cell edges, the continuity of different types of spheres across cell boundaries cannot be guaranteed. The BCT lattice has been used successfully by others [6-7], but is characterized by two degrees of freedom—the width and height of the unit cell. This introduces a degree of arbitrariness into the model, because the choice of cell dimensions affects the core leakage. Therefore, the BCC unit cell was kept as the basis for the core representation, with the size of the cubic cell adjusted so as to reproduce the required packing fraction. The basic dimensions of the unit cell and other key parameters appear in Table 6-12.

**Table 6-5
ASTRA Core Lattice Parameters**

<i>Parameter</i>	<i>Units</i>	<i>Value</i>
Packing fraction	—	0.625
Spheres:		
Dimension of BCC unit cell	cm	3.5631775
X-axis range of supercell	cm	-7.126355 \leq x \leq 7.126355
Y-axis range of supercell	cm	-7.126355 \leq y \leq 7.126355
Z-axis range of supercell	cm	-17.8158874 \leq z \leq 17.8158874
Coated Fuel Particles:		
Dimension of SC unit cell	cm	0.124988
Absorber Kernels:		
Dimension of SC unit cell	cm	0.02072235

The repeated cell was constructed by stacking five layers of four BCC unit cells each. The loading of each unit cell depended on the core zone under consideration. Thus, in the inner reflector zone, only graphite moderator spheres appeared in the unit cells. In the fuel zone, the repeated cell consisted of eighteen fuel-only unit cells and two fuel unit cells with an absorber sphere in the centre position. The two fuel-with-absorber unit cells were located diagonally apart in the second and fourth layers of the supercell. The mixed zone repeated cell consisted of nineteen moderator unit cells with a fuel sphere in the centre position, and one moderator unit cell with an absorber sphere in the centre position. The latter unit cell was located in the third layer of the repeated cell. The exact details may be found in the MCNP4B input file in Appendix C.1, and cross-sectional views of the core appear below in Figures 6-13 to 6-15 (blue spheres are moderator, purple are fuel and green are absorber spheres).

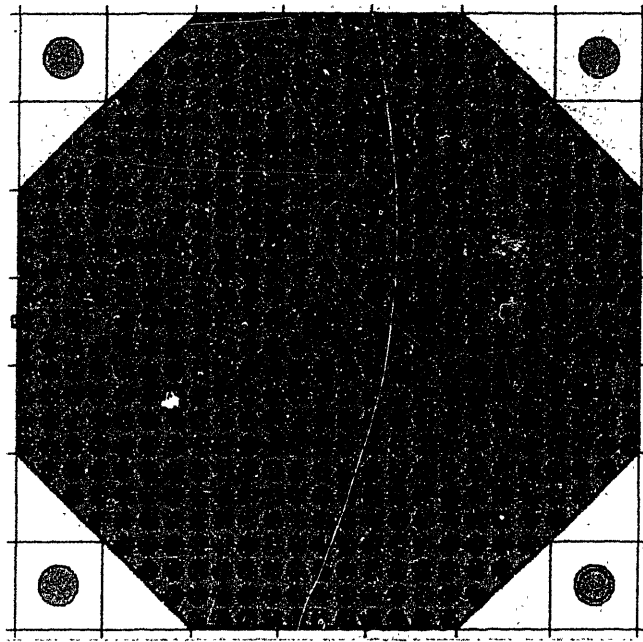


Figure 6-13. ASTRA Detailed MCNP4B Model—Horizontal View 1

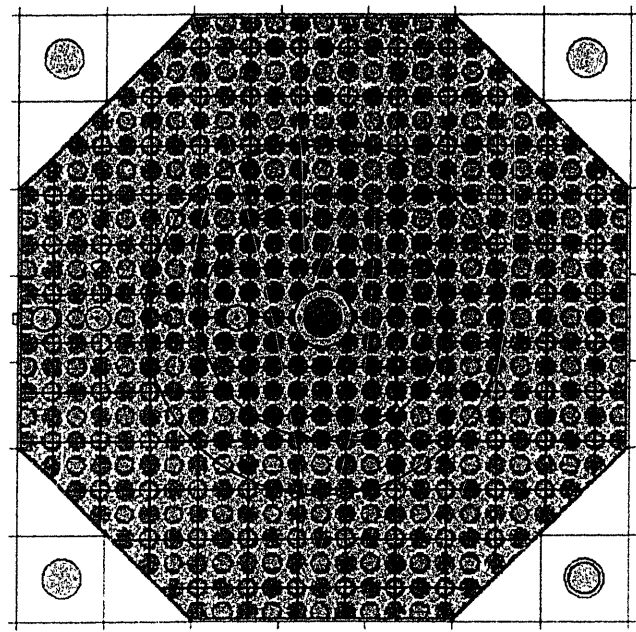


Figure 6-14. ASTRA Detailed MCNP4B Model—Horizontal View 2

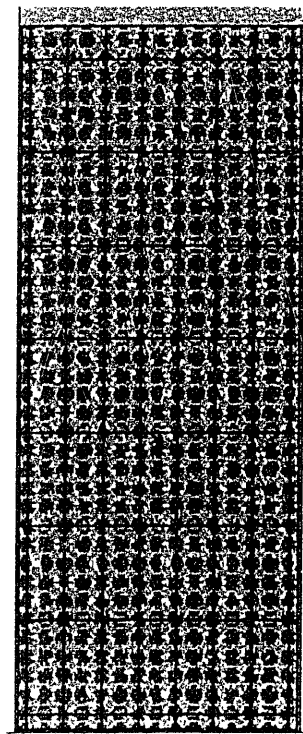


Figure 6-15. ASTRA Detailed MCNP4B Model – Vertical View

However, numerical experiments with the ‘super’ cell model have shown that the results are overly sensitive to the manner in which the absorber spheres are distributed within the repeated cell. This arbitrariness, as well as the long execution times, led to the conclusion that an approximate representation using a simple BCC unit cell with borated fuel spheres is more appropriate.

In the simplified model, the boron contained in the absorber spheres is smeared into the graphite shells of the fuel spheres (see Figures 6-16 and 6-17). Because of significant self-shielding among the boron carbide kernels, calculations were performed using infinite lattices of fuel spheres with explicitly modelled absorber spheres and borated fuel spheres. The boron concentration in the homogenized case was reduced by 17% in order to match the exact k_{∞} results, and the same borated boron composition was used in the ASTRA model. The MCNP4B model of the infinite lattice with a ‘super’ cell representation of the fuelled core region appears in Appendix C.2, that of the corresponding approximate infinite lattice in Appendix C.3, and of ASTRA with borated fuel spheres in Appendix C.4.

The octagonal shape of the ASTRA core precludes the use of an exclusion zone as a means for eliminating the contribution of partial spheres at the core boundaries (see Chapter 3). However, an alternative approach is to reduce the packing fraction of the pebble bed. The packing fraction of 0.625, which is specified in the ASTRA critical facility configuration report, already appears to include such a correction. The actual packing fraction of 0.636 can be calculated from the known core loading and volume.

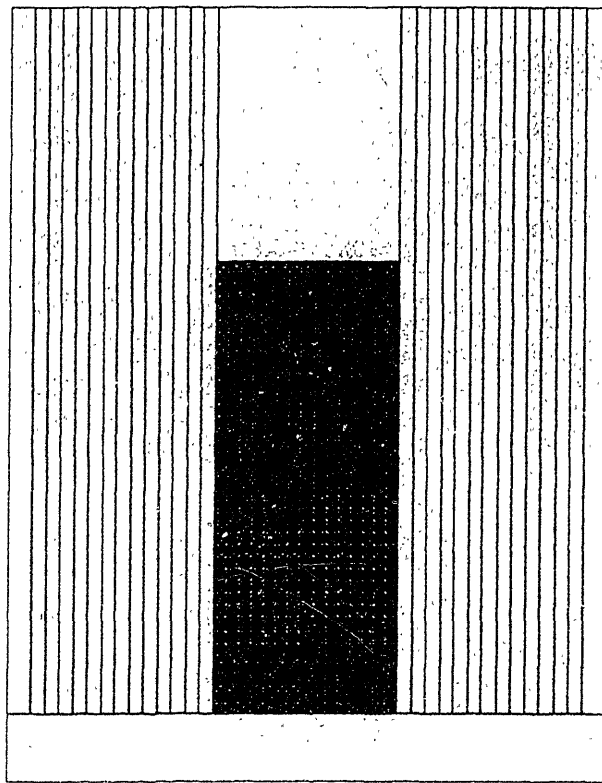


Figure 6-16. Approximate MCNP4B Model of ASTRA Facility—Vertical View

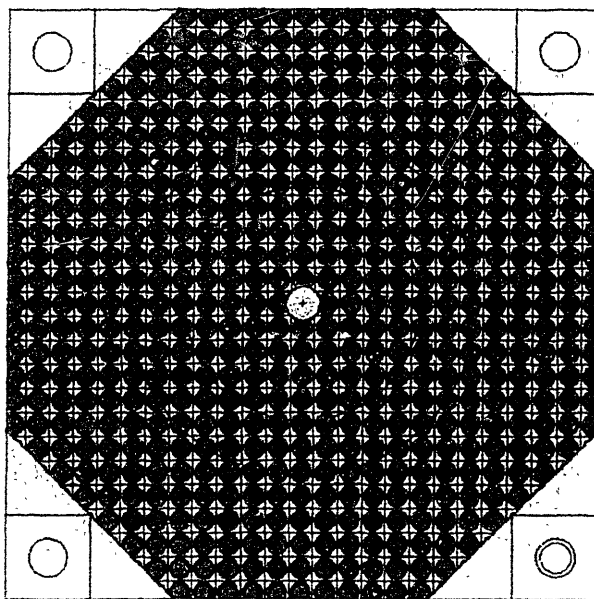


Figure 6-17. Approximate MCNP4B Model of ASTRA Facility—Horizontal View

A related modelling consideration involves the treatment of the (circular) interfaces between the core zones. Because of the overlapping of spheres and the different proportions of (borated) fuel and moderator spheres in the various zones, the boundaries between these zones should be shifted. Thus, applying the reverse approach to that used in the HTR-PROTEUS and HTR-10 models, the outer radii of the inner reflector and mixed zones are shifted inward by 1.5 cm to 34.75 cm and 51.25 cm, respectively. For example, the spheres in the fuelled zone would penetrate on average 3 cm into the mixed zone, while the fuel and absorber spheres in the mixed zone would penetrate into the fuelled zone by 1.5 cm on average. Therefore, the net inward adjustment of the interface is $3 - 1.5 = 1.5$ cm. The interface between the mixed and inner reflector zones is also shifted inwards by 1.5 cm, because of the 50% moderator sphere loading in the mixed zone. The resulting k_{eff} of the reference core confirms the validity of these modelling choices.

6.4 Results of MCNP4B Analysis

The results of the MCNP4B criticality analysis of the ASTRA core presented below were generated with the approximate model, which used fuel spheres with borated shells and no exclusion zones. The effective multiplication constant (k_{eff}) for the reference critical height of 268.9 cm was calculated to be 0.99977 ± 0.00082 with all the absorber rods fully withdrawn. All cases were run for a total of 1 million active histories from a source file generated in a separate run. The reactivity worths of individual control rods are given in Table 6-6, pairs of rods in Table 6-7, and combinations of three rods in Table 6-8. The differential reactivity worth of control rod CR5 appears in Table 6-9 and Figure 6-18.

Table 6-6
Individual Control Rod Worths in ASTRA Facility

<i>Control Rod</i>	<i>Reflector Position</i>	<i>Reactivity Worth (% Δk/k)</i>	
		<i>Measured</i>	<i>Calculated</i>
CR1	D8	-1.77 ± 0.01	-1.72 ± 0.11
CR2	H12	-1.84 ± 0.01	-1.89 ± 0.11
CR4	K5	-1.40 ± 0.01	-1.56 ± 0.11
CR5	H14	-1.83 ± 0.01	-2.01 ± 0.12
MR1	I8	-0.372 ± 0.002	-0.11 ± 0.12

Table 6-7
Reactivity Worth of Two-Rod Combinations in ASTRA

<i>Control Rods</i>	<i>Reactivity Worth (% Δk/k)</i>	
	<i>Measured</i>	<i>Calculated</i>
CR1 + CR5	-3.72 ± 0.019	-3.73 ± 0.12
CR2 + CR5	-4.01 ± 0.020	-3.97 ± 0.12
CR4 + CR5	-3.11 ± 0.016	-3.14 ± 0.12

Table 6-8
Reactivity Worths of Three-Rod Combinations in ASTRA

<i>Control Rods</i>	<i>Reactivity Worth (% Δk/k)</i>	
	<i>Measured</i>	<i>Calculated</i>
CR1 + CR2 + CR5	-6.06 ± 0.030	-6.15 ± 0.13
CR1 + CR4 + CR5	-5.16 ± 0.026	-5.36 ± 0.12
CR2 + CR4 + CR5	-5.45 ± 0.027	-5.41 ± 0.13

Table 6-9
Differential Worth of ASTRA Control Rod CR5

Control Rod Position	Control Rod Insertion (cm)	Reactivity Worth (% $\Delta k/k$)	
		Measured	Calculated
1	0	0	0
2	128.1	-0.0806 ± 0.0004	-0.150 ± 0.120
3	145.6	-0.149 ± 0.001	-0.234 ± 0.121
4	181.2	-0.384 ± 0.002	-0.458 ± 0.117
5	198.6	-0.545 ± 0.003	-0.759 ± 0.112
6	224.7	-0.823 ± 0.004	-0.912 ± 0.118
7	244.9	-1.058 ± 0.005	-1.248 ± 0.120
8	261.6	-1.251 ± 0.006	-1.439 ± 0.123
9	276.9	-1.404 ± 0.007	-1.525 ± 0.116
10	284.4	-1.488 ± 0.007	-1.552 ± 0.119
11	300.5	-1.622 ± 0.008	-1.765 ± 0.119
12	342.7	-1.831 ± 0.009	-2.006 ± 0.118

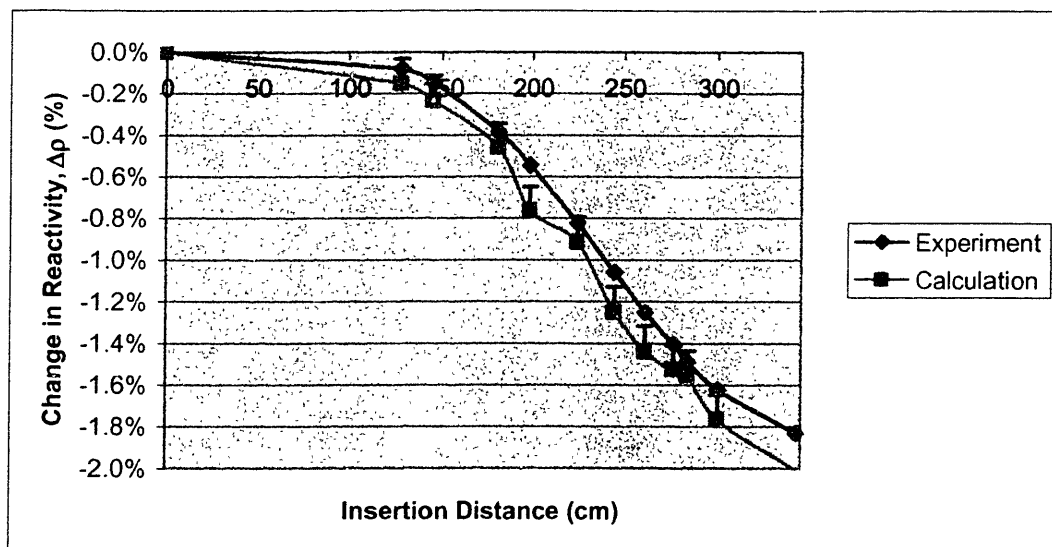


Figure 6-18. Differential Worth of ASTRA Control Rod CR5

The radial position dependence of the reactivity worths of control rods CR2 and CR4 is given in Table 6-10. Shown in the table are the reflector positions of the control rods and the distance from the core boundary.

Table 6-10
Dependence of ASTRA Control Rod Worth on Distance from Core

<i>Control Rod</i>	<i>Reflector Position</i>	<i>Distance (cm)</i>	<i>Reactivity Worth (%) $\Delta k/k$)</i>	
			<i>Measured[†]</i>	<i>Calculated</i>
CR2	H12	12.5	-1.80	-1.89 ± 0.11
CR2	H13	37.5	-0.63	-0.76 ± 0.11
CR2	H14	62.5	-0.16	-0.12 ± 0.11
CR2	H15	87.5	-0.02	-0.03 ± 0.11
CR4	K5	17.7	-1.40	-1.56 ± 0.11
CR4	L4	53.0	-0.25	-0.29 ± 0.12

[†] The relative error is 2.5% ($\beta_{\text{eff}} = 0.0072 \pm 0.0002$).

6.5 Discussion

The ASTRA critical experiments have highlighted the limitations of applying MCNP4B to the modeling of pebble-bed reactors. The ASTRA core has the following features, which were not found in the HTR-PROTEUS facility or the HTR-10 reactor: (a) an octagonal core vessel; (b) absorber spheres that make up 5% of the fuelled portion of the core; and (c) an annular core. Polygonal cores are not common in actual reactor designs, but absorber spheres may be required in start-up cores.

The octagonal core precluded the inclusion of a buffer zone to compensate for the appearance of partial spheres at core boundaries, and a reduced packing fraction (given by the experimenters) was used instead. The procedure used by the Kurchatov Institute to estimate the reduced packing fraction is unknown, but the resulting model correctly predicted the critical height of the core.

However, the mixing of absorber spheres with the fuel spheres complicated the construction of an exact core model considerably. The effective multiplication constant of

the core was found to depend strongly on the manner in which the relatively small number of absorber spheres was distributed in the core lattice, especially in the narrow mixed zone where the required ratio of absorber to fuel spheres is more difficult to realize because of boundary effects. The resulting variability in k_{eff} ($\sim \pm 1\% \Delta k/k$) and the long running time (~ 24 h) of the detailed model led to the development of a more approximate but equally accurate model, in which the boron from the boron carbide kernels was dispersed in the graphite shells of the fuel spheres.

Because dispersed boron leads to more absorptions than lumped boron carbide, its effective atom density should be reduced by an appropriate amount. The need for this correction can be demonstrated by considering the optical path of a neutron in the absorber sphere. For a spherical B_4C kernel with a diameter of 30 μm , the average chord length is $l_0 = \frac{4V_0}{S_0} = 0.002$ cm. The optical thickness for a single kernel is

$$\tau_0 = \Sigma_a l_0 = (83.45)(0.002) \approx 0.17,$$

and the thermal flux depression in the absorber kernel relative to the moderator is approximately given by the semi-empirical correlation

$$\frac{\bar{\phi}_m}{\bar{\phi}_a} \approx 0.87\tau_0 + \exp(-0.35\tau_0) \approx 1.09$$

[6-8]. As noted earlier, the actual atom density

correction of 17% was deduced from direct numerical experiments.

The annular core appears to pose a more serious computational challenge for MCNP4B partly because of the fuzzy interfaces between core zones, but also because of the greater neutronic decoupling caused by the large central reflector region and the presence of boron absorber among the fuel spheres. The decoupling was evident from the sensitivity of the MCNP4B results on the definition of starting fission source and the number of

neutron histories used to determine the effective multiplication constant. This possibly explains the differences observed in the reactivity worths of the symmetrically positioned control rods CR2 and CR5. There appears to be a flux tilt across the core, which changed the reactivity worths of CR4 and CR5 by ~10%, CR2 by 2.72% and CR1 by -2.82%. Other deviations between the calculated and measured reactivity worths are related to the uncertain design of the control rods and the manual regulating rod, which show up as biases of ~0.15% $\Delta k/k$ (see Figure 6-14) and 0.27% $\Delta k/k$, respectively.

Values of the interference coefficient ξ for the two-rod and three-rod combinations can be calculated from the results in Tables 6-6 to 6-8. The interference coefficient is defined as $\xi = \Delta R / \sum_{i=1}^n \rho_i$, where ΔR is the total reactivity worth of the entire rod system, ρ_i is the worth of control rod i , and n is the number of control rods in the system [6-4]. The results are presented in Table 6-11.

Table 6-11
Interference Coefficients for ASTRA Rod Combinations

<i>Control Rods</i>	ξ	
	<i>Measured</i>	<i>Calculated</i>
CR1 + CR5	1.03	1.00
CR2 + CR5	1.09	1.02
CR4 + CR5	0.96	0.88
CR1 + CR2 + CR5	1.11	1.09
CR1 + CR4 + CR5	1.03	1.01
CR2 + CR4 + CR5	1.07	0.99

As discussed in Reference 6-4, Table 6-11 shows that a complex pattern of interference exists between the control rods in the ASTRA facility. For control rods CR2 and CR5,

which are positioned symmetrically 180° apart, the interference coefficient is greater than unity ($\xi = 1.09$). Yet for control rods CR4 and CR5, which are 45° apart, the interference coefficient is less than unity ($\xi = 0.96$). The largest interference coefficient was measured for the combination of CR1, CR2 and CR5 ($\xi = 1.11$).

6.6 Summary

A detailed MCNP4B model was developed of the PBMR mock-up in the ASTRA critical facility at the Kurchatov Institute. This is an annular core composed of an inner reflector zone, a fuelled zone with 5% absorber spheres, and a transition zone with 50% moderator, 47.5% fuel and 2.5% absorber spheres. A primitive BCC lattice represents the randomly packed core, with the boron from the absorber spheres smeared into the shells of the fuel spheres. A simple-cubic lattice is used to arrange the explicitly modelled coated fuel particles inside the fuel spheres. The model predicts the critical height of the reference core exactly (0.99977 ± 0.00082), although the more neutronically decoupled annular core appears to make the spatial flux shape sensitive to the starting fission source and number of neutron histories. As a result, the reactivity worth of some control rods was predicted only within 10% of measurement. Greater accuracy would be required before this MCNP4B methodology can be applied to the annular PBMR core.

7. MCNP4B MODELLING OF PEBBLE BED CORES WITH BURNUP

The previous chapters established a method for the MCNP modelling of pebble-bed cores with fresh fuel. However, reactor design and analysis is most frequently carried out using a core with an equilibrium burnup distribution. The isotopic composition of the fuel in most reactors can be determined using a Monte Carlo burnup code like MONTEBURNS [7-1] or MOCUP [7-2], which couple MCNP4B [7-3] to ORIGEN2 [7-4]. However, the recycling of fuel spheres in pebble-bed reactors complicates this calculation considerably, because of the continuous movement and mixing of fuel in the core. An alternative approach is presented in this chapter, which utilizes a link between MCNP4B and VSOP94 [7-5]. The fuel management routine in VSOP94 is used to establish the equilibrium core, and the program MCARDS is used to prepare the corresponding MCNP4B material cards from the nuclide atom densities of the depleted fuel that were calculated by VSOP94. This method is demonstrated on the Pebble Bed Modular Reactor.

7.1 The Pebble Bed Modular Reactor

The 268 MW(t) Pebble Bed Modular Reactor (PBMR) currently being designed in South Africa is the latest development in the continuing evolution of pebble-bed reactors [7-6]. The advantages of modular HTGRs were already recognized by the 1980s, even though higher fuel enrichments are required to compensate for greater neutron leakage [7-7]. The inherent safety of a small reactor unit (~ 200 MWt) has the potential for significant cost reductions, because of its simpler design, standardization and the elimination of a gastight containment building. Two modular pebble-bed reactors were designed and licensed in

Germany by the late 1980s: the 80 MW(e) HTR-MODUL by Siemens/Interatom [7-8] and the 100 MW(e) HTR-100 by HRB/BBC. Interest in an inner reflector surfaced in the early 1990s, with the inclusion of a central graphite column in the 500 MW(e) Advanced High Temperature Reactor [7-9]. The ability to locate control rods in the central column of the AHTR-500 eliminated the need for the THTR-style in-core rods, which had to be pressed into the pebble bed [7-10]. An annular geometry was also proposed for increasing the power of a modular pebble-bed reactor from 200 MW(t) up to 350 MW [7-11]. The flux flattening effect of the central reflector also increases the reactivity worth of control rods located in the side reflector.

The PBMR features 18 control rods and 17 small-absorber-ball shutdown channels in the static side reflector, and a moving inner reflector created by dropping only graphite moderator spheres into the centre top of the core. Vertical and horizontal cross-sectional views of the reactor are shown in Figures 7-1 and 7-2, and detailed specifications of the PBMR reference core and fuel sphere appear in Tables 7-1 and 7-2 [7-6].

Fuel spheres are dropped into the core from nine equally spaced feeders located on a circle of 164.5 cm radius, and are removed from the core through a discharge tube at the bottom of the vessel. The fuel spheres are scanned with a γ -detector to determine the burnup and are reinserted at the top if the desired discharge burnup has not been reached.

Table 7-1
PBMR Reference Core Specifications

<i>Parameter</i>	<i>Value</i>	
Thermal power rating	268	MW
Core diameter	3.5	m
Average core height	8.52	m
Average burnup	80,000	MWd/tU
Refuelling strategy	Multiple pass ($\times 10$)	
Fuel	8.13	at. % (^{235}U)
Average irradiation time of fuel	874	days
Number of fuel zones	2	
Moderation ratio (N_C/N_U)	428	
Number of fuel spheres	334,000	
Number of graphite spheres	110,000	
Percent fuel in central/mixed/fuel zones	0/50/100	
Thickness of top reflector	1.35	m
Thickness of bottom reflector	2.61	m
Width of radial zones in side reflector	6/13/22.5/19/14.5 cm	
Graphite density in top reflector	1.54	g/cm^3
Graphite density in bottom reflector	1.53	g/cm^3
Graphite density profile in side reflector	1.7/1.17/1.7/1.48/1.7 g/cm^3	

Table 7-2
Reference Specifications for PBMR Fuel Elements

<i>Parameter</i>	<i>Value</i>	
Fuel Sphere (FS):		
Pebble radius	3.0	cm
Radius of fuelled zone	2.5	cm
Uranium loading	9.0	g/FS
Graphite density	1.75	g/cm^3
Coated Fuel Particle:		
Diameter of UO_2 kernel	500	μm
Density of UO_2	10.4	g/cm^3
Coating materials	C/PyC/SiC/PyC	
Layer thicknesses	95/40/35/40 μm	
Layer densities	1.05/1.90/3.18/1.90 g/cm^3	

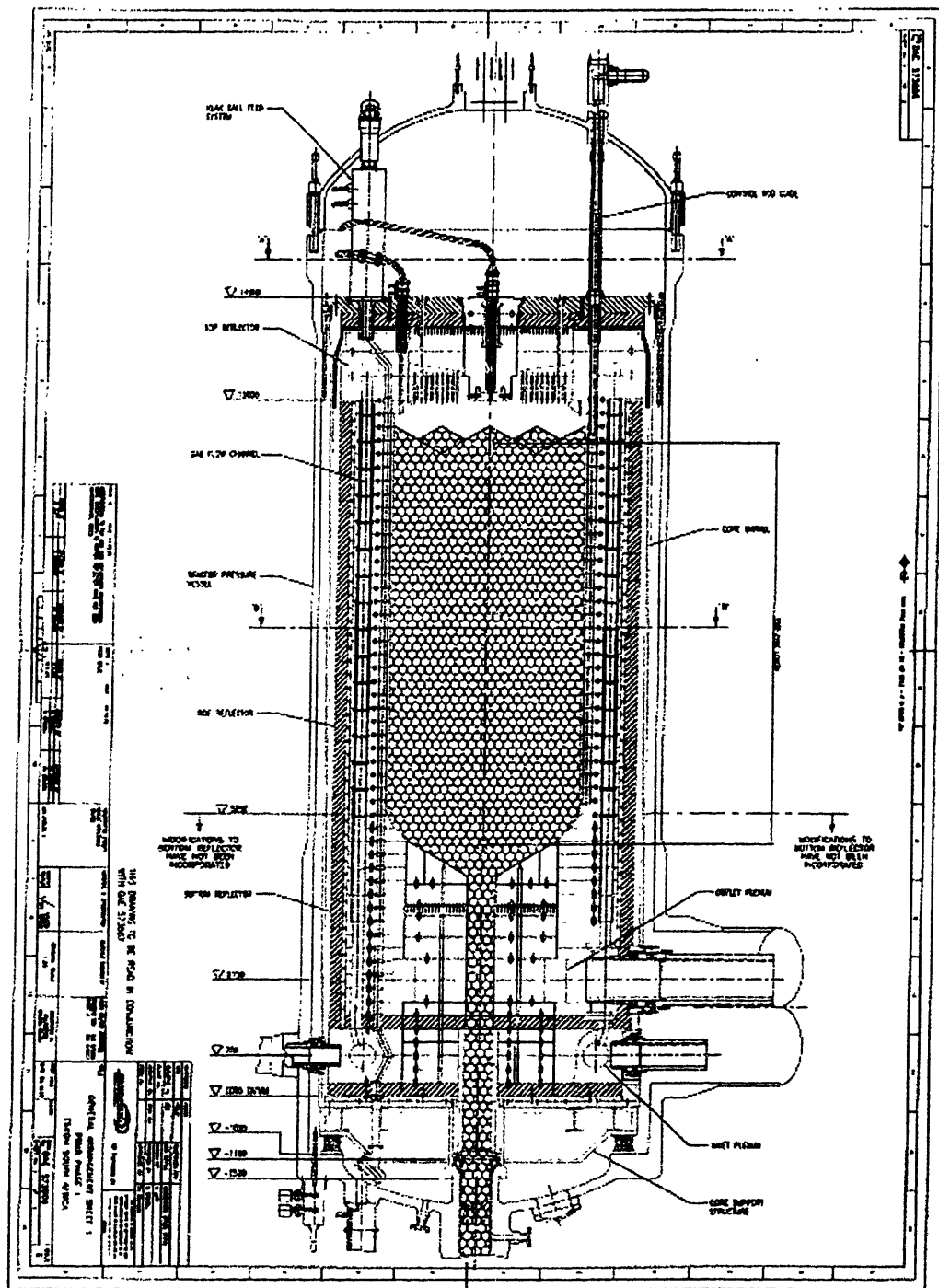


Figure 7-1. A Vertical View of the PBMR [7-6]

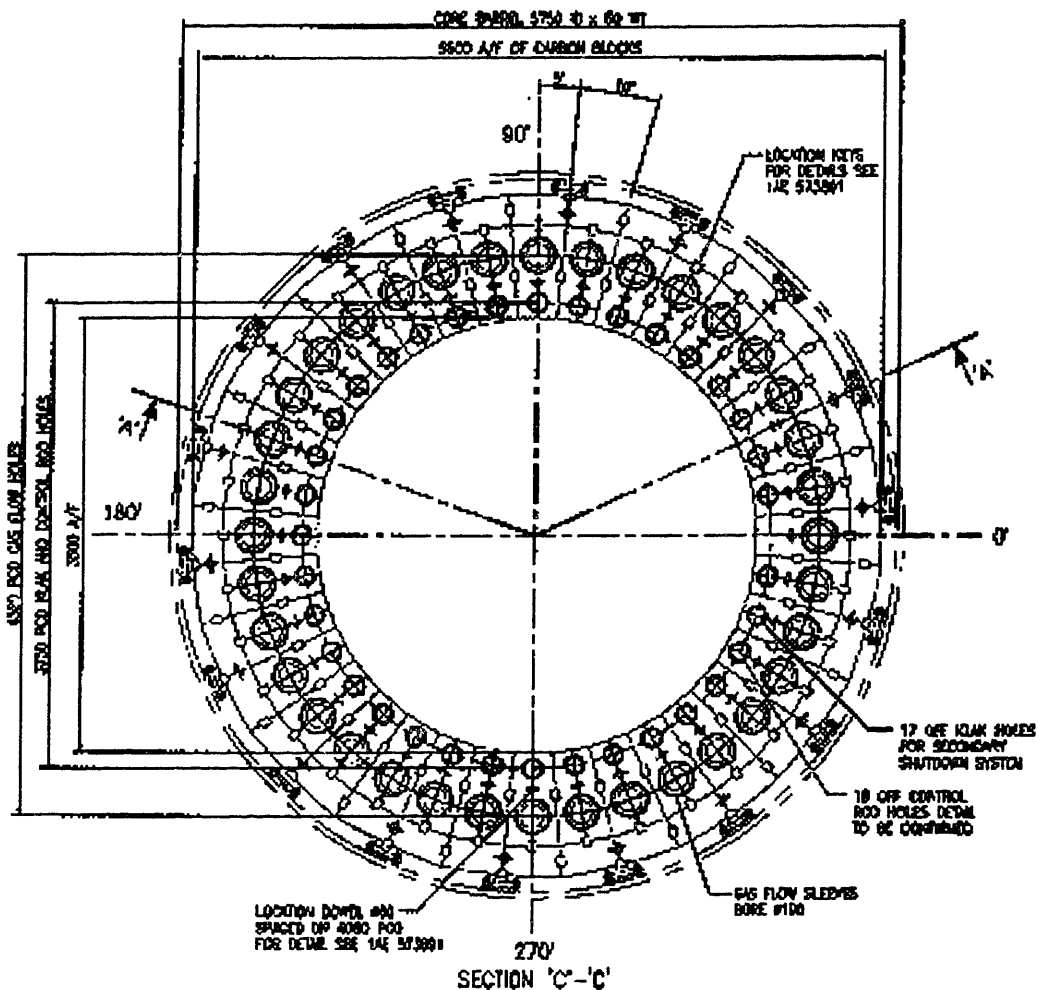


Figure 7-2. A Horizontal View of the PBMR Core [7-6]

7.2 The VSOP94 Model of the PBMR

The two-dimensional (R-Z geometry) VSOP94 model of the reference PBMR core is shown schematically in Figure 7-3 [7-6].[†] The model includes details of the core, the reflectors and the borated carbon thermal shields. The reactor pressure vessel, the core barrel and the associated helium gaps are lumped together in a single annular region. The

[†] The VSOP model of the PBMR was kindly provided by Dr. E.J. Mulder, PBMR (Pty) Limited.

control rods are modelled by homogenizing the boron carbide absorber into the surrounding graphite material. The various channels for the shutdown system and helium coolant are modelled by reducing the density of the appropriate graphite regions.

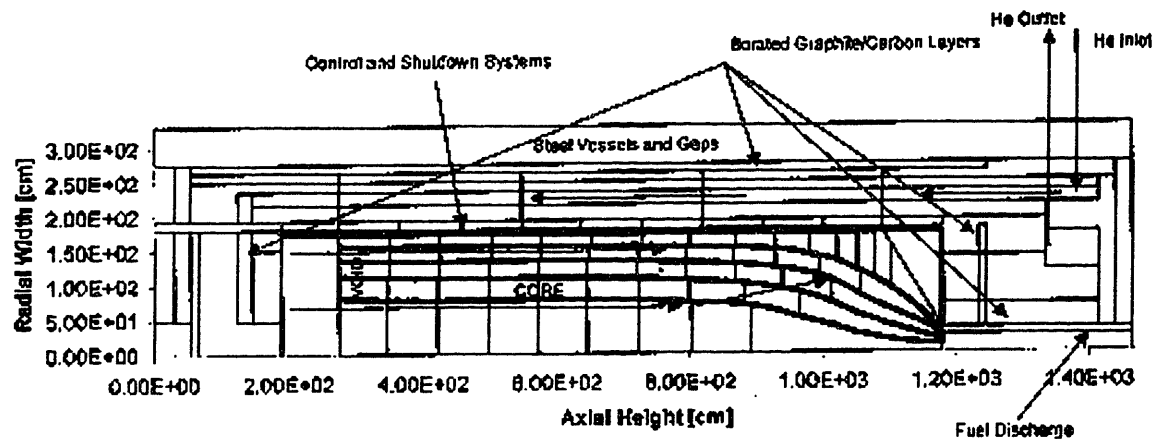


Figure 7-3. VSOP94 Model of the PBMR [7-6]

The model of the core comprises 57 equally sized regions called *layers*, each of which contains a mixture of 10 different fuel *batches*.[†] These batches represent the number of times that the fuel spheres have been through the core, from the first pass (batch 1) to the last pass (batch 10). The burnup of each batch is calculated individually using a fission-product chain of 44 isotopes (see Table 7-3). The second member of the chain is a non-saturating fission product chosen by comparison with ORIGEN-JÜL-II code predictions, which corresponds to low absorbing fission products not modeled explicitly [7-12]. The 43 explicit fission products cover 98.02% of the total fission-product absorptions, while the non-saturating fission product accounts for the remaining 1.98%.

[†] Each layer also contains an 11th batch in order to accommodate the presence of moderator spheres in the inner reflector.

Table 7-3
Fission Product Chain 44 in VSOP94

No.	Nuclide	No.	Nuclide	No.	Nuclide	No.	Nuclide
1	^{135}Xe	12	^{105}Rh	23	^{143}Pr	34	^{149}Sm
2	FP-44	13	^{105}Pd	24	^{143}Nd	35	^{150}Sm
3	^{136}Xe	14	^{108}Pd	25	^{144}Nd	36	^{151}Pm
4	^{83}Kr	15	^{109}Ag	26	^{145}Nd	37	^{151}Sm
5	^{95}Zr	16	^{113}Cd	27	^{146}Nd	38	^{152}Sm
6	^{95}Mo	17	^{131}I	28	^{147}Pm	39	^{153}Eu
7	^{97}Mo	18	^{131}Xe	29	$^{148}\text{Pm/m}$	40	^{154}Eu
8	^{99}Tc	19	^{133}Xe	30	$^{148}\text{Pm/g}$	41	^{155}Eu
9	^{101}Ru	20	^{133}Cs	31	^{147}Sm	42	^{155}Gd
10	^{103}Ru	21	^{134}Cs	32	^{148}Sm	43	^{156}Gd
11	^{103}Rh	22	^{141}Pr	33	^{149}Pm	44	^{157}Gd

Fuel depletion is modelled by means of burnup steps. Thus, approximately every 9 days, each layer and its associated batches are moved down to the position of the next layer. This movement of fuel occurs in *channels*, which are used to reproduce the characteristic flow of pebbles within the core vessel. This flow pattern was established by Pohl and Neubacher during the operation of the AVR [7-13], and from measurements performed by Kleine-Tebbe during the final defuelling of the THTR [7-14]. The layers at the bottom of the core are discharged, and corresponding batches (*i.e.*, with the same number of passes through the core) from different channels are grouped and mixed together. The batch numbers are then incremented (to initiate an additional pass through the core) and reinserted into the various channels. The oldest batches are discharged from the core, while a tenth of the volume of each top layer is filled with fresh fuel.

The neutronic calculation is performed using 29 spectral zones, which consist of user-specified groupings of layers. A similar procedure is used for the reflector regions where 25 spectrum zones are defined. The temperatures of the spectral zones are established

using the thermal-hydraulics module in VSOP94. The reference VSOP94 input file is included as Appendix D.1.

7.3 Link Between VSOP94 and MCNP4B

A convenient way to model an equilibrium pebble-bed core with MCNP4 is to perform a fuel management study with VSOP94 and transfer the resulting fuel compositions to an MCNP4B model of the same reactor. The most accurate method for establishing a link between the two codes would be to create a supercell VSOP94 model of a fuel kernel in a given layer, and deplete the fuel to the burnup determined from a separate VSOP94 fuel management study (see Section 7.6 for further details). The resulting fuel compositions could then be used in a detailed MCNP4B model of the pebble-bed core, which would include an explicit representation of the coated fuel kernels and the fuel spheres. A more approximate but direct approach is presented here, in which the nuclide densities obtained from a whole-core VSOP94 calculation are used directly in an MCNP4B model of the reactor.

An MCNP4B model of the PBMR equilibrium core was developed, which uses a regular lattice of spheres with homogenized fuel and graphite interiors. This lattice is subdivided into annular regions that reproduce exactly the core regions of the VSOP94 model. The fuel compositions used in these regions are the corresponding batch-averaged VSOP94 nuclide densities, which are adjusted to allow for the effect of fuel homogenization on resonance absorptions in ^{238}U and ^{240}Pu .

7.3.1 Modifications to VSOP94

Several modifications had to be made to VSOP94 in order to extract the necessary fuel compositions. These changes affected subroutine CH1 in chain 1 where the main problem definition data are read, and subroutine VORSHU in chain 7 where fuelling operations are simulated.

Subroutine VORSHU is called before fuel shuffling takes place. It reads instructions for the next burnup cycle, calculates average batch properties and accounts for isotope decay during the reshuffling. The subroutine was modified to calculate the total atom numbers and reaction rates for each isotope per layer, and write this information to data files FORT.98 and FORT.99, respectively. Also written to file FORT.98 is the cycle number, the layer number, the total number of all nuclides in the given layer, the volume of the layer, and the packing fraction. Two fields were added to the printout options card V21 [7-5], which specify the refuelling cycle whose fuel compositions are required. The specifications of the modified card are shown in Table 7-4, and listings of the source code are included as Appendix D.2.

7.3.2 Program MCARDS

VSOP94 output file FORT.98 contains, for each layer, the total number of all nuclides, the volume and the packing fraction. This is followed by the number of atoms for each nuclide used in the VSOP94 calculation (65 nuclides are used in the PBMR model). Output file FORT.99 contains the total absorption reaction rates that correspond to these nuclides. The FORTRAN program MCARDS reads these data and prepares an MCNP4B

material card for each layer. Because a one-to-one mapping does not exist between the nuclides available in the VSOP94 and MCNP4B libraries, ^{10}B is added such that the total absorption reaction rate in each layer is preserved. The materials cards are written consecutively to file MCARDS.DAT starting at material label M100 for the first layer with comment cards that specify the total atom density for the given layer, which can be “cut and pasted” into the MCNP4B input file. The listings of the source code are included as Appendix D.3.

7.4 MCNP4B Model of the PBMR

Because detailed engineering drawings of the PBMR were not available, the MCNP4B model was based on the two-dimensional VSOP94 model of the reactor. Key aspects of the VSOP94 model of the PBMR core and structural components were duplicated, including the pebble flow channels and layers (Figures 7-4 and 7-5).

The control rods, and the shutdown and helium coolant channels in the side reflector were modelled explicitly. However, the HTR-10 control rods described in Chapter 5 were used instead of the proprietary PBMR design (Figure 5-7). The model also uses the oval shutdown channels from the Chinese reactor (Figure 7-6). A simple BCC lattice without exclusion zones was used to represent the randomly packed pebble bed. This lattice was subdivided into layers exactly as in the VSOP94 model of the core. The spheres in each layer consisted of the homogenized mix of carbon, silicon, heavy metal and fission-product nuclides prepared with program MCARDS from the corresponding VSOP94 layer-averaged atom densities. Further details may be found in the MCNP4B input file included as Appendix D.4.

Table 7-4
Modified VSOP94 Card V21

Card V21		Format (18I4)
1	IPRIN(1)	<p>Spectrum calculation:</p> <ul style="list-style-type: none"> = 0: Thermal self shielding factors only. = 1: Same as 0, plus averaged thermal cross sections. = 2: Same as 1, plus fine-group neutron fluxes. = 3: Same as 2, plus broad-group averaged cross Sections for materials with concentration > 0. = 4: Same as 3, for all materials.
2	IPRIN(2)	<ul style="list-style-type: none"> = 0: No output. = 1: Print layout of batches before shuffling. = 2: Same as 1, plus atom densities (only in combination with IPRIN(3) ≥ 0).
3	IPRIN(3)	<p>Burnup calculation:</p> <ul style="list-style-type: none"> = -1: Global neutron balance. = 0: Detailed neutron balance. = 1: Same as 0, plus characteristic data for all fuel batches.
4	IPRIN(4)	<ul style="list-style-type: none"> = 0: Skip spectrum calculation if a set of cross sections is available. Instructions on card V22 are neglected. = 1: Repeat spectrum calculation as defined on Card V22. = 2: Same as 1, but only for the thermal spectrum. = 3: Same as 1, but not for zones without heavy metal (reflectors). = 4: Same as 2, but not for zones without heavy metal (reflectors).
5	IPRIN(5)	Cycle whose fuel compositions are to be written to file.
6	IPRIN(6)	<ul style="list-style-type: none"> = 0: Do not write fuel compositions to file. = 1: Write fuel compositions to file.

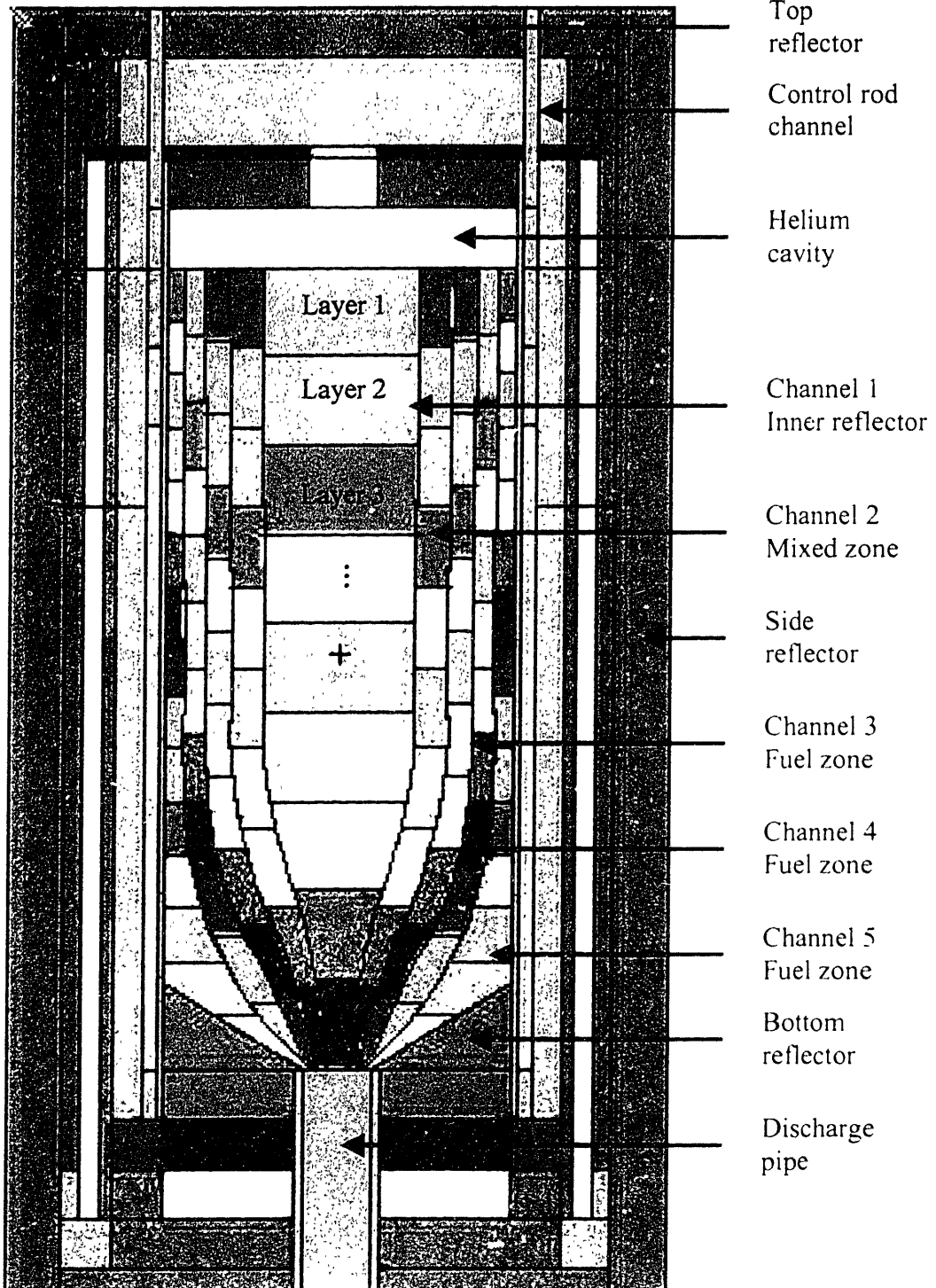


Figure 7-4. MCNP4B Model of the PBMR—Vertical View

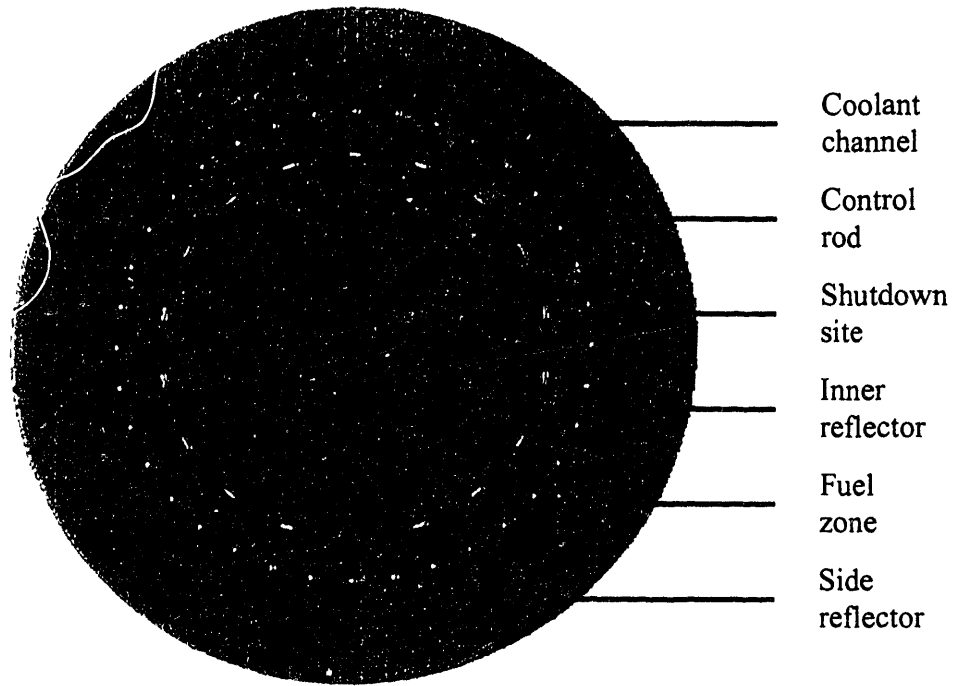


Figure 7-5. MCNP4B Model of the PBMR—Horizontal View

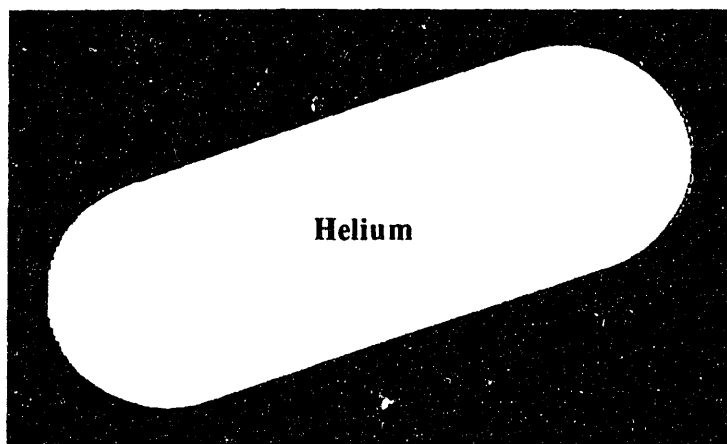


Figure 7-6. Channel for Small Absorber Balls in MCNP4B Model of PBMR

7.5 MCNP4B/VSOP94 Results

Preliminary analysis of the PBMR using the MCNP4B/VSOP94 model described above, but with unadjusted VSOP94 nuclide densities, yields an effective multiplication constant of 1.00873 ± 0.00096 . Typical core power and neutron flux distributions are shown in Figures 7-7 to 7-9 for fully homogenized layers. MCNP4B was unable to generate prompt fission power (F7) and neutron flux (F4) tallies for segments defined via an FS tally segmentation card for the detailed core. Although this result demonstrates in principle the linkage between VSOP94 and MCNP4B, further developments are needed before the method can be applied to actual reactor analysis.

VSOP94 performs the diffusion calculations on homogenized regions of the core, with self-shielding factors used to correct for double heterogeneity and a diffusion correction to allow for neutron streaming in core voids (see Chapter 2). Neutron streaming is handled in MCNP4B by modelling explicitly the lattice of spheres.

Figure 7-7. Power Density in PBMR Equilibrium Core
Control Rods 1/4 Inserted ($z = 201.25$ cm)

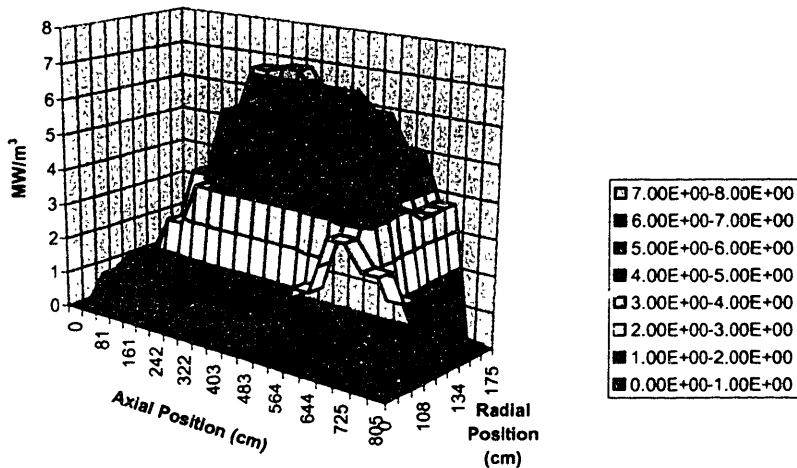


Figure 7-8. Fast Neutron Flux in PBMR Equilibrium Core
 Control Rods 1/4 Inserted ($z = 201.25 \text{ cm}$)

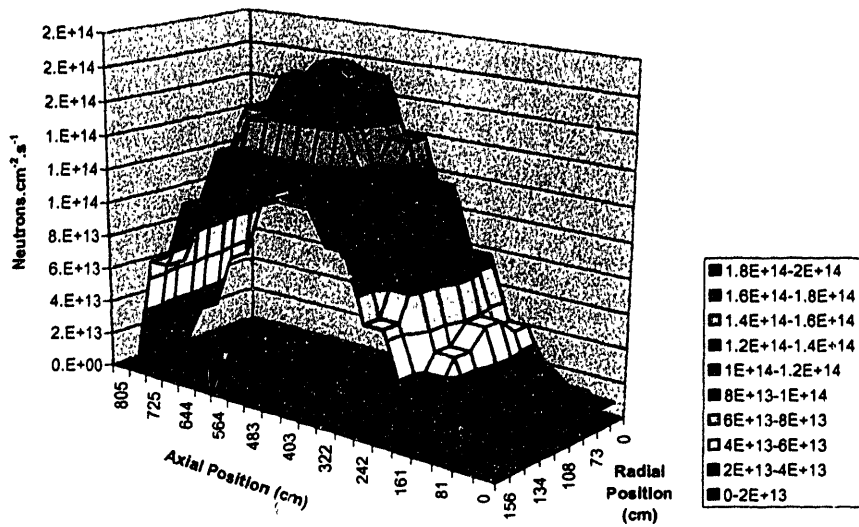
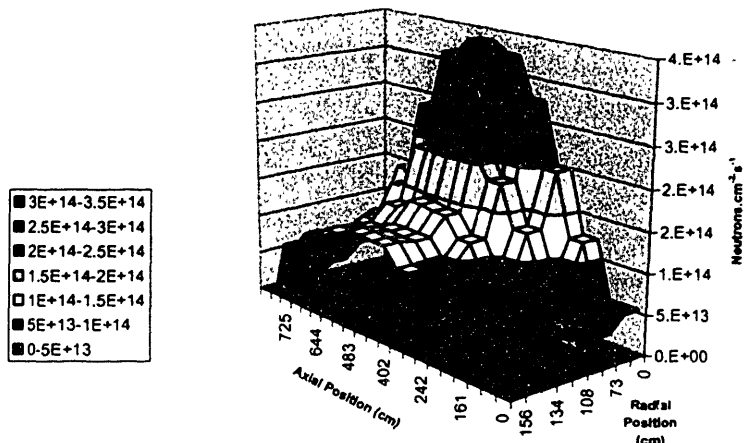


Figure 7-9. Thermal Neutron Flux in PBMR Equilibrium Core
 Control Rods 1/4 Inserted ($z = 201.25 \text{ cm}$)



However, the nuclide densities calculated by VSOP94 for each layer must also be adjusted to compensate for the approximate MCNP4B representation of fuel-sphere interiors. The effect of this homogenization was shown to decrease the reactivity of the core $\sim 4\% \Delta k/k$ by using an identical MCNP4B model in which the core layers were fully homogenized. Therefore, the ^{238}U (and ^{240}Pu that contributes to the resonance absorptions at high burnup) atom densities calculated by VSOP94 should be reduced (*i.e.*, adjust $\Sigma_i = N_i \sigma_i$ by modifying N_i instead of σ_i) to compensate for this change in reactivity. This would result in a k_{eff} of ~ 1.04 if temperature effects are not included in the simulation. Two-dimensional VSOP analysis of the PBMR core has established a total temperature reactivity coefficient of $-4.17 \times 10^{-5} \Delta k/\text{°C}$ (see Table 7-5) [7-6], which would reduce the reactivity of the core by $\sim 4\% \Delta k/k$ assuming an average fuel temperature of 950°C . The MCNP4B calculations reported here were performed at room temperature, because cross-section libraries at typical HTGR operating temperatures were not available.

**Table 7-5
Temperature Reactivity Coefficients in the PBMR [7-6]**

<i>Reactor Component</i>	$\Delta k/\text{°C}$
Fuel	-3.28×10^{-5}
Moderator in fuelled region of core	-3.30×10^{-5}
Central reflector	$+0.93 \times 10^{-5}$
Outer reflectors	$+1.48 \times 10^{-5}$
Total	-4.17×10^{-5}

7.6 Discussion

Monte Carlo methods are becoming the tool of choice for the physics design and analysis of nuclear reactors. Models prepared with a Monte Carlo code such as MCNP4B are capable of calculating very accurately all key core parameters, including the effective multiplication constant, the reactivity worths of control rods and shutdown absorbers, fission powers and neutron fluxes. The ability of MCNP4B to transport photons also makes it useful for shielding and heat deposition calculations. Furthermore, advances in computer hardware have made lengthy Monte Carlo runs cost effective.

Full-core calculations are increasingly being performed with code systems that couple Monte Carlo and stand-alone fuel depletion codes. An example of such a Monte Carlo burnup code is MOCUP, which couples MCNP4B and ORIGEN2. However, this code cannot be currently applied to pebble-bed reactors for several reasons: (a) the recirculation of fuel spheres in the core; (b) modelling the 10^4 discrete fuel particles in each fuel sphere in a large pebble-bed core is beyond the capabilities of the codes; and (c) the number of MCNP4B runs required to reach an equilibrium burnup distribution would be computationally prohibitive. Therefore, the best approach at this time is to perform the fuel management study separately using a diffusion- or transport-theory code and use the resulting fuel compositions in a snapshot MCNP4B calculation with a very detailed model of the reactor.

The method described in this chapter for obtaining the MCNP input for the composition of fuel spheres in a pebble-bed core with burnup is limited in its accuracy, because of the need to account for the effects of homogenization on resonance absorptions. Therefore, a

different approach is needed if the resulting MCNP4B model is to be of benchmark quality. Such a model should treat the double heterogeneity of the pebble bed core with the same degree of accuracy as the HTR-PROTEUS and HTR-10 models described in Chapters 4 and 5 (although one possible simplification is to lump the coatings of the fuel kernels together with the graphite matrix [7-15]). The composition of the fuel kernels could be generated directly using a lattice code with an accurate burnup capability, or a Monte Carlo burnup code. The proposed method is shown schematically in Figure 7-10 for the Dutch WIMS/PANTHERMIX code system (see Chapter 2), although VSOP94 could also be used to perform these calculations.

In the suggested procedure, a fuel management study would be performed to determine the burnup distribution in the core for a given refuelling strategy. These burnups (in MWD/THM) would be calculated using diffusion theory for a finite number of core regions (or layers in VSOP94). A neutronics code would then be used to deplete the fuel to the required burnup with a standard supercell model consisting of a single fuel sphere, with an explicit representation of the coated fuel particles, surrounded by a driver region. This procedure is similar to the single pebble, multi-kernel burnup calculations reported in References 7-15 and 7-16. Because each fuel sphere is expected to visit every region of the core during its multiple passes, an average fuel composition corresponding to the equilibrium core could be used for the driver fuel.

Any number of codes may be used to perform the supercell depletion calculation, including MOCUP and WIMS [7-18]. The model would have to be run to generate

separate fuel compositions for the burnup in each core region, and the MCNP4B material cards would be prepared with a modified version of MCARDS.

A more direct approach, which does not rely on a diffusion-theory code, would be to use the MONTEBURNS Monte Carlo burnup code to perform the entire fuel management study. The core would be modeled as in Section 7.4, although with an explicit representation of the double heterogeneity. Simple annular zones could be used to simplify the generation of flux and power distributions. The same fuel composition would be used in all fuel spheres in a given core region. MONTEBURNS already has the capability for shuffling fuel, but the code would have to be modified to perform the mixing of fuel spheres with different burnup that occurs when discharged fuel spheres are reinserted at the top of the core.

7.7 Summary

An approximate method for the MCNP4B modelling of pebble-bed reactors with burnup was presented. In this approach, the nuclide densities of the homogenized layers in the VSOP94 model of the reactor are used in the corresponding MCNP4B model with an adjustment for its explicit representation of the sphere lattice. The method was demonstrated in principle on the PBMR equilibrium core, although temperature-dependent cross sections would have to be generated for MCNP4B before the model can be applied to reactor design problems.

Two alternative approaches were proposed, which takes advantage of the ability to model the double heterogeneity of the PBMR core directly with MCNP4B. In the first method,

which uses a lattice code such as WIMS or the Monte-Carlo burnup code MOCUP, a supercell model of a fuel kernel would be used to deplete the fuel to the desired burnup in a representative core environment. The resulting nuclide densities could then be used without adjustment in a detailed (doubly heterogeneous) MCNP4B model. In both this and the MCNP4B/VSOP94 approaches, average fuel compositions are generated for a finite number of core regions (similar to the layers of VSOP94) to make the problem computationally manageable. In the second method, the Monte Carlo burnup code MONTEBURNS would be used to perform the entire fuel management study directly. However, this approach would require modifications to the code to facilitate the recycling of fuel spheres with different burnup.

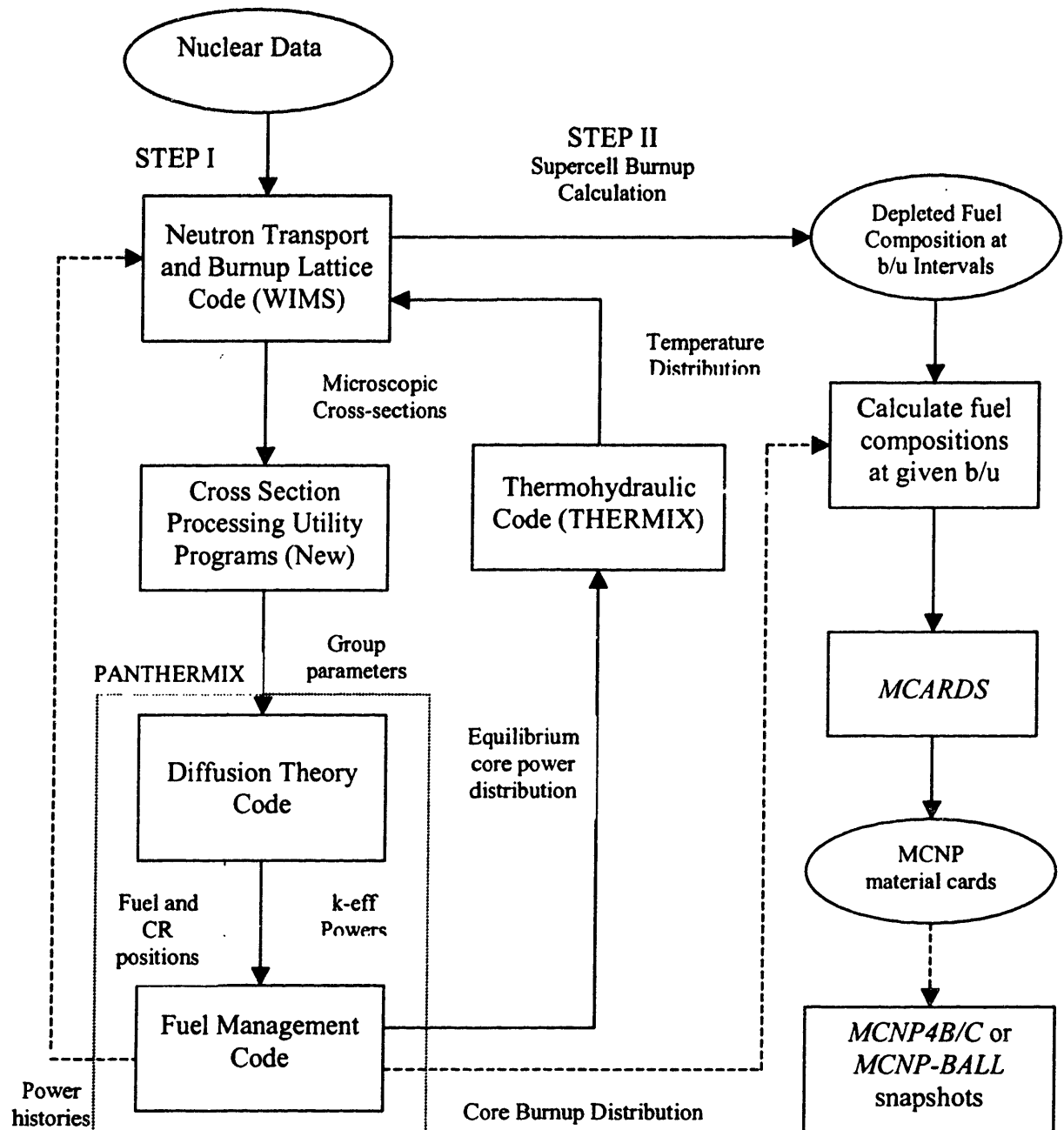


Figure 7-10. Proposed MCNP-Based Code System for Pebble-Bed Reactors with Burnup

8. PLUTONIUM PRODUCTION IN A PEBBLE BED REACTOR

Nuclear power is expected to play a significant role in meeting future electricity needs while reducing emissions of air pollutants and greenhouse gases [8-1]. However, several issues continue to trouble government and industry policymakers and segments of the public. These include nuclear power plant safety, waste, economics and weapons material proliferation. The modular pebble-bed reactor is a leading contender in a new generation of nuclear reactors, and is recognized for its simple design, thermodynamic efficiency, natural safety and environmental friendliness. The graphite pebbles with the embedded TRISO coated fuel particles serve as an excellent waste form for the direct disposal of spent fuel in a geological repository [8-2]. The focus of this chapter is the proliferation resistance of pebble-bed reactors.

Preliminary calculations were performed with the VSOP94, MCNP4B and ORIGEN2 physics codes to estimate the production of plutonium in a pebble-bed reactor. The ESKOM Pebble Bed Modular Reactor (PBMR) was used as the reference reactor [8-3]. The study examined the isotopic composition of normally discharged fuel, first-pass fuel spheres and depleted-uranium production spheres¹.

8-1. Modeling Methods

A description of the VSOP94 and MCNP4B physics codes appears in Chapter 2. The VSOP94 suite of codes, which relies on diffusion theory to solve the neutron transport equation, can be used to perform fuel management studies for pebble-bed reactors with multiple-pass refuelling strategies [8-4]. The Monte Carlo code MCNP4B is capable of accurate calculations involving the transport of neutrons and photons, including the determination of ^{238}U capture rates [8-5].

¹ The concept of depleted-uranium production spheres was proposed by J.S. Herring of the INEEL.

ORIGEN2 is a general-purpose point-depletion and generation code for calculating isotopes, decay heat, radiation source terms and radioactivity levels [8-6]. MOCUP is a Monte Carlo burnup code that couples MCNP4B and ORIGEN2 [8-7].

Models of the PBMR were used to examine the amount and isotopic composition of plutonium present in the normally discharged fuel spheres, fuel spheres diverted after a single pass through the core, and special production spheres loaded with depleted UO₂. The analysis consisted of a supercell calculation of plutonium production with special spheres using MCNP4B, and a full-core simulation of normal fuel spheres using VSOP94².

8.1.1 Supercell Model

The supercell model represents an attempt to represent accurately the environment that the production pebble experiences during its passage through the core. It consists of an MCNP4B model, in which a single production pebble is placed in the center of a reflected spherical core consisting of a regular lattice of driver fuel pebbles (see Figure 8-1).

The nuclide concentrations of the driver fuel were extracted from the VSOP94 model of the PBMR and corresponded to an average over all regions of the equilibrium core (see Chapter 7). The size of the supercell was adjusted to yield a critical assembly ($k_{\text{eff}} \sim 1$), and its power was normalized so as to match the VSOP94 core-averaged total neutron flux. The ²³⁹Pu production is estimated from a tally of the ²³⁸U(n, γ)²³⁹U reaction rate for the stand-alone MCNP4B, or by tracking the isotopic composition of the production ball in a MOCUP depletion calculation; the composition of the driver fuel is static. The supercell model permits the modeling of the inner reflector and transition zones.

² The VSOP model of the PBMR reference core was provided by Dr. E.J. Mulder, PBMR (Pty) Ltd.

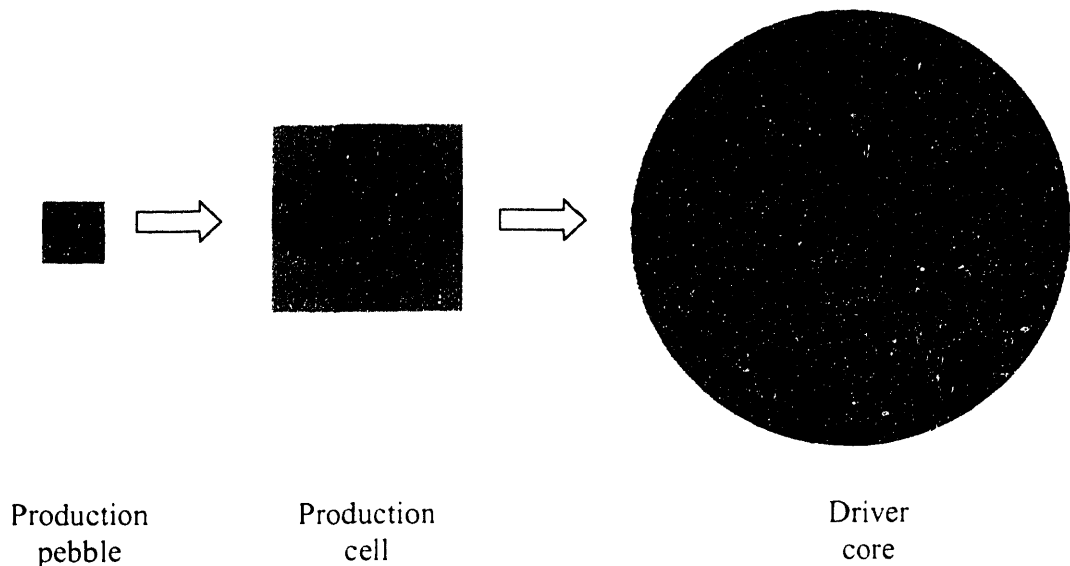
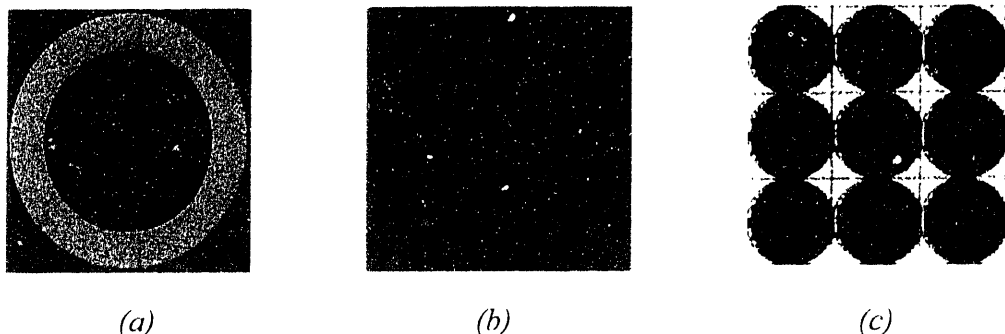


Figure 8-1. Supercell MCNP4B Model of Production Sphere

8.1.2 Production Pebbles

Three configurations of plutonium production pebbles containing depleted ($0.2\% {^{235}\text{U}}$) UO_2 were considered (see Figure 8-2): *(a)* a solid core (2.1 cm radius); *(b)* ten alternating shells (2 mm thick) of depleted fuel and pyrolytic carbon; *(c)* a densely packed simple cubic array of BISO coated depleted fuel particles (0.025 cm inner and 0.038 cm outer radius of pyrolytic carbon coating, and a 0.5 packing fraction). The BISO coating does not incorporate a silicon-carbide layer, and using such fuel particles would avoid problems associated with the removal of silicon carbide during reprocessing (the depleted uranium will not add a significant amount of fission-product contamination to the reactor cooling system).



(a)

(b)

(c)

Figure 8-2. Different configurations of production pebbles:
(a) solid core; (b) shells; (c) dense BISO.

8.2 Analysis and Results

The following sections provide some details of the analysis performed and a summary of the results obtained. Plutonium production in regular fuel pebbles was analyzed with VSOP94, while the special production pebbles was investigated using the supercell model described above. A further discussion of the proliferation resistance of pebble-bed reactor fuel cycles appears in Reference 8-8, and the simple-cell MCNP4B and MOCUP analysis of plutonium production in pebble-bed reactors performed at the INEEL may be found in Reference 8-9.

8.2.1 Regular Fuel Pebbles

VSOP94 analysis of the reference PBMR core showed (see Appendix E.2) that a diversion of 157,000 spent fuel pebbles would be needed over 1.2 years to obtain 6 kg of ^{239}Pu (which is taken to be a weapon's worth of plutonium). However, as is shown in Table 8-1 for a fuel discharge burnup of 80 MWd/kgU, the isotopic composition of plutonium in spent fuel at high burnup is not well suited for nuclear weapons production. Moreover, the percentage of ^{239}Pu is lower than 40%, which is a recognized level for lower proliferation risk [8-9].

Table 8-1
Plutonium Isotopic Composition of PBMR
Spent Fuel at 80 MWd/kgU[†]

Isotope	%
^{238}Pu	1.9
^{239}Pu	36.8
^{240}Pu	27.5
^{241}Pu	18.1
^{242}Pu	15.7

[†] Calculated with VSOP94.

Fuel pebbles, which are diverted after a single pass through the core, have a more favourable plutonium isotopic composition (Table 8-2). However, because of the shorter irradiation times (on average 73 days per pass), as many as 258,000 fuel pebbles would have to be diverted for 6 kg of ^{239}Pu (the amount of ^{239}Pu needed for a weapon varies between 4 and 8 kg). Since fuel pebbles are normally reinserted at the top of the core, the diversion of all first-pass fuel pebbles would result in an excessive loss of reactivity. Therefore, the duration of the diversion would be longer than the two years calculated for the normal discharge rate of such pebbles unless fresh fuel can be added.

Table 8-2
Plutonium Isotopic Composition of PBMR
First-Pass Fuel[†]

Isotope	%
^{238}Pu	~ 0
^{239}Pu	82.8
^{240}Pu	15.2
^{241}Pu	1.9
^{242}Pu	0.1

[†] Calculated with VSOP94 for reference fuel cycle.

8.2.2 Supercell Analysis of Production Pebbles

The purpose of using a supercell model of the production pebble is to simulate more accurately the neutron flux and spectrum that the pebble would experience during its single pass through the core. Calculations were performed for the three designs of production pebble described in Section 8.1.2, using a driver-fuel assembly representative of (a) the PBMR average core and (b) the PBMR inner reflector region. The MCNP4B analysis included tallies of the $^{238}\text{U}(\text{n},\gamma)$ reaction rates in the depleted uranium target and the eighth of a driver fuel pebble in each of the eight corners of the BCC production cell. The average neutron flux in the production cell was also tallied. In addition, a MOCUP depletion calculation was carried out for the production pebble with a solid UO₂ target to determine the plutonium isotopic composition at the end of the irradiation period. The results are presented in Tables 8-3 to 8-5.

Table 8-3
Neutron Fluxes Calculated With Supercell MCNP4B Model
(neutrons·cm⁻²·s⁻¹)

Case	Group 1 ^a	Group 2 ^b	Group 3 ^c	Group 4 ^d	Comments
VSOP reference	2.47e+13	4.85e+13	1.26e+13	1.18e+14	Average core
Solid UO ₂ target	3.46e+13 (3.41%)	6.18e+13 (2.91%)	1.63e+13 (4.91%)	9.33e+13 (2.26%)	
UO ₂ target shells	3.58e+13 (3.40%)	6.20e+13 (2.84%)	1.62e+13 (4.81%)	9.21e+13 (2.32%)	
Densely packed BISO targets	3.58e+13 (3.47%)	6.14e+13 (2.96%)	1.42e+13 (5.18%)	9.46e+13 (2.27%)	
VSOP reference	1.07e+13	2.64e+13	9.15e+12	2.02e+14	Inner reflector
Solid UO ₂ target	3.41e+12 (11.3%)	1.49e+12 (24.1%)	2.55e+11 (38.4%)	2.07e+14 (1.72%)	

^a) 0.1 MeV < E ≤ 20 MeV; ^b) 29 eV < E ≤ 0.1 MeV; ^c) 1.86 eV < E ≤ 29 eV; ^d) 0 eV < E ≤ 1.86 eV.

The standalone MCNP4B tallies were normalized using four million starting neutron histories for the core-averaged cases and eight million for the reflector case³, while the MOCUP calculation was limited to one million neutron histories at each burnup step because of time constraints. The reported percent relative errors (shown in brackets) correspond to the 1- σ confidence interval.

Table 8-4
 ^{239}Pu Production Calculated with Supercell MCNP4B Model

Production Pebble	Reaction Rate (1/s)		$\text{g } ^{239}\text{Pu} / \text{pass}$		Pebbles for 6 kg ^{239}Pu	Comments
	driver	target	driver	target		
Solid UO ₂ target	1.91e+13 (21.9%)	1.86e+14 (5.65%)	0.048 (21.9%)	0.466 (5.65%)	12,866 ± 727	Average core
Shell UO ₂ targets	1.28e+13 (21.0%)	1.54e+14 (6.63%)	0.032 (21.0%)	0.386 (6.63%)	15,526 ± 1,029	
Dense BISO targets	1.27e+13 (16.2%)	1.95e+14 (6.18%)	0.032 (16.2%)	0.487 (6.18%)	12,312 ± 761	
Solid UO ₂ target	3.41e+12 (4.67%)	2.12e+14 (3.86%)	0.007 (4.67%)	0.420 (3.86%)	14,132 ± 645	Inner reflector

Table 8-5
Isotopic Composition of Plutonium in Irradiated Solid UO₂ Target[†]

Isotope	%
^{238}Pu	~0
^{239}Pu	92.2
^{240}Pu	7.5
^{241}Pu	0.3
^{242}Pu	~0

[†] Calculated with supercell MOCUP model.

8.3 Discussion

The analysis has confirmed that spent fuel from pebble-bed reactors is proliferation resistant at high discharge burnup (≥ 80 MWd/kgU), because of its unfavourable plutonium isotopic composition and the large number of pebbles that would have to be diverted—about half a core

³ The large number of histories is needed to reduce the relative errors of the neutron flux and reaction rate tallies to acceptable levels (ideally < 5%).

load. The isotopes of first-pass fuel pebbles are more favourable, but an even larger number would be needed to accumulate 6 kg of ^{239}Pu . In addition, the large number of coated fuel particles that must be cracked to remove the SiC coating make TRISO fuel difficult to reprocess. Such reprocessing technology is yet to be demonstrated on irradiated fuel.

However, it is also possible to produce a significant quantity of plutonium in a pebble-bed reactor by inserting special pebbles with a high loading of depleted uranium. Analysis has also shown that the production of plutonium in such pebbles is limited by γ -heating and resonance self-shielding in the target regions [8-10]. As with any new fuel concept, the manufacturing of the special pebbles would require a sophisticated fuel development program and irradiation research facilities not commonly found in countries lacking a nuclear infrastructure. Fewer pebbles would be needed (13,000 to 20,000), although the duration of the diversion will depend on the ability to compensate for their reactivity effect. If the production pebbles comprise 1% of the core inventory, it would take a minimum of 1.5 years to accumulate the required amount of material at the normal fuel-pebble removal rate. By extrapolation from HTR-10 criticality calculations⁴, the reactivity worth of the PBMR core height may be estimated to be 0.02 %/cm. Therefore, the height of the core would have to be raised by approximately 50 cm to compensate for 1 $\% \Delta k/k$ loss in reactivity. It is unlikely that such a change in core height would go unnoticed in a safeguarded reactor.

The substitution of fuel pebbles with ones containing depleted uranium targets, or diverting regular pebbles after a single pass, could have a significant effect on the normal operation of the

⁴ For HTR-10, $\Delta\rho/\Delta H \approx 0.5\text{ %}/\text{cm}$. Since the PBMR core is 5 times taller, then this value scales as $(1/5)^2$ assuming a cosine flux shape. Thus, $\Delta\rho/\Delta H|_{\text{pbmr}} \approx 0.02\text{ %}/\text{cm}$.

reactor.⁵ A detailed analysis must be carried out using the VSOP94 fuel management code to model such effects, especially to determine the throughput of special pebbles. However, since the preparation of VSOP94 input files is time consuming, the preliminary calculations were performed with MCNP4B and MOCUP using simplified models of the PBMR core that limit the accuracy of the analysis. The standalone MCNP4B calculations are expected to be conservative because they neglect the depletion of bred plutonium. The supercell MCNP4B models predict a harder neutron spectrum than VSOP94 and, therefore, also tend to overestimate the $^{238}\text{U}(\text{n},\gamma)$ reaction rate.

The potential diversion of special plutonium production pebbles requires the use of extrinsic barriers to assure nonproliferation. While there are differences in estimates of the actual number (13,000 to over 20,000) and the time needed to accumulate these pebbles (1 to 2 years), the final conclusion is that intrinsic barriers alone are not sufficient for on-line refueling of pebble-bed reactors. IAEA safeguards and enhanced monitoring systems would be required to prevent the insertion of these pebbles, monitoring devices to detect their production, and seals to avoid tampering with the closed refueling system of the plant [8-11].

As is typical for IAEA safeguards programs for light-water reactors, inspections of fuel fabrication plants and fresh fuel deliveries would be required. Automatic weighing stations would also be required for fuel pebbles prior to their insertion into the core to detect the heavier production pebbles. Pebble-bed reactors already possess on-line burnup meters and failed pebble detectors to sort pebbles for reinsertion. However, by making “defected” production pebbles, this system could also be used to remove first-pass pebbles for plutonium recovery. The detection

⁵ It may be possible to design production pebbles that are reactivity neutral, e.g., by adding an outer fuel shell.

system would have to be enhanced to detect spectral differences caused by the presence of production pebbles. These technologies require an additional research and development effort to ensure that nonproliferation objectives are met.

This study also suggests that additional work on fuel management strategies may be helpful in improving intrinsic barriers by reducing ^{239}Pu production through the adjustment of enrichments and neutron spectra. Alternative intrinsic barriers are the OTTO (once through then out) fuel cycles, which include the Dutch PAP (*peu-á-peu*) concept [8-12] and the proposed PAP2 fuel with burnable poison [8-13], and potentially utilizing Th/LEU fuel to provide additional proliferation resistance of spent fuel. Irradiations of short duration are not possible in such non-recirculating cores (other than by the premature dumping of the entire inventory).

A final remark is appropriate regarding the relative proliferation risk of this technology. The pebble-bed reactor is not a likely target for a terrorist or sub-national group, because of the sophisticated nature of the fabrication and reprocessing of production pebbles. Plutonium production assemblies can be inserted into any reactor. However, while a single fuel assembly may suffice in a light-water reactor, thousands of pebbles would have to be diverted from a pebble-bed reactor to produce a single weapon. Any reactor may become a national threat by a country that chooses to abdicate the NPT and IAEA safeguards inspections. It is the purpose of international safeguards to provide advanced notice of such activity.

9. Conclusions and Future Directions

The research described in this report explored the applicability of the standard version of MCNP to the neutronic modeling of pebble-bed reactors. Previous MCNP (versions 4A or 4B) investigations only considered critical experiments involving regularly packed cores [9-1, 9-2]. The key issue for the practical application of MCNP4B to pebble-bed reactors is the use of regular lattices to describe their randomly packed cores. This modeling effort was very successful for the simple core configurations encountered in the HTR-PROTEUS critical experiments and the HTR-10 start-up core. The annular ASTRA core, which is representative of modern modular HTGR designs, proved to be much more difficult to model accurately. A summary of key results is provided in Table 9-1; further details may be found in the referenced chapters.

Table 9-1
Summary of key MCNP4B Criticality Calculations

<i>Experiment</i>	<i>Parameter</i>	<i>Measurement</i>	<i>Calculation</i>	<i>Chapter</i>
HTR-PROTEUS	k_{eff}	1.0134 ± 0.0011	$1.0208 \pm 0.0011^{\dagger}$	4
	k_{eff}	1.0129 ± 0.0008	$1.0172 \pm 0.0010^{\dagger}$	4
	k_{eff}	1.0132 ± 0.0007	$1.0176 \pm 0.0011^{\dagger}$	4
HTR-10	Critical load	16,890	16,841	5
ASTRA	k_{eff}	1.000	0.99977 ± 0.00082	6
	$\Delta\rho$	1.77 % [‡]	$1.72 \pm 0.11 \%$	6
	$\Delta\rho$	1.84 %	$1.89 \pm 0.11 \%$	6
	$\Delta\rho$	1.40 %	$1.56 \pm 0.11 \%$	6
	$\Delta\rho$	1.83 %	$2.01 \pm 0.12 \%$	6

[†] A reactivity bias is present because of graphite impurities; [‡] % $\Delta k/k$.

The method developed for the MCNP4B modeling of pebble-bed cores involves the use of a regular lattice of spheres, arranged either as a primitive BCC lattice or based on a repeating cell constructed from a number of BCC unit cells as shown in Figure 9-1. The

coated fuel particles are modeled in detail and are distributed over the fuelled portion of the fuel sphere using a simple cubic lattice. The enlarged cell approach is needed for modeling explicitly more complicated core configurations, especially when more than two types of spheres are present in the core (such as fuel, moderator, absorber, *etc.*). The results of such a model were found to depend very strongly on the distribution of spheres in the cell, and a generic modeling methodology is difficult to define. However, case-by-case treatment can be successful when supported by appropriate sensitivity studies.

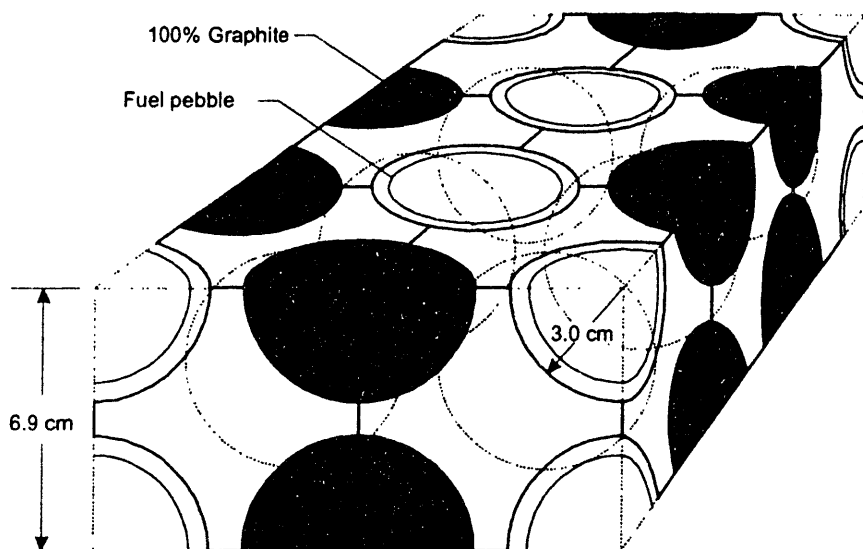


Figure 9-1. Six-cell BCC model used in the plutonium production study [9-3]

Because the repeated-structure feature of MCNP4B introduces partial spheres at the periphery of the core, a correction is required in order to eliminate excess fuel contributed by partial fuel spheres. This can be done either by reducing the volume of the core while keeping the sphere packing fraction unchanged, or by reducing the packing fraction while keeping the core volume unchanged. Both approaches rely on an exclusion zone, which balances the contributions from physically realizable and unrealizable partial spheres. For

circular cores, the procedure is straightforward because a distribution of partial spheres of various sizes exists at the core boundary. The size of the exclusion zone is given by the radius of the sphere scaled by the number ratio of fuel spheres to all spheres in the unit cell. However, such a distribution does not exist in polygonal cores and the exclusion zone must be determined explicitly from the volumes of partial spheres at the boundaries. This is possible because the positions of the spheres are known in a regular lattice, and an expression is available for the volume of a spherical segment [$V = \frac{1}{3}\pi h^2(3R-h)$, where R is the radius of the sphere and h is the height of the segment].

Ultimately of interest is the ability to model a realistic core with any number of types of spherical elements, including fuel spheres with different fissile materials, enrichments and burnup. A core representation constructed from a repeating cell with 100 spheres (arranged in 50 BCC unit cells) could be used in principle to describe such core loadings. However, as the ASTRA analysis has demonstrated, such a deterministic approach is very difficult and not likely to be accurate. If MCNP4B (or version 4C) is to be used, the recommended method is to use average material compositions in a finite number of core regions (such as the layers from the VSOP94 model), with an explicit treatment of the fuel kernels whose compositions are best generated with a separate fuel management code as discussed in Chapter 7. A 30% reduction in computation time is reportedly possible by smearing the multiple coatings of the fuel kernels into a single layer [9-4].

However, the best approach would appear to be to shift the Monte Carlo modeling effort to the stochastic geometry treatment of the MCNP-BALL code developed by JAERI [9-5], because this would eliminate the difficulties associated with specifying the pebble-bed

core explicitly. In this method, the geometry of the core is sampled during the neutron transport calculation using nearest-neighbour distribution functions (NND). Such distribution functions, which give the probability of finding the nearest neighbour in a spherical shell between radius r and $r+dr$, are generated using the Monte Carlo packing code MCRDF. (An exclusion zone is used during the sampling process to avoid including spheres that overlap the vessel boundary, although here the packing fraction is increased to achieve the correct inventory of spheres.) The NNDs are sampled during the transport of each neutron to determine its path through a sphere or coated fuel particle. This eliminates the need for the *a priori* specification of the pebble-bed geometry, because the positions of other spheres or coated fuel particles do not enter the calculation.

The current version of MCNP-BALL was developed by JAERI from MCNP3B by revising five existing subroutines and adding five new ones, and validated through analysis of the stochastic-core experiments at the HTR-PROTEUS facility [9-6]. However, all future applications and modifications of MCNP-BALL should be based on an MCNP4C implementation of the code. The most important enhancements required in MCNP-BALL relate to the modeling of separate core regions with different fuel compositions.

Apart from the recommendation to shift from MCNP4B (or 4C) to MCNP-BALL, several other aspects of the research discussed in this report require a follow-up. The most important of these concern the ASTRA critical assembly and the addition of a burnup capability to the MCNP4B modeling of pebble-bed reactors.

(a) ASTRA

The remaining experiments performed in ASTRA should be analyzed, including the investigation of critical parameters as a function of core height, the spatial distribution of relative reaction rates, and the reactivity effects of spherical elements. The latter measurements were carried out for both individual and groups of spheres (fuel, moderator and absorber) in the central channel. [9-7]

Calculation of the ASTRA control-rod worths was found to be sensitive to the number of neutron histories (both the total number and the number per cycle) and the definition of the fission source term used to initiate the run. This suggests that the annular core may be more neutronically decoupled than was previously thought to be the case. This should be investigated, including the effect of the boron absorber on the neutronic stability of the core (for example, by defining the starting fission source in one half of the core only and following the behaviour of the effective multiplication factor for successive cycles).

(b) Burnup

The method proposed in Chapter 7 for calculating the nuclide densities of depleted fuel should be implemented. This should be done initially by using VSOP94 to determine the equilibrium core burnup distribution, followed by a supercell MONTEBURNS [9-8] calculation of layer-averaged fuel compositions (see Figure 7-10). This could then be followed up by an investigation of whether MONTEBURNS could be used to perform the fuel management study directly. New routines would have to be added to

MONTEBURNS to simulate the out-of-pile decay of fission products and the mixing of fuel spheres with different burnup in each core region.

An interlaboratory burnup benchmark should be promoted similar to those done in the past for light-water reactor UOX and MOX fuel [9-9]. This would consist of a numerical benchmark comparison of the burnup reactivity and isotopes capabilities of the computer codes currently used by the international community engaged in HTGR analysis and design. The proposed benchmark would continue the work initiated in Reference 9-10, in which a single spherical unit cell was depleted with MONTEBURNS at several levels of complexity. The unit cell examined was taken from an ECN report [9-11], which modeled the LEUPRO-1 critical assembly tested at the HTR-PROTEUS facility. Such an international benchmark was recently proposed [9-12].

Several other areas also deserve further investigation. A more systematic study of neutron streaming in different types of lattices should be undertaken to determine the optimum packing order. As discussed in Chapter 3, a rhombohedral lattice is expected to provide a better representation of the arrangement of spheres in a pebble-bed reactor. A “super” lattice constructed from such unit cells was found to be too complicated for detailed modeling of the ASTRA core, but an approximate model that uses borated fuel spheres in a primitive rhombohedral unit cell may give better results than a BCC unit cell.

The predictions for the reactivity worths of the control rods in the HTR-10 reactor, which were calculated using the MCNP4B model described in Chapter 5, should be compared with the measured values when these become available. Good agreement in the worth of control rods signifies that the MCNP4B model is capable of predicting accurately the

neutron flux in the core, and, more importantly, in the radial reflector where diffusion theory treatments are suspect.

In conclusion, a comprehensive examination of the applicability of the MCNP4B Monte Carlo code to the modeling of pebble-bed reactors was undertaken in the course of this research. A modeling methodology was developed based on an analysis of three critical experiments—HTR-PROTEUS, ASTRA and the HTR-10 start-up core. The method uses a body-centred cubic core representation, and exclusion zones to compensate for the contribution of partial spheres generated by MCNP4B at the core boundaries. The critical core heights were predicted correctly in all cases. However, the calculation of the reactivity worths of control rods in the more decoupled annular ASTRA core was less accurate.

An approximate procedure was also developed for the MCNP4B modeling of pebble-bed reactors with burnup. The nuclide densities of the homogenized layers in the VSOP94 model of the reactor are used in the corresponding MCNP4B model with an explicit representation of the sphere lattice. The method was demonstrated in principle on the PBMR equilibrium core. The procedure for extracting fuel compositions from VSOP94 was also used to create a supercell MOCUP model of a special pebble loaded with depleted uranium. The model was then used to calculate the plutonium production capability of the PBMR.

For the modeling of realistic cores, the main recommendation of this report is a shift from MCNP4B (or version 4C), and its use of regular lattices of spheres to represent the core, to the stochastic geometry approach implemented in the JAERI code MCNP-BALL.

10. REFERENCES

Chapter 1

- [1-1] E. Teuchert, K.A. Haas, H.J. Rütten, H. Brockmann, H. Gerwin, U. Ohlig and W. Scherer, "V.S.O.P. ('94) Computer Code System for Reactor Physics and Fuel Cycle Simulation—Input Manual and Comments," Forschungszentrum Jülich GmbH, Jülich-2897, April 1994.
- [1-2] J. Oppe, J.B.M. de Haas and J.C. Kuijper, "PANTHERMIX—A PANTHER-MIX-THERMIX Interaction," ECN-I—96-022, May 1996.
- [1-3] J. Oppe, J.C. Kuijper, J.B.M. de Haas, E.C. Verkerk and H.T. Klippel, "Modeling of Continuous Reload HTR Systems by the PANTHERMIX Code System," M&C 2001, Salt Lake City, Utah, September 2001.
- [1-4] W. K. Terry, H. D. Gougar, and A. M. Ougouag, "Deterministic Method for Fuel Cycle Analysis in Pebble Bed Reactors", Transactions of the American Nuclear Society, 83, November 2000, pp. 278-9.
- [1-5] J.F. Briesmeister (Ed.), "MCNP—A General Monte Carlo N-Particle Transport Code, Version 4B," Los Alamos National Laboratory, Report LA-12625-M, March 1997.
- [1-6] F.C. Difilippo, "Applications of Monte Carlo Methods for the Analysis of MHTGR Case of the PROTEUS Benchmark," Oak Ridge National Laboratory. Report ORNL/TM-12711, April 1994.

- [1-7] I. Murata, A. Takahashi, T. Mori and M. Nakagawa, "New Sampling Method in Continuous Energy Monte Carlo Calculation for Pebble Bed Reactors," Journal of Nuclear Science and Technology, 34(8), August 1997, pp. 734-744.
- [1-8] G. Melese and R. Katz, Thermal and Flow Design of Helium-Cooled Reactors, American Nuclear Society, Illinois, 1984.
- [1-9] R.P.C Schram, E.H.P. Cordfunke and A.I. van Heek, "High-Temperature Reactor Development in the Netherlands," Proceedings of the 3rd JAERI Symposium on HTGR Technologies, JAERI-Conf96-010, JAERI, Ibarak-ken, Japan, 1996, pp. 76-88.
- [1-10] A.I. van Heek (Ed.), "Inherently safe nuclear COGENeration (INCOGEN)," Pre-Feasibility Study, Netherlands Energy Research Foundation (ECN), Petten, 1997.
- [1-11] A.C. Kadak and R.G. Ballinger, "3.1.1.2 Advanced Modular Pebble Bed Reactor," Nuclear Engineering Department Activities Report, MIT, August 1, 2001.
- [1-12] L. Massimo, Physics of High-Temperature Reactors, Pergamon Press, Oxford, 1976.
- [1-13] J. Spanier and E.M. Gelbard, Monte Carlo Principles and Neutron Transport Problems, Addison-Wesley, Reading, MA, 1969.

- [1-14] J.S. Tang and B.A. Worley, "Monte Carlo Calculations of Control-Rod Worth of a Medium-Size Pebble-Bed Reactor," Oak Ridge National Laboratory, Report ORNL/TM-8111, August 1982.
- [1-15] E.F. Mitenkova, N.V. Novikov and Yu. P. Sukharev, "Monte Carlo Investigation of the Neutron-Physical Characteristics of a Bulk-Fill Core of a High-Temperature Gas-Cooled Reactor," *Atomic Energy*, 77(3), September 1994.
- [1-16] A. Hogenbirk, R.C.L. van der Stad, A.J. Janssen, H. Th. Klippel and J.C. Kuijper, "HTR-PROTEUS Benchmark Calculations. Part 1: Unit cell results LEUPRO-1 and LEUPRO-2," Netherlands Energy Research Foundation, Report ECN-C-95-087, September 1995.
- [1-17] F.C. Difilippo, "Application of Monte Carlo Methods for the Analysis of MHTGR Case of the VHTGR Benchmark," Oak Ridge National Laboratory, Report ORNL/TM-12698, 1994.
- [1-18] J.R. Leibhaft and M.J. Driscoll, "MCNP4B Analysis of the HTR-10 Startup Core," *Transactions of the American Nuclear Society*, 84, June 2001, pp. 214-5.
- [1-19] R. Brogli, D. Mathews, R. Seiler, "HTR PROTEUS experiments," Proceedings of the 2nd JAERI Symposium on HTGR Technologies, Ibaraki, Japan, Japan, Atomic Energy Research Institute, Report JAERI-M-92-215, 1992, pp.233-239.

- [1-20] X. Jing and Y. Sun, "Benchmark Problem of the HTR-10 Initial Core (Version 2000-03)," Institute of Nuclear Energy Technology, Tsinghua University, Beijing, March 2000.
- [1-21] D. Naidoo, "ASTRA Critical Facility Configuration Report," PBMR (Pty) Ltd., Report 003402-34, Revision A, December 29, 2000.
- [1-22] E.J. Mulder, "Core Basic Design Report for the PBMR Nuclear Power Plant Project," PBMR (Pty) Ltd., Report 002979-34, November 2000.
- [1-23] E. Teuchert and H.J. Rütten, "Core Physics and Fuel Cycles of the Pebble Bed Reactor," Nuclear Engineering and Design, 34, 1975, pp. 109-118.
- [1-24] A.G. Croff, "ORIGEN 2.1—Isotope Generation and Depletion Code Matrix Exponential Method," Oak Ridge National Laboratory, CCC-371 (ORNL/TM-7175), July 1980.
- [1-25] "MOCUP: MCNP/ORIGEN Coupling Utility Programs," RSICC, Oak Ridge National Laboratory, PSR-365 (INEL-95/0523), October 1997.
- [1-26] J.S. Herring, J.R. Lebenthal, K.D. Weaver and M.J. Driscoll, "Plutonium Production in a Pebble Bed Reactor," MIT/INEEL, unpublished technical report, August 2000.

Chapter 2

- [2-1] J.S. Tang and B.A. Worley, "Monte Carlo Calculations of Control-Rod Worth of a Medium-Size Pebble-Bed Reactor," Oak Ridge National Laboratory, Report ORNL/TM-8111, August 1982.
- [2-2] L. Massimo, Physics of High-Temperature Reactors, Pergamon Press, Oxford, 1976.
- [2-3] D.R. Vondy and B.A. Worley, "Pebble Bed Reactor Core Physics and Fuel Cycle Analysis," Oak Ridge National Laboratory, Report ORNL-5484, October 1979.
- [2-4] R.J.J. Stammler and M.J. Abbate, Methods of Steady-State Reactor Physics in Nuclear Design, Academic Press, London, 1983.
- [2-5] L.W. Nordheim and J.B. Sampson, Transactions of the American Nuclear Society, 2, 1959, p. 84.
- [2-6] E. Teuchert and R. Breitbarth, "Resonanzintegralberechnung für mehrfach heterogene Anordnungen," KFA Jülich, Jül-551-RG, 1968.
- [2-7] E. Teuchert, K.A. Haas, H.J. Rütten, H. Brockmann, H. Gerwin, U. Ohlig and W. Scherer, "V.S.O.P. ('94) Computer Code System for Reactor Physics and Fuel Cycle Simulation—Input Manual and Comments," Forschungszentrum Jülich GmbH, Jül-2897, April 1994.

- [2-8] M. Segev and M. Caner, "A WIMS-Based Calculational Route for Pebble-Bed Fuel," *Nuclear Science and Engineering*, 112, 1992, pp. 43-53.
- [2-9] J.R. Askew, F.J. Fayers and P.B. Kemshell, "A General Description of the Lattice Code WIMS," *Journal of the British Nuclear Energy Society*, 5, 1966, pp.564-585.
- [2-10] J.L. Kloosterman, J.C. Kuijper and P.F.A. de Leege, "The OCTOPUS Burnup and Criticality Code System," *Proceedings of PHYSOR 96*, 1996.
- [2-11] D.J. Cumberland and R.J. Crawford, The Packing of Particles, Handbook of Powder Technology, Volume 6, Elsevier, Amsterdam, 1987.
- [2-12] G.D. Scott, "Packing of Spheres," *Nature*, 188, 1960, pp. 908-909.
- [2-13] J. Wadsworth, "Experimental Examination of Local Processes in Packed Beds of Homogeneous Spheres," National Research Council of Canada, Report NRC-5895, February 1960.
- [2-14] J. Lieberoth and A. Stojadinovic, "Neutron Streaming in Pebble Beds," *Nuclear Science and Engineering*, 76, 1980, pp. 336-344.
- [2-15] J.A. Young and J.U. Koppel, "Phonon Spectrum in Graphite," *Journal of Chemical Physics*, 42, 1968, p. 224.
- [2-16] J.H. Simmons, Radiation Damage in Graphite, Pergamon Press, Oxford, 1965.

- [2-17] G.F. Kuncir, "ZUT: A Program for the Calculation of Resonance Integrals," General Atomics, Report GA-2525, August 1961.
- [2-18] G.D. Joanou and J.S. Dudeck, "GAM-I: A Consistent P_1 Multigroup Code for the Calculation of Fast Neutron Spectra and Multigroup Constants," General Atomics, Report GA-1850, June 1961.
- [2-19] H.C. Honeck, "THERMOS—A Thermalization Transport Theory Code for Reactor Lattice Calculations," Brookhaven National Laboratory, Report BNL-5826, September 1961.
- [2-20] G.D. Joanou, C.V. Smith and H.A. Vieweg, "GATHER-II," General Atomics, Report GA-4132, 1963.
- [2-21] H. Brockmann and U. Ohlig, "Erstellung einer 68-Gruppen-Wirkungsquerschnittsbibliothek im GAM-I Format und einer 96-Gruppen Wirkungsquerschnittsbibliothek in THERMILIZATION Format," KFA Jülich, Report KFA-IRE-IB-3/89, June 1989.
- [2-22] U. Hansen and E. Teuchert, "Influence of Coated-Particle Structure in Thermal-Neutron Spectrum Energy Range," Nuclear Science and Engineering, 44, 1971, p. 12.
- [2-23] J. Darvas, "DATA-2, Head Programm zum VSOP Zyklus für Hochtemperaturreaktoren," KFA Jülich, Report KFA-IRE-70-4, 1970.
- [2-24] D.R. Vondy and T.B. Fowler, "CITATION," Oak Ridge National Laboratory, Report ORNL/TM-2496, March 1972; *ibid.*, ORNL/TM-3793, July 1972.

- [2-25] F. Todt, "FEVER—A One-Dimensional Few Group Depletion Program for Reactor Analysis," General Atomics, Report GA-2749, 1962.
- [2-26] J.C. Cleveland and S.R. Greene, "Application of THERMIX-KONVEK Code to Accident Analyses of Modular Pebble Bed High Temperature Reactors," Oak Ridge National Laboratory, Report ORNL/TM-9905, August 1986.
- [2-27] U. Hansen, "The VSOP System Present Worth Fuel Cycle Calculation Methods and Codes—KPD," Winfrith Atomic Energy Establishment, Dragon Project Report 915, 1975.
- [2-28] J. Spanier and E.M. Gelbard, Monte Carlo Principles and Neutron Transport Problems, Addison-Wesley, Reading, MA, 1969.
- [2-29] L.L. Carter and E.D. Cashwell, Particle Transport Simulation with the Monte Carlo Method, ERDA Critical Review Series, TID-26607, 1975.
- [2-30] I. Murata, "Studies on Monte Carlo Particle Transport in Irregularly Distributed Fuel Elements for High Temperature Gas-Cooled Reactors," PhD Thesis, Department of Nuclear Engineering, Osaka University, Japan, 1999.
- [2-31] J.F. Briesmeister (Ed.), "MCNP—A General Monte Carlo N-Particle Transport Code, Version 4B," Los Alamos National Laboratory, Report LA-12625-M, March 1997.

Chapter 3

- [3-1] J.F. Briesmeister (Ed.), "MCNP—A General Monte Carlo N-Particle Transport Code, Version 4B," Los Alamos National Laboratory, Report LA-12625-M, March 1997.
- [3-2] C.R. Craig, W.D. Nix and A.S. Tetelman, The Principles of Engineering Materials, Prentice-Hall, Englewood Cliffs, 1973.
- [3-3] Z. Karriem, C. Stoker and F. Reitsma, "MCNP Modelling of HTGR Pebble-Type Fuel," presented at the M&C 2000, Pittsburgh, Pennsylvania, May 7-12, 2000.
- [3-4] I. Murata, A. Takahashi, T. Mori and M. Nakagawa, "New Sampling Method in Continuous Energy Monte Carlo Calculation for Pebble Bed Reactors," Journal of Nuclear Science and Technology, 34(8), August 1997, pp. 734-744.

Chapter 4

- [4-1] R. Brogli, K.H. Bucher, R. Chawla, K. Foskolos, H. Luchsinger, D. Mathews, G. Sarlos and R. Seiler, "LEU-HTR Critical Experiment Program for the PROTEUS Facility in Switzerland," Energy, 16(1/2), 1991, pp. 507-519.
- [4-2] T. Williams, "LEU-HTR PROTEUS: Configuration Descriptions and Critical Balances for the Cores of the HTR-PROTEUS Experimental Programme," Paul Scherrer Institute, Report TM-41-95-18, November 1996.

- [4-3] "PROTEUS Critical Experiment Facility," Paul Scherrer Institute, unpublished report.
- [4-4] D. Mathews and R. Chawla, "LEU-HTR PROTEUS Calculational Benchmark Specifications," Paul Scherrer Institute, Report TM-41-90-32, October 1990.
- [4-5] T. Williams, O. Köberl, D. Mathews and R. Seiler, "New Experimental Insights to the Neutron Physics of Small, Low-Enriched, High Temperature Reactor Systems," Annex IV, Annual Report, Paul Scherrer Institute, 1995, pp. 109-118.
- [4-6] D. Mathews, Paul Scherrer Institute, personal communication, March 2001.
- [4-7] I. Murata and A. Takahashi, "Analysis of Critical Assembly Experiments by Continuous Energy Monte Carlo Method with Statistical Geometry Model," Technology Reports of the Osaka University, 48(2304), April 1998, pp. 19-31.

Chapter 5

- [5-1] D. Zhong *et al.*, "Present Status Of The HTR-10 Project," in Proceedings of the IAEA Technical Committee Meeting on Safety Related Design and Economic Aspects of High-Temperature Gas-Cooled Reactors, November 2-4 1998, Beijing.
- [5-2] X. Jing and Y. Sun, "Benchmark Problem of the HTR-10 Initial Core (Version 2000-03)," Institute of Nuclear Energy Technology, Tsinghua University, Beijing, March 2000.
- [5-3] Y. Sun, "HTR-10: Present Status and Future R&D," presentation at 3rd RCM, IAEA CRP-5, Oarai, Japan, March 12-16, 2001.

- [5-4] D.J. Cumberland and R.J. Crawford, The Packing of Particles, Handbook of Powder Technology, Volume 6, Elsevier, Amsterdam, 1987.
- [5-5] Nuclides and Isotopes: A Guide to the Chart of the Nuclides, 15th Edition, General Electric Nuclear, November 1996.
- [5-6] M. S. Abdelrahman and N.M. Abdurrahman, "Cross Section Libraries for Studies of Plutonium Disposition in Light Water Reactors," Amarillo National Resource Center for Plutonium, ANRCP-1999-28, October 1999.
- [5-7] R. E. MacFarlane and D. W. Muir, "The NJOY Nuclear Data Processing System Version 91," LA-12740-M (October 1994).
- [5-8] X. Jing and Y. Sun, "Benchmark Problem of the HTR-10 Initial Core (Draft Version)," Institute of Nuclear Energy Technology, Tsinghua University, Beijing, December 1998.
- [5-9] E. Teuchert *et al.*, "V.S.O.P. ('94): Computer Code System for Reactor Physics and Fuel Cycle Simulation—Input Manual and Comments," Forschungszentrum Jülich, JüL-2897, April 1994.
- [5-10] R. Shindo, K. Yamashita and I. Murata, "DELIGHT-7: One-Dimensional Fuel Cell Burnup Analysis Code for High Temperature Gas-Cooled Reactor (HTGR)," JAERI-M 90-048, 1990.

[5-11] H. Harada and K. Yamashita, "The Reactor Core Analysis Code CITATION-1000VP for High Temperature Engineering Test Reactor," JAERI-M 89-135, 1989.

[5-12] J.R. Askew, A.J. Fayers and P.B. Kemshell, "A General Description of the Lattice Code WIMS," Journal of British Nuclear Society, 5, 1966, p. 564.

Chapter 6

[6-1] E.J. Mulder, "Core Basic Design Report for the PBMR Nuclear Power Plant Project," PBMR (Pty) Limited, Document No. 002979-34, November 2000.

[6-2] V.P. Garin, *et al.*, "Selection and Substantiation of an Annular Core Critical Assembly Configuration Simulating the PBMR Reactor Core at the ASTRA Facility," Russian Research Centre, Kurchatov Institute, Moscow, April 1999.

[6-3] D. Naidoo, "ASTRA Critical Facility Calculational Tasks," PBMR (Pty) Limited, Document No. 003931-34, Revision A, December 2000.

[6-4] V.P. Garin, *et al.*, "Technical description of the ASTRA facility and the conclusion from the evaluation of possibility to carry out experiments on it," Stage A-1.1.1 Report, Russian Research Centre, Kurchatov Institute, Moscow, March 1999.

[6-5] V.P. Garin, *et al.*, "Investigation of critical parameters with varying height of the pebble bed, worth of control rods depending on the depth of its insertion, with

calculational analysis of results obtained," Stage A-1.2.3 Report, Russian Research Centre, Kurchatov Institute, Moscow, 2000.

- [6-6] V.P. Garin, *et al.*, "Measurement of reactivity effects of components and materials important for the PBMR reactor, and of spatial distribution of reaction rates, neutron fluxes and power in axial and radial directions in the ASTRA Facility Assembly," Stage A-1.2.4 Report, Russian Research Centre, Kurchatov Institute, Moscow, February 2000.
- [6-7] Z. Karriem, C. Stoker and F. Reitsma, "MCNP Modelling of HTGR Pebble-Type Fuel," presented at the M&C 2000, Pittsburgh, Pennsylvania, May 7-12, 2000.
- [6-8] M.J. Driscoll, Systems Analysis of the Nuclear Fuel Cycle, class notes for Course 22.351, MIT, Spring 2001.
- [6-9] J.J. Duderstadt and L.J. Hamilton, Nuclear Reactor Analysis, John Wiley & Sons, New York, 1976, p. 434.

Chapter 7

- [7-1] H.R. Trellue and D.I Poston, "User's Manual, Version 2.0 for MONTEBURNS, Version 5B," Los Alamos National Laboratory, Report LA-UR-99-4999, 1999.
- [7-2] J.F. Briesmeister (Ed.), "MCNP—A General Monte Carlo N-Particle Transport Code, Version 4B," Los Alamos National Laboratory, Report LA-12625-M, March 1997.

- [7-3] "ORIGEN 2.1: Isotope Generation and Depletion Code, Matrix Exponential Method," Oak Ridge National Laboratory, Report CCC-371, May 1999.
- [7-4] "MOCUP: MCNP/ORIGEN Coupling Utility Programs," Oak Ridge National Laboratory, Report PSR-365, October 1997.
- [7-5] E. Teuchert, K.A. Haas, H.J. Rütten, H. Brockmann, H. Gerwin, U. Ohlig and W. Scherer, "V.S.O.P. ('94) Computer Code System for Reactor Physics and Fuel Cycle Simulation—Input Manual and Comments," Forschungszentrum Jülich GmbH, JüL-2897, April 1994.
- [7-6] E.J. Mulder, "Core Basic Design Report for the PBMR Nuclear Power Plant Project," PBMR (Pty) Limited, Document No. 002979-34, November 2000.
- [7-7] H. Reutler and G.H. Lohnert, "Advantages of Going Modular in HTRs," Nuclear Engineering and Design, 78, 1984, pp. 129-136.
- [7-8] Siemens-INTERATOM *Hochtemperaturreaktor-Modul-Kraftwerksanlage-Kurzbeschreibung*, November 1988.
- [7-9] J. Singh, H. Hohn and H. Barnert, "Advanced Pebble Bed High Temperature Reactor with Central Graphite Column for Future Applications," Nuclear Engineering and Design, 128, 1991, pp. 383-390.
- [7-10] L. Massimo, Physics of High-Temperature Reactors, Pergamon Press, Oxford, 1976.

[7-11] A.I. van Heek, "Increasing the Power of the High Temperature Reactor Module," Nuclear Engineering and Design, 150, 1994, pp. 183-189.

[7-12] H.J. Rütten, "The Depletion Computer Code ORIGEN-JÜL," KFA Jülich, JÜL-2739, March 1993.

[7-13] Unpublished technical memoranda reporting on the investigation of pebble flow curves for the AVR:

- a) Pohl and Neubacher, *Das Kugelfließverhalten im Innen- und Außencore*
 - *Endauswertung des IC-Durchlaufversuchs*
 - *Simulation des Kugelfließens im AC*AVR GmbH, Ref. No.: H5-X1, P1/Neu/Bot, 4.8.86
- b) Pohl, "Generation of a new model for the flow of spheres for the AVR core following code," AVR GmbH, Ref. No.: H5-X1, P1/Bot, 29.9.87

[7-14] A. Kleine-Tebbe, *Arbeiten zu einen ringförmigen Kugelhaufenkern*, KFA Research Report, September 1995.

[7-15] Z. Karriem, C. Stoker and F. Reitsma, "MCNP Modelling of HTGR Pebble-Type Fuel," presented at the M&C 2000, Pittsburgh, Pennsylvania, May 7-12, 2000.

[7-16] J.R. Johnson, "Monte Carlo Study of Pebble Bed Reactor Fuel Reactivity and Isotopes", SB Thesis, Nuclear Engineering Department, MIT, June 2001.

[7-17] J.R. Johnson, J.R. Leibhaft and M.J. Driscoll, "Burnup Reactivity and Isotopes of an HTGR Fuel Pebble," to be presented at the 2001 ANS Winter Conference.

[7-18] J.R. Askew, A.J. Fayers and P.B. Kemshell, "A General Description of the Lattice Code WIMS," Journal of British Nuclear Society, 5, 1966, pp. 564-585.

Chapter 8

[8-1] "From Renaissance to Reality—Vision 2020," Nuclear Energy Institute, Washington, D.C., 2001.

[8-2] P.E. Owen and K.R. Czerwinski, "Waste Characteristics of Spent Nuclear Fuel from a Pebble Bed Reactor," MIT, Report MIT-NFC-TR-023, June 2000.

[8-3] E.J. Mulder, "Core Basic Design Report for the PBMR Nuclear Power Plant Project," PBMR (Pty) Ltd., Report 002979-34, November 2000.

[8-4] E. Teuchert *et al.*, "V.S.O.P. ('94) Computer Code System for Reactor Physics and Fuel Cycle Simulation – Input Manual and Comments," Forschungszentrum Jülich, JüL-2897, April 1994.

[8-5] J.F. Briesmeister, "MCNP – A General Monte Carlo N-Particle Transport Code, Version 4B," Los Alamos National Laboratory, LA-12625-M, Version 4B, March 1997.

[8-6] A.G. Croff, "ORIGEN 2.1 – Isotope Generation and Depletion Code Matrix Exponential Method," RSICC, Oak Ridge National Laboratory, CCC-371 (ORNL/TM-7175), July 1980.

- [8-7] "MOCUP: MCNP/ORIGEN Coupling Utility Programs," RSICC, Oak Ridge National Laboratory, PSR-365 (INEL-95/0523), October 1997.
- [8-8] E. Teuchert and K.A. Haas, "Nonproliferation Issue of the Pebble Bed High Temperature Reactor," Nuclear Technology, 72, February 1986, pp. 218-222.
- [8-9] "Technological Opportunities to Increase the Proliferation Resistance of Global Civilian Nuclear Power Systems (TOPS)," report by the TOPS task force to the Nuclear Research Advisory Committee (NERAC), January 2001.
- [8-10] J.S. Herring, J.R. Lebenhaft, K.D. Weaver and M.J. Driscoll, "Plutonium Production in a Pebble Bed Reactor," MIT/INEEL, unpublished technical report, August 2000.
- [8-11] E.F. Dean, "Analysis of the Proliferation Resistant Safeguards Applicable to the Fuel Handling and Storage System of the Modular Pebble Bed Reactor," B.S. Thesis, Department of Nuclear Engineering, MIT, September 2001.
- [8-12] B. R. W. Haverkate, A. I. Heek and J. N. T. Jehee, "Nuclear Cogeneration Based on the HTR Technology," Proceedings of the 6th International Conference on Nuclear Engineering, ICONE-6258, 10-14 May 1998.
- [8-13] E. Mulder and E. Teuchert, "OTTO-PAP2 – An Alternative Option to the PBMR Fuelling Philosophy," Technical Committee Meeting on HTGR Technology Development, Commercializing the HTGR, IAEA, Vienna, 13-15 November 1996.

Chapter 9

- [9-1] F.C. Difilippo, "Applications of Monte Carlo Methods for the Analysis of MHTGR Case of the PROTEUS Benchmark," Oak Ridge National Laboratory, Report ORNL/TM-12711, April 1994.
- [9-2] A. Hogenbirk, R.C.L. van der Stad, A.J. Janssen, H. Th. Klippe and J.C. Kuijper, "HTR-PROTEUS Benchmark Calculations. Part 1: Unit cell results LEUPRO-1 and LEUPRO-2," Netherlands Energy Research Foundation, Report ECN-C-95-087, September 1995.
- [9-3] J.S. Herring, J.R. Lebenhaft, K.D. Weaver and M.J. Driscoll, "Plutonium Production in a Pebble Bed Reactor," MIT/INEEL, unpublished technical report, August 2000.
- [9-4] Z. Karriem, C. Stoker and F. Reitsma, "MCNP Modelling of HTGR Pebble-Type Fuel," presented at the M&C 2000, Pittsburgh, Pennsylvania, May 7-12, 2000.
- [9-5] I. Murata, "Studies on Monte Carlo Particle Transport in Irregularly Distributed Fuel Elements for High Temperature Gas-Cooled Reactors," PhD Thesis, Osaka University, Japan, 1999.
- [9-6] I. Murata, A. Takahashi, T. Mori and M. Nakagawa, "New Sampling Method in Continuous Energy Monte Carlo Calculation for Pebble Bed Reactors," Journal of Nuclear Science and Technology, 34(8), August 1997, pp. 734-744.

- [9-7] V.P. Garin, *et al.*, "Measurement of reactivity effects of components and materials important for the PBMR reactor, and of spatial distribution of reaction rates, neutron fluxes and power in axial and radial directions in the ASTRA Facility Assembly," Stage A-1.2.4 Report, Russian Research Centre, Kurchatov Institute, Moscow, February 2000.
- [9-8] H.R. Trellue and D.I Poston, "User's Manual, Version 2.0 for MONTEBURNS, Version 5B," Los Alamos National Laboratory, Report LA-UR-99-4999, 1999.
- [9-9] X. Zhao, "Micro-Heterogeneous Thorium Based Fuel Concepts for Pressurized Water Reactors," Ph.D. thesis, Nuclear Engineering Department, MIT, June 2001.
- [9-10] J.R. Johnson, "Monte Carlo Study of Pebble Bed Reactor Fuel Reactivity and Isotopes", SB Thesis. Nuclear Engineering Department, MIT, June 2001.
- [9-11] A. Hogenbirk, R.C.L. van der Stad, A.J. Janssen, H. Th. Klippel and J.C. Kuijper, "HTR-PROTEUS Benchmark Calculations. Part 1: Unit cell results LEUPRO-1 and LEUPRO-2," Netherlands Energy Research Foundation, Report ECN-C-95-087, September 1995.
- [9-12] J.R. Johnson, J.R. Leibhaft and M.J. Driscoll, "Burnup Reactivity and Isotopes Of an HTGR Fuel Pebble," presented at the American Nuclear Society Winter Meeting, Reno, Nevada, November 11-15, 2001.

Appendix A

[A-1] J.F. Briesmeister (Ed.), "MCNP—A General Monte Carlo N-Particle Transport Code, Version 4B," Los Alamos National Laboratory, Report LA-12625-M, March 1997.

APPENDIX A. MCNP4B Models of the HTR-PROTEUS Facility

This Appendix contains the MCNP4B input files with models of the three HTR-PROTEUS stochastic cores. A description of the MCNP4B code, model creation and input cards may be found in the manual [A-1]. Details of the HTR-PROTEUS facility appear in Chapter 4.

All the calculations reported in this report were performed on a DEC Alpha Personal Workstation 600au running under the Digital UNIX Version 4.0E operating system. MCNP4B and VSOP94 were compiled using the Digital FORTRAN 77 compiler (V5.2-171-428BH and Driver V5.2-10).

APPENDIX A.1: MCNP4B Model of HTR-PROTEUS Core 4.1

```

HTR-PROTEUS EXPERIMENT 4.1 -- IRREGULAR CORE
c
c   MCNP4B model of critical experiment 4.1 in the PROTEUS facility
c   using the detailed geometry specification from the calculational
c   benchmark. The random packing is modeled using a loose BCC, with
c   F/M ratio of one, and a detailed model of coated fuel particles.
c   Uses a 1.5 cm exclusion zone and a detailed top reflector.
c
c   J.R. Lebenhaft, MIT, January 2001
c -----
c   CELL CARDS
c
c
1 0           -1: 11: 22          $ outside world
c
c   reactor structure
c
2 1  8.61e-02      1  -2  -20          $ bottom axial reflector
3 3  6.18e-02      5  -6  16  -21        $ Al ring
4 2  8.84e-02      1  -10 20  -22 #3    $ radial reflector
5 4  5.058e-05     10 -11 20  -22       $ air above rad reflector
6 4  5.058e-05     6  -11 19  -20       $ air between Al and refl
7 3  6.18e-02      6  -11 18  -19       $ outer Al cylinder
8 3  6.18e-02      6  -11 12  -13       $ inner Al cylinder
9 3  6.18e-02      6  -7  13  -18       $ lower Al plate
10 3 6.18e-02      8  -9  13  -18      $ upper Al plate - outer
11 3 6.18e-02      8  -9  -12        $ upper Al plate - inner
12 3 6.18e-02      7  -8  14  -15      $ middle Al cylinder
13 4  5.058e-05     7  -8  13  -14      $ inner air cavity
14 4  5.058e-05     7  -8  15  -18      $ outer air cavity
15 1  8.61e-02      9  -11  -12        $ inner axial reflector
16 1  8.61e-02      9  -11 13  -18      $ outer axial reflector
c
c   core cavity
c
20 4  5.058e-05     4  -8  -12        $ air above core center
21 4  5.058e-05     4  -6  12  -20 #3    $ rest of air above core
22 4  5.058e-05     2  -4  17  -20        $ radial exclusion zone
23 4  5.058e-05     2  -3  -17        $ bottom exclusion zone
24 0               3  -4  -17          $ pebble bed
c
c   universe 1: BCC lattice of pebbles
c
31 0           -51  52  -53  54  -55  56
lat=1  fill=2
u=i
c
c   universe 2: contents of unit cell
c
32 0           -60          fill=3  u=2  $ [ 0  0  0 ]
33 8  8.61659e-02    -61          u=2  $ [ 1  1  1 ]
34 8  8.61659e-02    -62          u=2  $ [ 1  1  -1 ]
35 8  8.61659e-02    -63          u=2  $ [ 1  -1  -1 ]

```

```

36   8  8.61659e-02      -64          u=2 $ [ 1 -1  1]
37   8  8.61659e-02      -65          u=2 $ [-1  1  1]
38   8  8.61659e-02      -66          u=2 $ [-1  1 -1]
39   8  8.61659e-02      -67          u=2 $ [-1 -1 -1]
40   8  8.61659e-02      -68          u=2 $ [-1 -1  1]
41   4  5.058e-05       60  61  62  63  64          $ air between
                                         65  66  67  68          u=2 $ pebbles
c
c      universe 3: contents of fuel pebble
c
45   6  8.64564e-02      85          u=3 $ graphite shell
46   0                   -85          fill=4 u=3 $ fueled region
c
c      universe 4: embedded coated fuel particles
c
50   0                   -87  88 -89  90 -91  92
     lat=1  fill=5
     u=4
c
c      universe 5: coated fuel particle
c
51   10 -10.88         -95          u=5 $ UO2 kernel
52   11 -1.1           95 -96        u=5 $ PyC layer 1
53   12 -1.9           96 -97        u=5 $ PyC layer 2
54   13 -3.2           97 -98        u=5 $ SiC layer
55   12 -1.89          98 -99        u=5 $ PyC layer 3
56   6   8.64564e-02    99          u=5 $ graphite matrix
c
c -----
c      SURFACE CARDS
c
c      reactor structure surfaces
c
1   pz    0.0          $ bottom of reactor
2   pz    78.0         $ bottom of pebble bed
3   pz    79.5         $ bottom exclusion zone
4   pz    234.5        $ top of core
5   pz    251.0        $ lower surface of Al ring
6   pz    252.0        $ upper surface of Al ring
7   pz    252.4        $ upper surface of bot. Al plate
8   pz    267.0        $ lower surface of top Al plate
9   pz    267.2        $ upper surface of top Al plate
10  pz    330.0        $ top of radial reflector
11  pz    345.3        $ top of reactor
12  cz    19.88        $ inside of inner Al cylinder
13  cz    20.38        $ outside of inner Al cylinder
14  cz    43.15        $ inside of middle Al cylinder
15  cz    43.55        $ outside of middle Al cylinder
16  cz    60.0          $ inner surface of Al ring
17  cz    61.0          $ radial exclusion zone
18  cz    61.95        $ inside of outer Al cylinder
19  cz    62.25        $ outside of outer Al cylinder
20  cz    62.5          $ inner surface of radial reflector
21  cz    70.0          $ outer surface of Al ring
22  cz    166.1         $ outer surface of radial reflector
c

```

```

c      Pebble bed surfaces
c
c      unit cell in core
c
51  px    3.6119940                      $ [ 1   0   0]
52  px    -3.6119940                     $ [-1   0   0]
53  py    3.6119940                      $ [ 0   1   0]
54  py    -3.6119940                     $ [ 0  -1   0]
55  pz    3.6119940                      $ [ 0   0   1]
56  pz    -3.6119940                     $ [ 0   0  -1]

c
c      balls in unit cells
c
60  so    3.0
61  s     3.6119940  3.6119940  3.6119940  3.0
62  s     3.6119940  3.6119940 -3.6119940  3.0
63  s     3.6119940 -3.6119940 -3.6119940  3.0
64  s     3.6119940 -3.6119940  3.6119940  3.0
65  s    -3.6119940  3.6119940  3.6119940  3.0
66  s    -3.6119940  3.6119940 -3.6119940  3.0
67  s    -3.6119940 -3.6119940 -3.6119940  3.0
68  s    -3.6119940 -3.6119940  3.6119940  3.0

c
c      inside fuel pebble
c
85  so    2.5                                $ fueled region
c
c      unit cell for CFP lattice
c
87  px    0.0955071
88  px    -0.0955071
89  py    0.0955071
90  py    -0.0955071
91  pz    0.0955071
92  pz    -0.0955071

c
c      coated fuel particle
95  so    0.02510                          $ UO2 kernel
96  so    0.03425                          $ buffer
97  so    0.03824                          $ inner PyC
98  so    0.04177                          $ SiC
99  so    0.04577                          $ outer PyC
c -----
c
c      RUN PARAMETERS
c
c      problem type
c
mode n
kcode 5000 1.0 10 110
ksrc  0  0  81.611994   0  0  88.835982   0  0  96.059970
      0  0 103.283958   0  0 110.507946   0  0 117.731934
      0  0 124.955922   0  0 132.179910   0  0 139.403898
      0  0 146.627886

totnu
print
dbcn 9j 300

```

```

prdmp j -60 1 2
c
c      neutron importance
c
imp:n 0                                $ outside world
    1 14r                                $ reactor structure
    1 4r                                $ core cavity
    1                                    $ u=1: lattice
    1 9r                                $ u=2: unit cell
    1 1                                $ u=3: fuel pebble
    1                                    $ u=4: CFP lattice
    1 5r                                $ u=5: CFP

c
c      transformations
c
tr1 0.0        0.0        81.6119940
c
c      material specifications
c
c      axial reflector
m1   6000.60c 8.61e-02     5011.60c 3.60e-08     5010.60c 9.00e-09
mt1  grph.01t
c
c      radial reflector
m2   6000.60c 8.84e-02     5011.60c 3.70e-08     5010.60c 9.20e-09
mt2  grph.01t
c
m3   13027.60c 1                         $ aluminum
c
c      humid air
m4   1001.60c 5.79913e-07   1002.60c 8.7e-11     7014.60c 3.98536e-05
    7015.60c 1.46400e-07   8016.60c 1.0e-05
c
c      pebble graphite shell
m6   5010.60c 2.47855e-08   5011.60c 1.00394e-07   6000.60c 8.64563e-02
mt6  grph.01t
c
c      moderator pebble (N = 8.38303e-02)
m8   5010.60c 2.40326e-08   5011.60c 9.73442e-08   6000.60c 8.38302e-02
mt8  grph.01t
c
c      fuel kernel (N = 7.292359e-02)
m10  92235.60c 4.11729e-03  92238.60c 2.01906e-02   8016.60c 4.86157e-02
c
c      buffer
m11  6000.60c 5.51511e-02   5011.60c 6.40418e-08   5010.60c 1.58108e-08
mt11 grph.01t
c
c      PyC
m12  6000.60c 9.52609e-02   5011.60c 1.10617e-07   5010.60c 2.73095e-08
mt12 grph.01t
c
c      SiC
m13  14000.60c 4.80603e-02   6000.60c 4.80603e-02   5011.60c 5.58080e-08
    5010.60c 1.37780e-08
mt13 grph.01t

```

APPENDIX A.2: MCNP4B Model of HTR-PROTEUS Core 4.2

```

HTR-PROTEUS EXPERIMENT 4.2 -- IRREGULAR CORE
c
c      MCNP4B model of critical experiment 4.2 in the PROTEUS facility
c      using the detailed geometry specification from the calculational
c      benchmark. The random packing is modeled using a loose BCC, with
c      F/M ratio of one, and a detailed model of coated fuel particles.
c      Uses a 1.5 cm exclusion zone and a detailed top reflector.
c
c      J.R. Lebenhaft, MIT, January 2001
c -----
c      CELL CARDS
c
1   0                      -1: 11: 22          $ outside world
c
c      reactor structure
c
2   1   8.61e-02           1   -2  -20          $ bottom axial reflector
3   3   6.18e-02           5   -6   16  -21          $ Al ring
4   2   8.84e-02           1  -10   20  -22  #3  $ radial reflector
5   4   5.058e-05          10  -11   20  -22          $ air above rad reflector
6   4   5.058e-05          6  -11   19  -20          $ air between Al and ref
7   3   6.18e-02           6  -11   18  -19          $ outer Al cylinder
8   3   6.18e-02           6  -11   12  -13          $ inner Al cylinder
9   3   6.18e-02           6   -7   13  -18          $ lower Al plate
10  3   6.18e-02           8   -9   13  -18          $ upper Al plate - outer
11  3   6.18e-02           8   -9  -12          $ upper Al plate - inner
12  3   6.18e-02           7   -8   14  -15          $ middle Al cylinder
13  4   5.058e-05          7   -8   13  -14          $ inner air cavity
14  4   5.058e-05          7   -8   15  -18          $ outer air cavity
15  1   8.61e-02           9  -11  -12          $ inner axial reflector
16  1   8.61e-02           9  -11   13  -18          $ outer axial reflector
c
c      core cavity
c
20  4   5.058e-05          4   -8  -12          $ air above core center
21  4   5.058e-05          4   -6   12  -20  #3  $ rest of air above core
22  4   5.058e-05          2   -4   17  -20          $ radial exclusion zone
23  4   5.058e-05          2   -3  -17          $ bottom exclusion zone
24  0                   3   -4  -17
                           fill=1(1)          $ pebble bed
c
c      universe 1: BCC lattice of pebbles
c
31  0                   -51   52  -53   54  -55   56
lat=1    fill=2
u=1
c
c      universe 2: contents of unit cell
c
32  0                   -60
                           fill=3  u=2  $ [ 0   0   0]
33  8   8.61659e-02       -61
                           u=2  $ [ 1   1   1]
34  8   8.61659e-02       -62
                           u=2  $ [ 1   1  -1]
35  8   8.61659e-02       -63
                           u=2  $ [ 1  -1  -1]
36  8   8.61659e-02       -64
                           u=2  $ [ 1  -1   1]

```

```

37  8  8.61659e-02      -65          u=2 $ [-1 1 1]
38  8  8.61659e-02      -66          u=2 $ [-1 1 -1]
39  8  8.61659e-02      -67          u=2 $ [-1 -1 -1]
40  8  8.61659e-02      -68          u=2 $ [-1 -1 1]
41  4  5.058e-05       60 61 62 63 64      u=2 $ air between
                                         65 66 67 68
pebbles
c
c      universe 3: contents of fuel pebble
c
45  6  8.64564e-02      85          u=3 $ graphite shell
46  0                  -85          fill=4 u=3 $ fueled region
c
c      universe 4: embedded coated fuel particles
c
50  0                  -87 88 -89 90 -91 92
    lat=1 fill=5
    u=4
c
c      universe 5: coated fuel particle
c
51  10 -10.88          -95          u=5 $ UO2 kernel
52  11 -1.1             95 -96        u=5 $ PyC layer 1
53  12 -1.9             96 -97        u=5 $ PyC layer 2
54  13 -3.2             97 -98        u=5 $ SiC layer
55  12 -1.89            98 -99        u=5 $ PyC layer 3
56  6   8.64564e-02     99          u=5 $ graphite matrix
c
c -----
c      SURFACE CARDS
c
c      reactor structure surfaces
c
1  pz    0.0           $ bottom of reactor
2  pz    78.0          $ bottom of pebble bed
3  pz    79.5          $ bottom exclusion zone
4  pz    228.5          $ top of pebble bed
5  pz    251.0          $ lower surface of Al ring
6  pz    252.0          $ upper surface of Al ring
7  pz    252.4          $ upper surface of bottom Al plate
8  pz    267.0          $ lower surface of top Al plate
9  pz    267.2          $ upper surface of top Al plate
10  pz   330.0          $ top of radial reflector
11  pz   345.3          $ top of reactor
12  cz   19.88          $ inside of inner Al cylinder
13  cz   20.38          $ outside of inner Al cylinder
14  cz   43.15          $ inside of middle Al cylinder
15  cz   43.55          $ outside of middle Al cylinder
16  cz   60.0           $ inner surface of Al ring
17  cz   61.0           $ radial exclusion zone
18  cz   61.95          $ inner surface of outer Al cylinder
19  cz   62.25          $ outer surface of outer Al cylinder
20  cz   62.5           $ inner surface of radial reflector
21  cz   70.0           $ outer surface of Al ring
22  cz   166.1          $ outer surface of radial reflector
c

```

```

c      pebble bed surfaces
c
c      Unit cell in core
c
51   px    3.5823865                      $ [-1  0  0]
52   px    -3.5823865                     $ [ 1  0  0]
53   py    3.5823865                      $ [ 0  1  0]
54   py    -3.5823865                     $ [ 0 -1  0]
55   pz    3.5823865                      $ [ 0  0  1]
56   pz    -3.5823865                     $ [ 0  0 -1]
c
c      Balls in unit cells
c
60   so    3.0
61   s     3.5823865  3.5823865  3.5823865  3.0
62   s     3.5823865  3.5823865 -3.5823865  3.0
63   s     3.5823865 -3.5823865 -3.5823865  3.0
64   s     3.5823865 -3.5823865  3.5823865  3.0
65   s     -3.5823865  3.5823865  3.5823865  3.0
66   s     -3.5823865  3.5823865 -3.5823865  3.0
67   s     -3.5823865 -3.5823865 -3.5823865  3.0
68   s     -3.5823865 -3.5823865  3.5823865  3.0
c
c      inside fuel pebble
c
85   so    2.5                                $ fueled region
c
c      unit cell for CFP lattice
c
87   px    0.0955071
88   px    -0.0955071
89   py    0.0955071
90   py    -0.0955071
91   pz    0.0955071
92   pz    -0.0955071
c
c      coated fuel particle
95   so    0.02510                          $ UO2 kernel
96   so    0.03425                          $ buffer
97   so    0.03824                          $ inner PyC
98   so    0.04177                          $ SiC
99   so    0.04577                          $ outer PyC
c
-----
```

c RUN PARAMETERS

c problem type

c

mode n

kcode 5000 1.0 10 110

ksrc	0 0 81.5823865	0 0 88.7471595	0 0 95.9119325
	0 0 103.0767055	0 0 110.2414785	0 0 117.4062515
	0 0 124.5710245	0 0 131.7357975	0 0 138.9005705
	0 0 146.0653435		

totnu

print

dbcn 9j 300

```

prdmp j -60 1 2
c
c      neutron importance
c
imp:n 0                                $ outside world
    1 14r                                $ reactor structure
    1 4r                                 $ core cavity
    1                                     $ u=1: lattice
    1 9r                                 $ u=2: unit cell
    1 1                                 $ u=3: fuel pebble
    1                                     $ u=4: CFP lattice
    1 5r                                 $ u=5: CFP

c
c      transformations
c
tr1 0.0        0.0        81.5823865
c
c      material specifications
c
c      axial reflector
m1   6000.60c 8.61e-02     5011.60c 3.60e-08     5010.60c 9.00e-09
mt1  grph.01t
c
c      radial reflector
m2   6000.60c 8.84e-02     5011.60c 3.70e-08     5010.60c 9.20e-09
mt2  grph.01t
c
m3   13027.60c 1                         $ aluminum
c
c      humid air
m4   1001.60c 5.79913e-07   1002.60c 8.7e-11      7014.60c 3.98536e-05
    7015.60c 1.46400e-07   8016.60c 1.0e-05
c
c      pebble graphite shell
m6   5010.60c 2.47855e-08   5011.60c 1.00394e-07   6000.60c 8.64563e-02
mt6  grph.01t
c
c      moderator pebble (N = 8.38303e-02)
m8   5010.60c 2.40326e-08   5011.60c 9.73442e-08   6000.60c 8.38302e-02
mt8  grph.01t
c
c      fuel kernel (N = 6.958395e-02)
m10  92235.60c 4.11729e-03  92238.60c 2.01906e-02   8016.60c 4.86157e-02
c
c      buffer
m11  6000.60c 5.51511e-02   5011.60c 6.40418e-08   5010.60c 1.58108e-08
mt11 grph.01t
c
c      PyC
m12  6000.60c 9.52609e-02   5011.60c 1.10617e-07   5010.60c 2.73095e-08
mt12 grph.01t
c
c      SiC
m13  14000.60c 4.80603e-02   6000.60c 4.80603e-02   5011.60c 5.58080e-08
    5010.60c 1.37780e-08
mt13 grph.01t

```

APPENDIX A.3: MCNP4B Model of HTR-PROTEUS Core 4.3

```

HTR-PROTEUS EXPERIMENT 4.3 -- IRREGULAR CORE
c
c      MCNP4B model of critical experiment 4.3 in the PROTEUS facility
c      using the detailed geometry specification from the calculational
c      benchmark. The random packing is modeled using a loose BCC, with
c      F/M ratio of one, and a detailed model of coated fuel particles.
c      Uses a 1.5 cm exclusion zone to account for partial pebbles at
c      core edge, and a detailed representation of the top reflector.
c
c      J.R. Lebenhaft, MIT, January 2001
c -----
c      CELL CARDS
c
c
1   0                      -1: 11: 22          $ outside world
c
c      reactor structure
c
2   1   8.61e-02           1  -2  -20          $ bottom axial reflector
3   3   6.18e-02           5  -6  16  -21          $ Al ring
4   2   8.84e-02           1  -10 20  -22 #3    $ radial reflector
5   4   5.058e-05          10 -11 20  -22          $ air above rad reflector
6   4   5.058e-05          6  -11 19  -20          $ air between Al and ref
7   3   6.18e-02           6  -11 18  -19          $ outer Al cylinder
8   3   6.18e-02           6  -11 12  -13          $ inner Al cylinder
9   3   6.18e-02           6  -7  13  -18          $ lower Al plate
10  3   6.18e-02           8  -9  13  -18          $ upper Al plate - outer
11  3   6.18e-02           8  -9  -12           $ upper Al plate - inner
12  3   6.18e-02           7  -8  14  -15          $ middle Al cylinder
13  4   5.058e-05          7  -8  13  -14          $ inner air cavity
14  4   5.058e-05          7  -8  15  -18          $ outer air cavity
15  1   8.61e-02           9  -11 -12           $ inner axial reflector
16  1   8.61e-02           9  -11 13  -18          $ outer axial reflector
c
c      core cavity
c
20  4   5.058e-05          4  -8  -12          $ air above core center
21  4   5.058e-05          4  -6  12  -20 #3    $ rest of air above core
22  4   5.058e-05          2  -4  17  -20          $ radial exclusion zone
23  4   5.058e-05          2  -3  -17           $ bottom exclusion zone
24  0                           3  -4  -17
                               fill=1(1)          $ pebble bed
c
c      universe 1: BCC lattice of pebbles
c
31  0                      -51  52  -53  54  -55  56
lat=1    fill=2
u=1
c
c      universe 2: contents of unit cell
c
32  0                      -60          fill=3  u=2  $ [ 0  0  0]
33  8   8.61659e-02        -61          u=2  $ [ 1  1  1]
34  8   8.61659e-02        -62          u=2  $ [ 1  1  -1]

```

```

35   8  8.61659e-02    -63          u=2 $ [ 1 -1 -1]
36   8  8.61659e-02    -64          u=2 $ [ 1 -1  1]
37   8  8.61659e-02    -65          u=2 $ [-1  1  1]
38   8  8.61659e-02    -66          u=2 $ [-1  1 -1]
39   8  8.61659e-02    -67          u=2 $ [-1 -1 -1]
40   8  8.61659e-02    -68          u=2 $ [-1 -1  1]
41   4  5.058e-05      60  61  62  63  64          u=2 $ air bet pebbles
c
c      universe 3: contents of fuel pebble
c
45   6  8.64564e-02    85          u=3 $ graphite shell
46   0                  -85          fill=4 u=3 $ fueled region
c
c      universe 4: embedded coated fuel particles
c
50   0                  -87  88 -89  90 -91  92
lat=1  fill=5
u=4
c
c      universe 5: coated fuel particle
c
51  10 -10.88         -95          u=5 $ UO2 kernel
52  11 -1.1           95 -96        u=5 $ PyC layer 1
53  12 -1.9           96 -97        u=5 $ PyC layer 2
54  13 -3.2           97 -98        u=5 $ SiC layer
55  12 -1.89          98 -99        u=5 $ PyC layer 3
56  6   8.64564e-02   99          u=5 $ graphite matrix
c
c -----
c      SURFACE CARDS
c
c      reactor structure surfaces
c
1   pz    0.0          $ bottom of reactor
2   pz    78.0         $ bottom of pebble bed
3   pz    79.5         $ bottom exclusion zone
4   pz    226.5        $ top of pebble bed minus exclusion
5   pz    251.0        $ lower surface of Al ring
6   pz    252.0        $ upper surface of Al ring
7   pz    252.4        $ upper surface of bottom Al plate
8   pz    267.0        $ lower surface of top Al plate
9   pz    267.2        $ upper surface of top Al plate
10  pz    330.0        $ top of radial reflector
11  pz    345.3        $ top of reactor
12  cz    19.88        $ inside of inner Al cylinder
13  cz    20.38        $ outside of inner Al cylinder
14  cz    43.15        $ inside of middle Al cylinder
15  cz    43.55        $ outside of middle Al cylinder
16  cz    60.0          $ inner surface of Al ring
17  cz    61.0          $ radial exclusion zone
18  cz    61.95        $ inner surface of outer Al cylinder
19  cz    62.25        $ outer surface of outer Al cylinder
20  cz    62.5          $ inner surface of radial reflector
21  cz    70.0          $ outer surface of Al ring
22  cz    166.1        $ outer surface of radial reflector

```

```

c
c      pebble bed surfaces
c
c      Unit cell in core
c
51   px    3.576580                      $ [-1  0  0]
52   px    -3.576580                     $ [ 1  0  0]
53   py    3.576580                      $ [ 0  1  0]
54   py    -3.576580                     $ [ 0 -1  0]
55   pz    3.576580                      $ [ 0  0  1]
56   pz    -3.576580                    $ [ 0  0 -1]
c
c      Balls in unit cells
c
60   so    3.0
61   s     3.576580    3.576580    3.576580  3.0
62   s     3.576580    3.576580   -3.576580  3.0
63   s     3.576580   -3.576580   -3.576580  3.0
64   s     3.576580   -3.576580    3.576580  3.0
65   s     -3.576580    3.576580    3.576580  3.0
66   s     -3.576580    3.576580   -3.576580  3.0
67   s     -3.576580   -3.576580   -3.576580  3.0
68   s     -3.576580   -3.576580    3.576580  3.0
c
c      inside fuel pebble
c
85   so    2.5                                $ fueled region
c
c      unit cell for CFP lattice
c
87   px    0.0955071
88   px    -0.0955071
89   py    0.0955071
90   py    -0.0955071
91   pz    0.0955071
92   pz    -0.0955071
c
c      coated fuel particle
95   so    0.02510                          $ UO2 kernel
96   so    0.03425                          $ buffer
97   so    0.03824                          $ inner PyC
98   so    0.04177                          $ SiC
99   so    0.04577                          $ outer PyC
c
-----
```

c RUN PARAMETERS

c problem type

c

mode n

kcode 5000 1.0 10 110

ksrc	0 0 81.576580	0 0 88.729740	0 0 95.882900
	0 0 103.036060	0 0 110.189220	0 0 117.342380
	0 0 124.495540	0 0 131.648700	0 0 138.801860
	0 0 145.955020		

totnu

print

```

dbcn 9j 300
prdmp j -60 1 2
c
c      neutron importance
c
imp:n 0                                $ outside world
    1 14r                                $ reactor structure
    1 4r                                 $ core cavity
    1                                     $ u=1: lattice
    1 9r                                 $ u=2: unit cell
    1 1                                 $ u=3: fuel pebble
    1                                     $ u=4: CFP lattice
    1 5r                                 $ u=5: CFP

c
c      transformations
c
tr1 0.0        0.0        81.576580
c
c      material specifications
c
c      axial reflector
m1   6000.60c 8.61e-02     5011.60c 3.60e-08     5010.60c 9.00e-09
mt1  grph.01t
c
c      radial reflector
m2   6000.60c 8.84e-02     5011.60c 3.70e-08     5010.60c 9.20e-09
mt2  grph.01t
c
m3   13027.60c 1                         $ aluminum
c
c      humid air
m4   1001.60c 5.79913e-07   1002.60c 8.7e-11     7014.60c 3.98536e-05
    7015.60c 1.46400e-07   8016.60c 1.0e-05
c
c      pebble graphite shell
m6   5010.60c 2.47855e-08   5011.60c 1.00394e-07   6000.60c 8.64563e-02
mt6  grph.01t
c
c      moderator pebble (N = 8.38303e-02)
m8   5010.60c 2.40326e-08   5011.60c 9.73442e-08   6000.60c 8.38302e-02
mt8  grph.01t
c
c      fuel kernel (N = 6.958395e-02)
m10  92235.60c 4.11729e-03  92238.60c 2.01906e-02   8016.60c 4.86157e-02
c
c      buffer
m11  6000.60c 5.51511e-02   5011.60c 6.40418e-08   5010.60c 1.58108e-08
mt11 grph.01t
c
c      PyC
m12  6000.60c 9.52609e-02   5011.60c 1.10617e-07   5010.60c 2.73095e-08
mt12 grph.01t
c
c      SiC
m13  14000.60c 4.80603e-02   6000.60c 4.80603e-02   5011.60c 5.58080e-08
    5010.60c 1.37780e-08
mt13 grph.01t

```

APPENDIX B. MCNP4B Models of HTR-10

This Appendix contains the MCNP4B input files with models of the HTR-10 reactor. The model of the initial critical core for benchmark problem B1, which uses the standard ENDF/B-VI cross-section libraries, appears in Appendix B.1. The model of the reactor for benchmark problem B2.1, with a full core and using the University of Texas at Austin libraries, appears in Appendix B.2. Details of the HTR-10 reactor appear in Chapter 5.

APPENDIX B-1: MCNP4B Model of HTR-10 Benchmark Problem B1

HTR-10 PEBBLE-BED REACTOR

c MCNP4B model of the HTR-10 initial core, based on IAEA benchmark
c problem CRP-5 specification. Benchmark problem B1.

c Modeling assumptions:

c A BCC lattice of spheres in core with 0.61 packing fraction and a
c 1:1 mix of fuel and moderator pebbles in cylindrical portion of
c core, but adjusted with moderator pebble size reduced to
c approximate a 57:43 fuel-to-moderator ratio. The control,
c irradiation, KLAK and He channels were modeled explicitly. A 1.71
c cm radial exclusion zone corrects for core-edge fuel pebbles.

c Prepared by J.R. Lebenhaft (MIT) December 2000

c -----

c Revision history:

c January 2001, J. Lebenhaft - detailed model of control rods

=====

c CELL CARDS

c

1	0	1:	-17:	29	\$ outside world		
Graphite reactor structure							
2	2	0.0762391	-1	2	-23	\$ zone 1	
3	3	0.0851467	-2	3	-23	\$ zone 2	
4	4	0.0145351	-3	4	-23	\$ zone 3	
5	5	0.0802920	-4	6	-23	\$ zone 4	
6	1	0.0851052	30	9	-23	\$ zone 0	
7	7	0.0538278	-9	14	-20	\$ zone 6	
8	7	0.0538278	-14	16	-20	\$ zone 7	
9	18	0.0797184	-16	17	-20	\$ zone 81	
10	8	0.0781412	-9	10	20	-23	\$ zone 8
11	9	0.0823755	-10	11	20	-23	\$ zone 9
12	10	0.0846632	-11	12	20	-21	\$ zone 10
13	11	0.0818665	-11	12	21	-23	\$ zone 11
14	12	0.0852881	-12	15	20	-21	\$ zone 12
15	13	0.0819526	-12	13	21	-23	\$ zone 13
16	14	0.0541695	-13	14	21	-22	\$ zone 14
17	15	0.0332112	-13	14	22	-23	\$ zone 15
18	16	0.0882170	-14	15	21	-23	\$ zone 16
19	17	0.0800619	-15	16	20	-24	\$ zone 17
20	18	0.0797184	-16	17	20	-24	\$ zone 18
21	19	0.0795574	-1	2	23	-24	\$ zone 19
22	20	0.0878379	-2	3	23	-24	\$ zone 20
23	21	0.0579699	-3	4	23	-24	\$ zone 21
24	22	0.0882423	-4	9	23	-24	\$ zone 22
25	22	0.0882423	-9	11	23	-24	\$ zone 23
26	23	0.0881225	-11	12	23	-24	\$ zone 24

27	22	0.0882423	-12	13	23	-24		\$ zone 25
28	24	0.0846759	-13	14	23	-24		\$ zone 26
29	22	0.0882423	-14	15	23	-24		\$ zone 80
30	25	8.55939e-02	-1	2	24	-25		\$ zone 27
			260	261	262	263	264	265
			266	267	268	269		
			(275:-276:(277		279)	: (280 -278))		
			(281:-282:(283		285)	: (286 -284))		
			(287:-288:(289		291)	: (292 -290))		
			(293:-294:(295		297)	: (298 -296))		
			(299:-300:(301		303)	: (304 -302))		
			(305:-306:(307		309)	: (310 -308))		
			(311:-312:(313		315)	: (316 ^14))		
			340	341	342			
31	26	9.43585e-02	-2	3	24	-25		\$ zone 28
			260	261	262	263	264	265
			266	267	268	269		
			(275:-276:(277		279)	: (280 -278))		
			(281:-282:(283		285)	: (286 -284))		
			(287:-288:(289		291)	: (292 -290))		
			(293:-294:(295		297)	: (298 -296))		
			(299:-300:(301		303)	: (304 -302))		
			(305:-306:(307		309)	: (310 -308))		
			(311:-312:(313		315)	: (316 -314))		
			340	341	342			
32	27	5.61302e-02	-3	4	24	-25		\$ zone 29
			260	261	262	263	264	265
			266	267	268	269		
			(275:-276:(277		279)	: (280 -278))		
			(281:-282:(283		285)	: (286 -284))		
			(287:-288:(289		291)	: (292 -290))		
			(293:-294:(295		297)	: (298 -296))		
			(299:-300:(301		303)	: (304 -302))		
			(305:-306:(307		309)	: (310 -308))		
			(311:-312:(313		315)	: (316 -314))		
			340	341	342			
33	26	9.43585e-02	-4	5	24	-25		\$ zone 82
			260	261	262	263	264	265
			266	267	268	269		
			(275:-276:(277		279)	: (280 -278))		
			(281:-282:(283		285)	: (286 -284))		
			(287:-288:(289		291)	: (292 -290))		
			(293:-294:(295		297)	: (298 -296))		
			(299:-300:(301		303)	: (304 -302))		
			(305:-306:(307		309)	: (310 -308))		
			(311:-312:(313		315)	: (316 -314))		
			340	341	342			
34	28	9.43396e-02	-5	6	24	-25		\$ zone 30
			260	261	262	263	264	265
			266	267	268	269		
			(275:-276:(277		279)	: (280 -278))		
			(281:-282:(283		285)	: (286 -284))		
			(287:-288:(289		291)	: (292 -290))		
			(293:-294:(295		297)	: (298 -296))		
			(299:-300:(301		303)	: (304 -302))		
			(305:-306:(307		309)	: (310 -308))		
			(311:-312:(313		315)	: (316 -314))		

35	29	8.81642e-02		340	341	342		\$ zones 31-40
				-6	9	24	-25	
				260	261	262	263	264
				265	266	267	268	269
				(275:-276:(277	(279):(280	-278))		
				(281:-282:(283	(285):(286	-284))		
				(287:-288:(289	(291):(292	-290))		
				(293:-294:(295	(297):(298	-296))		
				(299:-300:(301	(303):(304	-302))		
				(305:-306:(307	(309):(310	-308))		
				(311:-312:(313	(315):(316	-314))		
				340	341	342		
76	45	9.43396e-02		-9	18	24	-25	\$ zone 41a -
260	261	262	263	264	265			\$ at bottom
				266	267	268	269	\$ of CR
				(275:-276:(277	(279):(280	-278))		
				(281:-282:(283	(285):(286	-284))		
				(287:-288:(289	(291):(292	-290))		
				(293:-294:(295	(297):(298	-296))		
				(299:-300:(301	(303):(304	-302))		
				(305:-306:(307	(309):(310	-308))		
				(311:-312:(313	(315):(316	-314))		
36	28	0.0678903		-18	11	24	-25	\$ zone 41b
37	30	0.0678011		-11	12	24	-25	\$ zone 42
38	31	0.0861481		-12	13	24	-25	\$ zone 43
39	32	0.0829070		-13	14	24	-25	\$ zone 44
40	31	0.0861481		-14	15	24	-25	\$ zone 45
41	33	0.0781618		-15	16	24	-25	\$ zone 46
42	18	0.0778265		-16	17	24	-25	\$ zone 47
43	17	0.0800619		-1	2	25	-28	\$ zone 74
44	22	0.0882423		-2	3	25	-27	\$ zone 66a
45	22	0.0882423		-2	9	27	-28	\$ zone 66b
46	35	0.0582702		-3	4	25	-26	\$ zone 48
47	22	0.0882423		-4	9	25	-26	\$ zone 49
48	22	0.0882423		-9	11	25	-26	\$ zone 50
49	23	0.0881225		-11	12	25	-26	\$ zone 51
50	22	0.0882423		-12	13	25	-26	\$ zone 52
51	36	0.0855865		-13	14	25	-26	\$ zone 53
52	22	0.0882423		-14	15	25	-26	\$ zone 54
53	17	0.0800619		-15	16	25	-26	\$ zone 55
54	18	0.0797184		-16	17	25	-26	\$ zone 56
55	37	0.0728266		-3	4	26	-27	\$ zone 57
56	38	0.0760372		-4	9	26	-27	\$ zone 58
				320	321	322	323	324
				325	326	327	328	329
				330	331	332	333	334
				335	336	337	338	339
57	38	0.0760372		-9	11	26	-27	\$ zone 59
58	39	0.0759340		-11	12	26	-27	\$ zone 60
59	38	0.0760372		-12	13	26	-27	\$ zone 61
60	40	0.0737488		-13	14	26	-27	\$ zone 62
61	38	0.0760372		-14	15	26	-27	\$ zone 63
62	41	0.0689883		-15	16	26	-27	\$ zone 64
63	18	0.0686924		-16	17	26	-27	\$ zone 65
64	22	0.0882423		-9	11	27	-28	\$ zone 67
65	23	0.0881225		-11	12	27	-28	\$ zone 68
66	22	0.0882423		-12	13	27	-28	\$ zone 69

```

67  43  0.0861505    -13   14   27  -28      $ zone 70
68  22  0.0882423    -14   15   27  -28      $ zone 71
69  17  0.0800619    -15   16   27  -28      $ zone 72
70  18  0.0797184    -16   17   27  -28      $ zone 73
71  17  0.0800619    -1    2   28  -29      $ zone 75
72  17  0.0800619    -2   13   28  -29      $ zone 76
73  44  0.0783836    -13   14   28  -29      $ zone 77
74  17  0.0800619    -14   16   28  -29      $ zone 78
75  17  0.0800619    -16   17   28  -29      $ zone 79
c
c   Cavity above core
c
80  50  5.058e-05     -6    7  -23      $ air
c
c   -----
c   Cylindrical Region of Core
c
84  50  5.058e-05     -7    8   19  -23      $ radial gap
85  0           -7    8  -19      fill=10(1) $ pebble bed
c
c   Universe 10: BCC lattice of fuel and dummy spheres
c
86  0           45  -46  -47   48  -49   50
lat=1  fill=11
u=10
c
c   Universe 11: unit cell
c
87  0           -51      fill=12  u=11  $ fuel [ 0  0  0]
88  64  9.225716e-02 -52
89  64  9.225716e-02 -53
90  64  9.225716e-02 -54
91  64  9.225716e-02 -55
92  64  9.225716e-02 -56
93  64  9.225716e-02 -57
94  64  9.225716e-02 -58
95  64  9.225716e-02 -59
96  50  5.058e-05     51   52   53   54   55
                           56   57   58   59      u=11  $ air in between
c
c   Universe 12: details of fuel element
c
97  65  8.674180e-02  41      u=12  $ graphite shell
98  0           -41      fill=13  u=12  $ fuel region
c
c   Universe 13: embedded coated fuel particles
c
99  0           -250  251  -252  253  -254  255
lat=1  fill=14
u=13
c
c   Universe 14: coated fuel particle
c
100 61  6.970994e-02 -245      u=14  $ UO2 kernel
101 62  -1.1          245  -246      u=14  $ PyC layer 1
102 62  -1.9          246  -247      u=14  $ PyC layer 2
103 63  -3.18         247  -248      u=14  $ SiC layer

```

```

104 62 -1.9          248 -249           u=14 $ PyC layer 3
105 65 8.674180e-02 249           u=14 $ graphite matrix
c
c -----
c   Conus Region of Core (dummy balls)
c
110 0                 -8   9 -30       fill=20(2)
c
c   Universe 20: BCC lattice of dummy spheres
c
111 0                 45 -46 -47  48 -49  50
lat=1  fill=21
u=20
c
c   Universe 21: unit cell
c
112 64 9.225716e-02 -51           u=21 $ mod [ 0  0  0]
113 64 9.225716e-02 -52           u=21 $ mod [ 1  1  1]
114 64 9.225716e-02 -53           u=21 $ mod [ 1  1 -1]
115 64 9.225716e-02 -54           u=21 $ mod [ 1 -1 -1]
116 64 9.225716e-02 -55           u=21 $ mod [ 1 -1  1]
117 64 9.225716e-02 -56           u=21 $ mod [-1  1  1]
118 64 9.225716e-02 -57           u=21 $ mod [-1  1 -1]
119 64 9.225716e-02 -58           u=21 $ mod [-1 -1 -1]
120 64 9.225716e-02 -59           u=21 $ mod [-1 -1  1]
121 50 5.058e-05      51  52  53  54  55
                           56  57  58  59           u=21 $ air in between
c
c -----
c   Control rod sites
c
130 0                 -1  18 -260       fill=25(15)    $ CR1
131 0                 -1  18 -261       fill=25(16)    $ CR2
132 0                 -1  18 -262       fill=25(17)    $ CR3
133 0                 -1  18 -263       fill=25(18)    $ CR4
134 0                 -1  18 -264       fill=25(19)    $ CR5
135 0                 -1  18 -265       fill=25(20)    $ CR6
136 0                 -1  18 -266       fill=25(21)    $ CR7
137 0                 -1  18 -267       fill=25(22)    $ CR8
138 0                 -1  18 -268       fill=25(23)    $ CR9
139 0                 -1  18 -269       fill=25(24)    $ CR10
c
c   Universe 25: contents of CR guide tubes
c
145 50 5.058e-05     367           u=25 $ air around CR
146 50 5.058e-05     -367 -350      u=25 $ air below CR
147 0                 -367  350       fill=26   u=25 $ CR
c
c   Universe 26: control rod
c
148 51 -7.9          -351  362       u=26 $ lower end
c
c   segment 1
c
149 51 -7.9          351 -352  362 -363      u=26 $ inner sleeve
150 50 5.058e-05     351 -352  363 -364      u=26 $ gap
151 52 -1.7          351 -352  364 -365      u=26 $ B4C

```

152	50	5.058e-05	351	-352	365	-366	u=26	\$ gap
153	51	-7.9	351	-352	366		u=26	\$ outer sleeve
c								
154	51	-7.9	352	-353	362		u=26	\$ joint 1
c								
c	segment 2							
c								
155	51	-7.9	353	-354	362	-363	u=26	\$ inner sleeve
156	50	5.058e-05	353	-354	363	-364	u=26	\$ gap
157	52	-1.7	353	-354	364	-365	u=26	\$ B4C
158	50	5.058e-05	353	-354	365	-366	u=26	\$ gap
159	51	-7.9	353	-354	366		u=26	\$ outer sleeve
c								
160	51	-7.9	354	-355	362		u=26	\$ joint 2
c								
c	segment 3							
c								
161	51	-7.9	355	-356	362	-363	u=26	\$ inner sleeve
162	50	5.058e-05	355	-356	363	-364	u=26	\$ gap
163	52	-1.7	355	-356	364	-365	u=26	\$ B4C
164	50	5.058e-05	355	-356	365	-366	u=26	\$ gap
165	51	-7.9	355	-356	366		u=26	\$ outer sleeve
c								
166	51	-7.9	356	-357	362		u=26	\$ joint 3
c								
c	segment 4							
c								
167	51	-7.9	357	-358	362	-363	u=26	\$ inner sleeve
168	50	5.058e-05	357	-358	363	-364	u=26	\$ gap
169	52	-1.7	357	-358	364	-365	u=26	\$ B4C
170	50	5.058e-05	357	-358	365	-366	u=26	\$ gap
171	51	-7.9	357	-358	366		u=26	\$ outer sleeve
c								
172	51	-7.9	358	-359	362		u=26	\$ joint 4
c								
c	segment 5							
c								
173	51	-7.9	359	-360	362	-363	u=26	\$ inner sleeve
174	50	5.058e-05	359	-360	363	-364	u=26	\$ gap
175	52	-1.7	359	-360	364	-365	u=26	\$ B4C
176	50	5.058e-05	359	-360	365	-366	u=26	\$ gap
177	51	-7.9	359	-360	366		u=26	\$ outer sleeve
c								
178	51	-7.9	360	-361	362		u=26	\$ upper end
179	50	5.058e-05	-361	-362			u=26	\$ centre channel
180	50	5.058e-05	361				u=26	\$ above rod
c								
c	-----							
c	Absorber ball KLAk sites							
c								
190	50	5.058e-05	-1	18	-275	276 (-277:-279) (278:-280)		\$ KL1
191	50	5.058e-05	-1	18	-281	282 (-283:-285) (284:-286)		\$ KL2
192	50	5.058e-05	-1	18	-287	288 (-289:-291) (290:-292)		\$ KL3
193	50	5.058e-05	-1	18	-293	294 (-295:-297) (296:-298)		\$ KL4
194	50	5.058e-05	-1	18	-299	300 (-301:-303) (302:-304)		\$ KL5
195	50	5.058e-05	-1	18	-305	306 (-307:-309) (308:-310)		\$ KL6
196	50	5.058e-05	-1	18	-311	312 (-313:-315) (314:-316)		\$ KL7

```

c
c -----
c      Helium flow channels
c
200  50  5.058e-05    -4   9  -320          $ HE1
201  50  5.058e-05    -4   9  -321          $ HE2
202  50  5.058e-05    -4   9  -322          $ HE3
203  50  5.058e-05    -4   9  -323          $ HE4
204  50  5.058e-05    -4   9  -324          $ HE5
205  50  5.058e-05    -4   9  -325          $ HE6
206  50  5.058e-05    -4   9  -326          $ HE7
207  50  5.058e-05    -4   9  -327          $ HE8
208  50  5.058e-05    -4   9  -328          $ HE9
209  50  5.058e-05    -4   9  -329          $ HE10
210  50  5.058e-05   -4   9  -330          $ HE11
211  50  5.058e-05   -4   9  -331          $ HE12
212  50  5.058e-05   -4   9  -332          $ HE13
213  50  5.058e-05   -4   9  -333          $ HE14
214  50  5.058e-05   -4   9  -334          $ HE15
215  50  5.058e-05   -4   9  -335          $ HE16
216  50  5.058e-05   -4   9  -336          $ HE17
217  50  5.058e-05   -4   9  -337          $ HE18
218  50  5.058e-05   -4   9  -338          $ HE19
219  50  5.058e-05   -4   9  -339          $ HE20
c
c -----
c      Irradiation channels
c
230  50  5.058e-05   -1   9  -340          $ IR1
231  50  5.058e-05   -1   9  -341          $ IR2
232  50  5.058e-05   -1   9  -342          $ IR3
c
=====
c      SURFACE CARDS
c
1   pz      0.0          $ Top of borated C bricks at reactor top
2   pz     -40.0         $ Bottom of borated C bricks @ reactor top
3   pz     -95.0         $ Upper surface of cold He chamber
4   pz    -105.0         $ Lower surface of cold He chamber
5   pz    -114.7         $ Surface between axial regions 30 and 82
6   pz    -130.0         $ Lower surface of top reflector
c   7   pz    -171.698     $ Top of fueled region (full core)
7   pz    -224.318       $ Top of fueled region (initial critical)
8   pz    -351.818       $ Upper surface of cone region
9   pz    -388.764       $ Lower surface of cone region
10  pz    -402.0         $ Surface between axial regions 8 and 9
11  pz    -430.0         $ Surface between axial regions 9 and 10
12  pz    -450.0         $ Surface between axial regions 10 and 12
13  pz    -465.0         $ Surface between axial regions 13 and 14
14  pz    -495.0         $ Surface between axial regions 6 and 7
15  pz    -510.0         $ Surface between axial regions 16 and 17
16  pz    -540.0         $ Surface between axial regions 7 and 81
17  pz    -610.0         $ Bottom of reactor
18  pz    -394.2         $ Bottom of CR guide hole
c
19  cz     88.29        $ radial fuel exclusion zone

```

```

20  cz      25.0
21  cz      41.75
22  cz      70.75
23  cz      90.0      $ Inner surface of radial reflector
24  cz      95.6      $ Inner surface of control rod region
25  cz      108.6     $ Outer surface of control rod region
26  cz      140.6     $ Inner surface of He flow region
27  cz      148.6     $ Outer surface of He flow region
28  cz      167.793    $ Outer surface of side graphite reflector
29  cz      190.0     $ Outside of radial borated C bricks
c
30  kz      -402.974  3.09522 1  $ Outer surface of bottom cone
c
c   Fuel element
c
41  so      2.5          $ fuel region
c
c   Unit cell in core
c
45  px      -3.4386     $ [ -1  0  0]
46  px      3.4386      $ [  1  0  0]
47  py      3.4386      $ [  0  1  0]
48  py      -3.4386     $ [  0 -1  0]
49  pz      3.4386      $ [  0  0  1]
50  pz      -3.4386     $ [  0  0 -1]
c
c   Pebbles in unit BCC cells
c
51  so      3.0          $ centre fuel
52  s       3.4386  3.4386  3.4386  2.731   $
53  s       3.4386  3.4386 -3.4386  2.731   $
54  s       3.4386 -3.4386 -3.4386  2.731   $
55  s       3.4386 -3.4386  3.4386  2.731   $ reduced
56  s       -3.4386  3.4386  3.4386  2.731   $ radius
57  s       -3.4386  3.4386 -3.4386  2.731   $ moderator
58  s       -3.4386 -3.4386 -3.4386  2.731   $ spheres
59  s       -3.4386 -3.4386  3.4386  2.731   $
c
c   Coated Fuel Particles
c
245 so      0.025      $ kernel
246 so      0.034      $ 1st PyC layer
247 so      0.038      $ 2nd PyC layer
248 so      0.0415     $ SiC layer
249 so      0.0455     $ 3rd PyC layer
c
c   Unit cell for CFP lattice in graphite matrix
c
250 px      0.09938918
251 px      -0.09938918
252 py      0.09938918
253 py      -0.09938918
254 pz      0.09938918
255 pz      -0.09938918
c
c   Control rod channels
c

```

```

260 c/z    90.972   46.352   6.49   $ CR1
261 c/z    46.352   90.972   6.49   $ CR2
262 c/z   -15.972   100.843   6.49   $ CR3
263 c/z   -72.196   72.196   6.49   $ CR4
264 c/z  -100.843   15.972   6.49   $ CR5
265 c/z  -90.972  -46.352   6.49   $ CR6
266 c/z  -46.352  -90.972   6.49   $ CR7
267 c/z   15.972  -100.843   6.49   $ CR8
268 c/z   72.196  -72.196   6.49   $ CR9
269 c/z  100.843  -15.972   6.49   $ CR10
c
c      Small absorber ball channels
c
c      .. KL1
275 5   px     3.0
276 5   px    -3.0
277 5   py     5.0
278 5   py    -5.0
279 5   c/z    0.0   5.0   3.0
280 5   c/z    0.0  -5.0   3.0
c
c      .. KL2
281 6   px     3.0
282 6   px    -3.0
283 6   py     5.0
284 6   py    -5.0
285 6   c/z    0.0   5.0   3.0
286 6   c/z    0.0  -5.0   3.0
c
c      .. KL3
287 7   px     3.0
288 7   px    -3.0
289 7   py     5.0
290 7   py    -5.0
291 7   c/z    0.0   5.0   3.0
292 7   c/z    0.0  -5.0   3.0
c
c      .. KL4
293 8   px     3.0
294 8   px    -3.0
295 8   py     5.0
296 8   py    -5.0
297 8   c/z    0.0   5.0   3.0
298 8   c/z    0.0  -5.0   3.0
c
c      .. KL5
299 9   px     3.0
300 9   px    -3.0
301 9   py     5.0
302 9   py    -5.0
303 9   c/z    0.0   5.0   3.0
304 9   c/z    0.0  -5.0   3.0
c
c      .. KL6
305 10  px     3.0
306 10  px    -3.0
307 10  py     5.0

```

```

308 10  py    -5.0
309 10  c/z    0.0   5.0   3.0
310 10  c/z    0.0  -5.0   3.0
c
c .. KL7
311 11  px     3.0
312 11  px    -3.0
313 11  py     5.0
314 11  py    -5.0
315 11  c/z    0.0   5.0   3.0
316 11  c/z    0.0  -5.0   3.0
c
c Helium flow channels
c
320 c/z  142.820  22.620  3.99      $ HE1
321 c/z  128.840  65.647  3.99      $ HE2
322 c/z  102.248  102.248 3.99      $ HE3
323 c/z   65.647  128.840 3.99      $ HE4
324 c/z   22.620  142.820 3.99      $ HE5
325 c/z  -22.620  142.820 3.99      $ HE6
326 c/z  -65.647  128.840 3.99      $ HE7
327 c/z -102.248  102.248 3.99      $ HE8
328 c/z -128.840   65.647  3.99      $ HE9
329 c/z -142.82   22.620  3.99      $ HE10
330 c/z -142.82  -22.620 3.99      $ HE11
331 c/z -128.84  -65.647 3.99      $ HE12
332 c/z -102.248 -102.248 3.99      $ HE13
333 c/z  -65.647 -128.840 3.99      $ HE14
334 c/z  -22.620 -142.820 3.99      $ HE15
335 c/z   22.620 -142.820 3.99      $ HE16
336 c/z   65.647 -128.840 3.99      $ HE17
337 c/z  102.248 -102.248 3.99      $ HE18
338 c/z  128.840  -65.647 3.99      $ HE19
339 c/z  142.820  -22.620 3.99      $ HE20
c
c Irradiation Channels
c
340 c/z  100.843  15.972  6.49      $ IR1
341 c/z -100.843 -15.972  6.49      $ IR2
342 c/z  -15.972 -100.843  6.49      $ IR3
c
c Control Rods
c
350 25  pz     0.001      $ bottom of control rod
351 25  pz     4.501      $ segment 1 -
bottom
352 25  pz     53.201     $ segment 1 - top
353 25  pz     56.801     $ segment 2 -
bottom
354 25  pz    105.501     $ segment 2 - top
355 25  pz    109.101     $ segment 3 -
bottom
356 25  pz    157.801     $ segment 3 - top
357 25  pz    161.401     $ segment 4 - bottom
358 25  pz    210.101     $ segment 4 - top
359 25  pz    213.701     $ segment 5 - bot

```

```

360 25  pz    262.401                      $ segment 5 - top
361 25  pz    264.701                      $ top of rod
362      cz    2.751                        $ inner sleeve - in
363      cz    2.951                        $ inner sleeve - out
364      cz    3.001                        $ absorber - inside
365      cz    5.251                        $ absorber - outside
366      cz    5.301                        $ outer sleeve - in
367      cz    5.501                        $ outer sleeve - out
c
=====
c      RUN PARAMETERS
c
c      NEUTRON IMPORTANCES
imp:n
    0                                $ outside world
    1 74r                            $ graphite structure
    1 1                               $ helium cavity
    1 20r                            $ fuel region
    1 9r                             $ control rod sites
    1 2r                             $ control rod guide tubes
    1 32r                            $ control rod
    1 11r                            $ conus
    1 6r                             $ KLAK sites
    1 19r                            $ Helium flow channels
    1 2r                             $ Irradiation sites
c
c      TRANSFORMATIONS
c
c      Center positions of unit cells in fill zones
tr1  0.0  0.0  -348.3794                  $ fuel sphere
tr2  0.0  0.0  -355.2566                  $ mod sphere
c
c      Small absorber ball channels (centered on r = 98.61 cm)
*tr5  69.728  69.728  0.0    45  45  90  135  45  90  90  90  0  $ KL1
*tr6  15.426  97.396  0.0    81   9  90  171  81  90  90  90  0  $ KL2
*tr7  -44.768  87.862  0.0   117  27  90  153  117  90  90  90  0  $ KL3
*tr8  -87.862  44.768  0.0   153  63  90  117  153  90  90  90  0  $ KL4
*tr9  -69.728  -69.728  0.0   135  135  90   45  135  90  90  90  0  $ KL5
*tr10 44.768  -87.862  0.0    63  153  90   27   63  90  90  90  0  $ KL6
*tr11 87.862  -44.768  0.0    27  117  90   63   27  90  90  90  0  $ KL7
c
c      Control rod radial positions
c
tr15  90.972  46.352  0.0                  $ CR1
tr16  46.352  90.972  0.0                  $ CR2
tr17 -15.972  100.843  0.0                  $ CR3
tr18 -72.196  72.196  0.0                  $ CR4
tr19 -100.843  15.972  0.0                  $ CR5
tr20 -90.972  -46.352  0.0                 $ CR6
tr21 -46.352  -90.972  0.0                 $ CR7
tr22  15.972  -100.843 0.0                 $ CR8
tr23  72.196  -72.196  0.0                 $ CR9
tr24 100.843  -15.972  0.0                 $ CR10
c
c      Control rod insertion (length = 264.7 cm)
c

```

```

tr25      0.0      0.0    -119.2          $ fully out
c       tr25      0.0      0.0    -394.2          $ fully in
c
c      MATERIAL SPECIFICATIONS
c      Graphite Structure
c
m1      6000.60c   8.51047e-02   5010.60c   9.09283e-08
      5011.60c   3.65998e-07
mt1     grph.01t
c
m2      6000.60c   7.29410e-02   5010.60c   6.56324e-04
      5011.60c   2.64179e-03
mt2     grph.01t
c
m3      6000.60c   8.51462e-02   5010.60c   9.09725e-08
      5011.60c   3.66176e-07
mt3     grph.01t
c
m4      6000.60c   1.45350e-02   5010.60c   1.55296e-08
      5011.60c   6.25088e-08
mt4     grph.01t
c
m5      6000.60c   8.02916e-02   5010.60c   8.57857e-08
      5011.60c   3.45298e-07
mt5     grph.01t
c
m7      6000.60c   5.38275e-02   5010.60c   5.75108e-08
      5011.60c   2.31488e-07
mt7     grph.01t
c
m8      6000.60c   7.81408e-02   5010.60c   8.34879e-08
      5011.60c   3.36049e-07
mt8     grph.01t
c
m9      6000.60c   8.23751e-02   5010.60c   8.80119e-08
      5011.60c   3.54259e-07
mt9     grph.01t
c
m10     6000.60c   8.43647e-02   5010.60c   5.94023e-05
      5011.60c   2.39102e-04
mt10    grph.01t
c
m11     6000.60c   8.17101e-02   5010.60c   3.11268e-05
      5011.60c   1.25289e-04
mt11    grph.01t
c
m12     6000.60c   8.50790e-02   5010.60c   4.16093e-05
      5011.60c   1.67483e-04
mt12    grph.01t
c
m13     6000.60c   8.19167e-02   5010.60c   7.13473e-06
      5011.60c   2.87182e-05
mt13    grph.01t
c
m14     6000.60c   5.41118e-02   5010.60c   1.14914e-05
      5011.60c   4.62542e-05
mt14    grph.01t

```

c				
m15	6000.60c	3.32110e-02	5010.60c	3.54835e-08
	5011.60c	1.42826e-07		
mt15	grph.01t			
c				
m16	6000.60c	8.81811e-02	5010.60c	7.14143e-06
	5011.60c	2.87452e-05		
mt16	grph.01t			
c				
m17	6000.60c	7.65948e-02	5010.60c	6.89235e-04
	5011.60c	2.77426e-03		
mt17	grph.01t			
c				
m18	6000.60c	1		
mt18	grph.01t			
c				
m19	6000.60c	7.61157e-02	5010.60c	6.84890e-04
	5011.60c	2.75677e-03		
mt19	grph.01t			
c				
m20	6000.60c	8.78374e-02	5010.60c	9.38478e-08
	5011.60c	3.77749e-07		
mt20	grph.01t			
c				
m21	6000.60c	5.79696e-02	5010.60c	6.19364e-08
	5011.60c	2.49302e-07		
mt21	grph.01t			
c				
m22	6000.60c	8.82418e-02	5010.60c	9.42800e-08
	5011.60c	3.79489e-07		
mt22	grph.01t			
c				
m23	6000.60c	8.79541e-02	5010.60c	3.35054e-05
	5011.60c	1.34864e-04		
mt23	grph.01t			
c				
m24	6000.60c	8.46754e-02	5010.60c	9.04696e-08
	5011.60c	3.64151e-07		
mt24	grph.01t			
c				
m25	6000.60c	8.18911e-02	5010.60c	7.36859e-04
	5011.60c	2.96595e-03		
mt25	grph.01t			
c				
m26	6000.60c	9.43390e-02	5010.60c	3.87139e-06
	5011.60c	1.55828e-05		
mt26	grph.01t			
c				
m27	6000.60c	5.61108e-02	5010.60c	3.87139e-06
	5011.60c	1.55828e-05		
mt27	grph.01t			
c				
m28	6000.60c	9.43390e-02	5010.60c	1.00795e-07
	5011.60c	4.05711e-07		
mt28	grph.01t			
c				
m29	6000.60c	8.81637e-02	5010.60c	9.41966e-08

	5011.60c	3.79153e-07
mt29	grph.01t	
c		
m30	6000.60c	6.76758e-02
	5011.60c	1.00390e-04
mt30	grph.01t	
c		
m31	6000.60c	8.61476e-02
	5011.60c	3.70483e-07
mt31	grph.01t	
c		
m32	6000.60c	8.29066e-02
	5011.60c	3.56544e-07
mt32	grph.01t	
c		
m33	6000.60c	7.47805e-02
	5011.60c	2.70841e-03
mt33	grph.01t	
c		
m35	6000.60c	5.82699e-02
	5011.60c	2.50593e-07
mt35	grph.01t	
c		
m36	6000.60c	8.55860e-02
	5011.60c	3.68068e-07
mt36	grph.01t	
c		
m37	6000.60c	7.28262e-02
	5011.60c	3.13193e-07
mt37	grph.01t	
c		
m38	6000.60c	7.60368e-02
	5011.60c	3.27000e-07
mt38	grph.01t	
c		
m39	6000.60c	7.57889e-02
	5011.60c	1.16211e-04
mt39	grph.01t	
c		
m40	6000.60c	7.37484e-02
	5011.60c	3.17159e-07
mt40	grph.01t	
c		
m41	6000.60c	6.60039e-02
	5011.60c	2.39054e-03
mt41	grph.01t	
c		
m43	6000.60c	8.61500e-02
	5011.60c	3.70493e-07
mt43	grph.01t	
c		
m44	6000.60c	7.49927e-02
	5011.60c	2.71609e-03
mt44	grph.01t	
c		
m45	6000.60c	9.43390e-02
	5011.60c	4.05711e-07

```

mt45 grph.01t
c
c      Humid air
c
m50   1001.60c  5.79913e-07  1002.60c  8.7e-11
      7014.60c  3.98536e-05  7015.60c  1.46400e-07
      8016.60c  1.0e-05

c
c      Control rod
c
m51   24000.50c -0.18      26000.50c -0.681    28000.50c -0.1
      14000.60c -0.01      25055.60c -0.02     6000.60c -0.001
      22000.60c -0.008

c
m52   6000.60c  0.2       5010.60c  0.1584
      5011.60c  0.6416
c
c      Fuel element
c
c      .. fuel kernel (N = 6.970994e-02)
m61   92235.60c 3.992067e-03  92238.60c  1.924449e-02
      8016.60c  4.647329e-02  5011.60c  7.445022e-08
      5010.60c  1.849637e-08

c
c      .. graphite layers of CFP
m62   6000.60c  1

c
c      .. SiC layer of CFP
m63   14000.60c 0.5       6000.60c  0.5

c
c      .. moderator graphite (N = 9.225716e-02)
m64   6000.60c 9.225714e-02  5011.60c  9.248780e-09
      5010.60c  2.283365e-09

mt64 grph.01t
c
c      .. graphite matrix in fuel pebble (N = 8.674180e-02)
m65   6000.60c 8.674169e-02  5011.60c  9.032424e-08
      5010.60c  2.244010e-08

mt65 grph.01t
c
c      PROBLEM TYPE
c
mode n
totnu
kcode 5000 1.0 10 210
c
sdef pos=0 0 -351.818 axs=0 0 1 rad=d1 ext=d2
si1 0 88.29
sp1 0 1
si2 0 127.5
sp2 0 1
c
c      Printing and cutoff cards
c
print
dbcn 9j 300
prdmp j -60 1 2

```

APPENDIX B-2: MCNP4B Model of HTR-10 Benchmark Problem B2.1

```
HTR-10 PEBBLE-BED REACTOR (CASE B21 UTX)
c
c
=====
c
c MCNP4B model of the HTR-10 initial core, based on IAEA benchmark
c problem CRP-5 specification. Benchmark problem B21.
c
c Modeling assumptions:
c
c A BCC lattice of spheres in core with 0.61 packing fraction and a
c 1:1 mix of fuel and moderator balls in cylindrical portion of core,
c but with a reduced moderator pebble size to approximate a 57/43 f/m
c pebble ratio. The control, irradiation, KLAK and He channels are
c modeled explicitly. Pressurized helium atmosphere.
c
c Benchmark problem B2.1, calculated using the U of Texas cross
c sections at 300K.
c
c Prepared by J.R. Lebenhaft (MIT) May 2001.
c
c -----
c Revision history:
c
c January 2001, J. Lebenhaft - detailed model of control rod; radial
c core exclusion zone to correct for partial pebbles at boundary.
c
c May 2001, J. Lebenhaft - revised moderator density and boron
c content; reduced fueled region in fuel spheres; corrected size of
c CFP unit cell.
c
=====
c CELL CARDS
c
1 0           1: -17: 29          $ outside world
c
c Graphite reactor structure
c
2 2  0.0762391    -1   2  -23      $ zone 1
3 3  0.0851467    -2   3  -23      $ zone 2
4 4  0.0145351    -3   4  -23      $ zone 3
5 5  0.0802920    -4   6  -23      $ zone 4
6 1  0.0851052    30   9  -23      $ zone 0
7 7  0.0538278    -9   14  -20     $ zone 6
8 7  0.0538278    -14  16  -20     $ zone 7
9 18 0.0797184    -16  17  -20     $ zone 81
10 8  0.0781412    -9   10  20  -23  $ zone 8
11 9  0.0823755    -10  11  20  -23  $ zone 9
12 10 0.0846632    -11  12  20  -21  $ zone 10
13 11 0.0818665    -11  12  21  -23  $ zone 11
14 12 0.0852881    -12  15  20  -21  $ zone 12
15 13 0.0819526    -12  13  21  -23  $ zone 13
16 14 0.0541695    -13  14  21  -22  $ zone 14
17 15 0.0332112    -13  14  22  -23  $ zone 15
```

18	16	0.0882170	-14	15	21	-23		\$ zone 16
19	17	0.0800619	-15	16	20	-24		\$ zone 17
20	18	0.0797184	-16	17	20	-24		\$ zone 18
21	19	0.0795574	-1	2	23	-24		\$ zone 19
22	20	0.0878379	-2	3	23	-24		\$ zone 20
23	21	0.0579699	-3	4	23	-24		\$ zone 21
24	22	0.0882423	-4	9	23	-24		\$ zone 22
25	22	0.0882423	-9	11	23	-24		\$ zone 23
26	23	0.0881225	-11	12	23	-24		\$ zone 24
27	22	0.0882423	-12	13	23	-24		\$ zone 25
28	24	0.0846759	-13	14	23	-24		\$ zone 26
29	22	0.0882423	-14	15	23	-24		\$ zone 80
30	25	8.55939e-02	-1	2	24	-25		\$ zone 27
			260	261	262	263	264	265
			266	267	268	269		
			(275:-276:(277			279):	(280	-278))
			(281:-282:(283			285):	(286	-284))
			(287:-288:(289			291):	(292	-290))
			(293:-294:(295			297):	(298	-296))
			(299:-300:(301			303):	(304	-302))
			(305:-306:(307			309):	(310	-308))
			(311:-312:(313			315):	(316	-314))
			340	341	342			
31	26	9.43585e-02	-2	3	24	-25		\$ zone 28
			260	261	262	263	264	265
			266	267	268	269		
			(275:-276:(277			279):	(280	-278))
			(281:-282:(283			285):	(286	-284))
			(287:-288:(289			291):	(292	-290))
			(293:-294:(295			297):	(298	-296))
			(299:-300:(301			303):	(304	-302))
			(305:-306:(307			309):	(310	-308))
			(311:-312:(313			315):	(316	-314))
			340	341	342			
32	27	5.61302e-02	-3	4	24	-25		\$ zone 29
			260	261	262	263	264	265
			266	267	268	269		
			(275:-276:(277			279):	(280	-278))
			(281:-282:(283			285):	(286	-284))
			(287:-288:(289			291):	(292	-290))
			(293:-294:(295			297):	(298	-296))
			(299:-300:(301			303):	(304	-302))
			(305:-306:(307			309):	(310	-308))
			(311:-312:(313			315):	(316	-314))
			340	341	342			
33	26	9.43585e-02	-4	5	24	-25		\$ zone 82
			260	261	262	263	264	265
			266	267	268	269		
			(275:-276:(277			279):	(280	-278))
			(281:-282:(283			285):	(286	-284))
			(287:-288:(289			291):	(292	-290))
			(293:-294:(295			297):	(298	-296))
			(299:-300:(301			303):	(304	-302))
			(305:-306:(307			309):	(310	-308))
			(311:-312:(313			315):	(316	-314))
			340	341	342			
34	28	9.43396e-02	-5	6	24	-25		\$ zone 30

			260	261	262	263	264	265	
			266	267	268	269			
			(275:-276:(277		(279):(280 -278))				
			(281:-282:(283		(285):(286 -284))				
			(287:-288:(289		(291):(292 -290))				
			(293:-294:(295		(297):(298 -296))				
			(299:-300:(301		(303):(304 -302))				
			(305:-306:(307		(309):(310 -308))				
			(311:-312:(313		(315):(316 -314))				
			340	341	342				
35	29	8.81642e-02	-6	9	24	-25			\$ zones 31 to
40			260	261	262	263	264		
			265	266	267	268	269		
			(275:-276:(277		(279):(280 -278))				
			(281:-282:(283		(285):(286 -284))				
			(287:-288:(289		(291):(292 -290))				
			(293:-294:(295		(297):(298 -296))				
			(299:-300:(301		(303):(304 -302))				
			(305:-306:(307		(309):(310 -308))				
			(311:-312:(313		(315):(316 -314))				
			340	341	342				
76	45	9.43396e-02	-9	18	24	-25			\$ zone 41a -
			260	261	262	263	264	265	\$ CR bottom
			266	267	268	269			
			(275:-276:(277		(279):(280 -278))				
			(281:-282:(283		(285):(286 -284))				
			(287:-288:(289		(291):(292 -290))				
			(293:-294:(295		(297):(298 -296))				
			(299:-300:(301		(303):(304 -302))				
			(305:-306:(307		(309):(310 -308))				
			(311:-312:(313		(315):(316 -314))				
36	28	0.0678903	-18	11	24	-25			\$ zone 41b
37	30	0.0678011	-11	12	24	-25			\$ zone 42
38	31	0.0861481	-12	13	24	-25			\$ zone 43
39	32	0.0829070	-13	14	24	-25			\$ zone 44
40	31	0.0861481	-14	15	24	-25			\$ zone 45
41	33	0.0781618	-15	16	24	-25			\$ zone 46
42	18	0.0778265	-16	17	24	-25			\$ zone 47
43	17	0.0800619	-1	2	25	-28			\$ zone 74
44	22	0.0882423	-2	3	25	-27			\$ zone 66a
45	22	0.0882423	-2	9	27	-28			\$ zone 66b
46	35	0.0582702	-3	4	25	-26			\$ zone 48
47	22	0.0882423	-4	9	25	-26			\$ zone 49
48	22	0.0882423	-9	11	25	-26			\$ zone 50
49	23	0.0881225	-11	12	25	-26			\$ zone 51
50	22	0.0882423	-12	13	25	-26			\$ zone 52
51	36	0.0855865	-13	14	25	-26			\$ zone 53
52	22	0.0882423	-14	15	25	-26			\$ zone 54
53	17	0.0800619	-15	16	25	-26			\$ zone 55
54	18	0.0797184	-16	17	25	-26			\$ zone 56
55	37	0.0728266	-3	4	26	-27			\$ zone 57
56	38	0.0760372	-4	9	26	-27			\$ zone 58
			320	321	322	323	324		
			325	326	327	328	329		
			330	331	332	333	334		
			335	336	337	338	339		

```

57 38 0.0760372    -9   11   26  -27      $ zone 59
58 39 0.0759340    -11   12   26  -27      $ zone 60
59 38 0.0760372    -12   13   26  -27      $ zone 61
60 40 0.0737488    -13   14   26  -27      $ zone 62
61 38 0.0760372    -14   15   26  -27      $ zone 63
62 41 0.0689883    -15   16   26  -27      $ zone 64
63 18 0.0686924    -16   17   26  -27      $ zone 65
64 22 0.0882423    -9    11   27  -28      $ zone 67
65 23 0.0881225    -11   12   27  -28      $ zone 68
66 22 0.0882423    -12   13   27  -28      $ zone 69
67 43 0.0861505    -13   14   27  -28      $ zone 70
68 22 0.0882423    -14   15   27  -28      $ zone 71
69 17 0.0800619    -15   16   27  -28      $ zone 72
70 18 0.0797184    -16   17   27  -28      $ zone 73
71 17 0.0800619    -1    2    28  -29      $ zone 75
72 17 0.0800619    -2    13   28  -29      $ zone 76
73 44 0.0783836    -13   14   28  -29      $ zone 77
74 17 0.0800619    -14   16   28  -29      $ zone 78
75 17 0.0800619    -16   17   28  -29      $ zone 79
c
c   Cavity above core
c
80 50 -4.814e-03     -6     7  -23
c
c -----
c   Cylindrical Region of Core
c
84 50 -4.814e-03     -7     8   19  -23      $ radial gap
85 0                  -7     8  -19           fill=10(1) $ pebble bed
c
c   Universe 10: BCC lattice of fuel and dummy spheres
c
86 0                  45  -46  -47   48  -49   50
lat=1  fill=11
u=10
c
c   Universe 11: unit cell
c
87 0                  -51           fill=12  u=11  $ fuel [ 0  0  0]
88 64 9.225716e-02  -52           u=11  $ mod  [ 1  1  1]
89 64 9.225716e-02  -53           u=11  $ mod  [ 1  1  -1]
90 64 9.225716e-02  -54           u=11  $ mod  [ 1  -1  -1]
91 64 9.225716e-02  -55           u=11  $ mod  [ 1  -1  1]
92 64 9.225716e-02  -56           u=11  $ mod  [-1  1  1]
93 64 9.225716e-02  -57           u=11  $ mod  [-1  1  -1]
94 64 9.225716e-02  -58           u=11  $ mod  [-1  -1  -1]
95 64 9.225716e-02  -59           u=11  $ mod  [-1  -1  1]
96 50 -4.814e-03     51   52   53   54   55
                           56   57   58   59           u=11  $ helium between
c
c   Universe 12: details of fuel element
c
97 65 8.674180e-02   41           u=12  $ graphite shell
98 0                  -41           fill=13  u=12  $ fuel region
c
c   Universe 13: embedded coated fuel particles
c

```

```

99  0           -250  251 -252  253 -254  255
    lat=1  fill=14
    u=13
c
c      Universe 14: coated fuel particle
c
100 61  6.970994e-02 -245                      u=14 $ UO2 kernel
101 62 -1.1          245 -246                  u=14 $ PyC layer 1
102 62 -1.9          246 -247                  u=14 $ PyC layer 2
103 63 -3.18         247 -248                  u=14 $ SiC layer
104 62 -1.9          248 -249                  u=14 $ PyC layer 3
105 65  8.674180e-02  249                      u=14 $ graphite matrix
c
c      -----
c      Conus Region of Core (dummy balls)
c
110 0           -8     9 -30          fill=20(2)
c
c      Universe 20: BCC lattice of moderator spheres
c
111 0           45 -46 -47  48 -49  50
    lat=1  fill=21
    u=20
c
c      Universe 21: unit cell
c
112 64  9.225716e-02 -51                      u=21 $ mod [ 0  0  0]
113 64  9.225716e-02 -52                      u=21 $ mod [ 1  1  1]
114 64  9.225716e-02 -53                      u=21 $ mod [ 1  1 -1]
115 64  9.225716e-02 -54                      u=21 $ mod [ 1 -1 -1]
116 64  9.225716e-02 -55                      u=21 $ mod [ 1 -1  1]
117 64  9.225716e-02 -56                      u=21 $ mod [-1  1  1]
118 64  9.225716e-02 -57                      u=21 $ mod [-1  1 -1]
119 64  9.225716e-02 -58                      u=21 $ mod [-1 -1 -1]
120 64  9.225716e-02 -59                      u=21 $ mod [-1 -1  1]
121 50 -4.814e-03      51  52  53  54  55
                                         56  57  58  59          u=21 $ helium between
c
c      -----
c      Control rod sites
c
130 0           -1  18 -260          fill=25(15)   $ CR1
131 0           -1  18 -261          fill=25(16)   $ CR2
132 0           -1  18 -262          fill=25(17)   $ CR3
133 0           -1  18 -263          fill=25(18)   $ CR4
134 0           -1  18 -264          fill=25(19)   $ CR5
135 0           -1  18 -265          fill=25(20)   $ CR6
136 0           -1  18 -266          fill=25(21)   $ CR7
137 0           -1  18 -267          fill=25(22)   $ CR8
138 0           -1  18 -268          fill=25(23)   $ CR9
139 0           -1  18 -269          fill=25(24)   $ CR10
c
c      Universe 25: contents of CR guide tubes
c
145 50 -4.814e-03   367          u=25 $ He around CR
146 50 -4.814e-03  -367 -350      u=25 $ He below CR
147 0             -367   350          fill=26   u=25 $ CR

```

```

c
c      Universe 26: control rod
c
148  51 -5.0          -351  362                      u=26 $ lower end
c
c      segment 1
c
149  51 -5.0          351 -352  362 -363          u=26 $ inner sleeve
150  50 -4.814e-03    351 -352  363 -364          u=26 $ gap
151  52 -1.7          351 -352  364 -365          u=26 $ B4C
152  50 -4.814e-03    351 -352  365 -366          u=26 $ gap
153  51 -5.0          351 -352  366              u=26 $ outer sleeve
c
154  51 -5.0          352 -353  362              u=26 $ joint 1
c
c      segment 2
c
155  51 -5.0          353 -354  362 -363          u=26 $ inner sleeve
156  50 -4.814e-03    353 -354  363 -364          u=26 $ gap
157  52 -1.7          353 -354  364 -365          u=26 $ B4C
158  50 -4.814e-03    353 -354  365 -366          u=26 $ gap
159  51 -5.0          353 -354  366              u=26 $ outer sleeve
c
160  51 -5.0          354 -355  362              u=26 $ joint 2
c
c      segment 3
c
161  51 -5.0          355 -356  362 -363          u=26 $ inner sleeve
162  50 -4.814e-03    355 -356  363 -364          u=26 $ gap
163  52 -1.7          355 -356  364 -365          u=26 $ B4C
164  50 -4.814e-03    355 -356  365 -366          u=26 $ gap
165  51 -5.0          355 -356  366              u=26 $ outer sleeve
c
166  51 -5.0          356 -357  362              u=26 $ joint 3
c
c      segment 4
c
167  51 -5.0          357 -358  362 -363          u=26 $ inner sleeve
168  50 -4.814e-03    357 -358  363 -364          u=26 $ gap
169  52 -1.7          357 -358  364 -365          u=26 $ B4C
170  50 -4.814e-03    357 -358  365 -366          u=26 $ gap
171  51 -5.0          357 -358  366              u=26 $ outer sleeve
c
172  51 -5.0          358 -359  362              u=26 $ joint 4
c
c      segment 5
c
173  51 -5.0          359 -360  362 -363          u=26 $ inner sleeve
174  50 -4.814e-03    359 -360  363 -364          u=26 $ gap
175  52 -1.7          359 -360  364 -365          u=26 $ B4C
176  50 -4.814e-03    359 -360  365 -366          u=26 $ gap
177  51 -5.0          359 -360  366              u=26 $ outer sleeve
c
178  51 -5.0          360 -361  362              u=26 $ upper end
179  50 -4.814e-03    -361 -362              u=26 $ centre channel
180  50 -4.814e-03    361                  u=26 $ above rod
c

```

```

c -----
c Absorber ball KLAk sites
c
190 50 -4.814e-03    -1  18 -275  276 (-277:-279) (278:-280)   $ KL1
191 50 -4.814e-03    -1  18 -281  282 (-283:-285) (284:-286)   $ KL2
192 50 -4.814e-03    -1  18 -287  288 (-289:-291) (290:-292)   $ KL3
193 50 -4.814e-03    -1  18 -293  294 (-295:-297) (296:-298)   $ KL4
194 50 -4.814e-03    -1  18 -299  300 (-301:-303) (302:-304)   $ KL5
195 50 -4.814e-03    -1  18 -305  306 (-307:-309) (308:-310)   $ KL6
196 50 -4.814e-03    -1  18 -311  312 (-313:-315) (314:-316)   $ KL7
c
c -----
c Helium flow channels
c
200 50 -4.814e-03    -4   9 -320                           $ HE1
201 50 -4.814e-03    -4   9 -321                           $ HE2
202 50 -4.814e-03    -4   9 -322                           $ HE3
203 50 -4.814e-03    -4   9 -323                           $ HE4
204 50 -4.814e-03    -4   9 -324                           $ HE5
205 50 -4.814e-03    -4   9 -325                           $ HE6
206 50 -4.814e-03    -4   9 -326                           $ HE7
207 50 -4.814e-03    -4   9 -327                           $ HE8
208 50 -4.814e-03    -4   9 -328                           $ HE9
209 50 -4.814e-03    -4   9 -329                           $ HE10
210 50 -4.814e-03   -4   9 -330                           $ HE11
211 50 -4.814e-03   -4   9 -331                           $ HE12
212 50 -4.814e-03   -4   9 -332                           $ HE13
213 50 -4.814e-03   -4   9 -333                           $ HE14
214 50 -4.814e-03   -4   9 -334                           $ HE15
215 50 -4.814e-03   -4   9 -335                           $ HE16
216 50 -4.814e-03   -4   9 -336                           $ HE17
217 50 -4.814e-03   -4   9 -337                           $ HE18
218 50 -4.814e-03   -4   9 -338                           $ HE19
219 50 -4.814e-03   -4   9 -339                           $ HE20
c
c -----
c Irradiation channels
c
230 50 -4.814e-03    -1   9 -340                           $ IR1
231 50 -4.814e-03    -1   9 -341                           $ IR2
232 50 -4.814e-03    -1   9 -342                           $ IR3
c
=====
c SURFACE CARDS
c
1  pz      0.0          $ Top of borated C bricks at reactor top
2  pz     -40.0         $ Bottom of borated C bricks @ reactor top
3  pz     -95.0         $ Upper surface of cold He chamber
4  pz    -105.0         $ Lower surface of cold He chamber
5  pz    -114.7         $ Surface between axial regions 30 and 82
6  pz    -130.0         $ Lower surface of top reflector
7  pz   -173.408        $ Top of fueled region minus 1.71 cm
8  pz   -351.818        $ Upper surface of cone region
9  pz   -388.764        $ Lower surface of cone region
10 pz   -402.0          $ Surface between axial regions 8 and 9
11 pz   -430.0          $ Surface between axial regions 9 and 10

```

```

12  pz    -450.0      $ Surface between axial regions 10 and 12
13  pz    -465.0      $ Surface between axial regions 13 and 14
14  pz    -495.0      $ Surface between axial regions 6 and 7
15  pz    -510.0      $ Surface between axial regions 16 and 17
16  pz    -540.0      $ Surface between axial regions 7 and 81
17  pz    -610.0      $ Bottom of reactor
18  pz    -394.2      $ Bottom of CR guide hole
c
19  cz    88.29       $ radial fuel exclusion zone
20  cz    25.0
21  cz    41.75
22  cz    70.75
23  cz    90.0        $ Outer radius of fueled region
24  cz    95.6        $ Inner surface of control rod region
25  cz    108.6       $ Outer surface of control rod region
26  cz    140.6       $ Inner surface of He flow region
27  cz    148.6       $ Outer surface of He flow region
28  cz    167.793     $ Outer surface of side graphite reflector
29  cz    190.0       $ Outside of radial borated C bricks
c
30  kz    -402.974 3.09522 1 $ Outer surface of cone at bottom of core
c
c  Fuel element
c
41  so    2.5         $ fuel region
c
c  Unit cell in core
c
45  px    -3.4386     $ [-1  0  0]
46  px    3.4386      $ [ 1  0  0]
47  py    3.4386      $ [ 0  1  0]
48  py    -3.4386     $ [ 0 -1  0]
49  pz    3.4386      $ [ 0  0  1]
50  pz    -3.4386     $ [ 0  0 -1]
c
c  Balls in unit cells
c
51  so    3.0
52  s     3.4386  3.4386  3.4386  2.731
53  s     3.4386  3.4386 -3.4386  2.731
54  s     3.4386 -3.4386 -3.4386  2.731
55  s     3.4386 -3.4386  3.4386  2.731
56  s     -3.4386  3.4386  3.4386  2.731
57  s     -3.4386  3.4386 -3.4386  2.731
58  s     -3.4386 -3.4386 -3.4386  2.731
59  s     -3.4386 -3.4386  3.4386  2.731
c
c  Coated Fuel Particles
c
245 so    0.025      $ kernel
246 so    0.034      $ 1st PyC layer
247 so    0.038      $ 2nd PyC layer
248 so    0.0415     $ SiC layer
249 so    0.0455     $ 3rd PyC layer
c
c  Unit cell for CFP lattice in graphite matrix
c

```

```

250 px      0.09938918
251 px     -0.09938918
252 py      0.09938918
253 py     -0.09938918
254 pz      0.09938918
255 pz     -0.09938918
c
c   Control rod channels
c
260 c/z    90.972   46.352   6.49   $ CR1
261 c/z    46.352   90.972   6.49   $ CR2
262 c/z   -15.972  100.843   6.49   $ CR3
263 c/z   -72.196   72.196   6.49   $ CR4
264 c/z  -100.843   15.972   6.49   $ CR5
265 c/z  -90.972  -46.352   6.49   $ CR6
266 c/z  -46.352  -90.972   6.49   $ CR7
267 c/z   15.972  -100.843   6.49   $ CR8
268 c/z   72.196  -72.196   6.49   $ CR9
269 c/z  100.843  -15.972   6.49   $ CR10
c
C   Small absorber ball channels
C
C   .. KL1
275 5   px      3.0
276 5   px     -3.0
277 5   py      5.0
278 5   py     -5.0
279 5   c/z     0.0   5.0   3.0
280 5   c/z     0.0  -5.0   3.0
C
C   .. KL2
281 6   px      3.0
282 6   px     -3.0
283 6   py      5.0
284 6   py     -5.0
285 6   c/z     0.0   5.0   3.0
286 6   c/z     0.0  -5.0   3.0
C
C   .. KL3
287 7   px      3.0
288 7   px     -3.0
289 7   py      5.0
290 7   py     -5.0
291 7   c/z     0.0   5.0   3.0
292 7   c/z     0.0  -5.0   3.0
C
C   .. KL4
293 8   px      3.0
294 8   px     -3.0
295 8   py      5.0
296 8   py     -5.0
297 8   c/z     0.0   5.0   3.0
298 8   c/z     0.0  -5.0   3.0
C
C   .. KL5
299 9   px      3.0
300 9   px     -3.0

```

```

301 9   py    5.0
302 9   py   -5.0
303 9   c/z    0.0  5.0  3.0
304 9   c/z    0.0 -5.0  3.0
C
C   .. KL6
305 10  px    3.0
306 10  px   -3.0
307 10  py    5.0
308 10  py   -5.0
309 10  c/z    0.0  5.0  3.0
310 10  c/z    0.0 -5.0  3.0
C
C   .. KL7
311 11  px    3.0
312 11  px   -3.0
313 11  py    5.0
314 11  py   -5.0
315 11  c/z    0.0  5.0  3.0
316 11  c/z    0.0 -5.0  3.0
C
C   Helium flow channels
C
320 c/z  142.820  22.620  3.99      $ HE1
321 c/z  128.840  65.647  3.99      $ HE2
322 c/z  102.248  102.248 3.99      $ HE3
323 c/z  65.647  128.840 3.99      $ HE4
324 c/z  22.620  142.820 3.99      $ HE5
325 c/z  -22.620  142.820 3.99     $ HE6
326 c/z  -65.647  128.840 3.99     $ HE7
327 c/z  -102.248 102.248 3.99     $ HE8
328 c/z  -128.840 65.647  3.99     $ HE9
329 c/z  -142.82  22.620  3.99     $ HE10
330 c/z  -142.82  -22.620 3.99    $ HE11
331 c/z  -128.84  -65.647 3.99    $ HE12
332 c/z  -102.248 -102.248 3.99   $ HE13
333 c/z  -65.647 -128.840 3.99   $ HE14
334 c/z  -22.620 -142.820 3.99   $ HE15
335 c/z  22.620  -142.820 3.99   $ HE16
336 c/z  65.647  -128.840 3.99   $ HE17
337 c/z  102.248 -102.248 3.99   $ HE18
338 c/z  128.840  -65.647 3.99   $ HE19
339 c/z  142.820  -22.620 3.99   $ HE20
C
C   Irradiation Channels
C
340 c/z  100.843  15.972  6.49      $ IR1
341 c/z  -100.843 -15.972  6.49      $ IR2
342 c/z  -15.972 -100.843 6.49      $ IR3
C
C   Control Rods
C
350 25  pz    0.001      $ bottom of CR
351 25  pz    4.501      $ segment 1 - bottom
352 25  pz    53.201     $ segment 1 - top
353 25  pz    56.801     $ segment 2 - bottom
354 25  pz   105.501     $ segment 2 - top

```

```

    . 355 25  pz   109.101      $ segment 3 - bottom
    . 356 25  pz   157.801      $ segment 3 - top
    . 357 25  pz   161.401      $ segment 4 - bottom
    . 358 25  pz   210.101      $ segment 4 - top
    . 359 25  pz   213.701      $ segment 5 - bottom
    . 360 25  pz   262.401      $ segment 5 - top
    . 361 25  pz   264.701      $ top of rod
    . 362   cz   2.751          $ inner sleeve - in
    . 363   cz   2.951          $ inner sleeve - out
    . 364   cz   3.001          $ absorber - inside
    . 365   cz   5.251          $ absorber - outside
    . 366   cz   5.301          $ outer sleeve - in
    . 367   cz   5.501          $ outer sleeve - out
c
=====
c      RUN PARAMETERS
c
c      NEUTRON IMPORTANCES
imp:n
    0          $ outside world
    1 74r      $ graphite structure
    1          $ helium cavity
    1 21r      $ fuel region
    1 11r      $ conus
    1 9r       $ control rod sites
    1 2r       $ control rod guide tubes
    1 32r      $ control rod
    1 6r       $ KLAK sites
    1 19r      $ Helium flow channels
    1 2r       $ Irradiation sites
c
c      TRANSFORMATIONS
c
c      Center positions of unit cells in fill zones
c
tr1  0.0  0.0  -348.3794          $ fuel ball region
tr2  0.0  0.0  -355.2566          $ dummy ball region
c
c      Small absorber ball channels (centered on r = 98.61 cm)
c
*tr5  69.728  69.728  0.0   45  45  90  135  45  90  90  90  0  $ KL1
*tr6  15.426  97.396  0.0   81   9  90  171  81  90  90  90  0  $ KL2
*tr7  -44.768  87.862  0.0  117  27  90  153  117  90  90  90  0  $ KL3
*tr8  -87.862  44.768  0.0  153  63  90  117  153  90  90  90  0  $ KL4
*tr9  -69.728  -69.728  0.0  135  135  90   45  135  90  90  90  0  $ KL5
*tr10 44.768  -87.862  0.0   63  153  90   27   63  90  90  90  0  $ KL6
*tr11 87.862  -44.768  0.0   27  117  90   63   27  90  90  90  0  $ KL7
c
c      Control rod radial positions
c
tr15 90.972  46.352  0.0          $ CR1
tr16 46.352  90.972  0.0          $ CR2
tr17 -15.972 100.843  0.0          $ CR3
tr18 -72.196  72.196  0.0          $ CR4
tr19 -100.843 15.972  0.0          $ CR5
tr20 -90.972 -46.352  0.0          $ CR6

```

```

tr21 -46.352 -90.972 0.0           $ CR7
tr22 15.972 -100.843 0.0           $ CR8
tr23 72.196 -72.196 0.0           $ CR9
tr24 100.843 -15.972 0.0           $ CR10
c
c      Control rod insertion (length = 264.7 cm)
c
tr25 0.0      0.0    -119.2          $ fully out
c      tr25 0.0      0.0    -394.2          $ fully in
c
c      MATERIAL SPECIFICATIONS
c
c      Graphite Structure
c
m1   6000.62c  8.51047e-02  5010.62c  9.09283e-08
      5011.62c  3.65998e-07
mt1  grph.01t
c
m2   6000.62c  7.29410e-02  5010.62c  6.56324e-04
      5011.62c  2.64179e-03
mt2  grph.01t
c
m3   6000.62c  8.51462e-02  5010.62c  9.09725e-08
      5011.62c  3.66176e-07
mt3  grph.01t
c
m4   6000.62c  1.45350e-02  5010.62c  1.55296e-08
      5011.62c  6.25088e-08
mt4  grph.01t
c
m5   6000.62c  8.02916e-02  5010.62c  8.57857e-08
      5011.62c  3.45298e-07
mt5  grph.01t
c
m7   6000.62c  5.38275e-02  5010.62c  5.75108e-08
      5011.62c  2.31488e-07
mt7  grph.01t
c
m8   6000.62c  7.81408e-02  5010.62c  8.34879e-08
      5011.62c  3.36049e-07
mt8  grph.01t
c
m9   6000.62c  8.23751e-02  5010.62c  8.80119e-08
      5011.62c  3.54259e-07
mt9  grph.01t
c
m10  6000.62c  8.43647e-02  5010.62c  5.94023e-05
      5011.62c  2.39102e-04
mt10 grph.01t
c
m11  6000.62c  8.17101e-02  5010.62c  3.11268e-05
      5011.62c  1.25289e-04
mt11 grph.01t
c
m12  6000.62c  8.50790e-02  5010.62c  4.16093e-05
      5011.62c  1.67483e-04
mt12 grph.01t

```

```

c
m13  6000.62c 8.19167e-02 5010.62c 7.13473e-06
      5011.62c 2.87182e-05
mt13 grph.01t
c
m14  6000.62c 5.41118e-02 5010.62c 1.14914e-05
      5011.62c 4.62542e-05
mt14 grph.01t
c
m15  6000.62c 3.32110e-02 5010.62c 3.54835e-08
      5011.62c 1.42826e-07
mt15 grph.01t
c
m16  6000.62c 8.81811e-02 5010.62c 7.14143e-06
      5011.62c 2.87452e-05
mt16 grph.01t
c
m17  6000.62c 7.65948e-02 5010.62c 6.89235e-04
      5011.62c 2.77426e-03
mt17 grph.01t
c
m18  6000.62c 1
mt18 grph.01t
c
m19  6000.62c 7.61157e-02 5010.62c 6.84890e-04
      5011.62c 2.75677e-03
mt19 grph.01t
c
m20  6000.62c 8.78374e-02 5010.62c 9.38478e-08
      5011.62c 3.77749e-07
mt20 grph.01t
c
m21  6000.62c 5.79696e-02 5010.62c 6.19364e-08
      5011.62c 2.49302e-07
mt21 grph.01t
c
m22  6000.62c 8.82418e-02 5010.62c 9.42800e-08
      5011.62c 3.79489e-07
mt22 grph.01t
c
m23  6000.62c 8.79541e-02 5010.62c 3.35054e-05
      5011.62c 1.34864e-04
mt23 grph.01t
c
m24  6000.62c 8.46754e-02 5010.62c 9.04696e-08
      5011.62c 3.64151e-07
mt24 grph.01t
c
m25  6000.62c 8.18911e-02 5010.62c 7.36859e-04
      5011.62c 2.96595e-03
mt25 grph.01t
c
m26  6000.62c 9.43390e-02 5010.62c 3.87139e-06
      5011.62c 1.55828e-05
mt26 grph.01t
c
m27  6000.62c 5.61108e-02 5010.62c 3.87139e-06

```

	5011.62c	1.55828e-05		
mt27	grph.01t			
c				
m28	6000.62c	9.43390e-02	5010.62c	1.00795e-07
	5011.62c	4.05711e-07		
mt28	grph.01t			
c				
m29	6000.62c	8.81637e-02	5010.62c	9.41966e-08
	5011.62c	3.79153e-07		
mt29	grph.01t			
c				
m30	6000.62c	6.76758e-02	5010.62c	2.49409e-05
	5011.62c	1.00390e-04		
mt30	grph.01t			
c				
m31	6000.62c	8.61476e-02	5010.62c	9.20425e-08
	5011.62c	3.70483e-07		
mt31	grph.01t			
c				
m32	6000.62c	8.29066e-02	5010.62c	8.85797e-08
	5011.62c	3.56544e-07		
mt32	grph.01t			
c				
m33	6000.62c	7.47805e-02	5010.62c	6.72877e-04
	5011.62c	2.70841e-03		
mt33	grph.01t			
c				
m35	6000.62c	5.82699e-02	5010.62c	6.22572e-08
	5011.62c	2.50593e-07		
mt35	grph.01t			
c				
m36	6000.62c	8.55860e-02	5010.62c	9.14425e-08
	5011.62c	3.68068e-07		
mt36	grph.01t			
c				
m37	6000.62c	7.28262e-02	5010.62c	7.78096e-08
	5011.62c	3.13193e-07		
mt37	grph.01t			
c				
m38	6000.62c	7.60368e-02	5010.62c	8.12398e-08
	5011.62c	3.27000e-07		
mt38	grph.01t			
c				
m39	6000.62c	7.57889e-02	5010.62c	2.88713e-05
	5011.62c	1.16211e-04		
mt39	grph.01t			
c				
m40	6000.62c	7.37484e-02	5010.62c	7.87948e-08
	5011.62c	3.17159e-07		
mt40	grph.01t			
c				
m41	6000.62c	6.60039e-02	5010.62c	5.93904e-04
	5011.62c	2.39054e-03		
mt41	grph.01t			
c				
m43	6000.62c	8.61500e-02	5010.62c	9.20451e-08
	5011.62c	3.70493e-07		

```

mt43 grph.01t
c
m44 6000.62c 7.49927e-02 5010.62c 6.74785e-04
      5011.62c 2.71609e-03
mt44 grph.01t
c
m45 6000.62c 9.43390e-02 5010.62c 1.00795e-07
      5011.62c 4.05711e-07
mt45 grph.01t
c
c   Helium coolant (4.814e-3 g/cc at 300K)
c
m50 2003.62c 0.00000137 2004.62c 0.99999863
c
c   Control-rod metallic structure
c   (iron at a reduced density of 5 g/cm3)
c
m51 26054.62c 0.05845     26056.62c 0.91754     26057.62c 0.02119
      26058.62c 0.00282
c
c   Control-rod B4C absorber
c
m52 6000.62c 0.2          5010.62c 0.1584       5011.62c 0.6416
c
c   Fuel element
c
c   .. fuel kernel (N = 6.970994e-02)
m61 92235.62c 3.992067e-03 92238.62c 1.924449e-02
      8016.62c 4.647329e-02 5011.62c 7.445022e-08
      5010.62c 1.849637e-08
c
c   .. graphite layers of CFP
m62 6000.62c 1
c
c   .. SiC layer of CFP
m63 14000.60c 0.5         6000.62c 0.5
c
c   .. graphite matrix in fuel pebble (N = 9.225716e-02)
m64 6000.62c 9.225714e-02 5011.62c 9.248780e-09
      5010.62c 2.283365e-09
mt64 grph.01t
c
c   .. graphite matrix in fuel pebble (N = 8.674180e-02)
m65 6000.62c 8.674169e-02 5011.62c 9.032424e-08
      5010.62c 2.244010e-08
mt65 grph.01t
c
c   define U of Texas cross-section libraries at 300K
c
xs1 2003.62c 2.989032 he3.300 0 1 1 2841 0 0 2.585E-08 $ He-3
xs2 2004.62c 4.001500 he4.300 0 1 1 2761 0 0 2.585E-08 $ He-4
xs3 5010.62c 9.926921 b10.300 0 1 1 29335 0 0 2.585E-08 $ B-10
xs4 5011.62c 10.914700 b11.300 0 1 1 107576 0 0 2.585E-08 $ B-11
xs5 6000.62c 11.898000 cnat.300 0 1 1 25106 0 0 2.585E-08 $ C-nat
xs6 8016.62c 15.853160 o16.300 0 1 1 60016 0 0 2.585E-08 $ O-16
xs7 26054.62c 53.476002 fe54.300 0 1 1 190627 0 0 2.585E-08 $ Fe-54
xs8 26056.62c 55.453999 fe56.300 0 1 1 338423 0 0 2.585E-08 $ Fe-56

```

```
xs9  26057.62c 56.445999 fe57.300 0 1 1 167418 0 0 2.585E-08 $ Fe-57
xs10 26058.62c 57.436001 fe58.300 0 1 1 109347 0 0 2.585E-08 $ Fe-58
xs11 92235.62c 233.025000 u235.300 0 1 1 452322 0 0 2.585E-08 $ U-235
xs12 92238.62c 236.006000 u238.300 0 1 1 491254 0 0 2.585E-08 $ U-238
c
c      PROBLEM TYPE
c
mode n
totnu
kcode 5000 1.0 10 210
c
sdef pos=0 0 -351.818 axs=0 0 1 rad=d1 ext=d2
si1 0 88.29
sp1 0 1
si2 0 178.41
sp2 0 1
c
c      Printing and cutoff cards
c
print
dbcn 9j 300
prdmp j -60 1 2
```

APPENDIX C. MCNP4B Models of ASTRA Facility

Appendix C collects the MCNP4B input files for the models of the ASTRA facility. Appendix C.1 contains the model with an exact ‘super’ cell core representation. Appendix C.2 contains the model of an infinite lattice with the exact ‘super’ cell representation of the fuelled region of the ASTRA core. In Appendix C.3, the same infinite lattice is approximated by a primitive BCC unit cell with borated fuel spheres. This approximate core representation is applied to the ASTRA core in Appendix C.4. Details on the ASTRA facility may be found in Chapter 6.

APPENDIX C.1: MCNP4B model of ASTRA, supercell core representation

ASTRA - PBMR CRITICAL EXPERIMENT

c
c MCNP4B model of the PEMR mockup in ASTRA facility at the Kurchatov
c Institute, Moscow

c Control/shutoff rod positions:

c	SD rods fully withdrawn	h = 395.3	cm
c	CR2 in position 1	h = 382.7	cm
c	all other CRs in position 1	h = 382.7	cm
c	MR1 at reference critical height	h = 366.5	cm

c No top reflector
c Packing fraction = 0.625
c BCC lattice
c No exclusion zones

c J.R. Lebenhaft, MIT, July 2001

C CELLS

§ outside world

c reactor structure

```

2   9   -1.65      8   -9  -32                                $ bottom reflector
c   3   9   -1.65      25  -26
c           -35  36  -37  38  -39  -40  41  42
c           28 183 184 185 186 187                                $ top reflector
4   0           9  -26  -32
                   (35:-36: 37:-38: 39: 40:-41:-42)
fill=1(5)                                $ radial reflector

```

c radial reflector lattice

```
5      0          -55   56  -57   58  
lat=1  u=1  
fill=-12:4 -8:8 0:0
```

```

0 0 0 0 0      0 0      5 5      5 0      0      0      0 0 0 0
c
c -----
c
c      universe 5: solid graphite block
c
10   9    -1.65      -68                      u=5
c
c      universe 6: graphite block with empty center hole
c
15   9    -1.65      54                      u=6    $ graphite
16   11   5.058e-05  -54                      u=6    $ air
c
c      universe 7: graphite block with filled center hole
c
20   9    -1.65      54                      u=7    $ graphite
21   11   5.058e-05  -54      53          u=7    $ air gap
22   9    -1.65      -53                     u=7    $ graphite plug
c
c      universe 8: graphite block with small experimental channel
c          and empty center hole
c
25   9    -1.65      54 (199:-200:-198)      u=8    $ graphite
26   11   5.058e-05  198 -199   200          u=8    $ channel
27   11   5.058e-05  -54                     u=8    $ hole
c
c      universe 9: graphite block with small experimental channel
c          and plug in center hole
c
30   9    -1.65      54 (199:-200:-198)      u=9    $ graphite
31   11   5.058e-05  198 -199   200          u=9    $ channel
32   11   5.058e-05  -54      53          u=9    $ air gap
33   9    -1.65      -53                     u=9    $ plug
c
c -----
c
c      universe 11: control-rod spider
c
35   7    -7.9       203                      u=11   $ outer ring
36   7    -7.9       -202                     u=11   $ center
37   7    -7.9       202 -203 -205   206         u=11   $ x-tie
38   7    -7.9       202 -203 -207   208         u=11   $ y-tie
39   11   5.058e-05  202 -203   205   207         u=11   $ gap - top right
40   11   5.058e-05  202 -203 -206   207         u=11   $ gap - top left
41   11   5.058e-05  202 -203   205 -206        u=11   $ gap - bot right
42   11   5.058e-05  202 -203 -206 -208        u=11   $ gap - bot left
c
c -----
c
c      universe 12: control rod end-plate
c
920  7    -7.9       203   521   522   523   524   525
                  526   527   528   529   530   531
                  532   533   534   535
                                         u=12   $ outer ring
c
921  11   5.058e-05 -521
922  11   5.058e-05 -522
                                         u=12   $ pin 1 holder
                                         u=12   $ pin 2 holder

```

```

923 11 5.058e-05 -523 u=12 $ pin 3 holder
924 11 5.058e-05 -524 u=12 $ pin 4 holder
925 11 5.058e-05 -525 u=12 $ pin 5 holder
926 11 5.058e-05 -526 u=12 $ pin 6 holder
927 11 5.058e-05 -527 u=12 $ pin 7 holder
928 11 5.058e-05 -528 u=12 $ pin 8 holder
929 11 5.058e-05 -529 u=12 $ pin 9 holder
930 11 5.058e-05 -530 u=12 $ pin 10 holder
931 11 5.058e-05 -531 u=12 $ pin 11 holder
932 11 5.058e-05 -532 u=12 $ pin 12 holder
933 11 5.058e-05 -533 u=12 $ pin 13 holder
934 11 5.058e-05 -534 u=12 $ pin 14 holder
935 11 5.058e-05 -535 u=12 $ pin 15 holder
c
936 7 -7.9 -202 u=12 $ center
937 7 -7.9 202 -203 -205 206 u=12 $ x-tie
938 7 -7.9 202 -203 -207 208 u=12 $ y-tie
939 11 5.058e-05 202 -203 205 207 u=12 $ gap - top right
940 11 5.058e-05 202 -203 -206 207 u=12 $ gap - top left
941 11 5.058e-05 202 -203 205 -208 u=12 $ gap - bot right
942 11 5.058e-05 202 -203 -206 -208 u=12 $ gap - bot left
c
c -----
c
c universe 15: control/shutdown pin assembly
c
45 0 -95 fill=16(21) u=15 $ pin 1
46 0 -96 fill=16(22) u=15 $ pin 2
47 0 -97 fill=16(23) u=15 $ pin 3
48 0 -98 fill=16(24) u=15 $ pin 4
49 0 -99 fill=16(25) u=15 $ pin 5
50 0 -100 fill=16(26) u=15 $ pin 6
51 0 -101 fill=16(27) u=15 $ pin 7
52 0 -102 fill=16(28) u=15 $ pin 8
53 0 -103 fill=16(29) u=15 $ pin 9
54 0 -104 fill=16(30) u=15 $ pin 10
55 0 -105 fill=16(31) u=15 $ pin 11
56 0 -106 fill=16(32) u=15 $ pin 12
57 0 -107 fill=16(33) u=15 $ pin 13
58 0 -108 fill=16(34) u=15 $ pin 14
59 0 -109 fill=16(35) u=15 $ pin 15
c
60 11 5.058e-05 95 96 97 98 99 100
          101 102 103 104 105 106
          107 108 109 u=15 $ air
c
c universe 16: contents of absorber pin
c
61 7 -7.9 110 u=16 $ s/s clad
62 5 -1.53 -110 u=16 $ B4C
c
c -----
c
c universe 17: air-filled portion of control/shutdown pins
c
64 0 -95 fill=18(21) u=17 $ pin 1
65 0 -96 fill=18(22) u=17 $ pin 2

```

```

66 0 -97 fill=18(23) u=17 $ pin 3
67 0 -98 fill=18(24) u=17 $ pin 4
68 0 -99 fill=18(25) u=17 $ pin 5
69 0 -100 fill=18(26) u=17 $ pin 6
70 0 -101 fill=18(27) u=17 $ pin 7
71 0 -102 fill=18(28) u=17 $ pin 8
72 0 -103 fill=18(29) u=17 $ pin 9
73 0 -104 fill=18(30) u=17 $ pin 10
74 0 -105 fill=18(31) u=17 $ pin 11
75 0 -106 fill=18(32) u=17 $ pin 12
76 0 -107 fill=18(33) u=17 $ pin 13
77 0 -108 fill=18(34) u=17 $ pin 14
78 0 -109 fill=18(35) u=17 $ pin 15
79 11 5.058e-05 95 96 97 98 99 100
           101 102 103 104 105 106
           107 108 109                               u=17 $ air
c
c   universe 18: contents of absorber pin
c
80 7 -7.9 110                               u=18 $ s/s clad
81 11 5.058e-05 -110                         u=18 $ air
c
c -----
c   universe 19: upper pin holder
c
82 0 -501 fill=20(21) u=19 $ pin 1
83 0 -502 fill=20(22) u=19 $ pin 2
84 0 -503 fill=20(23) u=19 $ pin 3
85 0 -504 fill=20(24) u=19 $ pin 4
86 0 -505 fill=20(25) u=19 $ pin 5
87 0 -506 fill=20(26) u=19 $ pin 6
88 0 -507 fill=20(27) u=19 $ pin 7
89 0 -508 fill=20(28) u=19 $ pin 8
90 0 -509 fill=20(29) u=19 $ pin 9
91 0 -510 fill=20(30) u=19 $ pin 10
92 0 -511 fill=20(31) u=19 $ pin 11
93 0 -512 fill=20(32) u=19 $ pin 12
94 0 -513 fill=20(33) u=19 $ pin 13
95 0 -514 fill=20(34) u=19 $ pin 14
96 0 -515 fill=20(35) u=19 $ pin 15
97 11 5.058e-05 501 502 503 504 505 506
           507 508 509 510 511 512
           513 514 515                               u=19 $ air
c
c   universe 20: hollow interior
c
98 7 -7.9 201                               u=20 $ s/s holder
99 11 5.058e-05 -201                         u=20 $ air
c
c -----
c   universe 21: control rod CR1 (with small experiment channel)
c
100 9 -1.65 54 (199:-200:-198)             u=21 $ graphite
101 11 5.058e-05 198 -199 200               u=21 $ expt. channel
102 11 5.058e-05 -54 204                   u=21 $ surrounding air

```

```

103 11 5.058e-05 -204 -215 u=21 $ air below rod
104 0 -204 215 fill=210 u=21 $ rod

c
c universe 22: control rod CR2
c
105 9 -1.65 54 u=22 $ graphite
106 11 5.058e-05 -54 204 u=22 $ surrounding air
107 11 5.058e-05 -204 -215 u=22 $ air below rod
108 0 -204 215 fill=210 u=22 $ rod

c
c
c universe 23: control rod CR3
c
110 9 -1.65 54 u=23 $ graphite
111 11 5.058e-05 -54 204 u=23 $ surrounding air
112 11 5.058e-05 -204 -215 u=23 $ air below rod
113 0 -204 215 fill=210 u=23 $ rod

c
c
c universe 24: control rod CR4
c
115 9 -1.65 54 u=24 $ graphite
116 11 5.058e-05 -54 204 u=24 $ surrounding air
117 11 5.058e-05 -204 -215 u=24 $ air below rod
118 0 -204 215 fill=210 u=24 $ rod

c
c
c universe 25: control rod CR5
c
120 9 -1.65 54 u=25 $ graphite
121 11 5.058e-05 -54 204 u=25 $ surrounding air
122 11 5.058e-05 -204 -215 u=25 $ air below rod
123 0 -204 215 fill=210 u=25 $ rod

c
c
c -----
c
c universe 26: manual rod MR1
c
125 9 -1.65 54 u=26 $ graphite
126 11 5.058e-05 -54 213 u=26 $ surrounding air
127 11 5.058e-05 -213 -315 u=26 $ air below rod
128 0 -213 315 fill=220 u=26 $ rod

c
c
c -----
c
c universe 31: control rod SR1
c
130 9 -1.65 54 u=31 $ graphite
131 11 5.058e-05 -54 204 u=31 $ surrounding air
132 11 5.058e-05 -204 -215 u=31 $ air below rod
133 0 -204 215 fill=210 u=31 $ rod

c
c
c universe 32: control rod SR2
c
135 9 -1.65 54 u=32 $ graphite

```

```

136 11 5.058e-05 -54 204 u=32 $ surrounding air
137 11 5.058e-05 -204 -215 u=32 $ air below rod
138 0 -204 215 fill=210 u=32 $ rod
c
c
c      universe 33: control rod SR3
c
140 9 -1.65 54 u=33 $ graphite
141 11 5.058e-05 -54 204 u=33 $ surrounding air
142 11 5.058e-05 -204 -215 u=33 $ air below rod
143 0 -204 215 fill=210 u=33 $ rod
c
c
c      universe 34: control rod SR4
c
145 9 -1.65 54 u=34 $ graphite
146 11 5.058e-05 -54 204 u=34 $ surrounding air
147 11 5.058e-05 -204 -215 u=34 $ air below rod
148 0 -204 215 fill=210 u=34 $ rod
c
c
c      universe 35: control rod SR5
c
150 9 -1.65 54 u=35 $ graphite
151 11 5.058e-05 -54 204 u=35 $ surrounding air
152 11 5.058e-05 -204 -215 u=35 $ air below rod
153 0 -204 215 fill=210 u=35 $ rod
c
c
c      universe 36: control rod SR6
c
155 9 -1.65 54 u=36 $ graphite
156 11 5.058e-05 -54 204 u=36 $ surrounding air
157 11 5.058e-05 -204 -215 u=36 $ air below rod
158 0 -204 215 fill=210 u=36 $ rod
c
c
c      universe 37: control rod SR7
c
160 9 -1.65 54 u=37 $ graphite
161 11 5.058e-05 -54 204 u=37 $ surrounding air
162 11 5.058e-05 -204 -215 u=37 $ air below rod
163 0 -204 215 fill=210 u=37 $ rod
c
c
c      universe 38: control rod SR8
c
165 9 -1.65 54 u=38 $ graphite
166 11 5.058e-05 -54 204 u=38 $ surrounding air
167 11 5.058e-05 -204 -215 u=38 $ air below rod
168 0 -204 215 fill=210 u=38 $ rod
c
c -----
c
c      universe 210: details of control/shutoff rod
c
170 7 -7.9 -216 u=210 $ lower endplate

```

```

171 0 216 -217 fill=12 u=210 $ lower pin holder
172 0 217 -218 fill=17 u=210 $ empty pin zone
173 0 218 -219 fill=15 u=210 $ absorber
174 0 219 -220 fill=17 u=210 $ empty pin zone
175 0 220 -221 fill=19 u=210 $ upper pin holder
176 0 221 -222 fill=11 u=210 $ spider
177 11 5.058e-05 222 -223 202 u=210 $ middle gap
178 7 -7.9 222 -223 -202 u=210 $ middle joint
179 7 -7.9 223 -224 u=210 $ lower endplate
180 0 224 -225 fill=12 u=210 $ lower pin holder
181 0 225 -226 fill=17 u=210 $ empty pin zone
182 0 226 -227 fill=15 u=210 $ absorber region
183 0 227 -228 fill=17 u=210 $ empty pin zone
184 0 228 -229 fill=19 u=210 $ upper pin holder
185 0 229 -230 fill=11 u=210 $ spider
186 11 5.058e-05 230 u=210 $ air above rod
c
c universe 220: details of manual rod
c
190 12 -2.69 -316 210 u=220 $ solid bottom
191 12 -7.69 316 -317 210 -211 u=220 $ inner wall
192 11 5.058e-05 316 -317 211 -212 u=220 $ air gap
193 12 -2.69 316 -317 212 u=220 $ outer wall
194 12 -2.69 317 -318 210 u=220 $ solid top
195 11 5.058e-05 -318 -210 u=220 $ center gap
196 12 -2.69 318 -319 u=220 $ upper mid plate
c
c -----
-
c
c core cavity
c
510 11 5.058e-05 17 -26 31 -35 36 -37 38
      -39 -40 41 42 186 187 $ above fuel zone
511 11 5.058e-05 18 -26 30 -31 185 $ above mixed zone
512 11 5.058e-05 19 -26 28 -30 183 184 $ above inner reflect
c
c core regions
c
529 0 9 -19 28 -30 184 $ inner reflector
      fill=50(2)
530 0 9 -18 30 -31 185 $ mixed zone
      fill=52(3)
531 0 9 -17 31 -35 36 -37
      38 -39 -40 41 42 186
      187 fill=54(4) $ fuel outer zone
c
c experimental channels
c
532 0 9 -26 -28 fill=68 $ central channel
533 0 9 -26 -183 fill=70 $ E1
534 0 9 -26 -184 fill=75 $ E2
535 0 9 -26 -185 fill=80 $ E3
536 0 9 -26 -186 fill=85 $ E4
537 0 9 -26 -187 fill=90 $ E5
c

```

```

c -----
c
c      universe 50: inner reflector
c
540 0           -70   69  -72   71  -74   73
    lat=1  fill=51(7)
    u=50
541 0           -170  169  -172  171  -174  173
    lat=1  u=51
    fill=0:1 0:1 -2:2
        56 56 56 56
        56 56 56 56
        56 56 56 56
        56 56 56 56
        56 56 56 56
c -----
c
c      universe 52: mixed fuel/moderator/absorber zone
c
542 0           -70   69  -72   71  -74   73
    lat=1  fill=53(7)
    u=52
543 0           -170  169  -172  171  -174  173
    lat=1  u=53
    fill=0:1 0:1 -2:2
        57 57 57 57
        57 57 57 57
        57 57 58 57
        57 57 57 57
        57 57 57 57
c -----
c
c      universe 54: outer fuel zone
c
544 0           -70   69  -72   71  -74   73
    lat=1  fill=55(7)
    u=54
545 0           -170  169  -172  171  -174  173
    lat=1  u=55
    fill=0:1 0:1 -2:2
        59 59 59 59
        59 60 59 59
        59 59 59 59
        59 59 60 59
        59 59 59 59
c -----
c
c      Universe 56: bcc unit cell (moderator)
c
550 4  -1.68      -641                      u=56
551 4  -1.68      -642                      u=56
552 4  -1.68      -643                      u=56
553 4  -1.68      -644                      u=56
554 4  -1.68      -645                      u=56

```

```

555 4 -1.68      -646                      u=56
556 4 -1.68      -647                      u=56
557 4 -1.68      -648                      u=56
558 4 -1.68      -649                      u=56
c
c     air between spheres
c
559 11 5.058e-05    641  642  643  644  645  646
                           647  648  649
u=56
c
c -----
c
c     Universe 57: bcc unit cell (moderator + 1 fuel sphere)
c
565 4 -1.68      -641                      u=57
566 4 -1.68      -642                      u=57
567 4 -1.68      -643                      u=57
568 4 -1.68      -644                      u=57
569 0            -645          fill=62(645) u=57
570 4 -1.68      -646                      u=57
571 4 -1.68      -647                      u=57
572 4 -1.68      -648                      u=57
573 4 -1.68      -649                      u=57
c
c     air between spheres
c
574 11 5.058e-05    641  642  643  644  645  646
                           647  648  649
u=57
c
c -----
c
c     Universe 58: bcc unit cell (moderator + 1 absorber sphere)
c
580 4 -1.68      -641                      u=58
581 4 -1.68      -642                      u=58
582 4 -1.68      -643                      u=58
583 4 -1.68      -644                      u=58
584 0            -645          fill=65(645) u=58
585 4 -1.68      -646                      u=58
586 4 -1.68      -647                      u=58
587 4 -1.68      -648                      u=58
588 4 -1.68      -649                      u=58
c
c     air between spheres
c
589 11 5.058e-05    641  642  643  644  645  646
                           647  648  649
u=58
c
c -----
c
c     Universe 59: bcc unit cell (fuel)
c
595 0            -641          fill=62(641)  u=59
596 0            -642          fill=62(642)  u=59

```

```

597 0 -643 fill=62(643) u=59
598 0 -644 fill=62(644) u=59
599 0 -645 fill=62(645) u=59
600 0 -646 fill=62(646) u=59
601 0 -647 fill=62(647) u=59
602 0 -648 fill=62(648) u=59
603 0 -649 fill=62(649) u=59
c
c   air between spheres
c
604 11 5.058e-05 641 642 643 644 645 646
          647 648 649
u=59
c
c -----
c
c   Universe 60: bcc unit cell (fuel + 1 absorber sphere)
c
610 0 -641 fill=62(641) u=60
611 0 -642 fill=62(642) u=60
612 0 -643 fill=62(643) u=60
613 0 -644 fill=62(644) u=60
614 0 -645 fill=65(645) u=60
615 0 -646 fill=62(646) u=60
616 0 -647 fill=62(647) u=60
617 0 -648 fill=62(648) u=60
618 0 -649 fill=62(649) u=60
c
c   air between spheres
c
619 11 5.058e-05 641 642 643 644 645 646
          647 648 649
u=60
c
c -----
c
c   Universe 62: details of fuel sphere
c
625 4 -1.85 75 u=62 $ shell
626 0 -75 fill=63 u=62 $ fuel region
c
c   Universe 63: embedded coated fuel particles
c
627 0 -76 77 -78 79 -80 81
lat=1 fill=64
u=63
c
c   Universe 64: coated fuel particle
c
628 1 -10.1 -82 u=64 $ UO2 kernel
629 2 -1.1 82 -83 u=64 $ PyC layer 1
630 2 -1.8 83 -84 u=64 $ PyC layer 2
631 3 -3.2 84 -85 u=64 $ SiC layer
632 2 -1.8 85 -86 u=64 $ PyC layer 3
633 4 -1.85 86 u=64 $ graphite
c
c -----

```

```

c
c      universe 65: absorber sphere
c
640  4   -1.75          87                               u=65  $ shell
641  0            -87                               fill=66  u=65  $ absorber
c
c      universe 66: absorber region
c
642  0           -88  89 -90  91 -92  93
    lat=1  fill=67
    u=66                               $ simple cubic
c
c      universe 67: absorber kernel
c
643  5   -2.4          -94                               u=67  $ B4C
644  4   -1.75          94                               u=67  $ graphite
c
c -----
c      universe 68: central channel
c
650  10  -2.69          27                               u=68  $ Al wall
651  11  5.058e-05  -27                               u=68  $ air
c
c -----
c      universe 70: experimental tube E1
c
655  10  -2.69          188                             u=70  $ Al wall
656  11  5.058e-05  -188                             u=70  $ air
c
c      universe 75: experimental tube E2
c
660  10  -2.69          189                             u=75  $ Al wall
661  11  5.058e-05  -189                             u=75  $ air
c
c      universe 80: experimental tube E3
c
670  10  -2.69          190                             u=80  $ Al wall
671  11  5.058e-05  -190                             u=80  $ air
c
c      universe 85: experimental tube E4
c
680  10  -2.69          191                             u=85  $ Al wall
681  11  5.058e-05  -191                             u=85  $ air
c
c      universe 90: experimental tube E5
c
690  10  -2.69          192                             u=90  $ Al wall
691  11  5.058e-05  -192                             u=90  $ air
c
c -----
c      SURFACES
c
8   pz     0.0                               $ bottom of reactor
9   pz     40.0                             $ bottom of core

```

```

c
c    core height
c
17  pz    308.9                      $ top of outer fuel zone
18  pz    308.9                      $ top of mixed fuel zone
19  pz    308.9                      $ top of inner reflector
c
20  pz    360.8                      $ bottom of Al structure
25  pz    399.5                      $ bottom of upper reflector
26  pz    460.0                      $ top of reactor
27  cz    5.0                        $ center tube - inner surface
28  cz    5.25                       $ center tube - outer surface
30  cz    34.75                      $ inner reflector boundary
31  cz    51.25                      $ mixed- zone boundary
32  cz    190.0                      $ outer surface of reactor
c
c    core boundary (x-y plane)
c
35  px    87.5                       $ right
36  px    -87.5                      $ left
37  py    87.5                       $ top
38  py    -87.5                      $ bottom
39  p     1.0   1.0   0.0   125.0    $ top right
40  p     -1.0  1.0   0.0   125.0    $ top left
41  p     1.0   1.0   0.0  -125.0   $ bottom left
42  p     -1.0  1.0   0.0  -125.0   $ bottom right
c
c    reflector blocks (x-y plane)
c
53  cz    5.6                        $ graphite plug
54  cz    5.7                        $ hole in graphite block
55  px    12.5                       $ right
56  px    -12.5                      $ left
57  py    12.5                       $ top
58  py    -12.5                      $ bottom
c
68  cz    17.68                      $ universe boundary
c
c    pebble-bed lattice
c
69  px    -7.126355                 $ -x
70  px    7.126355                  $ +x
71  py    -7.126355                 $ -y
72  py    7.126355                  $ +y
73  pz    -17.8158874                $ bottom
74  pz    17.8158874                $ top
c
c    inside fuel pebble
c
75  so    2.5                        $ fueled region
c
c    unit cell for CFP lattice
c
76  px    0.124988
77  px    -0.124988
78  py    0.124988
79  py    -0.124988

```

```

80  pz      0.124988
81  pz     -0.124988
c
c   coated fuel particle
c
82  so      0.025          $ UO2 kernel
83  so      0.034          $ buffer
84  so      0.041          $ inner PyC
85  so      0.047          $ SiC
86  so      0.053          $ outer PyC
c
c   inside absorber sphere
c
87  so      2.0            $ radius of absorber region
c
c   unit absorber cell
c
88  px      0.02072235
89  px     -0.02072235
90  py      0.02072235
91  py     -0.02072235
92  pz      0.02072235
93  pz     -0.02072235
c
94  so      0.003          $ absorber kernel radius
c
c   absorber pins - outer surfaces
c
95  c/z    3.8      0.0      0.625
96  c/z   3.47147  1.5456   0.625
97  c/z   2.5427   2.82395  0.625
98  c/z   1.17426  3.61401  0.625
99  c/z   -0.39721 3.77918  0.625
100 c/z   -1.9      3.2909   0.625
101 c/z   -3.07426 2.23358  0.625
102 c/z   -3.71696  0.79006  0.625
103 c/z   -3.71696 -0.79006 0.625
104 c/z   -3.07426 -2.23358 0.625
105 c/z   -1.9      -3.2909  0.625
106 c/z   -0.39721 -3.77918 0.625
107 c/z   1.17426 -3.61401  0.625
108 c/z   2.5427  -2.82395  0.625
109 c/z   3.47147 -1.5456   0.625
c
110 cz     0.505          $ absorber outer surface
c
c   bcc unit cell
c
169 px    -3.5631775      $ -x
170 px     3.5631775      $ +x
171 py    -3.5631775      $ -y
172 py     3.5631775      $ +y
173 pz    -3.5631775      $ bottom
174 pz     3.5631775      $ top
c
c   aluminum experiment tubes - outer surfaces
c

```

```

183 c/z -5.8501 0.0 0.6 $ E1
184 c/z -25.0 0.0 0.6 $ E2
185 c/z -45.0 0.0 0.6 $ E3
186 c/z -65.0 0.0 0.6 $ E4
187 c/z -80.0 0.0 0.6 $ E5
c
c      aluminum experiment tubes - inner surfaces
c
188 c/z -5.8501 0.0 0.5 $ E1
189 c/z -25.0 0.0 0.5 $ E2
190 c/z -45.0 0.0 0.5 $ E3
191 c/z -65.0 0.0 0.5 $ E4
192 c/z -80.0 0.0 0.5 $ E5
c
c      small experiment channels
c
198 px 11.0
199 py 1.5
200 py -1.5
c
c      control and shutoff rod surfaces
c
201 cz 0.3 $ radius of pin end-region
202 cz 1.5 $ joint
203 cz 3.1 $ inside of pin holder
204 cz 4.5 $ outside of pin holder
205 px 0.50 $ pin support
206 px -0.50 $ pin support
207 py 0.50 $ pin support
208 py -0.50 $ pin support
c
c      manual rod
210 cz 3.5 $ inside of inner surface
211 cz 3.75 $ outside of inner surface
212 cz 4.5 $ inside of outer surface
213 cz 4.75 $ outer surface of rod
c
c      CR1
c
215 pz 0.0 $ bottom of lower endplate
216 pz 0.1 $ bottom of lower pin holder
217 pz 1.0 $ bottom of lower pins
218 pz 2.0 $ bottom of B4C in lower pins
219 pz 189.5 $ top of B4C in lower pins
220 pz 190.5 $ bottom of lower pin holder
221 pz 191.2 $ bottom of lower spider
222 pz 192.2 $ bottom of middle gap
223 pz 192.7 $ bottom of upper endplate
224 pz 192.8 $ bottom of pin holder
225 pz 193.7 $ bottom of upper pins
226 pz 194.7 $ bottom of B4C in upper pins
227 pz 382.2 $ top of B4C in upper pins
228 pz 383.2 $ bottom of upper holder
229 pz 383.9 $ bottom of upper spider
230 pz 384.9 $ top of upper spider
c
c      MR1

```

```

c
315 45 pz 0.0           $ bottom of rod
316 45 pz 2.0           $ bottom of air gap
317 45 pz 383.5         $ top of air gap
318 45 pz 385.5         $ bottom of top plate
319 45 pz 388.5         $ top of rod

c
c    upper pin holder
c
501 c/z 3.8 0.0 0.7
502 c/z 3.47147 1.5456 0.7
503 c/z 2.5427 2.82395 0.7
504 c/z 1.17426 3.61401 0.7
505 c/z -0.39721 3.77918 0.7
506 c/z -1.9 3.2909 0.7
507 c/z -3.07426 2.23358 0.7
508 c/z -3.71696 0.79006 0.7
509 c/z -3.71696 -0.79006 0.7
510 c/z -3.07426 -2.23358 0.7
511 c/z -1.9 -3.2909 0.7
512 c/z -0.39721 -3.77918 0.7
513 c/z 1.17426 -3.61401 0.7
514 c/z 2.5427 -2.82395 0.7
515 c/z 3.47147 -1.5456 0.7

c
c    control rod end-plate
c
521 c/z 3.8 0.0 0.3
522 c/z 3.47147 1.5456 0.3
523 c/z 2.5427 2.82395 0.3
524 c/z 1.17426 3.61401 0.3
525 c/z -0.39721 3.77918 0.3
526 c/z -1.9 3.2909 0.3
527 c/z -3.07426 2.23358 0.3
528 c/z -3.71696 0.79006 0.3
529 c/z -3.71696 -0.79006 0.3
530 c/z -3.07426 -2.23358 0.3
531 c/z -1.9 -3.2909 0.3
532 c/z -0.39721 -3.77918 0.3
533 c/z 1.17426 -3.61401 0.3
534 c/z 2.5427 -2.82395 0.3
535 c/z 3.47147 -1.5456 0.3

c
c    spheres
c
641 s -3.5631775 -3.5631775 -3.5631775 3.0 $ [-a/2 -a/2 -b/2]
642 s 3.5631775 -3.5631775 -3.5631775 3.0 $ [ a/2 -a/2 -b/2]
643 s -3.5631775 3.5631775 -3.5631775 3.0 $ [-a/2 a/2 -b/2]
644 s 3.5631775 3.5631775 -3.5631775 3.0 $ [ a/2 a/2 -b/2]
645 so                                3.0 $ [ 0 0 0 ]
646 s -3.5631775 -3.5631775 3.5631775 3.0 $ [-a/2 -a/2 b/2]
647 s 3.5631775 -3.5631775 3.5631775 3.0 $ [ a/2 -a/2 b/2]
648 s -3.5631775 3.5631775 3.5631775 3.0 $ [-a/2 a/2 b/2]
649 s 3.5631775 3.5631775 3.5631775 3.0 $ [ a/2 a/2 b/2]

```

c

c

```

c      RUN PARAMETERS
c
c      problem type
c
mode n
kcode 5000 1.0 10 210
c
sdef pos=0 0 40 axs=0 0 1 rad=d1 ext=d2
si1 5.25 90.5
sp1 0 1
si2 0 268.7
sp2 0 1
c
totnu
print
dbcn 9j 300
prdmp j -60 1 2
c
c      neutron importance
c
imp:n 0
    1 1          $ outside world
    1
    1
    1 1          $ reactor structure
    1 2r         $ u=1: radial reflector lattice
    1 2r         $ u=5: solid graphite block
    1 3r         $ u=6: graphite block with hole
    1 7r         $ u=7: graphite block/plug
    1 22r        $ u=8: graphite block/hole/channel
    1 17r        $ u=9: graphite block/plug/channel
    1 17r        $ u=11: control rod end-plate
    1 17r        $ u=12: lower pin holder
    1 17r        $ u=15 and 16: B4C pins
    1 17r        $ u=17 and 18: gap in pins
    1 17r        $ u=19 and 20: pin holder
    1 4r  1 3r  1 3r  1 3r  1 3r  $ u=21 to 25: CRs
    1 3r          $ u=26: MR1
    1 3r  1 3r  1 3r  1 3r  $ u=31 to 38: SD rods
    1 3r  1 3r  1 3r
    1 16r         $ u=210: details of CR
    1 6r          $ u=220: details of MR
    1 2r          $ cavity above core
    1 2r          $ core regions
    1 5r          $ experimental channels
    1 5r          $ u=50 to 55: unit cells
    1 9r          $ u=56: moderator
    1 9r          $ u=57: moderator + 1 fuel
    1 9r          $ u=58: moderator + 1 absorber
    1 9r          $ u=59: fuel
    1 9r          $ u=60: fuel + absorber
    1 8r          $ u=62 to 64: fuel sphere
    1 4r          $ u=65 to 67: absorber sphere
    1 1           $ u=65: center channel
    1 1           $ u=70: E1
    1 1           $ u=75: E2
    1 1           $ u=80: E3
    1 1           $ u=85: E4
    1 1           $ u=90: E5

```

c

```

c      transformations
c
tr2      0.0        21.3790649    57.8158874    $ inner reflector origin
tr3      0.0        42.7581298    57.8158874    $ mixed zone origin
tr4      0.0        71.2635496    57.8158874    $ fuel zone origin
tr5     100.0        0.0          0.0          $ reflector origin
tr7     -3.5631775   -3.5631775   0.0          $ origin of unit cell fill
c
c      absorber pins - inner surfaces
c
tr21     3.8        0.0          1.0
tr22     3.47147   1.5456       1.0
tr23     2.5427    2.82395     1.0
tr24     1.17426   3.61401     1.0
tr25    -0.39721   3.77918     1.0
tr26     -1.9       3.2909      1.0
tr27    -3.07426   2.23358     1.0
tr28    -3.71696   0.79006     1.0
tr29    -3.71696  -0.79006     1.0
tr30    -3.07426  -2.23358     1.0
tr31     -1.9      -3.2909      1.0
tr32    -0.39721  -3.77918     1.0
tr33     1.17426  -3.61401     1.0
tr34     2.5427   -2.82395     1.0
tr35     3.47147  -1.5456      1.0
c
c      control rod positions
c
tr41     0          0          382.7      $ CR1      1
tr42     0          0          382.7      $ CR2      1
tr43     0          0          382.7      $ CR3      1
tr44     0          0          382.7      $ CR4      1
tr45     0          0          382.7      $ CR5      1
tr46     0          0          366.5      $ MR1     (critical)
c
c      shutdown rod positions
c
tr51     0          0          395.3      $ SD1      out
tr52     0          0          395.3      $ SD2
tr53     0          0          395.3      $ SD3
tr54     0          0          395.3      $ SD4
tr55     0          0          395.3      $ SD5
tr56     0          0          395.3      $ SD6
tr57     0          0          395.3      $ SD7
tr58     0          0          395.3      $ SD8
c
c      sphere positions
c
tr641    -3.5631775  -3.5631775  -3.5631775
tr642     3.5631775  -3.5631775  -3.5631775
tr643    -3.5631775   3.5631775  -3.5631775
tr644     3.5631775   3.5631775  -3.5631775
tr645     0.0         0.0         0.0
tr646    -3.5631775  -3.5631775   3.5631775
tr647     3.5631775  -3.5631775   3.5631775
tr648    -3.5631775   3.5631775   3.5631775
tr649     3.5631775   3.5631775   3.5631775

```

```

c
c      material specifications
c
m1    92234.60c  0.0015      92235.60c  0.2066
      92236.60c  0.0009      92238.60c  0.7910
      8016.60c  2.0
                                         $ UO2
c
m2    6000.60c  1
mt2   grph.01t
c
m3    14000.60c  0.5
mt3   grph.01t
c
m4    6000.60c -0.999999      5010.60c -0.198e-06
      5011.60c -0.802e-06
                                         $ graphite
mt4   grph.01t
c
m5    6000.60c  0.2
      5011.60c  0.6416
                                         $ B4C
mt5   grph.01t
c
c      control and shutdown rods
c
m7    26000.50c -0.691      6000.60c -0.0012
      14000.60c -0.0008      25055.60c -0.02
      24000.50c -0.18        28000.50c -0.1
      22000.60c -0.007
                                         $ s/steel
c
c      reflector graphite
c
m9    6000.60c -0.99999945    5010.60c -0.1089e-06
      5011.60c -0.4411e-06
mt9   grph.01t
c
c      aluminum experiment tubes
c
m10   13027.60c -0.9999986    5010.60c -0.0000014
c
c      humid air
c
m11   1001.60c  5.79913e-07    1002.60c  8.7e-11
      7014.60c  3.98536e-05    7015.60c  1.46400e-07
      8016.60c  1.0e-05
c
c      aluminum manual rod
c
m12   29000.50c -0.0035      25055.60c -0.0035
      26000.50c -0.0050      14000.60c -0.0085
      24000.50c -0.0025      13027.60c -0.9770

```

APPENDIX C.2: Infinite ASTRA lattice using exact supercell model

ASTRA SUPERCELL MODEL

```

c
c MCNP4B supercell model with 40 fuel spheres with borated shells.
c The CFPs are modeled explicitly. The boron and carbon in these
c spheres reproduce the 95/5 fuel-to-absorber sphere ratio. The
c repeating unit geometry is an enlarged BCC cell.
c
c -----
c
c CELLS
c
1 0           60: -59:  62: -61          $ outside world
2 0           -60   59   -62   61
fill=1
3 0           -70   69   -72   71   -74   73          $ periodic BC
lat=1
fill=2(7)
u=1          $ inside world
c
c universe 1: super cell
c
4 0           -170  169 -172  171 -174  173
lat=1 u=2
fill=0:1 0:1 -2:2
  59 59 59 59
  59 60 59 59
  59 59 59 59
  59 59 60 59
  59 59 59 59
c
c -----
c
c Universe 59: bcc unit cell (fuel)
c
10 0           -641          fill=62(641)  u=59
11 0           -642          fill=62(642)  u=59
12 0           -643          fill=62(643)  u=59
13 0           -644          fill=62(644)  u=59
14 0           -645          fill=62(645)  u=59
15 0           -646          fill=62(646)  u=59
16 0           -647          fill=62(647)  u=59
17 0           -648          fill=62(648)  u=59
18 0           -649          fill=62(649)  u=59
c
c air between spheres
c
19 11  5.058e-05    641  642  643  644  645  646
                           647  648  649
u=59
c
c -----
c
c Universe 60: bct unit cell (fuel + 1 absorber sphere)
c
25 0           -641          fill=62(641)  u=60

```

```

26 0 -642 fill=62(642) u=60
27 0 -643 fill=62(643) u=60
28 0 -644 fill=62(644) u=60
29 0 -645 fill=65(645) u=60
30 0 -646 fill=62(646) u=60
31 0 -647 fill=62(647) u=60
32 0 -648 fill=62(648) u=60
33 0 -649 fill=62(649) u=60
c
c      air between spheres
c
34 11 5.058e-05 641 642 643 644 645 646
          647 648 649
u=60
c
c -----
c
c      Universe 62: details of fuel sphere
c
45 4 -1.85 75 u=62 $ shell
46 0 -75 fill=63 u=62 $ fuel region
c
c      Universe 63: embedded coated fuel particles
c
47 0 -76 77 -78 79 -80 81
lat=1 fill=64
u=63
c
c      Universe 64: coated fuel particle
c
48 1 -10.1 -82 u=64 $ UO2 kernel
49 2 -1.1 82 -83 u=64 $ PyC layer 1
50 2 -1.8 83 -84 u=64 $ PyC layer 2
51 3 -3.2 84 -85 u=64 $ SiC layer
52 2 -1.8 85 -86 u=64 $ PyC layer 3
53 4 -1.85 86 u=64 $ graphite
c
c -----
c
c      universe 65: absorber sphere
c
60 4 -1.75 87 u=65 $ shell
61 0 -87 fill=66 u=65 $ absorber
c
c      universe 66: absorber region
c
62 0 -88 89 -90 91 -92 93
lat=1 fill=67
u=66 $ simple cubic
c
c      universe 67: absorber kernel
c
63 5 -2.4 -94 u=67 $ B4C
64 4 -1.75 94 u=67 $ graphite
c
c      SURFACES

```

```

c
c      pebble-bed lattice
c
59   -60  px    -10.6895325          $ -x
60   -59  px     10.6895325          $ +x
61   -62  py    -10.6895325          $ -y
62   -61  py     10.6895325          $ +y
c
69   px     -7.126355             $ -x
70   px     7.126355             $ +x
71   py     -7.126355             $ -y
72   py     7.126355             $ +y
73   pz    -17.8158874           $ bottom
74   pz    17.8158874           $ top
c
c      inside fuel pebble
c
75   so     2.5                  $ fueled region
c
c      unit cell for CFP lattice
c
76   px     0.124988
77   px     -0.124988
78   py     0.124988
79   py     -0.124988
80   pz     0.124988
81   pz     -0.124988
c
c      coated fuel particle
c
82   so     0.025              $ UO2 kernel
83   so     0.034              $ buffer
84   so     0.041              $ inner PyC
85   so     0.047              $ SiC
86   so     0.053              $ outer PyC
c
c      inside absorber sphere
c
87   so     2.0                  $ radius of absorber region
c
c      unit absorber cell
c
88   px     0.02072235
89   px     -0.02072235
90   py     0.02072235
91   py     -0.02072235
92   pz     0.02072235
93   pz     -0.02072235
c
94   so     0.003              $ absorber kernel radius
c
c      bcc unit cell
c
169  px     -3.5631775          $ -x
170  px     3.5631775           $ +x
171  py     -3.5631775          $ -y
172  py     3.5631775           $ +y

```

```

173  pz     -3.5631775          $ bottom
174  pz     3.5631775          $ top
c
c      spheres
c
641  s    -3.5631775  -3.5631775  -3.5631775  3.0   $ [-a/2 -a/2 -b/2]
642  s    3.5631775  -3.5631775  -3.5631775  3.0   $ [ a/2 -a/2 -b/2]
643  s    -3.5631775  3.5631775  -3.5631775  3.0   $ [-a/2 a/2 -b/2]
644  s    3.5631775  3.5631775  -3.5631775  3.0   $ [ a/2 a/2 -b/2]
645  so           3.0   $ [ 0  0  0 ]
646  s    -3.5631775  -3.5631775  3.5631775  3.0   $ [-a/2 -a/2 b/2]
647  s    3.5631775  -3.5631775  3.5631775  3.0   $ [ a/2 -a/2 b/2]
648  s    -3.5631775  3.5631775  3.5631775  3.0   $ [-a/2 a/2 b/2]
649  s    3.5631775  3.5631775  3.5631775  3.0   $ [ a/2 a/2 b/2]
c
c      TRANSFORMATIONS
c
tr7      -3.5631775  -3.5631775  0.0       $ origin of unit cell fill
c
c      sphere positions
c
tr641     -3.5631775  -3.5631775  -3.5631775
tr642     3.5631775  -3.5631775  -3.5631775
tr643    -3.5631775  3.5631775  -3.5631775
tr644     3.5631775  3.5631775  -3.5631775
tr645     0.0        0.0        0.0
tr646    -3.5631775  -3.5631775  3.5631775
tr647     3.5631775  -3.5631775  3.5631775
tr648    -3.5631775  3.5631775  3.5631775
tr649     3.5631775  3.5631775  3.5631775
c
c      MATERIALS
c
m1      92234.60c  0.0015      92235.60c  0.2066
         92236.60c  0.0009      92238.60c  0.7910
         8016.60c  2.0          $ UO2
c
m2      6000.60c  1            $ PyC
mt2     grph.01t
c
m3      14000.60c  0.5         6000.60c  0.5          $ Sic
mt3     grph.01t
c
m4      6000.60c -0.999999    5010.60c -0.198e-06
         5011.60c -0.802e-06
mt4     grph.01t          $ graphite
c
m5      6000.60c  0.2         5010.60c  0.1584
         5011.60c  0.6416
mt5     grph.01t          $ B4C
c
c      humid air
c
m11     1001.60c  5.79913e-07  1002.60c  8.7e-11
         7014.60c  3.98536e-05   7015.60c  1.46400e-07
         8016.60c  1.0e-05

```

```

c
c      RUN PARAMETERS
c
mode n
kcode 5000 1.0 10 110
c
sdef pos=0 0 -17.8158874 axs=0 0 1 rad=d1 ext=d2
s1 0 7.126355
sp1 0 1
s12 0 35.6317748
sp2 0 1
c
imp:n 0                      $ outside world
    1                         $ inside world
    1                         $ u=1
    1                         $ u=2: super cell
    1 9r                       $ u=59
    1 9r                       $ u=60
    1 8r                       $ u=62 to u=64
    1 4r                       $ u=65 to u=67
c
totnu
print
dbcn 9j 300
prdmp j -60 1 2

```

APPENDIX C.3: Infinite ASTRA lattice using borated fuel shell

```

ASTRA SUPERCELL MODEL
c
c      MCNP4B model of an infinite BCC lattice of fuel spheres with
c      borated shells.
c
c -----
c
c      CELLS
c
1   0          60: -59:  62: -61                                $ outside world
2   0          -60    59   -62    61
fill=1
3   0          -70    69   -72    71   -74    73
fill=2  lat=1
u=1                                         $ lattice
c
c      Universe 2: bcc unit cell
c
25  0          -641          fill=62(641)  u=2
26  0          -642          fill=62(642)  u=2
27  0          -643          fill=62(643)  u=2
28  0          -644          fill=62(644)  u=2
29  0          -645          fill=62(645)  u=2
30  0          -646          fill=62(646)  u=2
31  0          -647          fill=62(647)  u=2
32  0          -648          fill=62(648)  u=2
33  0          -649          fill=62(649)  u=2
c
c      air between spheres
c
34  11  5.058e-05    641  642  643  644  645  646
                           647  648  649
u=2
c
c -----
c
c      Universe 62: details of fuel sphere
c
45  6  -1.850087    75                                u=62  $ borated
shell
46  0          -75          fill=63      u=62  $ fuel region
c
c      Universe 63: embedded coated fuel particles
c
47  0          -76  77  -78  79  -80  81
lat=1  fill=64
u=63
c
c      Universe 64: coated fuel particle
c
48  1  -10.1        -82                                u=64  $ UO2 kernel
49  2  -1.1         82  -83                            u=64  $ PyC layer 1
50  2  -1.8         83  -84                            u=64  $ PyC layer 2
51  3  -3.2         84  -85                            u=64  $ SiC layer

```

```

52   2    -1.8          85  -86          u=64 $ PyC layer 3
53   4    -1.85         86          u=64 $ graphite
c

c      SURFACES
c
c      pebble-bed lattice
c
59   -60  px    -5.34476625      $ -x
60   -59  px    5.34476625      $ +x
61   -62  py    -5.34476625      $ -y
62   -61  py    5.34476625      $ +y
c
c      bcc unit cell (packing fraction = 0.625)
c
69   px    -3.5631775      $ -x
70   px    3.5631775      $ +x
71   py    -3.5631775      $ -y
72   py    3.5631775      $ +y
73   pz    -3.5631775      $ bottom
74   pz    3.5631775      $ top
c
c      inside fuel pebble
c
75   so    2.5          $ fueled region
c
c      unit cell for CFP lattice
c
76   px    0.124988
77   px    -0.124988
78   py    0.124988
79   py    -0.124988
80   pz    0.124988
81   pz    -0.124988
c
c      coated fuel particle
c
82   so    0.025          $ UO2 kernel
83   so    0.034          $ buffer
84   so    0.041          $ inner PyC
85   so    0.047          $ SiC
86   so    0.053          $ outer PyC
c
c      spheres
c
641  s    -3.5631775  -3.5631775  -3.5631775  3.0  $ [-a/2 -a/2 -b/2]
642  s    3.5631775   -3.5631775  -3.5631775  3.0  $ [ a/2 -a/2 -b/2]
643  s    -3.5631775  3.5631775   -3.5631775  3.0  $ [-a/2 a/2 -b/2]
644  s    3.5631775   3.5631775   -3.5631775  3.0  $ [ a/2 a/2 -b/2]
645  so   3.5631775   3.5631775   3.5631775  3.0  $ [ 0   0   0   ]
646  s    -3.5631775  -3.5631775  3.5631775  3.0  $ [-a/2 -a/2 b/2]
647  s    3.5631775   -3.5631775  3.5631775  3.0  $ [ a/2 -a/2 b/2]
648  s    -3.5631775  3.5631775   3.5631775  3.0  $ [-a/2 a/2 b/2]
649  s    3.5631775   3.5631775   3.5631775  3.0  $ [ a/2 a/2 b/2]
c
c      TRANSFORMATIONS

```

```

c
c      sphere positions
c
tr641      -3.5631775  -3.5631775  -3.5631775
tr642       3.5631775  -3.5631775  -3.5631775
tr643      -3.5631775   3.5631775  -3.5631775
tr644       3.5631775   3.5631775  -3.5631775
tr645        0.0        0.0        0.0
tr646      -3.5631775  -3.5631775   3.5631775
tr647       3.5631775  -3.5631775   3.5631775
tr648      -3.5631775   3.5631775   3.5631775
tr649       3.5631775   3.5631775   3.5631775
c
c      MATERIALS
m1    92234.60c  0.0015          92235.60c  0.2066
      92236.60c  0.0009          92238.60c  0.7910
      8016.60c   2.0
                                         $ UO2
c
m2    6000.60c   1
mt2   grph.01t
c
m3    14000.60c  0.5           6000.60c   0.5
mt3   grph.01t
c
m4    6000.60c -0.999999     5010.60c -0.198e-06
      5011.60c -0.802e-06
mt4   grph.01t
c
m6    6000.60c -0.9999521    5010.60c -9.485733e-06
      5011.60c -3.842201e-05
mt6   grph.01t
c
c      humid air
m11   1001.60c  5.79913e-07   1002.60c  8.7e-11
      7014.60c  3.98536e-05    7015.60c  1.46400e-07
      8016.60c  1.0e-05
c
c      RUN PARAMETERS
mode  n
kcode 5000 1.0 10 60
c
sdef pos=0 0 -3.5631775 axs=0 0 1 rad=d1 ext=d2
sil 0 3.5631775
sp1 0 1
si2 0 7.126355
sp2 0 1
c
imp:n 0
      1
      1
      1 9r
      1 8r
                                         $ outside world
                                         $ inside world
                                         $ u=1
                                         $ u=2: bcc unit
                                         $ u=62 to u=64
c
totnu
print
dbcn 9j 300
prdmp j -60 1 2

```

APPENDIX C.4: MCNP4B model of ASTRA using BCC core representation

ASTRA - PBMR EXPERIMENT

```
c  
c MCNP4B model of the PBMR mockup in ASTRA facility at the Kurchatov  
c Institute, Moscow.  
c  
c Task 3: Differential reactivity worth of control rods.  
c  
c No top reflector  
c SD rods fully withdrawn h = 395.3 cm  
c CR2 in position 1 h = 382.7 cm  
c all other CRs in position 1 h = 382.7 cm  
c MR1 at reference critical height h = 366.5 cm  
c  
c Packing fraction = 0.625  
c Simple BCC lattice with borated fuel spheres  
c No exclusion zones  
c  
c J.R. Lebenhaft, MIT, August 2001  
c -----  
c CELLS  
c  
1 0 -8: 26: 32 $ outside world  
c  
c reactor structure  
c  
2 9 -1.65 8 -9 -32 $ bottom reflector  
c 3 9 -1.65 25 -26  
c -35 36 -37 38 -39 -40 41 42  
c 28 183 184 185 186 187 $ top reflector  
4 0 9 -26 -32  
c (35:-36: 37:-38: 39: 40:-41:-42)  
fill=1(5) $ radial reflector  
c  
c radial reflector lattice  
c  
5 0 -55 56 -57 58  
lat=1 u=1  
fill=-12:4 -8:8 0:0  
c  
0 0 0 0 0 0 5 5 5 0 0 0 0 0 0 0 0 0 0 0 0 0 0 0  
0 0 0 0 5 5 5 6 6 6 5 5 5 5 0 0 0 0 0 0 0 0 0 0 0  
0 0 0 5 6 6 6 6 6 6 6 6 6 6 6 6 5 0 0 0 0 0 0 0 0  
0 0 5 6 6 6 7 7 7 7 7 7 6 6 6 6 6 5 0 0 0 0 0 0  
0 5 6 6 6 7 33(53) 6 25(45) 6 37(57) 7 6 6 6 6 6 6 6 5 0 0  
0 5 6 6 6 7 6 5 0 0 0 5 24(44) 7 6 6 6 6 6 6 5 0 0  
0 5 6 7 31(51) 5 0 0 0 0 0 5 36(56) 7 6 5 0 0 0 0 0 0  
5 6 6 7 6 0 0 0 0 0 0 0 0 6 7 7 6 5 0 0 0 0 0 0 0 0  
5 8 8 9 21(41) 0 0 0 0 0 0 0 0 0 26(46) 7 6 6 5 0 0 0 0  
5 6 6 7 6 0 0 0 0 0 0 0 0 0 35(55) 7 6 6 5 0 0 0 0 0 0  
0 5 6 7 32(52) 5 0 0 0 0 0 0 5 23(43) 7 6 5 0 0 0 0 0 0 0 0
```

```

0 5 6 6 7      6 5 0 0 0 5 6 7      6 6 5 0
0 5 6 6 6      7 38(58) 6 22(42) 6 34(54) 7 6 6 5 0
0 0 5 6 6      7 7 7 7 7 7 6 6 6 5 0 0
0 0 0 5 6      6 6 6 6 6 6 6 5 0 0 0
0 0 0 0 5      5 5 7 6 6 5 5 5 0 0 0
0 0 0 0 0      0 0 5 5 5 0 0 0 0 0 0

c
c -----
c
c universe 5: solid graphite block
c
10 9 -1.65      -68                      u=5
c
c universe 6: graphite block with empty center hole
c
15 9 -1.65      54                      u=6 $ graphite
16 11 5.058e-05 -54                      u=6 $ air
c
c universe 7: graphite block with filled center hole
c
20 9 -1.65      54                      u=7 $ graphite
21 11 5.058e-05 -54 53                  u=7 $ air gap
22 9 -1.65      -53                     u=7 $ graphite plug
c
c universe 8: graphite block with small experimental channel
c           and empty center hole
c
25 9 -1.65      54 (199:-200:-198)      u=8 $ graphite
26 11 5.058e-05 198 -199 200          u=8 $ channel
27 11 5.058e-05 -54                     u=8 $ hole
c
c universe 9: graphite block with small experimental channel
c           and plug in center hole
c
30 9 -1.65      54 (199:-200:-198)      u=9 $ graphite
31 11 5.058e-05 198 -199 200          u=9 $ channel
32 11 5.058e-05 -54 53                 u=9 $ air gap
33 9 -1.65      -53                     u=9 $ plug
c
c -----
c
c universe 11: control-rod spider
c
35 7 -7.9       203                      u=11 $ outer ring
36 7 -7.9       -202                     u=11 $ center
37 7 -7.9       202 -203 -205 206        u=11 $ x-tie
38 7 -7.9       202 -203 -207 208        u=11 $ y-tie
39 11 5.058e-05 202 -203 205 207       u=11 $ gap - top right
40 11 5.058e-05 202 -203 -206 207       u=11 $ gap - top left
41 11 5.058e-05 202 -203 205 -208       u=11 $ gap - bot right
42 11 5.058e-05 202 -203 -206 -208      u=11 $ gap - bot left
c
c -----
c
c universe 12: control rod end-plate
c
920 7 -7.9      203 521 522 523 524 525

```

```

      526  527  528  529  530  531
      532  533  534  535

c                               u=12 $ outer ring
921 11  5.058e-05 -521          u=12 $ pin 1 holder
922 11  5.058e-05 -522          u=12 $ pin 2 holder
923 11  5.058e-05 -523          u=12 $ pin 3 holder
924 11  5.058e-05 -524          u=12 $ pin 4 holder
925 11  5.058e-05 -525          u=12 $ pin 5 holder
926 11  5.058e-05 -526          u=12 $ pin 6 holder
927 11  5.058e-05 -527          u=12 $ pin 7 holder
928 11  5.058e-05 -528          u=12 $ pin 8 holder
929 11  5.058e-05 -529          u=12 $ pin 9 holder
930 11  5.058e-05 -530          u=12 $ pin 10 holder
931 11  5.058e-05 -531         u=12 $ pin 11 holder
932 11  5.058e-05 -532         u=12 $ pin 12 holder
933 11  5.058e-05 -533         u=12 $ pin 13 holder
934 11  5.058e-05 -534         u=12 $ pin 14 holder
935 11  5.058e-05 -535         u=12 $ pin 15 holder

c
936 7   -7.9       -202          u=12 $ center
937 7   -7.9       202  -203  -205  206  u=12 $ x-tie
938 7   -7.9       202  -203  -207  208  u=12 $ y-tie
939 11  5.058e-05 202  -203  205  207  u=12 $ gap - top right
940 11  5.058e-05 202  -203  -206  207  u=12 $ gap - top left
941 11  5.058e-05 202  -203  205  -208  u=12 $ gap - bot right
942 11  5.058e-05 202  -203  -206  -208 u=12 $ gap - bot left

c
c -----
c
c   universe 15: control/shutdown pin assembly
c
45  0           -95          fill=16(21)  u=15 $ pin 1
46  0           -96          fill=16(22)  u=15 $ pin 2
47  0           -97          fill=16(23)  u=15 $ pin 3
48  0           -98          fill=16(24)  u=15 $ pin 4
49  0           -99          fill=16(25)  u=15 $ pin 5
50  0           -100         fill=16(26) u=15 $ pin 6
51  0           -101         fill=16(27) u=15 $ pin 7
52  0           -102         fill=16(28) u=15 $ pin 8
53  0           -103         fill=16(29) u=15 $ pin 9
54  0           -104         fill=16(30) u=15 $ pin 10
55  0           -105         fill=16(31) u=15 $ pin 11
56  0           -106         fill=16(32) u=15 $ pin 12
57  0           -107         fill=16(33) u=15 $ pin 13
58  0           -108         fill=16(34) u=15 $ pin 14
59  0           -109         fill=16(35) u=15 $ pin 15

c
60  11  5.058e-05  95   96   97   98   99   100
                           101  102  103  104  105  106
                           107  108  109
                                         u=15 $ air

c
c   universe 16: contents of absorber pin
c
61  7   -7.9       110          u=16 $ s/s clad
62  5   -1.53      -110         u=16 $ B4C

c
c -----

```

```

c
c      universe 17: air-filled portion of control/shutdown pins
c
64   0          -95           fill=18(21)  u=17  $ pin 1
65   0          -96           fill=18(22)  u=17  $ pin 2
66   0          -97           fill=18(23)  u=17  $ pin 3
67   0          -98           fill=18(24)  u=17  $ pin 4
68   0          -99           fill=18(25)  u=17  $ pin 5
69   0         -100           fill=18(26)  u=17  $ pin 6
70   0         -101           fill=18(27)  u=17  $ pin 7
71   0         -102           fill=18(28)  u=17  $ pin 8
72   0         -103           fill=18(29)  u=17  $ pin 9
73   0         -104           fill=18(30)  u=17  $ pin 10
74   0         -105           fill=18(31)  u=17  $ pin 11
75   0         -106           fill=18(32)  u=17  $ pin 12
76   0         -107           fill=18(33)  u=17  $ pin 13
77   0         -108           fill=18(34)  u=17  $ pin 14
78   0         -109           fill=18(35)  u=17  $ pin 15
79   11    5.058e-05   95   96   97   98   99   100
                           101  102  103  104  105  106
                           107  108  109
                                         u=17  $ air
c
c      universe 18: contents of absorber pin
c
80   7     -7.9        110
81   11   5.058e-05  -110
                                         u=18  $ s/s clad
                                         u=18  $ air
c
c      -----
c
c      universe 19: upper pin holder
c
82   0          -501           fill=20(21)  u=19  $ pin 1
83   0          -502           fill=20(22)  u=19  $ pin 2
84   0          -503           fill=20(23)  u=19  $ pin 3
85   0          -504           fill=20(24)  u=19  $ pin 4
86   0          -505           fill=20(25)  u=19  $ pin 5
87   0          -506           fill=20(26)  u=19  $ pin 6
88   0          -507           fill=20(27)  u=19  $ pin 7
89   0          -508           fill=20(28)  u=19  $ pin 8
90   0          -509           fill=20(29)  u=19  $ pin 9
91   0          -510           fill=20(30)  u=19  $ pin 10
92   0          -511           fill=20(31)  u=19  $ pin 11
93   0          -512           fill=20(32)  u=19  $ pin 12
94   0          -513           fill=20(33)  u=19  $ pin 13
95   0          -514           fill=20(34)  u=19  $ pin 14
96   0          -515           fill=20(35)  u=19  $ pin 15
97   11    5.058e-05  501  502  503  504  505  506
                           507  508  509  510  511  512
                           513  514  515
                                         u=19  $ air
c
c      universe 20: hollow interior
c
98   7     -7.9        201
99   11   5.058e-05  -201
                                         u=20  $ s/s holder
                                         u=20  $ air
c
c      -----

```

```

c      universe 21: control rod CR1 (with small experiment channel)
c
100  9    -1.65      54 (199:-200:-198)           u=21 $ graphite
101  11   5.058e-05  198 -199  200             u=21 $ expt. channel
102  11   5.058e-05  -54  204               u=21 $ surrounding air
103  11   5.058e-05  -204 -215             u=21 $ air below rod
104  0        -204  215             fill=210 u=21 $ rod
c
c      universe 22: control rod CR2
c
105  9    -1.65      54           u=22 $ graphite
106  11   5.058e-05  -54  204         u=22 $ surrounding air
107  11   5.058e-05  -204 -215       u=22 $ air below rod
108  0        -204  215             fill=210 u=22 $ rod
c
c
c      universe 23: control rod CR3
c
110  9    -1.65      54           u=23 $ graphite
111  11   5.058e-05  -54  204         u=23 $ surrounding air
112  11   5.058e-05  -204 -215       u=23 $ air below rod
113  0        -204  215             fill=210 u=23 $ rod
c
c
c      universe 24: control rod CR4
c
115  9    -1.65      54           u=24 $ graphite
116  11   5.058e-05  -54  204         u=24 $ surrounding air
117  11   5.058e-05  -204 -215       u=24 $ air below rod
118  0        -204  215             fill=210 u=24 $ rod
c
c
c      universe 25: control rod CR5
c
120  9    -1.65      54           u=25 $ graphite
121  11   5.058e-05  -54  204         u=25 $ surrounding air
122  11   5.058e-05  -204 -215       u=25 $ air below rod
123  0        -204  215             fill=210 u=25 $ rod
c
c
c      -----
c
c      universe 26: manual rod MR1
c
125  9    -1.65      54           u=26 $ graphite
126  11   5.058e-05  -54  213         u=26 $ surrounding air
127  11   5.058e-05  -213 -315       u=26 $ air below rod
128  0        -213  315             fill=220 u=26 $ rod
c
c
c      -----
c
c      universe 31: control rod SR1
c
130  9    -1.65      54           u=31 $ graphite
131  11   5.058e-05  -54  204         u=31 $ surrounding air
132  11   5.058e-05  -204 -215       u=31 $ air below rod
133  0        -204  215             fill=210 u=31 $ rod

```

```

c
c
c      universe 32: control rod SR2
c
135  9   -1.65      54          u=32 $ graphite
136 11   5.058e-05  -54  204    u=32 $ surrounding air
137 11   5.058e-05  -204 -215    u=32 $ air below rod
138 0        -204  215          fill=210 u=32 $ rod
c
c
c      universe 33: control rod SR3
c
140  9   -1.65      54          u=33 $ graphite
141 11   5.058e-05  -54  204    u=33 $ surrounding air
142 11   5.058e-05  -204 -215    u=33 $ air below rod
143 0        -204  215          fill=210 u=33 $ rod
c
c
c      universe 34: control rod SR4
c
145  9   -1.65      54          u=34 $ graphite
146 11   5.058e-05  -54  204    u=34 $ surrounding air
147 11   5.058e-05  -204 -215    u=34 $ air below rod
148 0        -204  215          fill=210 u=34 $ rod
c
c
c      universe 35: control rod SR5
c
150  9   -1.65      54          u=35 $ graphite
151 11   5.058e-05  -54  204    u=35 $ surrounding air
152 11   5.058e-05  -204 -215    u=35 $ air below rod
153 0        -204  215          fill=210 u=35 $ rod
c
c
c      universe 36: control rod SR6
c
155  9   -1.65      54          u=36 $ graphite
156 11   5.058e-05  -54  204    u=36 $ surrounding air
157 11   5.058e-05  -204 -215    u=36 $ air below rod
158 0        -204  215          fill=210 u=36 $ rod
c
c
c      universe 37: control rod SR7
c
160  9   -1.65      54          u=37 $ graphite
161 11   5.058e-05  -54  204    u=37 $ surrounding air
162 11   5.058e-05  -204 -215    u=37 $ air below rod
163 0        -204  215          fill=210 u=37 $ rod
c
c
c      universe 38: control rod SR8
c
165  9   -1.65      54          u=38 $ graphite
166 11   5.058e-05  -54  204    u=38 $ surrounding air
167 11   5.058e-05  -204 -215    u=38 $ air below rod
168 0        -204  215          fill=210 u=38 $ rod

```

```

c -----
c
c      universe 210: details of control/shutoff rod
c
170 7 -7.9      -216                               u=210 $ lower endplate
171 0           216 -217      fill=12   u=210 $ lower pin holder
172 0           217 -218      fill=17   u=210 $ empty pin zone
173 0           218 -219      fill=15   u=210 $ absorber
174 0           219 -220      fill=17   u=210 $ empty pin zone
175 0           220 -221      fill=19   u=210 $ upper pin holder
176 0           221 -222      fill=11   u=210 $ spider
177 11 5.058e-05 222 -223 202                  u=210 $ middle gap
178 7 -7.9      222 -223 -202                 u=210 $ middle joint
179 7 -7.9      223 -224      fill=12   u=210 $ lower endplate
180 0           224 -225      fill=17   u=210 $ lower pin holder
181 0           225 -226      fill=15   u=210 $ empty pin zone
182 0           226 -227      fill=15   u=210 $ absorber region
183 0           227 -228      fill=17   u=210 $ empty pin zone
184 0           228 -229      fill=19   u=210 $ upper pin holder
185 0           229 -230      fill=11   u=210 $ spider
186 11 5.058e-05 230                  u=210 $ air above rod
c
c -----
c
c      universe 220: details of manual rod
c
190 12 -2.69     -316 210                         u=220 $ solid bottom
191 12 -7.69     316 -317 210 -211             u=220 $ inner wall
192 11 5.058e-05 316 -317 211 -212             u=220 $ air gap
193 12 -2.69     316 -317 212                  u=220 $ outer wall
194 12 -2.69     317 -318 210                  u=220 $ solid top
195 11 5.058e-05 -318 -210                     u=220 $ center gap
196 12 -2.69     318 -319                         u=220 $ upper mid plate
c
c -----
c
c      core cavity
c
510 11 5.058e-05 17 -26 31 -35 36 -37 38      $ above outer fuel
zone
511 11 5.058e-05 18 -26 30 -31 185            $ above mixed zone
512 11 5.058e-05 19 -26 28 -30 183 184        $ above inner
reflector
c
c      core regions
c
529 0           9 -19 28 -30 184                $ inner reflector
      fill=50(2)
530 0           9 -18 30 -31 185                $ mixed zone
      fill=52(3)
531 0           9 -17 31 -35 36 -37
      38 -39 -40 41 42 186
      187
      fill=54(4)                                $ fuel outer zone
c
c      experimental channels

```

```

c
532 0           9 -26 -28          fill=65 $ central channel
533 0           9 -26 -183         fill=70 $ E1
534 0           9 -26 -184         fill=75 $ E2
535 0           9 -26 -185         fill=80 $ E3
536 0           9 -26 -186         fill=85 $ E4
537 0           9 -26 -187         fill=90 $ E5
c
c -----
c
c      universe 50: inner reflector
c
540 0           -70   69  -72   71  -74   73
    lat=1  fill=51
    u=50
c
c      Universe 51: bcc unit cell (moderator)
c
541 4  -1.68     -121             u=51
542 4  -1.68     -122             u=51
543 4  -1.68     -123             u=51
544 4  -1.68     -124             u=51
545 4  -1.68     -125             u=51
546 4  -1.68     -126             u=51
547 4  -1.68     -127             u=51
548 4  -1.68     -128             u=51
549 4  -1.68     -129             u=51
c
c      air between spheres
c
550 11  5.058e-05    121  122  123  124  125  126
                           127  128  129
    u=51
c
c -----
c
c      universe 52: mixed fuel/moderator/absorber zone
c
555 0           -70   69  -72   71  -74   73
    lat=1  fill=53
    u=52
c
c      Universe 53: BCC unit cell (moderator/borated fuel)
c
556 0           -121             fill=60 u=53 $ [ 0  0  0]
557 4  -1.68     -122             u=53 $ [ 1  1  1]
558 4  -1.68     -123             u=53 $ [ 1  1 -1]
559 4  -1.68     -124             u=53 $ [ 1 -1 -1]
560 4  -1.68     -125             u=53 $ [ 1 -1  1]
561 4  -1.68     -126             u=53 $ [-1  1  1]
562 4  -1.68     -127             u=53 $ [-1  1 -1]
563 4  -1.68     -128             u=53 $ [-1 -1 -1]
564 4  -1.68     -129             u=53 $ [-1 -1  1]
c
565 11  5.058e-05    121 122 123 124 125
                           126 127 128 129             u=53 $ air
c

```

```

c -----
c
c      universe 54: outer borated fuel zone
c
570  0           -70   69   -72    71   -74    73
     lat=1  fill=55
     u=54
c
c      Universe 55: BCC unit cell
c
572  0           -121      fill=60      u=55  $ [ 0  0  0]
573  0           -122      fill=60(11)  u=55  $ [ 1  1  1]
574  0           -123      fill=60(12)  u=55  $ [ 1  1 -1]
575  0           -124      fill=60(13)  u=55  $ [ 1 -1 -1]
576  0           -125      fill=60(14)  u=55  $ [ 1 -1  1]
577  0           -126      fill=60(15)  u=55  $ [-1  1  1]
578  0           -127      fill=60(16)  u=55  $ [-1  1 -1]
579  0           -128      fill=60(17)  u=55  $ [-1 -1 -1]
580  0           -129      fill=60(18)  u=55  $ [-1 -1  1]
c
581  11   5.058e-05   121 122 123 124 125
                           126 127 128 129
                                         u=55  $ air
c
c -----
c
c      Universe 60: details of fuel element
c
585  6   -1.850087    75
586  0           -75      fill=61      u=60  $ borated shell
                                         u=60  $ fuel region
c
c      Universe 61: embedded coated fuel particles
c
590  0           -76   77   -78    79   -80    81
     lat=1  fill=62
     u=61
c
c      Universe 62: coated fuel particle
c
591  1   -10.1       -82      u=62  $ UO2 kernel
592  2   -1.1        82  -83   u=62  $ PyC layer 1
593  2   -1.8        83  -84   u=62  $ PyC layer 2
594  3   -3.2        84  -85   u=62  $ SiC layer
595  2   -1.8        85  -86   u=62  $ PyC layer 3
596  4   -1.85       86      u=62  $ graphite
c
c -----
c
c      universe 65: central channel
c
650  10  -2.69       27      u=65  $ Al wall
651  11   5.058e-05  -27
                                         u=65  $ air
c
c -----
c
c      universe 70: experimental tube E1
c
655  10  -2.69       188
                                         u=70  $ Al wall

```

```

656 11 5.058e-05 -188 u=70 $ air
c
c   universe 75: experimental tube E2
c
660 10 -2.69      189 u=75 $ Al wall
661 11 5.058e-05 -189 u=75 $ air
c
c   universe 80: experimental tube E3
c
670 10 -2.69      190 u=80 $ Al wall
671 11 5.058e-05 -190 u=80 $ air
c
c   universe 85: experimental tube E4
c
680 10 -2.69      191 u=85 $ Al wall
681 11 5.058e-05 -191 u=85 $ air
c
c   universe 90: experimental tube E5
c
690 10 -2.69      192 u=90 $ Al wall
691 11 5.058e-05 -192 u=90 $ air
c
c -----
c   SURFACES
c
8  pz    0.0          $ bottom of reactor
9  pz    40.0         $ bottom of core
c
c   core height
c
17 pz    308.9        $ top of outer fuel zone
18 pz    308.9        $ top of mixed fuel zone
19 pz    308.9        $ top of inner reflector
c
c   20  pz    360.8     $ bottom of Al structure
c   25  pz    399.5     $ bottom of upper reflector
26  pz    460.0        $ top of reactor
27  cz    5.0          $ center tube - inner surface
28  cz    5.25         $ center tube - outer surface
30  cz    34.75        $ inner reflector boundary (36.25)
31  cz    51.25        $ mixed- zone boundary (52.75)
32  cz    190.0         $ outer surface of reactor
c
c   core boundary (x-y plane)
c
35 px    87.5          $ right
36 px   -87.5          $ left
37 py    87.5          $ top
38 py   -87.5          $ bottom
39 p     1.0    1.0    0.0    125.0 $ top right
40 p    -1.0    1.0    0.0    125.0 $ top left
41 p     1.0    1.0    0.0   -125.0 $ bottom left
42 p    -1.0    1.0    0.0   -125.0 $ bottom right
c
c   reflector blocks (x-y plane)
c

```

```

53  cz      5.6          $ graphite plug
54  cz      5.7          $ hole in graphite block
55  px      12.5         $ right
56  px     -12.5         $ left
57  py      12.5         $ top
58  py     -12.5         $ bottom
c
68  cz      17.68        $ universe boundary
c
c  pebble-bed lattice
c
69  px     -3.5631775    $ -x
70  px      3.5631775    $ +x
71  py     -3.5631775    $ -y
72  py      3.5631775    $ +y
73  pz     -3.5631775    $ bottom
74  pz      3.5631775    $ top
c
c  inside fuel pebble
c
75  so      2.5          $ fueled region
c
c  unit cell for CFP lattice
c
76  px      0.124988
77  px     -0.124988
78  py      0.124988
79  py     -0.124988
80  pz      0.124988
81  pz     -0.124988
c
c  coated fuel particle
c
82  so      0.025        $ UO2 kernel
83  so      0.034        $ buffer
84  so      0.041        $ inner PyC
85  so      0.047        $ SiC
86  so      0.053        $ outer PyC
c
c  absorber pins - outer surfaces
c
95  c/z     3.8          0.0          0.625
96  c/z     3.47147      1.5456       0.625
97  c/z     2.5427       2.82395      0.625
98  c/z     1.17426      3.61401      0.625
99  c/z     -0.39721     3.77918      0.625
100 c/z     -1.9          3.2909       0.625
101 c/z     -3.07426     2.23358       0.625
102 c/z     -3.71696     0.79006       0.625
103 c/z     -3.71696     -0.79006      0.625
104 c/z     -3.07426     -2.23358      0.625
105 c/z     -1.9          -3.2909      0.625
106 c/z     -0.39721     -3.77918      0.625
107 c/z     1.17426      -3.61401      0.625
108 c/z     2.5427       -2.82395      0.625
109 c/z     3.47147      -1.5456       0.625
c

```

```

110 cz     0.505                      $ absorber outer surface
c
c   spheres in unit cell
c
121 so     3.0
122 s      3.5631775    3.5631775    3.5631775 3.0
123 s      3.5631775    3.5631775   -3.5631775 3.0
124 s      3.5631775   -3.5631775   -3.5631775 3.0
125 s      3.5631775   -3.5631775    3.5631775 3.0
126 s     -3.5631775    3.5631775    3.5631775 3.0
127 s     -3.5631775    3.5631775   -3.5631775 3.0
128 s     -3.5631775   -3.5631775   -3.5631775 3.0
129 s     -3.5631775   -3.5631775    3.5631775 3.0
c
c   aluminum experiment tubes - outer surfaces
c
183 c/z   -5.8501    0.0      0.6      $ E1
184 c/z   -25.0       0.0      0.6      $ E2
185 c/z   -45.0       0.0      0.6      $ E3
186 c/z   -65.0       0.0      0.6      $ E4
187 c/z   -80.0       0.0      0.6      $ E5
c
c   aluminum experiment tubes - inner surfaces
c
188 c/z   -5.8501    0.0      0.5      $ E1
189 c/z   -25.0       0.0      0.5      $ E2
190 c/z   -45.0       0.0      0.5      $ E3
191 c/z   -65.0       0.0      0.5      $ E4
192 c/z   -80.0       0.0      0.5      $ E5
c
c   small experiment channels
c
198 px    11.0
199 py    1.5
200 py   -1.5
c
c   control and shutoff rod surfaces
c
201 cz    0.3          $ radius of pin end-region
202 cz    1.5          $ joint
203 cz    3.1          $ inside of pin holder
204 cz    4.5          $ outside of pin holder
205 px    0.50         $ pin support
206 px   -0.50         $ pin support
207 py    0.50         $ pin support
208 py   -0.50         $ pin support
c
c   manual rod
210 cz    3.5          $ inside of inner surface
211 cz    3.75         $ outside of inner surface
212 cz    4.5          $ inside of outer surface
213 cz    4.75         $ outer surface of rod
c
c   Control rod
c
215 pz    0.0          $ bottom of lower endplate
216 pz    0.1          $ bottom of lower pin holder

```

```

217 pz    1.0      $ bottom of lower pins
218 pz    2.0      $ bottom of B4C in lower pins
219 pz   189.5     $ top of B4C in lower pins
220 pz   190.5     $ bottom of lower pin holder
221 pz   191.2     $ bottom of lower spider
222 pz   192.2     $ bottom of middle gap
223 pz   192.7     $ bottom of upper endplate
224 pz   192.8     $ bottom of pin holder
225 pz   193.7     $ bottom of upper pins
226 pz   194.7     $ bottom of B4C in upper pins
227 pz   382.2     $ top of B4C in upper pins
228 pz   383.2     $ bottom of upper holder
229 pz   383.9     $ bottom of upper spider
230 pz   384.9     $ top of upper spider

c
c      Manual regulating rod
c
315 45 pz    0.0      $ bottom of rod
316 45 pz    2.0      $ bottom of air gap
317 45 pz   383.5     $ top of air gap
318 45 pz   385.5     $ bottom of top plate
319 45 pz   388.5     $ top of rod

c
c      upper pin holder
c
501 c/z   3.8      0.0      0.7
502 c/z   3.47147   1.5456   0.7
503 c/z   2.5427    2.82395  0.7
504 c/z   1.17426   3.61401  0.7
505 c/z   -0.39721  3.77918  0.7
506 c/z   -1.9       3.2909   0.7
507 c/z   -3.07426  2.23358  0.7
508 c/z   -3.71696  0.79006  0.7
509 c/z   -3.71696  -0.79006 0.7
510 c/z   -3.07426 -2.23358  0.7
511 c/z   -1.9       -3.2909  0.7
512 c/z   -0.39721 -3.77918  0.7
513 c/z   1.17426   -3.61401 0.7
514 c/z   2.5427    -2.82395 0.7
515 c/z   3.47147   -1.5456  0.7

c
c      control rod end-plate
c
521 c/z   3.8      0.0      0.3
522 c/z   3.47147   1.5456   0.3
523 c/z   2.5427    2.82395  0.3
524 c/z   1.17426   3.61401  0.3
525 c/z   -0.39721  3.77918  0.3
526 c/z   -1.9       3.2909   0.3
527 c/z   -3.07426  2.23358  0.3
528 c/z   -3.71696  0.79006  0.3
529 c/z   -3.71696  -0.79006 0.3
530 c/z   -3.07426 -2.23358  0.3
531 c/z   -1.9       -3.2909  0.3
532 c/z   -0.39721 -3.77918  0.3
533 c/z   1.17426   -3.61401 0.3
534 c/z   2.5427    -2.82395 0.3

```



```

c      transformations
c
tr2    0.0      21.379065 43.5631775      $ inner reflector origin
tr3    0.0      42.758130 43.5631775      $ mixed zone origin
tr4    0.0      71.263550 43.5631775      $ fuel zone origin
tr5   100.0      0.0      0.0      $ reflector origin
c
c      unit cell positions
c
tr11   3.5631775  3.5631775  3.5631775
tr12   3.5631775  3.5631775 -3.5631775
tr13   3.5631775 -3.5631775 -3.5631775
tr14   3.5631775 -3.5631775  3.5631775
tr15  -3.5631775  3.5631775  3.5631775
tr16  -3.5631775  3.5631775 -3.5631775
tr17  -3.5631775 -3.5631775 -3.5631775
tr18  -3.5631775 -3.5631775  3.5631775
c
c      absorber pins - inner surfaces
c
tr21   3.8      0.0      1.0
tr22   3.47147  1.5456   1.0
tr23   2.5427   2.82395  1.0
tr24   1.17426  3.61401  1.0
tr25  -0.39721  3.77918  1.0
tr26   -1.9     3.2909   1.0
tr27  -3.07426  2.23358  1.0
tr28  -3.71696  0.79006  1.0
tr29  -3.71696 -0.79006  1.0
tr30  -3.07426 -2.23358  1.0
tr31   -1.9    -3.2909   1.0
tr32  -0.39721 -3.77918  1.0
tr33   1.17426 -3.61401  1.0
tr34   2.5427  -2.82395  1.0
tr35   3.47147 -1.5456   1.0
c
c      control rod positions
c
tr41   0      0      382.7      position
tr42   0      0      382.7      $ CR1      1
tr43   0      0      382.7      $ CR2      1
tr44   0      0      382.7      $ CR3      1
tr45   0      0      382.7      $ CR4      1
tr46   0      0      366.5      $ CR5      1
tr46   0      0      366.5      $ MR1      (critical)
c
c      shutdown rod positions
c
tr51   0      0      395.3      $ SD1      out
tr52   0      0      395.3      $ SD2
tr53   0      0      395.3      $ SD3
tr54   0      0      395.3      $ SD4
tr55   0      0      395.3      $ SD5
tr56   0      0      395.3      $ SD6
tr57   0      0      395.3      $ SD7
tr58   0      0      395.3      $ SD8
c
c      material specifications

```

c				
m1	92234.60c 0.0015	92235.60c 0.2066		
	92236.60c 0.0009	92238.60c 0.7910		
	8016.60c 2.0			\$ UO2
c				
m2	6000.60c 1			\$ PyC
mt2	grph.01t			
c				
m3	14000.60c 0.5	6000.60c 0.5		\$ SiC
mt3	grph.01t			
c				
m4	6000.60c -0.999999	5010.60c -1.98e-07		\$ graphite
	5011.60c -8.02e-07			\$ matrix
mt4	grph.01t			
c				
m5	6000.60c 0.2	5010.60c 0.1584		\$ B4C
	5011.60c 0.6416			
mt5	grph.01t			
c				
m6	6000.60c -0.9999521	5010.60c -9.485733e-06		\$ borated shell
	5011.60c -3.842201e-05			
mt6	grph.01t			
c				
c	control and shutdown rods			
c				
m7	26000.50c -0.691	6000.60c -0.0012		
	14000.60c -0.0008	25055.60c -0.02		
	24000.50c -0.18	28000.50c -0.1		
	22000.60c -0.007			\$ s/steel
c				
c	reflector graphite			
c				
m9	6000.60c -0.99999945	5010.60c -0.1089e-06		
	5011.60c -0.4411e-06			
mt9	grph.01t			
c				
c	aluminum experiment tubes			
c				
m10	13027.60c -0.9999986	5010.60c -0.0000014		
c				
c	humid air			
c				
m11	1001.60c 5.79913e-07	1002.60c 8.7e-11		
	7014.60c 3.98536e-05	7015.60c 1.46400e-07		
	8016.60c 1.0e-05			
c				
c	aluminum manual rod			
c				
m12	29000.50c -0.0035	25055.60c -0.0035		
	26000.50c -0.0050	14000.60c -0.0085		
	24000.50c -0.0025	13027.60c -0.9770		

APPENDIX D. MCNP4B/VSOP94 Models of PBMR

This Appendix contains the key files used to model the PBMR core with burnup. The VSOP94 input file for the reference PBMR core is attached as Appendix D.1, while the corresponding MCNP4B model is in Appendix D.2. The modified VSOP94 subroutine VORSHU is included as Appendix D.3. Program MCARDS, which generates the MCNP4B material cards from the layer-averaged fuel compositions extracted from VSOP94, is in Appendix D.4. Details on the PBMR reactor, the VSOP94 and MCNP4B models and the link between these codes appear in Chapter 7.

APPENDIX D.1-VSOP94 input file for reference PBMR core

*1999 MS; 0.3%BE IN MS; 265 MW; 44 FISPRD; 9 G/K; 18 RODS + 16 KLAK	V 1
07730 0 15 20 0 25 0 0	V 2
65 42 0 4 350 45 9 3 0 3 0	V 3
44 44 0 0 0 1	V 4
1 3 1 1 2 2 0 0 0 0.0001	1. 0 V 10
301 0 0 0 0 1	1 K1 V 11
0 1 0 0 0 2	12 V 11
0 1 0 0 0 3	23 V 11
0 1 0 0 0 4	34 V 11
0 1 0 0 0 5	45 V 11
0 1 0 0 0 6	56 V 11
0 1 0 0 0 7	67 V 11
0 1 0 0 0 8	78 V 11
0 1 0 0 0 10	89 V 11
0 1 0 0 0 1	100 K2 V 11
0 1 0 0 0 2	111 V 11
0 1 0 0 0 3	122 V 11
0 1 0 0 0 4	133 V 11
0 1 0 0 0 5	144 V 11
0 1 0 0 0 6	155 V 11
0 1 0 0 0 7	166 V 11
0 1 0 0 0 8	177 V 11
0 1 0 0 0 9	188 V 11
0 1 0 0 0 10	199 V 11
0 1 0 0 0 26	210 K3 V 11
0 1 0 0 0 27	221 V 11
0 1 0 0 0 28	232 V 11
0 1 0 0 0 29	243 V 11
0 1 0 0 0 30	254 V 11
0 1 0 0 0 31	265 V 11
0 1 0 0 0 32	276 V 11
0 1 0 0 0 33	287 V 11
0 1 0 0 0 34	298 V 11
0 1 0 0 0 35	309 V 11
0 1 0 0 0 0	320 V 11
0 1 0 0 0 26	331 K4 V 11
0 1 0 0 0 27	342 V 11
0 1 0 0 0 28	353 V 11
0 1 0 0 0 29	364 V 11
0 1 0 0 0 30	375 V 11
0 1 0 0 0 31	386 V 11
0 1 0 0 0 32	397 V 11
0 1 0 0 0 33	408 V 11
0 1 0 0 0 34	419 V 11
0 1 0 0 0 35	430 V 11
0 1 0 0 0 0	441 V 11
0 1 0 0 0 0	452 V 11
0 1 0 0 0 26	463 K5 V 11
0 1 0 0 0 27	474 V 11
0 1 0 0 0 28	485 V 11
0 1 0 0 0 29	496 V 11
0 1 0 0 0 30	507 V 11
0 1 0 0 0 31	518 V 11
0 1 0 0 0 32	529 V 11
0 1 0 0 0 33	540 V 11

0	1	0	0	0	34		551	V 11
0	1	0	0	0	35		562	V 11
0	1	0	0	0	0		573	V 11
0	1	0	0	0	0		584	V 11
0	1	0	0	0	0		595	V 11
0	1	0	0	0	0		606	V 11
0	1	0	0	0	0		617	V 11
2	0	0	0	0	14		628	KON V11
63		2.30577	-02					V 12
64		7.86962	-02					V 12
4	0	0	0	0	11		1 B 1	V11
58		0.0	-04					V 12
59		0.0	-03					V 12
63		2.49736	-02					V 12
64		8.52341	-02					V 12
2	0	0	0	0			2 B 2	V11
63		2.48234	-02					V 12
64		8.47225	-02					V 12
2	0	0	0	0			3 B 3	V11
63		2.22115	-02					V 12
64		7.58082	-02					V 12
1	0	0	0	0	12		4 B 4	V11
64		9.02479	-04					V 12
2	0	0	0	0	13		5 B 5	V11
63		1.55	-02					V 12
64		5.28	-02					V 12
2	0	0	0	0			6 B 6	V11
63		2.64423	-02					V 12
64		9.02479	-02					V 12
2	0	0	0	0	14		7 B 7	V11
63		2.45094	-02					V 12
64		8.36508	-02					V 12
2	0	0	0	0	15		8 B 8	V11
63		1.93792	-02					V 12
64		6.61415	-02					V 12
0	1	0	0	0			9 B 9	V11
2	0	0	0	0	16		10 B10	V11
63		2.64423	-02					V 12
64		9.02479	-02					V 12
0	10	0	0	0	17		11 B11	V11
0	10	0	0	0	18		12 B12	V11
0	10	0	0	0	19		13 B13	V11
0	10	0	0	0	20		14 B14	V11
0	10	0	0	0	15		15 B15	V11
3	0	0	0	0	16		16 B16	V11
58		1.453	-06					V 12
63		1.81923	-02					V 12
64		6.20906	-02					V 12
0	16	0	0	0			17 B17	V11
0	16	0	0	0	17		18 B18	V11
0	16	0	0	0			19 B19	V11
3	0	0	0	0			20 B20	V11
58		0.0	-06					V 12
63		1.81923	-02					V 12
64		6.20906	-02					V 12
0	20	0	0	0	18		21 B21	V11
0	20	0	0	0			22 B22	V11

0	20	0	0	0		23	B23	V11
0	20	0	0	0	19	24	B24	V11
0	20	0	0	0	20	27	B27	V11
0	1	0	0	0	21	28	B28	V11
0	2	0	0	0		29	B29	V11
0	10	0	0	0		30	B30	V11
0	10	0	0	0	22	31	B31	V11
0	10	0	0	0	23	32	B32	V11
0	10	0	0	0	24	33	B33	V11
0	10	0	0	0	25	34	B34	V11
4	0	0	0	0	21	35	B35	V11
58	0.0	-04						V 12
59	0.0	-03						V 12
63	2.49736	-02						V 12
64	8.52341	-02						V 12
0	35	0	0	0	22	36	B36	V11
0	35	0	0	0	23	37	B37	V11
0	35	0	0	0	24	38	B38	V11
0	35	0	0	0	25	39	B39	V11
4	0	0	0	0	21	40	B40	V11
58	0.0	-04						V 12
59	0.0	-03						V 12
63	1.82734	-02						V 12
64	6.23664	-02						V 12
0	40	0	0	0	22	41	B41	V11
0	40	0	0	0	23	42	B42	V11
0	40	0	0	0	24	43	B43	V11
4	0	0	0	0	37	44	B44	V11
58	0.0	-04						V 12
59	0.0	-03						V 12
63	2.49736	-02						V 12
64	8.52341	-02						V 12
0	44	0	0	0	38	45	B45	V11
0	44	0	0	0	39	46	B46	V11
0	44	0	0	0	40	47	B47	V11
0	44	0	0	0	41	48	B48	V11
2	0	0	0	0	36	49	B49	V11
60	4.08572	-02						V 12
64	9.02479	-04						V 12
4	0	0	0	0	42	50	B50	V11
58	5.01175	-05						V 12
59	2.04286	-04						V 12
63	2.29165	-02						V 12
64	7.82771	-02						V 12
4	0	0	0	0	42	51	B51	V11
58	5.40700	-05						V 12
59	2.20397	-04						V 12
63	2.47238	-02						V 12
64	8.44504	-02						V 12
0	10	0	0	0	11	52	B52	V11
0	52	0	0	0	11	53	B53	V11
0	1	0	0	0	15	54	B54	V11
0	40	0	0	0	25	-55	B55	V11
	0.00347	265.+06						V 15
2	10							V 16
1	0	0	0	261	1			V 21
0								V 22

										V	23
1										G	1
5015	180	515	30	3	3	5	0	0	0	685.	G2/R19
	575.		590.		612.		637.		663.		
	702.		712.		794.		647.		0.		0. G2/R19
	0.		0.		0.		0.		0.		0. G2/R19
	0.		0.		0.		0.		0.		0. G2/R19
	0.		594.		629.		681.		738.		793. G2/R19
	844.		887.		920.		944.		927.		0. G2/R19
	0.		0.		0.		0.		0.		0. G2
1	1	1	1	1	1	1	1	1	3	3	G 3
3	3	3	3	3	3	3	3	3	3	3	G 3
3	2	2	2	2	2	2	2	2	2	3	G 3
3	3	3	3	3	3						G 3
1	0										G 4
6	901	902	903	904	905	906					G 4
1	0										G 4
6	901	902	903	904	905	906					G 4
1	0										G 4
1	0										G 4
1000000.		29.		1.86							G 5
2	3	2	11	-1	0						T 1
1600	1601	1603	1604	1605	1606	1607	1608	1609	1610	1612	T 2
	573.		587.		608.		633.		658.		680. T3/R20
	697.		708.		788.		644.		551.		566. T3/R20
	751.		883.		745.		553.		602.		702. T3/R20
	780.		836.		503.		534.		541.		546. T3/R20
	589.		589.		622.		670.		725.		780. T3/R20
	830.		874.		909.		934.		921.		200. T3/R20
	503.		534.		541.		546.		589.		883. T3
1121	1122	1123	1124	1125							T 2
	575.		590.		612.		637.		663.		685. T3/R20
	702.		712.		794.		647.		0.		0. T3/R20
	0.		0.		0.		0.		0.		0. T3/R20
	0.		0.		0.		0.		0.		0. T3/R20
	0.		594.		629.		681.		738.		793. T3/R20
	844.		887.		920.		944.		927.		200. T3/R20
	0.		0.		0.		0.		0.		0. T3
	4.0	6	12	29							T 4
1	4	1	1	1	1	1	1	1	1	1	T 5
3	3	3	3	3	3	3	3	3	3	3	T 5
3	3	3	1	1	1	1	1	1	1	1	T 5
1	3	3	3	3	3	3	3	3			T 5
	1.5		0.61		1.		1.		-1.		1. T 6
11111111122220000000											
4	01	0.0		1.	0.						T 9
6	00	-1.0		0.	1.						T 9
26	01	1.0		0.	0.						T 9
130	01	-2.0		0.0	0.						T 9
150	01	-2.0		0.0	0.0						T 9
-1001	01	-2.0		0.0	0.0						T 9
	1.5		0.61		0.		1.		-1.		1. T 6
1111111112223333300	1	1		.025		.046		.14537		1.0694	T 7
	2.5		3.0		3.985						T 8
4	01	0.0		1.	0.		0.				T 9
6	00	1.0		0.	1.		1.				T 9
26	01	1.0		0.	0.		0.				T 9
130	01	0.0		1.0	0.		0.				T 9

150	01	.24682	.17968	.57350	0.		T	9	
-1001	01	.24682	.17968	.57350	0.		T	9	
	1.5	1.0	0.0	1.	0.	0.	T	6	
10000000000000000000							T	7	
	1.0						T	8	
-4	00	1.					T	9	
	1.5	1.0	0.0	1.	-1.	1.	T	6	
11112222220000000000	1 0		0.0	0.0	0.0	0.0	T	7	
	0.375	1.0466					T	8	
4	00	0.	1.				T	9	
130	01	1.	0.				T	9	
164	01	1.	0.				T	9	
-1001	01	0.01445	0.98555				T	9	
	0.61	0.0	2.5	3.0	0.6		T	11	
120000							C0	1	
7730	MEDUL H/R=805/175; CITA 2-Z						C0	2	
KOPPLUNG: VSOP - CITATION							C0	3	
001							C1	1	
0	0	1	0	0	0	0	C1	2	
0	0	0	0	0	0	0	C1	3	
840	0	0	0	0	0	0	C1	4	
	0.	0.	0.	0.	0.	0.	C1	5	
003							C3	1	
0	0	0	0	7	0	0	C3	2	
	0.0001	0.0001		0.	0.	0.	C3	3	
	9999.	0.		0.	3.287800-11	1.	C3	4	
1	1						C7	1	
1	204	204					C7	2	
							C7	3	
							C7	4	
	175.	0.1	0.5				C7	5	
14	81	18	0				CX	1	
7730	33	75	3	0	0	0	\$1000MILL		
	0.80	0.43	30.	1.			K	1	
	0.00	0.00	0.15	0.00	0.00	0.06	K	2	
	0.002	0.00	1.00	0.0	0.00		K	3	
	20.90	6.0	100.	0.0026	0.00	0.00	K	4	
	10.00	-1.25	0.0				K	5	
	6.	0.10	0.	890.	371.		TP1	K	6
	0.0	0.0	0.0	0.0			K	7	
	0.	0.	0.	0.	0.		K	8	
	0.	0.	0.				K	9	
	6.	0.10	0.	728.	371.		TP2	K	10
	0.0	0.0	0.0	0.0			K	7	
	0.	0.	0.	0.	0.		K	8	
	0.	0.	0.				K	9	
	6.	0.10	0.	890.	371.		TP3	K	10
	0.0	0.0	0.0	0.0			K	7	
	0.	0.	0.	0.	0.		K	8	
	0.	0.	0.				K	9	
	0.0	0.0	0.99	0.99	0.99	0.99	R	1	
	0.99	0.0	0.0	0.0	0.0	0.0	R	1	
	0.0	1.0	0.0	0.0	0.0	0.0	R	1	
	0.0	0.0	0.0	0.0	0.0	0.0	R	1	
	0.0	0.0	0.0	0.0	0.0	0.0	R	1	
	0.0	0.0	0.0	0.0	0.0	0.0	R	1	
	0.0	0.0	0.0	0.0	0.0	0.0	R	1	

0.0	0.0	0.0	0.0	0.0	0.0	R 1
0.0	0.0	0.0	0.0	0.0	0.0	R 1
0.0	0.0	0.0	1.0	1.0	1.0	R 1
1.0	1.0	1.0	1.0	1.0	1.0	R 1
0.	0.	365.	0.8	0.	0.	R 2
1 0 0 0 0						R 3
1 0.636417E+6	-101		1.			R 5
2 2.396666E+6	-201		2.			R 5
3 0.636417E+6	-301		3.			R 5
1 3 2 1 2 0 0 0 1 1 0 3 0 0 1 1 1 1 0 0 0 0 0 0 0 0						R 9
2 0 0 0	0.5					R 14
1						R 16
1						R 17
554.5	571.1	595.1	622.8	651.0	676.3	G2/R19
698.4	717.2	799.7	630.4	0.0	0.0	G2/R19
0.0	0.0	0.0	0.0	0.0	0.0	G2/R19
0.0	0.0	0.0	0.0	0.0	0.0	G2/R19
0.0	577.8	614.7	669.4	733.1	796.2	G2/R19
852.8	900.9	940.7	968.9	955.2	0.0	G2/R19
0.0	0.0	0.0	0.0	0.0	0.0	G2/R19
551.7	566.9	589.1	615.3	642.6	667.6	T3/R20
689.9	708.9	787.5	624.6	514.4	541.1	T3/R20
703.3	931.1	708.7	517.3	589.3	735.8	T3/R20
867.6	910.7	484.6	559.1	616.0	665.4	T3/R20
647.8	571.0	604.5	654.4	713.6	774.0	T3/R20
829.9	878.6	920.0	950.5	941.9	314.9	T3/R20
428.3	466.9	467.4	467.9	468.2	867.6	T3/R20
554.5	571.1	595.1	622.8	651.0	676.3	T3/R20
698.4	717.2	799.7	630.4	0.0	0.0	T3/R20
0.0	0.0	0.0	0.0	0.0	0.0	T3/R20
0.0	0.0	0.0	0.0	0.0	0.0	T3/R20
0.0	577.8	614.7	669.4	733.1	796.2	T3/R20
852.8	900.9	940.7	968.9	955.2	0.0	T3/R20
0.0	0.0	0.0	0.0	0.0	0.0	T3/R20
1		3 1		0.20000		R24
2		3 1		0.20000		R24
3		3 1		0.20000		R24
4		3 1		0.20000		R24
5		3 1		0.20000		R24
6		3 1		0.20000		R24
7		3 1		0.20000		R24
8		3 1		0.20000		R24
9		3 1		0.20000		R24
10		3 1		0.20000		R24
11		3 1		1.		R24
89	78 1					R24
90	79 2					R24
91	80 3					R24
92	81 4					R24
93	82 5					R24
94	83 6					R24
95	84 7					R24
96	85 8					R24
97	86 9					R24
98	87					R24
99	88					R24
100		3 1		0.20000		R24

101		3	1	0.20000	R24
102		3	1	0.20000	R24
103		3	1	0.20000	R24
104		3	1	0.20000	R24
105		3	1	0.20000	R24
106		3	1	0.20000	R24
107		3	1	0.20000	R24
108		3	1	0.20000	R24
109		3	1	0.20000	R24
110		3	1	1.	R24
199	188 1				R24
200	189 2				R24
201	190 3				R24
202	191 4				R24
203	192 5				R24
204	193 6				R24
205	194 7				R24
206	195 8				R24
207	196 9				R24
208	197				R24
209	198				R24
210		3	1	0.20000	R24
211		3	1	0.20000	R24
212		3	1	0.20000	R24
213		3	1	0.20000	R24
214		3	1	0.20000	R24
215		3	1	0.20000	R24
216		3	1	0.20000	R24
217		3	1	0.20000	R24
218		3	1	0.20000	R24
219		3	1	0.20000	R24
220		3	1	0.20000	R24
320	309 1			1.	R24
321	310 2				R24
322	311 3				R24
323	312 4				R24
324	313 5				R24
325	314 6				R24
326	315 7				R24
327	316 8				R24
328	317 9				R24
329	318				R24
330	319				R24
331		3	1	0.20000	R24
332		3	1	0.20000	R24
333		3	1	0.20000	R24
334		3	1	0.20000	R24
335		3	1	0.20000	R24
336		3	1	0.20000	R24
337		3	1	0.20000	R24
338		3	1	0.20000	R24
339		3	1	0.20000	R24
340		3	1	0.20000	R24
341		3	1	1.	R24
452	441 1				R24
453	442 2				R24
454	443 3				R24

455	444	4		R24
456	445	5		R24
457	446	6		R24
458	447	7		R24
459	448	8		R24
460	449	9		R24
461	450			R24
462	451			R24
463		3 1	0.20000	R24
464		3 1	0.20000	R24
465		3 1	0.20000	R24
466		3 1	0.20000	R24
467		3 1	0.20000	R24
468		3 1	0.20000	R24
469		3 1	0.20000	R24
470		3 1	0.20000	R24
471		3 1	0.20000	R24
472		3 1	0.20000	R24
473		3 1	1.	R24
617	606	1		R24
618	607	2		R24
619	608	3		R24
620	609	4		R24
621	610	5		R24
622	611	6		R24
623	612	7		R24
624	613	8		R24
625	614	9		R24
626	615			R24
-627	616			R24
1	0	0 -1	0 0 0 0 1 1 0 3 0 0 0 1 0 0 0 0 0 0 0 0 0 0 0	R 9
2	0	0 0	3.2030	R14
1		1 1	0.00100	R24
210001			0.00143	R24
310002			0.00143	R24
410003			0.00143	R24
510004			0.00143	R24
610005			0.00143	R24
710006			0.00143	R24
810007			0.00143	R24
910008			0.00143	R24
1010009			0.00143	R24
11		2 1	1.	R24
89	78	1		R24
90	79	2		R24
91	80	3		R24
92	81	4		R24
93	82	5		R24
94	83	6		R24
95	84	7		R24
96	85	8		R24
97	86	9		R24
98	87			R24
99	88			R24
100		1 1	0.00000	R24
10110001			0.14285	R24
10210002			0.14285	R24

10310003			0.14285	R24
10410004			0.14285	R24
10510005			0.14285	R24
10610006			0.14285	R24
10710007			0.14285	R24
10810008			0.14285	R24
10910009			0.14285	R24
110	2	1	1.	R24
199	188	1		R24
200	189	2		R24
201	190	3		R24
202	191	4		R24
203	192	5		R24
204	193	6		R24
205	194	7		R24
206	195	8		R24
207	196	9		R24
208	197			R24
209	198			R24
210		1	0.20000	R24
21110001			0.28571	R24
21210002			0.28571	R24
21310003			0.28571	R24
21410004			0.28571	R24
21510005			0.28571	R24
21610006			0.28571	R24
21710007			0.28571	R24
21810008			0.28571	R24
21910009			0.28571	R24
220	2	1	1.	R24
320	309	1		R24
321	310	2		R24
322	311	3		R24
323	312	4		R24
324	313	5		R24
325	314	6		R24
326	315	7		R24
327	316	8		R24
328	317	9		R24
329	318			R24
330	319			R24
331		1	0.20000	R24
33210001			0.28571	R24
33310002			0.28571	R24
33410003			0.28571	R24
33510004			0.28571	R24
33610005			0.28571	R24
33710006			0.28571	R24
33810007			0.28571	R24
33910008			0.28571	R24
34010009			0.28571	R24
341	2	1	1.	R24
452	441	1		R24
453	442	2		R24
454	443	3		R24
455	444	4		R24
456	445	5		R24

1	0	0	-2	0	0	0	0	1	1	0	0	0	0	0	0	0	0	0	0	0	R 9
15	0	0	-2	0	0	0	0	0	1	0	0	0	0	0	0	0	0	0	0	0	R 9
1	0	0	-1	0	0	0	0	1	1	0	0	0	0	0	0	0	0	0	0	0	R 9
1	0	0	-1	0	0	0	1	0	1	0	0	0	0	0	0	0	0	0	0	0	R 9
1	3	2	1	2	0	0	0	0	1	0	0	0	0	0	0	0	0	0	0	1	R 9

APPENDIX D.2: MCNP4B MODEL OF PBMR

ESKOM PEBBLE BED MODULAR REACTOR

c
c MCNP4B model of the Eskom PBMR using geometry and material specifications
c from the VSOP model of the reactor core. Detailed description of a multi-
c zoned core using a BCC lattice with homogenized pebbles.
c
c J.R. Lebenhaft, MIT, June 2000.
c -----
c CELL CARDS
c
1 0 5: -25: 41 \$ outside world
c
c reactor structure (using VSOP specifications)
c
2 1 1.10208e-01 -5 6 -35 \$ B1 upper shield
3 1 1.10208e-01 -5 6 36 -40 \$ B28 upper shield
4 49 4.17597e-02 -5 25 40 -41 \$ B49 vessel and gaps
5 6 1.16690e-01 -6 7 -35 \$ B52 top graphite
6 6 1.16690e-01 -6 7 36 -37 \$ B30 radial reflector, middle
7 1 2.49736e-02 -6 7 37 -39 \$ B29 bottom shield
8 1 2.49736e-02 -6 10 39 -40 \$ B44 radial shield
9 6 1.16690e-01 -7 8 -30 \$ B52 top graphite
10 2 1.09546e-01 -7 8 30 -35 \$ B2 cold helium chamber
11 2 1.09546e-01 -7 8 36 -39 \$ B29 radial reflector, middle
12 0 -8 9 -30 \$ B53 helium gap
13 3 9.80197e-02 -8 9 30 -34 \$ B3 top reflector
14 6 1.16690e-01 -8 21 34 -35 \$ B10-B14 radial reflect, inside
15 6 1.16690e-01 -8 10 36 -37 \$ B30 radial reflector, middle
17 40 8.06398e-02 -8 10 38 -39 \$ B40 radial reflector, outside
18 0 -9 10 -34 \$ B4 helium cavity
19 6 1.16690e-01 -10 13 36 -37 \$ B31 radial reflector, middle
21 40 8.06398e-02 -10 13 38 -39 \$ B41 radial reflector, outside
22 1 1.10208e-01 -10 13 39 -40 \$ B45 radial shield, inside
23 6 1.16690e-01 -13 21 36 -37 \$ B32-B34 rad reflector, mid/out
25 40 8.06398e-02 -13 23 38 -39 \$ B42-B55 rad reflector, out/bot
26 1 1.10208e-01 -13 22 39 -40 \$ B46-B48 rad shield, insulate
27 7 1.08160e-01 -20 21 31 -34 \$ B7 bottom reflector
28 6 1.16690e-01 -20 21 35 -36 \$ B14 radial reflector, inside
29 50 1.01448e-01 -21 22 31 -34 \$ B50 bottom shield, insulate
30 51 1.63465e-01 -21 22 34 -37 \$ B51
31 8 8.55207e-02 -22 23 31 -34 \$ B8 hot He chamber
32 1 1.10208e-01 -22 23 34 -37 \$ B54 shield of discharge tube
33 1 1.10208e-01 -23 24 31 -37 \$ B54
34 6 1.16690e-01 -22 23 39 -40 \$ B15
35 6 1.16690e-01 -23 24 37 -40 \$ B15
36 1 1.10208e-01 -24 25 31 -40 \$ B9
37 7 1.08160e-01 20 -34 45 \$ Bxx conus reflector
38 6 1.16690e-01 -20 25 30 -31 \$ B6 discharge pipe wall
c
c control/shutdown zone
c
40 6 1.16690e-01 -5 20 35 -36
(440:-441: 442:-443)
(444:-445: 446:-447)
(448:-449: 450:-451)

(452:-453: 454:-455)
 (456:-457: 458:-459)
 (460:-461: 462:-463)
 (464:-465: 466:-467)
 (468:-469: 470:-471)
 (472:-473: 474:-475)
 (476:-477: 478:-479)
 (480:-481: 482:-483)
 (484:-485: 486:-487)
 (488:-489: 490:-491)
 (492:-493: 494:-495)
 (496:-497: 498:-499)
 (500:-501: 502:-503)
 (504:-505: 506:-507)
 (508:-509: 510:-511)
 (271:-272: (273 275) : (276 -274))
 (277:-278: (279 281) : (282 -280))
 (283:-284: (285 287) : (288 -286))
 (289:-290: (291 293) : (294 -292))
 (295:-296: (297 299) : (300 -298))
 (301:-302: (303 305) : (306 -304))
 (307:-308: (309 311) : (312 -310))
 (313:-314: (315 317) : (318 -316))
 (319:-320: (321 323) : (324 -322))
 (325:-326: (327 329) : (330 -328))
 (331:-332: (333 335) : (336 -334))
 (337:-338: (339 341) : (342 -340))
 (343:-344: (345 347) : (348 -346))
 (349:-350: (351 353) : (354 -352))
 (355:-356: (357 359) : (360 -358))
 (361:-362: (363 365) : (366 -364))
 (367:-368: (369 371) : (372 -370))

c

c helium channel zone

c

41	6	1.16690e-01	-8	23	37	-38		
			375	376	377	378	379	380
			381	382	383	384	385	386
			387	388	389	390	391	392
			393	394	395	396	397	398
			399	400	401	402	403	404
			405	406	407	408	409	410

c

c control sites

c

45	0	-5	20	-440	441	-442	443	fill=300(61)	\$ CR1
46	0	-5	20	-444	445	-446	447	fill=300(62)	\$ CR2
47	0	-5	20	-448	449	-450	451	fill=300(63)	\$ CR3
48	0	-5	20	-452	453	-454	455	fill=300(64)	\$ CR4
49	0	-5	20	-456	457	-458	459	fill=300(65)	\$ CR5
50	0	-5	20	-460	461	-462	463	fill=300(66)	\$ CR6
51	0	-5	20	-464	465	-466	467	fill=300(67)	\$ CR7
52	0	-5	20	-468	469	-470	471	fill=300(68)	\$ CR8
53	0	-5	20	-472	473	-474	475	fill=300(69)	\$ CR9
54	0	-5	20	-476	477	-478	479	fill=300(70)	\$ CR10
55	0	-5	20	-480	481	-482	483	fill=300(71)	\$ CR11
56	0	-5	20	-484	485	-486	487	fill=300(72)	\$ CR12

57	0	-5	20	-488	489	-490	491	fill1=300(73)	\$ CR13
58	0	-5	20	-492	493	-494	495	fill1=300(74)	\$ CR14
59	0	-5	20	-496	497	-498	499	fill1=300(75)	\$ CR15
60	0	-5	20	-500	501	-502	503	fill1=300(76)	\$ CR16
61	0	-5	20	-504	505	-506	507	fill1=300(77)	\$ CR17
62	0	-5	20	-508	509	-510	511	fill1=300(78)	\$ CR18
c									
c shutdown sites									
c									
65	60	-3.429e-03	-5	20	-271	272	(-273:-275)	(274:-276)	\$ KL1
66	60	-3.429e-03	-5	20	-277	278	(-279:-281)	(280:-282)	\$ KL2
67	60	-3.429e-03	-5	20	-283	284	(-285:-287)	(286:-288)	\$ KL3
68	60	-3.429e-03	-5	20	-289	290	(-291:-293)	(292:-294)	\$ KL4
69	60	-3.429e-03	-5	20	-295	296	(-297:-299)	(298:-300)	\$ KL5
70	60	-3.429e-03	-5	20	-301	302	(-303:-305)	(304:-306)	\$ KL6
71	60	-3.429e-03	-5	20	-307	308	(-309:-311)	(310:-312)	\$ KL7
72	60	-3.429e-03	-5	20	-313	314	(-315:-317)	(316:-318)	\$ KL8
73	60	-3.429e-03	-5	20	-319	320	(-321:-323)	(322:-324)	\$ KL9
74	60	-3.429e-03	-5	20	-325	326	(-327:-329)	(328:-330)	\$ KL10
75	60	-3.429e-03	-5	20	-331	332	(-333:-335)	(334:-336)	\$ KL11
76	60	-3.429e-03	-5	20	-337	338	(-339:-341)	(340:-342)	\$ KL12
77	60	-3.429e-03	-5	20	-343	344	(-345:-347)	(346:-348)	\$ KL13
78	60	-3.429e-03	-5	20	-349	350	(-351:-353)	(352:-354)	\$ KL14
79	60	-3.429e-03	-5	20	-355	356	(-357:-359)	(358:-360)	\$ KL15
80	60	-3.429e-03	-5	20	-361	362	(-363:-365)	(364:-366)	\$ KL16
81	60	-3.429e-03	-5	20	-367	368	(-369:-371)	(370:-372)	\$ KL17
c									
c helium coolant channels									
c									
85	60	-3.429e-03	-8	23	-375				
86	60	-3.429e-03	-8	23	-376				
87	60	-3.429e-03	-8	23	-377				
88	60	-3.429e-03	-8	23	-378				
89	60	-3.429e-03	-8	23	-379				
90	60	-3.429e-03	-8	23	-380				
91	60	-3.429e-03	-8	23	-381				
92	60	-3.429e-03	-8	23	-382				
93	50	-3.429e-03	-8	23	-383				
94	60	-3.429e-03	-8	23	-384				
95	60	-3.429e-03	-8	23	-385				
96	60	-3.429e-03	-8	23	-386				
97	60	-3.429e-03	-8	23	-387				
98	60	-3.429e-03	-8	23	-388				
99	60	-3.429e-03	-8	23	-389				
100	60	-3.429e-03	-8	23	-390				
101	60	-3.429e-03	-8	23	-391				
102	60	-3.429e-03	-8	23	-392				
103	60	-3.429e-03	-8	23	-393				
104	60	-3.429e-03	-8	23	-394				
105	60	-3.429e-03	-8	23	-395				
106	60	-3.429e-03	-8	23	-396				
107	60	-3.129e-03	-8	23	-397				
108	60	-3.429e-03	-8	23	-398				
109	60	-3.429e-03	-8	23	-399				
110	60	-3.429e-03	-8	23	-400				
111	60	-3.429e-03	-8	23	-401				
112	60	-3.429e-03	-8	23	-402				

```

113 60 -3.429e-03    -8  23 -403
114 60 -3.429e-03    -8  23 -404
115 60 -3.429e-03    -8  23 -405
116 60 -3.429e-03    -8  23 -406
117 60 -3.429e-03    -8  23 -407
118 60 -3.429e-03    -8  23 -408
119 60 -3.429e-03    -8  23 -409
120 60 -3.429e-03    -8  23 -410
c
c -----
c   universe 300: control site
c
125 0                  520          fill=301  u=300 $ control rod region
126 6  1.16690e-01    -520  538          u=300 $ graphite surroundings
127 60 -3.429e-03    -520 -538          u=300 $ region below control
rod
c
c   universe 301: absorber lattice
c
128 0                  -523  524 -525  526 -530
                           533
lat=1 fill=302
u=301
c
c   .. universe 302: unit cell
c
129 6  1.16690e-01    538          u=302 $ graphite surroundings
130 60 -3.429e-03    -538  537          u=302 $ helium-filled gap
131 61 -8.0            -537  534  531          u=302 $ upper half joint
132 61 -8.0            -537  536 -531  532          u=302 $ outer sleeve of abs
133 62 -1.7            -536  535 -531  532          u=302 $ absorber
134 61 -8.0            -535  534 -531  532          u=302 $ inner sleeve of abs
135 61 -8.0            -537  534 -532          u=302 $ lower half joint
136 60 -3.429e-03    -534          u=302 $ helium-filled inside
c
c -----
c   core
c
300 0  -10  20  -34  -45          fill=5
c
c   discharge pipe
c
301 0  -20  25  -30          fill=78(58)
c
c   channel 1
302 0  (-115 155): (-116 -155 156): (-117 -156 157):
                   (-118 -157 158): (-119 -158 159): (-120 -159)
fill=10 u=5
c
c   channel 2
303 0  (115 -125 155): (116 -126 -155 156): (117 -127 -156 157):
                   (118 -128 -157 158): (119 -129 -158 159): (120 -130 -159)
fill=11 u=5
c
c   channel 3
304 0  (125 -135 155): (126 -136 -155 156): (127 -137 -156 157):
                   (128 -138 -157 158): (129 -139 -158 159): (130 -140 -159)

```

```

fill=12 u=5
c
c channel 4
305 0 (135 -145 155): (136 -146 -155 156): (137 -147 -156 157):
      (138 -148 -157 158): (139 -149 -158 159): (140 -150 -159)
      fill=13 u=5
c
c channel 5
306 0 (145 155): (146 -155 156): (147 -156 157): (148 -157 158):
      (149 -158 19): (149 -19 159): (150 -159)
      fill=14 u=5
c
c core layers
c
c .. channel 1
c
307 0 50 fill=21(1) u=10 $ layer 1
308 0 -50 51 fill=22(2) u=10 $ layer 2
309 0 -51 52 fill=23(3) u=10 $ layer 3
310 0 -52 53 fill=24(4) u=10 $ layer 4
311 0 -53 54 fill=25(5) u=10 $ layer 5
312 0 -54 55 fill=26(6) u=10 $ layer 6
313 0 -55 56 fill=27(7) u=10 $ layer 7
314 0 -56 57 fill=28(8) u=10 $ layer 8
315 0 -57 fill=29(9) u=10 $ layer 9
c
c .. channel 2
c
316 0 60 fill=30(10) u=11 $ layer 10
317 0 -60 61 fill=31(11) u=11 $ layer 11
318 0 -61 62 fill=32(12) u=11 $ layer 12
319 0 -62 63 fill=33(13) u=11 $ layer 13
320 0 -63 64 fill=34(14) u=11 $ layer 14
321 0 -64 65 fill=35(15) u=11 $ layer 15
322 0 -65 66 fill=36(16) u=11 $ layer 16
323 0 -66 67 fill=37(17) u=11 $ layer 17
324 0 -67 68 fill=38(18) u=11 $ layer 18
325 0 -68 fill=39(19) u=11 $ layer 19
c
c .. channel 3
c
326 0 70 fill=40(20) u=12 $ layer 20
327 0 -70 71 fill=41(21) u=12 $ layer 21
328 0 -71 72 fill=42(22) u=12 $ layer 22
329 0 -72 73 fill=43(23) u=12 $ layer 23
330 0 -73 74 fill=44(24) u=12 $ layer 24
331 0 -74 75 fill=45(25) u=12 $ layer 25
332 0 -75 76 fill=46(26) u=12 $ layer 26
333 0 -76 77 fill=47(27) u=12 $ layer 27
334 0 -77 78 fill=48(28) u=12 $ layer 28
335 0 -78 79 fill=49(29) u=12 $ layer 29
336 0 -79 fill=50(30) u=12 $ layer 30
c
c .. channel 4
c
337 0 85 fill=51(31) u=13 $ layer 31
338 0 -85 86 fill=52(32) u=13 $ layer 32

```

```

339 0 -86 87 fill=53(33) u=13 $ layer 33
340 0 -87 88 fill=54(34) u=13 $ layer 34
341 0 -88 89 fill=55(35) u=13 $ layer 35
342 0 -89 90 fill=56(36) u=13 $ layer 36
343 0 -90 91 fill=57(37) u=13 $ layer 37
344 0 -91 92 fill=58(38) u=13 $ layer 38
345 0 -92 93 fill=59(39) u=13 $ layer 39
346 0 -93 94 fill=60(40) u=13 $ layer 40
347 0 -94 95 fill=61(41) u=13 $ layer 41
348 0 -95 fill=62(42) u=13 $ layer 42
c
c .. channel 5
c
349 0 100 fill=63(43) u=14 $ layer 43
350 0 -100 101 fill=64(44) u=14 $ layer 44
351 0 -101 102 fill=65(45) u=14 $ layer 45
352 0 -102 103 fill=66(46) u=14 $ layer 46
353 0 -103 104 fill=67(47) u=14 $ layer 47
354 0 -104 105 fill=68(48) u=14 $ layer 48
355 0 -105 106 fill=69(49) u=14 $ layer 49
356 0 -106 107 fill=70(50) u=14 $ layer 50
357 0 -107 108 fill=71(51) u=14 $ layer 51
358 0 -108 109 fill=72(52) u=14 $ layer 52
359 0 -109 110 fill=73(53) u=14 $ layer 53
360 0 -110 111 fill=74(54) u=14 $ layer 54
361 0 -111 112 fill=75(55) u=14 $ layer 55
362 0 -112 113 fill=76(56) u=14 $ layer 56
363 0 -113 fill=77(57) u=14 $ layer 57
c
c -----
c channel 1: inner graphite reflector with trace U
c -----
c
c universe 21: layer 1
c
375 0 -206 205 -207 208 -209 210
lat=1 fill=80
u=21
c
c unit cell with graphite balls
c
376 100 1.1655800e-01 -211 u=80 $ [ 0 0 0]
377 100 1.1655800e-01 -212 u=80 $ [ 1 1 1]
378 100 1.1655800e-01 -213 u=80 $ [ 1 1 -1]
379 100 1.1655800e-01 -214 u=80 $ [ 1 -1 -1]
380 100 1.1655800e-01 -215 u=80 $ [ 1 -1 1]
381 100 1.1655800e-01 -216 u=80 $ [-1 1 1]
382 100 1.1655800e-01 -217 u=80 $ [-1 1 -1]
383 100 1.1655800e-01 -218 u=80 $ [-1 -1 -1]
384 100 1.1655800e-01 -219 u=80 $ [-1 -1 1]
385 60 -3.42900e-03 211 212 213 214 215
216 217 218 219 u=80 $ helium between balls
c
c -----
c universe 22: layer 2
c
386 0 -206 205 -207 208 -209 210

```

```

lat=1 fill=81
u=22
c
c unit cell with graphite balls
c
387 101 1.1655800e-01 -211      u=81   $ [ 0  0  0]
388 101 1.1655800e-01 -212      u=81   $ [ 1  1  1]
389 101 1.1655800e-01 -213      u=81   $ [ 1  1 -1]
390 101 1.1655800e-01 -214      u=81   $ [ 1 -1 -1]
391 101 1.1655800e-01 -215      u=81   $ [ 1 -1  1]
392 101 1.1655800e-01 -216      u=81   $ [-1  1  1]
393 101 1.1655800e-01 -217      u=81   $ [-1  1 -1]
394 101 1.1655800e-01 -218      u=81   $ [-1 -1 -1]
395 101 1.1655800e-01 -219      u=81   $ [-1 -1  1]
396 60  -3.42900e-03    211  212  213  214  215      u=81   $ helium between balls
216  217  218  219
c
c -----
c universe 23: layer 3
c
397 0           -206  205 -207  208 -209  210
lat=1 fill=82
u=23
c
c unit cell with graphite balls
c
398 102 1.1655800e-01 -211      u=82   $ [ 0  0  0]
399 102 1.1655800e-01 -212      u=82   $ [ 1  1  1]
400 102 1.1655800e-01 -213      u=82   $ [ 1  1 -1]
401 102 1.1655800e-01 -214      u=82   $ [ 1 -1 -1]
402 102 1.1655800e-01 -215      u=82   $ [ 1 -1  1]
403 102 1.1655800e-01 -216      u=82   $ [-1  1  1]
404 102 1.1655800e-01 -217      u=82   $ [-1  1 -1]
405 102 1.1655800e-01 -218      u=82   $ [-1 -1 -1]
406 102 1.1655800e-01 -219      u=82   $ [-1 -1  1]
407 60  -3.429e-03    211  212  213  214  215      u=82   $ helium between balls
216  217  218  219
c
c -----
c universe 24: layer 4
c
408 0           -206  205 -207  208 -209  210
lat=1 fill=83
u=24
c
c unit cell with graphite balls
c
409 103 1.1655800e-01 -211      u=83   $ [ 0  0  0]
410 103 1.1655800e-01 -212      u=83   $ [ 1  1  1]
411 103 1.1655800e-01 -213      u=83   $ [ 1  1 -1]
412 103 1.1655800e-01 -214      u=83   $ [ 1 -1 -1]
413 103 1.1655800e-01 -215      u=83   $ [ 1 -1  1]
414 103 1.1655800e-01 -216      u=83   $ [-1  1  1]
415 103 1.1655800e-01 -217      u=83   $ [-1  1 -1]
416 103 1.1655800e-01 -218      u=83   $ [-1 -1 -1]
417 103 1.1655800e-01 -219      u=83   $ [-1 -1  1]
418 60  -3.429e-03    211  212  213  214  215

```

```

216 217 218 219      u=83 $ helium between balls
c
c -----
c   universe 25: layer 5
c
419 0           -206 205 -207 208 -209 210
    lat=1 fill=84
    u=25
c
c   unit cell with graphite balls
c
420 104 1.1655800e-01 -211      u=84 $ [ 0 0 0]
421 104 1.1655800e-01 -212      u=84 $ [ 1 1 1]
422 104 1.1655800e-01 -213      u=84 $ [ 1 1 -1]
423 104 1.1655800e-01 -214      u=84 $ [ 1 -1 -1]
424 104 1.1655800e-01 -215      u=84 $ [ 1 -1 1]
425 104 1.1655800e-01 -216      u=84 $ [-1 1 1]
426 104 1.1655800e-01 -217      u=84 $ [-1 1 -1]
427 104 1.1655800e-01 -218      u=84 $ [-1 -1 -1]
428 104 1.1655800e-01 -219      u=84 $ [-1 -1 1]
429 60 -3.429e-03     211 212 213 214 215
                           216 217 218 219      u=84 $ helium between balls
c
c -----
c   universe 26: layer 6
c
430 0           -206 205 -207 208 -209 210
    lat=1 fill=85 u=26
c   unit cell with graphite balls
431 105 1.1655800e-01 -211      u=85 $ [ 0 0 0]
432 105 1.1655800e-01 -212      u=85 $ [ 1 1 1]
433 105 1.1655800e-01 -213      u=85 $ [ 1 1 -1]
434 105 1.1655800e-01 -214      u=85 $ [ 1 -1 -1]
435 105 1.1655800e-01 -215      u=85 $ [ 1 -1 1]
436 105 1.1655800e-01 -216      u=85 $ [-1 1 1]
437 105 1.1655800e-01 -217      u=85 $ [-1 1 -1]
438 105 1.1655800e-01 -218      u=85 $ [-1 -1 -1]
439 105 1.1655800e-01 -219      u=85 $ [-1 -1 1]
440 60 -3.42900e-03    211 212 213 214 215
                           216 217 218 219      u=85 $ helium between balls
c
c -----
c   universe 27: layer 7
c
441 0           -206 205 -207 208 -209 210
    lat=1 fill=86 u=27
c   unit cell with graphite balls
442 106 1.1655800e-01 -211      u=86 $ [ 0 0 0]
443 106 1.1655800e-01 -212      u=86 $ [ 1 1 1]
444 106 1.1655800e-01 -213      u=86 $ [ 1 1 -1]
445 106 1.1655800e-01 -214      u=86 $ [ 1 -1 -1]
446 106 1.1655800e-01 -215      u=86 $ [ 1 -1 1]
447 106 1.1655800e-01 -216      u=86 $ [-1 1 1]
448 106 1.1655800e-01 -217      u=86 $ [-1 1 -1]
449 106 1.1655800e-01 -218      u=86 $ [-1 -1 -1]
450 106 1.1655800e-01 -219      u=86 $ [-1 -1 1]
451 60 -3.42900e-03    211 212 213 214 215

```

```

          216 217 218 219      u=86 $ helium between balls
c
c -----
c   universe 28: layer 8
c
452 0           -206 205 -207 208 -209 210
               lat=1 fill=87 u=28
c   unit cell with graphite balls
453 107 1.1655800e-01 -211      u=87 $ [ 0 0 0]
454 107 1.1655800e-01 -212      u=87 $ [ 1 1 1]
455 107 1.1655800e-01 -213      u=87 $ [ 1 1 -1]
456 107 1.1655800e-01 -214      u=87 $ [ 1 -1 -1]
457 107 1.1655800e-01 -215      u=87 $ [ 1 -1 1]
458 107 1.1655800e-01 -216      u=87 $ [-1 1 1]
459 107 1.1655800e-01 -217      u=87 $ [-1 1 -1]
460 107 1.1655800e-01 -218      u=87 $ [-1 -1 -1]
461 107 1.1655800e-01 -219      u=87 $ [-1 -1 1]
462 60 -3.429e-03    211 212 213 214 215
               216 217 218 219      u=87 $ helium between balls
c
c -----
c   universe 29: layer 9
c
463 0           -206 205 -207 208 -209 210
               lat=1 fill=88 u=29
c   unit cell with graphite balls
464 108 1.1655800e-01 -211      u=88 $ [ 0 0 0]
465 108 1.1655800e-01 -212      u=88 $ [ 1 1 1]
466 108 1.1655800e-01 -213      u=88 $ [ 1 1 -1]
467 108 1.1655800e-01 -214      u=88 $ [ 1 -1 -1]
468 108 1.1655800e-01 -215      u=88 $ [ 1 -1 1]
469 108 1.1655800e-01 -216      u=88 $ [-1 1 1]
470 108 1.1655800e-01 -217      u=88 $ [-1 1 -1]
471 108 1.1655800e-01 -218      u=88 $ [-1 -1 -1]
472 108 1.1655800e-01 -219      u=88 $ [-1 -1 1]
473 60 -3.429e-03    211 212 213 214 215
               216 217 218 219      u=88 $ helium between balls
c
c -----
c   channel 2: mixed fuel and moderator
c
c
c   universe 30: layer 10
c
484 0           -206 205 -207 208 -209 210      $ unit cell boundaries
               lat=1 fill=89 u=30
c   .. contents of unit cell
485 109 4.2400759e-01 -211      u=89 $ [ 0 0 0]
486 109 4.2400759e-01 -212      u=89 $ [ 1 1 1]
487 109 4.2400759e-01 -213      u=89 $ [ 1 1 -1]
488 109 4.2400759e-01 -214      u=89 $ [ 1 -1 -1]
489 109 4.2400759e-01 -215      u=89 $ [ 1 -1 1]
490 109 4.2400759e-01 -216      u=89 $ [-1 1 1]
491 109 4.2400759e-01 -217      u=89 $ [-1 1 -1]
492 109 4.2400759e-01 -218      u=89 $ [-1 -1 -1]
493 109 4.2400759e-01 -219      u=89 $ [-1 -1 1]
494 60 -3.429e-03    211 212 213 214 215

```

```

          216  217  218  219      u=89    $ helium between balls
c
c -----
c   universe 31: layer 11
c
495  0           -206  205 -207  208 -209  210      $ unit cell boundaries
c       lat=1   fill=93   u=31
c   .. contents of unit cell
496 110  4.2400819e-01 -211                  u=93    $ [ 0  0  0]
497 110  4.2400819e-01 -212                  u=93    $ [ 1  1  1]
498 110  4.2400819e-01 -213                  u=93    $ [ 1  1 -1]
499 110  4.2400819e-01 -214                  u=93    $ [ 1 -1 -1]
500 110  4.2400819e-01 -215                  u=93    $ [ 1 -1  1]
501 110  4.2400819e-01 -216                  u=93    $ [-1  1  1]
502 110  4.2400819e-01 -217                  u=93    $ [-1  1 -1]
503 110  4.2400819e-01 -218                  u=93    $ [-1 -1 -1]
504 110  4.2400819e-01 -219                  u=93    $ [-1 -1  1]
505 60   -3.429e-03     211  212  213  214  215
c               216  217  218  219      u=93    $ helium between balls
c
c -----
c   universe 32: layer 12
c
506  0           -206  205 -207  208 -209  210      $ unit cell boundaries
c       lat=1   fill=97   u=32
c   .. contents of unit cell
507 111  4.2400879e-01 -211                  u=97    $ [ 0  0  0]
508 111  4.2400879e-01 -212                  u=97    $ [ 1  1  1]
509 111  4.2400879e-01 -213                  u=97    $ [ 1  1 -1]
510 111  4.2400879e-01 -214                  u=97    $ [ 1 -1 -1]
511 111  4.2400879e-01 -215                  u=97    $ [ 1 -1  1]
512 111  4.2400879e-01 -216                  u=97    $ [-1  1  1]
513 111  4.2400879e-01 -217                  u=97    $ [-1  1 -1]
514 111  4.2400879e-01 -218                  u=97    $ [-1 -1 -1]
515 111  4.2400879e-01 -219                  u=97    $ [-1 -1  1]
516 60   -3.429e-03     211  212  213  214  215
c               216  217  218  219      u=97    $ helium between balls
c
c -----
c   universe 33: layer 13
c
517  0           -206  205 -207  208 -209  210      $ unit cell boundaries
c       lat=1   fill=101  u=33
c   .. contents of unit cell
518 112  4.2400929e-01 -211                  u=101   $ [ 0  0  0]
519 112  4.2400929e-01 -212                  u=101   $ [ 1  1  1]
520 112  4.2400929e-01 -213                  u=101   $ [ 1  1 -1]
521 112  4.2400929e-01 -214                  u=101   $ [ 1 -1 -1]
522 112  4.2400929e-01 -215                  u=101   $ [ 1 -1  1]
523 112  4.2400929e-01 -216                  u=101   $ [-1  1  1]
524 112  4.2400929e-01 -217                  u=101   $ [-1  1 -1]
525 112  4.2400929e-01 -218                  u=101   $ [-1 -1 -1]
526 112  4.2400929e-01 -219                  u=101   $ [-1 -1  1]
527 60   -3.429e-03     211  212  213  214  215
c               216  217  218  219      u=101  $ helium between balls
c
c -----

```

```

c      universe 34: layer 14
c
528 0           -206 205 -207 208 -209 210    $ unit cell boundaries
c          lat=1 fill=105 u=34
c      .. contents of unit cell
529 113 4.2401019e-01 -211                  u=105 $ [ 0 0 0]
530 113 4.2401019e-01 -212                  u=105 $ [ 1 1 1]
531 113 4.2401019e-01 -213                  u=105 $ [ 1 1 -1]
532 113 4.2401019e-01 -214                  u=105 $ [ 1 -1 -1]
533 113 4.2401019e-01 -215                  u=105 $ [ 1 -1 1]
534 113 4.2401019e-01 -216                  u=105 $ [-1 1 1]
535 113 4.2401019e-01 -217                  u=105 $ [-1 1 -1]
536 113 4.2401019e-01 -218                  u=105 $ [-1 -1 -1]
537 113 4.2401019e-01 -219                  u=105 $ [-1 -1 1]
538 60 -3.429e-03     211 212 213 214 215
c          216 217 218 219                  u=105 $ helium between balls
c
c      -----
c      universe 35: layer 15
c
539 0           -206 205 -207 208 -209 210    $ unit cell boundaries
c          lat=1 fill=109 u=35
c      .. contents of unit cell
540 114 4.2401039e-01 -211                  u=109 $ [ 0 0 0]
541 114 4.2401099e-01 -212                  u=109 $ [ 1 1 1]
542 114 4.2401099e-01 -213                  u=109 $ [ 1 1 -1]
543 114 4.2401099e-01 -214                  u=109 $ [ 1 -1 -1]
544 114 4.2401099e-01 -215                  u=109 $ [ 1 -1 1]
545 114 4.2401099e-01 -216                  u=109 $ [-1 1 1]
546 114 4.2401099e-01 -217                  u=109 $ [-1 1 -1]
547 114 4.2401099e-01 -218                  u=109 $ [-1 -1 -1]
548 114 4.2401099e-01 -219                  u=109 $ [-1 -1 1]
549 60 -3.429e-03     211 212 213 214 215
c          216 217 218 219                  u=109 $ helium between balls
c
c      -----
c      universe 36: layer 16
c
550 0           -206 205 -207 208 -209 210    $ unit cell boundaries
c          lat=1 fill=113 u=36
c      .. contents of unit cell
551 115 4.2401180e-01 -211                  u=113 $ [ 0 0 0]
552 115 4.2401180e-01 -212                  u=113 $ [ 1 1 1]
553 115 4.2401180e-01 -213                  u=113 $ [ 1 1 -1]
554 115 4.2401180e-01 -214                  u=113 $ [ 1 -1 -1]
555 115 4.2401180e-01 -215                  u=113 $ [ 1 -1 1]
556 115 4.2401180e-01 -216                  u=113 $ [-1 1 1]
557 115 4.2401180e-01 -217                  u=113 $ [-1 1 -1]
558 115 4.2401180e-01 -218                  u=113 $ [-1 -1 -1]
559 115 4.2401180e-01 -219                  u=113 $ [-1 -1 1]
560 60 -3.429e-03     211 212 213 214 215
c          216 217 218 219                  u=113 $ helium between balls
c
c      -----
c      universe 37: layer 17
c
561 0           -206 205 -207 208 -209 210    $ unit cell boundaries

```

```

lat=1 fill=117 u=37
c .. contents of unit cell
562 116 4.2401239e-01 -211 u=117 $ [ 0 0 0]
563 116 4.2401239e-01 -212 u=117 $ [ 1 1 1]
564 116 4.2401239e-01 -213 u=117 $ [ 1 1 -1]
565 116 4.2401239e-01 -214 u=117 $ [ 1 -1 -1]
566 116 4.2401239e-01 -215 u=117 $ [ 1 -1 1]
567 116 4.2401239e-01 -216 u=117 $ [-1 1 1]
568 116 4.2401239e-01 -217 u=117 $ [-1 1 -1]
569 116 4.2401239e-01 -218 u=117 $ [-1 -1 -1]
570 116 4.2401239e-01 -219 u=117 $ [-1 -1 1]
571 60 -3.429e-03 211 212 213 214 215 u=117 $ helium between balls
c
c -----
c universe 38: layer 18
c
572 0 -206 205 -207 208 209 210 $ unit cell boundaries
    lat=1 fill=121
    u=38
c
c .. contents of unit cell
c
573 117 4.2401290e-01 -211 u=121 $ [ 0 0 0]
574 117 4.2401290e-01 -212 u=121 $ [ 1 1 1]
575 117 4.2401290e-01 -213 u=121 $ [ 1 1 -1]
576 117 4.2401290e-01 -214 u=121 $ [ 1 -1 -1]
577 117 4.2401290e-01 -215 u=121 $ [ 1 -1 1]
578 117 4.2401290e-01 -216 u=121 $ [-1 1 1]
579 117 4.2401290e-01 -217 u=121 $ [-1 1 -1]
580 117 4.2401290e-01 -218 u=121 $ [-1 -1 -1]
581 117 4.2401290e-01 -219 u=121 $ [-1 -1 1]
582 60 -3.429e-03 211 212 213 214 215 u=121 $ helium between balls
c
c -----
c universe 39: layer 19
c
583 0 -206 205 -207 208 -209 210 $ unit cell boundaries
    lat=1 fill=125
    u=39
c
c .. contents of unit cell
c
584 118 4.2401350e-01 -211 u=125 $ [ 0 0 0]
585 118 4.2401350e-01 -212 u=125 $ [ 1 1 1]
586 118 4.2401350e-01 -213 u=125 $ [ 1 1 -1]
587 118 4.2401350e-01 -214 u=125 $ [ 1 -1 -1]
588 118 4.2401350e-01 -215 u=125 $ [ 1 -1 1]
589 118 4.2401350e-01 -216 u=125 $ [-1 1 1]
590 118 4.2401350e-01 -217 u=125 $ [-1 1 -1]
591 118 4.2401350e-01 -218 u=125 $ [-1 -1 -1]
592 118 4.2401350e-01 -219 u=125 $ [-1 -1 1]
593 60 -3.429e-03 211 212 213 214 215 u=125 $ helium between balls
c
c -----

```

```

c      channel 3: fuel
c -----
c      universe 40: layer 20
c
603 0           -206 205 -207 208 -209 210
    lat=1 fill=129
    u=40

c
c .. contents of unit cell
c
604 119 7.3386878e-01 -211          u=129 $ [ 0 0 0]
605 119 7.3386878e-01 -212          u=129 $ [ 1 1 1]
606 119 7.3386878e-01 -213          u=129 $ [ 1 1 -1]
607 119 7.3386878e-01 -214          u=129 $ [ 1 -1 -1]
608 119 7.3386878e-01 -215          u=129 $ [ 1 -1 1]
609 119 7.3386878e-01 -216          u=129 $ [-1 1 1]
610 119 7.3386878e-01 -217          u=129 $ [-1 1 -1]
611 119 7.3386878e-01 -218          u=129 $ [-1 -1 -1]
612 119 7.3386878e-01 -219          u=129 $ [-1 -1 1]
613 60 -3.429e-03      211 212 213 214 215
                           216 217 218 219          u=129 $ helium between balls
c -----
c      universe 41: layer 21
c
614 0           -206 205 -207 208 -209 210
    lat=1 fill=133
    u=41                      $ unit cell

c
c .. contents of unit cell
c
615 120 7.3386961e-01 -211          u=133 $ [ 0 0 0]
616 120 7.3386961e-01 -212          u=133 $ [ 1 1 1]
617 120 7.3386961e-01 -213          u=133 $ [ 1 1 -1]
618 120 7.3386961e-01 -214          u=133 $ [ 1 -1 -1]
619 120 7.3386961e-01 -215          u=133 $ [ 1 -1 1]
620 120 7.3386961e-01 -216          u=133 $ [-1 1 1]
621 120 7.3386961e-01 -217          u=133 $ [-1 1 -1]
622 120 7.3386961e-01 -218          u=133 $ [-1 -1 -1]
623 120 7.3386961e-01 -219          u=133 $ [-1 -1 1]
624 60 -3.429e-03      211 212 213 214 215
                           216 217 218 219          u=133 $ helium between balls
c -----
c      universe 42: layer 22
c
625 0           -206 205 -207 208 -209 210
    lat=1 fill=137
    u=42                      $ unit cell

c
c .. contents of unit cell
c
626 121 7.3387039e-01 -211          u=137 $ [ 0 0 0]
627 121 7.3387039e-01 -212          u=137 $ [ 1 1 1]
628 121 7.3387039e-01 -213          u=137 $ [ 1 1 -1]
629 121 7.3387039e-01 -214          u=137 $ [ 1 -1 -1]
630 121 7.3387039e-01 -215          u=137 $ [ 1 -1 1]
631 121 7.3387039e-01 -216          u=137 $ [-1 1 1]
632 121 7.3387039e-01 -217          u=137 $ [-1 1 -1]

```

```

633 121 7.3387039e-01 -218 u=137 $ [-1 -1 -1]
634 121 7.3387039e-01 -219 u=137 $ [-1 -1 1]
635 60 -3.429e-03 211 212 213 214 215 u=137 $ helium between balls
c -----
c universe 43: layer 23
c
636 0 -206 205 -207 208 -209 210
lat=1 fill=141
u=43 $ unit cell
c
c .. contents of unit cell
c
637 122 7.3387140e-01 -211 u=141 $ [ 0 0 0]
638 122 7.3387140e-01 -212 u=141 $ [ 1 1 1]
639 122 7.3387140e-01 -213 u=141 $ [ 1 1 -1]
640 122 7.3387140e-01 -214 u=141 $ [ 1 -1 -1]
641 122 7.3387140e-01 -215 u=141 $ [ 1 -1 1]
642 122 7.3387140e-01 -216 u=141 $ [-1 1 1]
643 122 7.3387140e-01 -217 u=141 $ [-1 1 -1]
644 122 7.3387140e-01 -218 u=141 $ [-1 -1 -1]
645 122 7.3387140e-01 -219 u=141 $ [-1 -1 1]
646 60 -3.429e-03 211 212 213 214 215 u=141 $ helium between balls
c -----
c universe 44: layer 24
c
647 0 -206 205 -207 208 -209 210
lat=1 fill=145
u=44 $ unit cell
c
c .. contents of unit cell
c
648 123 7.3387212e-01 -211 u=145 $ [ 0 0 0]
649 123 7.3387212e-01 -212 u=145 $ [ 1 1 1]
650 123 7.3387212e-01 -213 u=145 $ [ 1 1 -1]
651 123 7.3387212e-01 -214 u=145 $ [ 1 -1 -1]
652 123 7.3387212e-01 -215 u=145 $ [ 1 -1 1]
653 123 7.3387212e-01 -216 u=145 $ [-1 1 1]
654 123 7.3387212e-01 -217 u=145 $ [-1 1 -1]
655 123 7.3387212e-01 -218 u=145 $ [-1 -1 -1]
656 123 7.3387212e-01 -219 u=145 $ [-1 -1 1]
657 60 -3.429e-03 211 212 213 214 215 u=145 $ helium between balls
c
c -----
c universe 45: layer 25
c
658 0 -206 205 -207 208 -209 210
lat=1 fill=149
u=45 $ unit cell
c
c .. contents of unit cell
c
659 124 7.3387319e-01 -211 u=149 $ [ 0 0 0]
660 124 7.3387319e-01 -212 u=149 $ [ 1 1 1]
661 124 7.3387319e-01 -213 u=149 $ [ 1 1 -1]

```

```

662 124 7.3387319e-01 -214 u=149 $ [ 1 -1 -1]
663 124 7.3387319e-01 -215 u=149 $ [ 1 -1 1]
664 124 7.3387319e-01 -216 u=149 $ [-1 1 1]
665 124 7.3387319e-01 -217 u=149 $ [-1 1 -1]
666 124 7.3387319e-01 -218 u=149 $ [-1 -1 -1]
667 124 7.3387319e-01 -219 u=149 $ [-1 -1 1]
668 60 -3.429e-03 211 212 213 214 215 u=149 $ helium between balls
c
c -----
c universe 46: layer 26
c
669 0 -206 205 -207 208 -209 210
    lat=1 fill=153
    u=46 $ unit cell
c
c .. contents of unit cell
c
670 125 7.3387408e-01 -211 u=153 $ [ 0 0 0]
671 125 7.3387408e-01 -212 u=153 $ [ 1 1 1]
672 125 7.3387408e-01 -213 u=153 $ [ 1 1 -1]
673 125 7.3387408e-01 -214 u=153 $ [ 1 -1 -1]
674 125 7.3387408e-01 -215 u=153 $ [ 1 -1 1]
675 125 7.3387408e-01 -216 u=153 $ [-1 1 1]
676 125 7.3387408e-01 -217 u=153 $ [-1 1 -1]
677 125 7.3387408e-01 -218 u=153 $ [-1 -1 -1]
678 125 7.3387408e-01 -219 u=153 $ [-1 -1 1]
679 60 -3.429e-03 211 212 213 214 215 u=153 $ helium between balls
c
c -----
c universe 47: layer 27
c
680 0 -206 205 -207 208 -209 210
    lat=1 fill=157 u=47 $ unit cell
c
c .. universe 128: contents of unit cell
c
681 126 7.3387527e-01 -211 u=157 $ [ 0 0 0]
682 126 7.3387527e-01 -212 u=157 $ [ 1 1 1]
683 126 7.3387527e-01 -213 u=157 $ [ 1 1 -1]
684 126 7.3387527e-01 -214 u=157 $ [ 1 -1 -1]
685 126 7.3387527e-01 -215 u=157 $ [ 1 -1 1]
686 126 7.3387527e-01 -216 u=157 $ [-1 1 1]
687 126 7.3387527e-01 -217 u=157 $ [-1 1 -1]
688 126 7.3387527e-01 -218 u=157 $ [-1 -1 -1]
689 126 7.3387527e-01 -219 u=157 $ [-1 -1 1]
690 60 -3.429e-03 211 212 213 214 215 u=157 $ helium between balls
c
c -----
c universe 48: layer 28
c
691 0 -206 205 -207 208 -209 210
    lat=1 fill=161
    u=48 $ unit cell
c

```

```

c .. contents of unit cell
c
692 127 7.3387587e-01 -211 u=161 $ [ 0 0 0]
693 127 7.3387587e-01 -212 u=161 $ [ 1 1 1]
694 127 7.3387587e-01 -213 u=161 $ [ 1 1 -1]
695 127 7.3387587e-01 -214 u=161 $ [ 1 -1 -1]
696 127 7.3387587e-01 -215 u=161 $ [ 1 -1 1]
697 127 7.3387587e-01 -216 u=161 $ [-1 1 1]
698 127 7.3387587e-01 -217 u=161 $ [-1 1 -1]
699 127 7.3387587e-01 -218 u=161 $ [-1 -1 -1]
700 127 7.3387587e-01 -219 u=161 $ [-1 -1 1]
701 60 -3.429e-03 211 212 213 214 215
                                216 217 218 219 u=161 $ helium between balls
c
c -----
c universe 49: layer 29
c
702 0 -206 205 -207 208 -209 210
lat=1 fill=165
u=49
$ unit cell
c .. contents of unit cell
703 128 7.3387688e-01 -211 u=165 $ [ 0 0 0]
704 128 7.3387688e-01 -212 u=165 $ [ 1 1 1]
705 128 7.3387688e-01 -213 u=165 $ [ 1 1 -1]
706 128 7.3387688e-01 -214 u=165 $ [ 1 -1 -1]
707 128 7.3387688e-01 -215 u=165 $ [ 1 -1 1]
708 128 7.3387688e-01 -216 u=165 $ [-1 1 1]
709 128 7.3387688e-01 -217 u=165 $ [-1 1 -1]
710 128 7.3387688e-01 -218 u=165 $ [-1 -1 -1]
711 128 7.3387688e-01 -219 u=165 $ [-1 -1 1]
712 60 -3.429e-03 211 212 213 214 215
                                216 217 218 219 u=165 $ helium between balls
c
c -----
c universe 50: layer 30
c
713 0 -206 205 -207 208 -209 210
lat=1 fill=169
u=50
$ unit cell
c
c .. contents of unit cell
c
714 129 7.3387718e-01 -211 u=169 $ [ 0 0 0]
715 129 7.3387718e-01 -212 u=169 $ [ 1 1 1]
716 129 7.3387718e-01 -213 u=169 $ [ 1 1 -1]
717 129 7.3387718e-01 -214 u=169 $ [ 1 -1 -1]
718 129 7.3387718e-01 -215 u=169 $ [ 1 -1 1]
719 129 7.3387718e-01 -216 u=169 $ [-1 1 1]
720 129 7.3387718e-01 -217 u=169 $ [-1 1 -1]
721 129 7.3387718e-01 -218 u=169 $ [-1 -1 -1]
722 129 7.3387718e-01 -219 u=169 $ [-1 -1 1]
723 60 -3.429e-03 211 212 213 214 215
                                216 217 218 219 u=169 $ helium between balls
c
c -----
c channel 4
c -----

```

```

c      universe 51: layer 31
c
733  0           -206  205 -207  208 -209  210
    lat=1  fill=173
    u=51                                         $ unit cell
c
c      .. contents of unit cell
c
734  130  7.3386890e-01 -211                 u=173  $ [ 0  0  0]
735  130  7.3386890e-01 -212                 u=173  $ [ 1  1  1]
736  130  7.3386890e-01 -213                 u=173  $ [ 1  1 -1]
737  130  7.3386890e-01 -214                 u=173  $ [ 1 -1 -1]
738  130  7.3386890e-01 -215                 u=173  $ [ 1 -1  1]
739  130  7.3386890e-01 -216                 u=173  $ [-1  1  1]
740  130  7.3386890e-01 -217                 u=173  $ [-1  1 -1]
741  130  7.3386890e-01 -218                 u=173  $ [-1 -1 -1]
742  130  7.3386890e-01 -219                 u=173  $ [-1 -1  1]
743  60   -3.429e-03      211  212  213  214  215
                           216  217  218  219             u=173  $ helium between balls
c
c      -----
c      universe 52: layer 32
c
744  0           -206  205 -207  208 -209  210
    lat=1  fill=177
    u=52                                         $ unit cell
c
c      .. contents of unit cell
c
745  131  7.3386949e-01 -211                 u=177  $ [ 0  0  0]
746  131  7.3386949e-01 -212                 u=177  $ [ 1  1  1]
747  131  7.3386949e-01 -213                 u=177  $ [ 1  1 -1]
748  131  7.3386949e-01 -214                 u=177  $ [ 1 -1 -1]
749  131  7.3386949e-01 -215                 u=177  $ [ 1 -1  1]
750  131  7.3386949e-01 -216                 u=177  $ [-1  1  1]
751  131  7.3386949e-01 -217                 u=177  $ [-1  1 -1]
752  131  7.3386949e-01 -218                 u=177  $ [-1 -1 -1]
753  131  7.3386949e-01 -219                 u=177  $ [-1 -1  1]
754  60   -3.429e-03      211  212  213  214  215
                           216  217  218  219             u=177  $ helium between balls
c
c      -----
c      universe 53: layer 33
c
755  0           -206  205 -207  208 -209  210
    lat=1  fill=181
    u=53                                         $ unit cell
c
c      .. contents of unit cell
c
756  132  7.3387033e-01 -211                 u=181  $ [ 0  0  0]
757  132  7.3387033e-01 -212                 u=181  $ [ 1  1  1]
758  132  7.3387033e-01 -213                 u=181  $ [ 1  1 -1]
759  132  7.3387033e-01 -214                 u=181  $ [ 1 -1 -1]
760  132  7.3387033e-01 -215                 u=181  $ [ 1 -1  1]
761  132  7.3387033e-01 -216                 u=181  $ [-1  1  1]
762  132  7.3387033e-01 -217                 u=181  $ [-1  1 -1]

```

```

763 132 7.3387033e-01 -218                               u=181   $ [-1 -1 -1]
764 132 7.3387033e-01 -219                               u=181   $ [-1 -1  1]
765 60 -3.429e-03      211  212  213  214  215      u=181   $ helium between balls
c
c -----
c   universe 54: layer 34
c
766 0           -206  205 -207  208 -209  210
    lat=1  fill=185
    u=54                                         $ unit cell
c
c   .. contents of unit cell
c
767 133 7.338711e-01 -211                               u=185   $ [ 0  0  0]
768 133 7.338711e-01 -212                               u=185   $ [ 1  1  1]
769 133 7.338711e-01 -213                               u=185   $ [ 1  1 -1]
770 133 7.338711e-01 -214                               u=185   $ [ 1 -1 -1]
771 133 7.338711e-01 -215                               u=185   $ [ 1 -1  1]
772 133 7.338711e-01 -216                               u=185   $ [-1  1  1]
773 133 7.338711e-01 -217                               u=185   $ [-1  1 -1]
774 133 7.338711e-01 -218                               u=185   $ [-1 -1 -1]
775 133 7.338711e-01 -219                               u=185   $ [-1 -1  1]
776 60 -3.429e-03      211  212  213  214  215      u=185   $ helium between balls
c
c -----
c   universe 55: layer 35
c
777 0           -206  205 -207  208 -209  210
    lat=1  fill=189
    u=55                                         $ unit cell
c
c   .. contents of unit cell
c
778 134 7.3387200e-01 -211                               u=189   $ [ 0  0  0]
779 134 7.3387200e-01 -212                               u=189   $ [ 1  1  1]
780 134 7.3387200e-01 -213                               u=189   $ [ 1  1 -1]
781 134 7.3387200e-01 -214                               u=189   $ [ 1 -1 -1]
782 134 7.3387200e-01 -215                               u=189   $ [ 1 -1  1]
783 134 7.3387200e-01 -216                               u=189   $ [-1  1  1]
784 134 7.3387200e-01 -217                               u=189   $ [-1  1 -1]
785 134 7.3387200e-01 -218                               u=189   $ [-1 -1 -1]
786 134 7.3387200e-01 -219                               u=189   $ [-1 -1  1]
787 60 -3.429e-03      211  212  213  214  215      u=189   $ helium between balls
c
c -----
c   universe 56: layer 36
c
788 0           -206  205 -207  208 -209  210
    lat=1  fill=193
    u=56                                         $ unit cell
c
c   .. contents of unit cell
c
789 135 7.3387271e-01 -211                               u=193   $ [ 0  0  0]

```

```

790 135 7.3387271e-01 -212          u=193   $ [ 1  1  1]
791 135 7.3387271e-01 -213          u=193   $ [ 1  1 -1]
792 135 7.3387271e-01 -214          u=193   $ [ 1 -1 -1]
793 135 7.3387271e-01 -215          u=193   $ [ 1 -1  1]
794 135 7.3387271e-01 -216          u=193   $ [-1  1  1]
795 135 7.3387271e-01 -217          u=193   $ [-1  1 -1]
796 135 7.3387271e-01 -218          u=193   $ [-1 -1 -1]
797 135 7.3387271e-01 -219          u=193   $ [-1 -1  1]
798 60  -3.429e-03      211  212  213  214  215
                                216  217  218  219          u=193   $ helium between balls
c
c -----
c  universe 57: layer 37
c
799 0           -206  205 -207  208 -209  210
lat=1  fill=197
u=57                                     $ unit cell
c
c .. universe 189: contents of unit cell
c
800 136 7.3387378e-01 -211          u=197   $ [ 0  0  0]
801 136 7.3387378e-01 -212          u=197   $ [ 1  1  1]
802 136 7.3387378e-01 -213          u=197   $ [ 1  1 -1]
803 136 7.3387378e-01 -214          u=197   $ [ 1 -1 -1]
804 136 7.3387378e-01 -215          u=197   $ [ 1 -1  1]
805 136 7.3387378e-01 -216          u=197   $ [-1  1  1]
806 136 7.3387378e-01 -217          u=197   $ [-1  1 -1]
807 136 7.3387378e-01 -218          u=197   $ [-1 -1 -1]
808 136 7.3387378e-01 -219          u=197   $ [-1 -1  1]
809 60  -3.429e-03      211  212  213  214  215
                                216  217  218  219          u=197   $ helium between balls
c
c -----
c  universe 58: layer 38
c
810 0           -206  205 -207  208 -209  210
lat=1  fill=201
u=58                                     $ unit cell
c
c .. contents of unit cell
c
811 137 7.3387462e-01 -211          u=201   $ [ 0  0  0]
812 137 7.3387462e-01 -212          u=201   $ [ 1  1  1]
813 137 7.3387462e-01 -213          u=201   $ [ 1  1 -1]
814 137 7.3387462e-01 -214          u=201   $ [ 1 -1 -1]
815 137 7.3387462e-01 -215          u=201   $ [ 1 -1  1]
816 137 7.3387462e-01 -216          u=201   $ [-1  1  1]
817 137 7.3387462e-01 -217          u=201   $ [-1  1 -1]
818 137 7.3387462e-01 -218          u=201   $ [-1 -1 -1]
819 137 7.3387462e-01 -219          u=201   $ [-1 -1  1]
820 60  -3.429e-03      211  212  213  214  215
                                216  217  218  219          u=201   $ helium between balls
c
c -----
c  universe 59: layer 39
c
821 0           -206  205 -207  208 -209  210

```

```

lat=1 fill=205
u=59                                         $ unit cell
c
c .. contents of unit cell
c
822 138 7.3387557e-01 -211                 u=205  $ [ 0  0  0]
823 138 7.3387557e-01 -212                 u=205  $ [ 1  1  1]
824 138 7.3387557e-01 -213                 u=205  $ [ 1  1 -1]
825 138 7.3387557e-01 -214                 u=205  $ [ 1 -1 -1]
826 138 7.3387557e-01 -215                 u=205  $ [ 1 -1  1]
827 138 7.3387557e-01 -216                 u=205  $ [-1  1  1]
828 138 7.3387557e-01 -217                 u=205  $ [-1  1 -1]
829 138 7.3387557e-01 -218                 u=205  $ [-1 -1 -1]
830 138 7.3387557e-01 -219                 u=205  $ [-1 -1  1]
831 60  -3.429e-03      211  212  213  214  215
                           216  217  218  219             u=205  $ helium between balls
c
c -----
c universe 60: layer 40
c
832 0           -206  205 -207  208 -209  210
lat=1 fill=209
u=60                                         $ unit cell
c
c .. contents of unit cell
c
833 139 7.3387623e-01 -211                 u=209  $ [ 0  0  0]
834 139 7.3387623e-01 -212                 u=209  $ [ 1  1  1]
835 139 7.3387623e-01 -213                 u=209  $ [ 1  1 -1]
836 139 7.3387623e-01 -214                 u=209  $ [ 1 -1 -1]
837 139 7.3387623e-01 -215                 u=209  $ [ 1 -1  1]
838 139 7.3387623e-01 -216                 u=209  $ [-1  1  1]
839 139 7.3387623e-01 -217                 u=209  $ [-1  1 -1]
840 139 7.3387623e-01 -218                 u=209  $ [-1 -1 -1]
841 139 7.3387623e-01 -219                 u=209  $ [-1 -1  1]
842 60  -3.429e-03      211  212  213  214  215
                           216  217  218  219             u=209  $ helium between balls
c
c -----
c universe 61: layer 41
c
843 0           -206  205 -207  208 -209  210
lat=1 fill=213
u=61                                         $ unit cell
c
c .. contents of unit cell
c
844 140 7.3387641e-01 -211                 u=213  $ [ 0  0  0]
845 140 7.3387641e-01 -212                 u=213  $ [ 1  1  1]
846 140 7.3387641e-01 -213                 u=213  $ [ 1  1 -1]
847 140 7.3387641e-01 -214                 u=213  $ [ 1 -1 -1]
848 140 7.3387641e-01 -215                 u=213  $ [ 1 -1  1]
849 140 7.3387641e-01 -216                 u=213  $ [-1  1  1]
850 140 7.3387641e-01 -217                 u=213  $ [-1  1 -1]
851 140 7.3387641e-01 -218                 u=213  $ [-1 -1 -1]
852 140 7.3387641e-01 -219                 u=213  $ [-1 -1  1]
853 60  -3.429e-03      211  212  213  214  215

```

```

          216  217  218  219      u=213 $ helium between balls
c
c -----
c   universe 62: layer 42
c
854  0           -206  205 -207  208 -209  210
    lat=1  fill=217
    u=62
                           $ unit cell
c
c   .. contents of unit cell
c
855  141  7.3387688e-01 -211      u=217  $ [ 0  0  0]
856  141  7.3387688e-01 -212      u=217  $ [ 1  1  1]
857  141  7.3387688e-01 -213      u=217  $ [ 1  1 -1]
858  141  7.3387688e-01 -214      u=217  $ [ 1 -1 -1]
859  141  7.3387688e-01 -215      u=217  $ [ 1 -1  1]
860  141  7.3387688e-01 -216      u=217  $ [-1  1  1]
861  141  7.3387688e-01 -217      u=217  $ [-1  1 -1]
862  141  7.3387688e-01 -218      u=217  $ [-1 -1 -1]
863  141  7.3387688e-01 -219      u=217  $ [-1 -1  1]
864  60   -3.429e-03       211  212  213  214  215      u=217  $ helium between balls
c
c -----
c   channel 5
c
c   universe 63: layer 43
c
874  0           -206  205 -207  208 -209  210
    lat=1  fill=221
    u=63
                           $ unit cell
c
c   .. contents of unit cell
c
875  142  7.3386949e-01 -211      u=221  $ [ 0  0  0]
876  142  7.3386949e-01 -212      u=221  $ [ 1  1  1]
877  142  7.3386949e-01 -213      u=221  $ [ 1  1 -1]
878  142  7.3386949e-01 -214      u=221  $ [ 1 -1 -1]
879  142  7.3386949e-01 -215      u=221  $ [ 1 -1  1]
880  142  7.3386949e-01 -216      u=221  $ [-1  1  1]
881  142  7.3386949e-01 -217      u=221  $ [-1  1 -1]
882  142  7.3386949e-01 -218      u=221  $ [-1 -1 -1]
883  142  7.3386949e-01 -219      u=221  $ [-1 -1  1]
884  60   -3.429e-03       211  212  213  214  215      u=221  $ helium between balls
c
c -----
c   universe 64: layer 44
c
885  0           -206  205 -207  208 -209  210
    lat=1  fill=225
    u=64
                           $ unit cell
c
c   .. contents of unit cell
c
886  143  7.3387003e-01 -211      u=225  $ [ 0  0  0]
887  143  7.3387003e-01 -212      u=225  $ [ 1  1  1]

```

```

888 143 7.3387003e-01 -213          u=225   $ [ 1  1 -1]
889 143 7.3387003e-01 -214          u=225   $ [ 1 -1 -1]
890 143 7.3387003e-01 -215          u=225   $ [ 1 -1  1]
891 143 7.3387003e-01 -216          u=225   $ [-1  1  1]
892 143 7.3387003e-01 -217          u=225   $ [-1  1 -1]
893 143 7.3387003e-01 -218          u=225   $ [-1 -1 -1]
894 143 7.3387003e-01 -219          u=225   $ [-1 -1  1]
895 60  -3.429e-03      211  212  213  214  215
                                216  217  218  219          u=225   $ helium between balls
c -----
c universe 65: layer 45
c
896 0                      -206  205 -207  208 -209  210
    lat=1  fill=229
    u=65                               $ unit cell
c
c .. contents of unit cell
c
897 144 7.3387092e-01 -211          u=229   $ [ 0  0  0]
898 144 7.3387092e-01 -212          u=229   $ [ 1  1  1]
899 144 7.3387092e-01 -213          u=229   $ [ 1  1 -1]
900 144 7.3387092e-01 -214          u=229   $ [ 1 -1 -1]
901 144 7.3387092e-01 -215          u=229   $ [ 1 -1  1]
902 144 7.3387092e-01 -216          u=229   $ [-1  1  1]
903 144 7.3387092e-01 -217          u=229   $ [-1  1 -1]
904 144 7.3387092e-01 -218          u=229   $ [-1 -1 -1]
905 144 7.3387092e-01 -219          u=229   $ [-1 -1  1]
906 60  -3.429e-03      211  212  213  214  215
                                216  217  218  219          u=229   $ helium between balls
c -----
c universe 66: layer 46
c
907 0                      -206  205 -207  208 -209  210
    lat=1  fill=233
    u=66                               $ unit cell
c
c .. contents of unit cell
c
908 145 7.3387158e-01 -211          u=233   $ [ 0  0  0]
909 145 7.3387158e-01 -212          u=233   $ [ 1  1  1]
910 145 7.3387158e-01 -213          u=233   $ [ 1  1 -1]
911 145 7.3387158e-01 -214          u=233   $ [ 1 -1 -1]
912 145 7.3387158e-01 -215          u=233   $ [ 1 -1  1]
913 145 7.3387158e-01 -216          u=233   $ [-1  1  1]
914 145 7.3387158e-01 -217          u=233   $ [-1  1 -1]
915 145 7.3387158e-01 -218          u=233   $ [-1 -1 -1]
916 145 7.3387158e-01 -219          u=233   $ [-1 -1  1]
917 60  -3.429e-03      211  212  213  214  215
                                216  217  218  219          u=233   $ helium between balls
c -----
c universe 67: layer 47
c
918 0                      -206  205 -207  208 -209  210
    lat=1  fill=237
    u=67                               $ unit cell

```

```

c
c .. contents of unit cell
c
919 146 7.3387271e-01 -211           u=237   $ [ 0  0  0]
920 146 7.3387271e-01 -212           u=237   $ [ 1  1  1]
921 146 7.3387271e-01 -213           u=237   $ [ 1  1 -1]
922 146 7.3387271e-01 -214           u=237   $ [ 1 -1 -1]
923 146 7.3387271e-01 -215           u=237   $ [ 1 -1  1]
924 146 7.3387271e-01 -216           u=237   $ [-1  1  1]
925 146 7.3387271e-01 -217           u=237   $ [-1  1 -1]
926 146 7.3387271e-01 -218           u=237   $ [-1 -1 -1]
927 146 7.3387271e-01 -219           u=237   $ [-1 -1  1]
928 60  -3.429e-03      211  212  213  214  215
                                216  217  218  219           u=237   $ helium between balls
c
c -----
c universe 68: layer 48
c
929 0          -206  205 -207  208 -209  210       $ unit cell
lat=1 fill=242
u=68
c
c .. contents of unit cell
c
930 147 7.3387343e-01 -211           u=242   $ [ 0  0  0]
931 147 7.3387343e-01 -212           u=242   $ [ 1  1  1]
932 147 7.3387343e-01 -213           u=242   $ [ 1  1 -1]
933 147 7.3387343e-01 -214           u=242   $ [ 1 -1 -1]
934 147 7.3387343e-01 -215           u=242   $ [ 1 -1  1]
935 147 7.3387343e-01 -216           u=242   $ [-1  1  1]
936 147 7.3387343e-01 -217           u=242   $ [-1  1 -1]
937 147 7.3387343e-01 -218           u=242   $ [-1 -1 -1]
938 147 7.3387343e-01 -219           u=242   $ [-1 -1  1]
939 60  -3.429e-03      211  212  213  214  215
                                216  217  218  219           u=242   $ helium between balls
c
c -----
c universe 69: layer 49
c
940 0          -206  205 -207  208 -209  210
lat=1 fill=246
u=69
$ unit cell
c
c .. contents of unit cell
c
941 148 7.3387438e-01 -211           u=246   $ [ 0  0  0]
942 148 7.3387438e-01 -212           u=246   $ [ 1  1  1]
943 148 7.3387438e-01 -213           u=246   $ [ 1  1 -1]
944 148 7.3387438e-01 -214           u=246   $ [ 1 -1 -1]
945 148 7.3387438e-01 -215           u=246   $ [ 1 -1  1]
946 148 7.3387438e-01 -216           u=246   $ [-1  1  1]
947 148 7.3387438e-01 -217           u=246   $ [-1  1 -1]
948 148 7.3387438e-01 -218           u=246   $ [-1 -1 -1]
949 148 7.3387438e-01 -219           u=246   $ [-1 -1  1]
950 60  -3.429e-03      211  212  213  214  215
                                216  217  218  219           u=246   $ helium between balls
c

```

```

c -----
c      universe 70: layer 50
c
951  0           -206  205 -207  208 -209  210
     lat=1  fill=250
     u=70                                         $ unit cell
c
c      .. contents of unit cell
c
952  149  7.3387527e-01 -211                  u=250   $ [ 0  0  0]
953  149  7.3387527e-01 -212                  u=250   $ [ 1  1  1]
954  149  7.3387527e-01 -213                  u=250   $ [ 1  1 -1]
955  149  7.3387527e-01 -214                  u=250   $ [ 1 -1 -1]
956  149  7.3387527e-01 -215                  u=250   $ [ 1 -1  1]
957  149  7.3387527e-01 -216                  u=250   $ [-1  1  1]
958  149  7.3387527e-01 -217                  u=250   $ [-1  1 -1]
959  149  7.3387527e-01 -218                  u=250   $ [-1 -1 -1]
960  149  7.3387527e-01 -219                  u=250   $ [-1 -1  1]
961  60   -3.429e-03    211  212  213  214  215
                           216  217  218  219          u=250   $ helium between balls
c
c -----
c      universe 71: layer 51
c
962  0           -206  205 -207  208 -209  210
     lat=1  fill=254
     u=71                                         $ unit cell
c
c      .. contents of unit cell
c
963  150  7.3387629e-01 -211                  u=254   $ [ 0  0  0]
964  150  7.3387629e-01 -212                  u=254   $ [ 1  1  1]
965  150  7.3387629e-01 -213                  u=254   $ [ 1  1 -1]
966  150  7.3387629e-01 -214                  u=254   $ [ 1 -1 -1]
967  150  7.3387629e-01 -215                  u=254   $ [ 1 -1  1]
968  150  7.3387629e-01 -216                  u=254   $ [-1  1  1]
969  150  7.3387629e-01 -217                  u=254   $ [-1  1 -1]
970  150  7.3387629e-01 -218                  u=254   $ [-1 -1 -1]
971  150  7.3387629e-01 -219                  u=254   $ [-1 -1  1]
972  60   -3.429e-03    211  212  213  214  215
                           216  217  218  219          u=254   $ helium between balls
c -----
c      universe 72: layer 52
c
973  0           -206  205 -207  208 -209  210
     lat=1  fill=258
     u=72                                         $ unit cell
c
c      .. contents of unit cell
c
974  151  7.3387671e-01 -211                  u=258   $ [ 0  0  0]
975  151  7.3387671e-01 -212                  u=258   $ [ 1  1  1]
976  151  7.3387671e-01 -213                  u=258   $ [ 1  1 -1]
977  151  7.3387671e-01 -214                  u=258   $ [ 1 -1 -1]
978  151  7.3387671e-01 -215                  u=258   $ [ 1 -1  1]
979  151  7.3387671e-01 -216                  u=258   $ [-1  1  1]
980  151  7.3387671e-01 -217                  u=258   $ [-1  1 -1]

```

```

981 151 7.3387671e-01 -218                               u=258   $ [-1 -1 -1]
982 151 7.3387671e-01 -219                               u=258   $ [-1 -1  1]
983 60  -3.429e-03      211  212  213  214  215      u=258   $ helium between balls
c -----
c universe 73: layer 53
c
984 0           -206  205 -207  208 -209  210
    lat=1  fill=262
    u=73                                         $ unit cell
c
c .. contents of unit cell
c
985 152 7.3387688e-01 -211                               u=262   $ [ 0  0  0]
986 152 7.3387688e-01 -212                               u=262   $ [ 1  1  1]
987 152 7.3387688e-01 -213                               u=262   $ [ 1  1 -1]
988 152 7.3387688e-01 -214                               u=262   $ [ 1 -1 -1]
989 152 7.3387688e-01 -215                               u=262   $ [ 1 -1  1]
990 152 7.3387688e-01 -216                               u=262   $ [-1  1  1]
991 152 7.3387688e-01 -217                               u=262   $ [-1  1 -1]
992 152 7.3387688e-01 -218                               u=262   $ [-1 -1 -1]
993 152 7.3387688e-01 -219                               u=262   $ [-1 -1  1]
994 60  -3.429e-03      211  212  213  214  215      u=262   $ helium between balls
c -----
c universe 74: layer 54
c
995 0           -206  205 -207  208 -209  210
    lat=1  fill=266
    u=74                                         $ unit cell
c
c .. contents of unit cell
c
996 153 7.3387748e-01 -211                               u=266   $ [ 0  0  0]
997 153 7.3387748e-01 -212                               u=266   $ [ 1  1  1]
998 153 7.3387748e-01 -213                               u=266   $ [ 1  1 -1]
999 153 7.3387748e-01 -214                               u=266   $ [ 1 -1 -1]
1999 153 7.3387748e-01 -215                               u=266   $ [ 1 -1  1]
2000 153 7.3387748e-01 -216                               u=266   $ [-1  1  1]
2001 153 7.3387748e-01 -217                               u=266   $ [-1  1 -1]
2002 153 7.3387748e-01 -218                               u=266   $ [-1 -1 -1]
2003 153 7.3387748e-01 -219                               u=266   $ [-1 -1  1]
2004 60  -3.429e-03      211  212  213  214  215      u=266   $ helium between balls
c -----
c universe 75: layer 55
c
2005 0           -206  205 -207  208 -209  210
    lat=1  fill=270
    u=75                                         $ unit cell
c
c .. contents of unit cell
c
2006 154 7.3387808e-01 -211                               u=270   $ [ 0  0  0]
2007 154 7.3387808e-01 -212                               u=270   $ [ 1  1  1]
2008 154 7.3387808e-01 -213                               u=270   $ [ 1  1 -1]
2009 154 7.3387808e-01 -214                               u=270   $ [ 1 -1 -1]

```

```

2010 154 7.3387808e-01 -215          u=270   $ [ 1 -1  1]
2011 154 7.3387808e-01 -216          u=270   $ [-1  1  1]
2012 154 7.3387808e-01 -217          u=270   $ [-1  1 -1]
2013 154 7.3387808e-01 -218          u=270   $ [-1 -1 -1]
2014 154 7.3387808e-01 -219          u=270   $ [-1 -1  1]
2015 60  -3.429e-03      211  212  213  214  215          u=270   $ helium between balls
c
c -----
c   universe 76: layer 56
c
2016 0           -206  205 -207  208 -209  210
    lat=1  fill=274
    u=76                               $ unit cell
c
c   .. contents of unit cell
c
2017 155 7.3387849e-01 -211          u=274   $ [ 0  0  0]
2018 155 7.3387849e-01 -212          u=274   $ [ 1  1  1]
2019 155 7.3387849e-01 -213          u=274   $ [ 1  1 -1]
2020 155 7.3387849e-01 -214          u=274   $ [ 1 -1 -1]
2021 155 7.3387849e-01 -215          u=274   $ [ 1 -1  1]
2022 155 7.3387849e-01 -216          u=274   $ [-1  1  1]
2023 155 7.3387849e-01 -217          u=274   $ [-1  1 -1]
2024 155 7.3387849e-01 -218          u=274   $ [-1 -1 -1]
2025 155 7.3387849e-01 -219          u=274   $ [-1 -1  1]
2026 60  -3.429e-03      211  212  213  214  215          u=274   $ helium between balls
c
c -----
c   universe 77: layer 57
c
2027 0           -206  205 -207  208 -209  210
    lat=1  fill=278
    u=77                               $ unit cell
c
c   .. contents of unit cell
c
2028 156 7.3387891e-01 -211          u=278   $ [ 0  0  0]
2029 156 7.3387891e-01 -212          u=278   $ [ 1  1  1]
2030 156 7.3387891e-01 -213          u=278   $ [ 1  1 -1]
2031 156 7.3387891e-01 -214          u=278   $ [ 1 -1 -1]
2032 156 7.3387891e-01 -215          u=278   $ [ 1 -1  1]
2033 156 7.3387891e-01 -216          u=278   $ [-1  1  1]
2034 156 7.3387891e-01 -217          u=278   $ [-1  1 -1]
2035 156 7.3387891e-01 -218          u=278   $ [-1 -1 -1]
2036 156 7.3387891e-01 -219          u=278   $ [-1 -1  1]
2037 60  -3.429e-03      211  212  213  214  215          u=278   $ helium between balls
c
c -----
c   universe 78: discharge pipe
c
2038 0           -206  205 -207  208 -209  210
    lat=1  fill=282
    u=78                               $ unit cell
c
c   .. contents of unit cell

```

```

c
2039 156 7.3387891e-01 -211          u=282   $ [ 0  0  0]
2040 156 7.3387891e-01 -212          u=282   $ [ 1  1  1]
2041 156 7.3387891e-01 -213          u=282   $ [ 1  1 -1]
2042 156 7.3387891e-01 -214          u=282   $ [ 1 -1 -1]
2043 156 7.3387891e-01 -215          u=282   $ [ 1 -1  1]
2044 156 7.3387891e-01 -216          u=282   $ [-1  1  1]
2045 156 7.3387891e-01 -217          u=282   $ [-1  1 -1]
2046 156 7.3387891e-01 -218          u=282   $ [-1 -1 -1]
2047 156 7.3387891e-01 -219          u=282   $ [-1 -1  1]
2048 60 -3.429e-03      211  212  213  214  215
                           216  217  218  219          u=282   $ helium between balls
c
c -----
c     SURFACE CARDS
c
c     reactor structure axial divisions
5    pz      0.0
6    pz     -50.0
7    pz    -140.0
8    pz    -150.0
9    pz    -200.0
10   pz   -261.2
13   pz   -500.6
19   pz  -979.4
20   pz -1066.2
21   pz -1116.2
22   pz -1166.2
23   pz -1216.2
24   pz -1266.2
25   pz -1291.2
c
c     reactor structure radial divisions
30   cz      35.0
31   cz      45.0
34   cz     175.0
35   cz     181.0
36   cz     194.0
37   cz     225.0
38   cz     235.0
39   cz     257.0
40   cz     275.0
41   cz     331.0
c
c     conus
45   z    -979.4  175.0    -1066.2  35.0
c
c     layers in channel 1                                bottom of:
50   pz    -325.8662          $ layer 1
51   pz    -391.5263          $ layer 2
52   pz    -457.4383          $ layer 3
53   pz    -523.4468          $ layer 4
54   pz    -590.0280          $ layer 5
55   pz    -658.3862          $ layer 6
56   pz    -728.9344          $ layer 7
57   pz    -803.4993          $ layer 8

```

```

c
c    layers in channel 2
60  pz   -325.9992      $ layer 10
61  pz   -391.1913      $ layer 11
62  pz   -456.7378      $ layer 12
63  pz   -522.6889      $ layer 13
64  pz   -589.1911      $ layer 14
65  pz   -656.5009      $ layer 15
66  pz   -725.3721      $ layer 16
67  pz   -797.0067      $ layer 17
68  pz   -870.4246      $ layer 18
c
c    layers in channel 3
70  pz   -328.1101      $ layer 20
71  pz   -394.5977      $ layer 21
72  pz   -460.6103      $ layer 22
73  pz   -526.1077      $ layer 23
74  pz   -591.0684      $ layer 24
75  pz   -655.4955      $ layer 25
76  pz   -719.5168      $ layer 26
77  pz   -783.4268      $ layer 27
78  pz   -846.7093      $ layer 28
79  pz   -911.2618      $ layer 29
c
c    layers in channel 4
85  pz   -327.7736      $ layer 31
86  pz   -393.1451      $ layer 32
87  pz   -458.4412      $ layer 33
88  pz   -524.1719      $ layer 34
89  pz   -590.2695      $ layer 35
90  pz   -656.0625      $ layer 36
91  pz   -720.2756      $ layer 37
92  pz   -781.3543      $ layer 38
93  pz   -838.8892      $ layer 39
94  pz   -896.3219      $ layer 40
95  pz   -952.4894      $ layer 41
c
c    layers in channel 5
100 pz   -329.0798      $ layer 43
101 pz   -397.1589      $ layer 44
102 pz   -465.1485      $ layer 45
103 pz   -532.6207      $ layer 46
104 pz   -599.0450      $ layer 47
105 pz   -663.8527      $ layer 48
106 pz   -727.6718      $ layer 49
107 pz   -791.0222      $ layer 50
108 pz   -846.8144      $ layer 51
109 pz   -889.1656      $ layer 52
110 pz   -922.5213      $ layer 53
111 pz   -948.9672      $ layer 54
112 pz   -971.4881      $ layer 55
113 pz   -993.7430      $ layer 56
c
c    channel 1 outer boundary
115 z    -261.2  79.689   -476.3  78.376   -685.4  75.201
116 z    -685.4  75.201   -810.9  67.429   -841.3  59.001
117 z    -841.3  59.001   -871.7  49.587   -902.1  41.487

```

```

118 z -902.1 41.487 -932.5 31.635 -962.9 24.848
119 z -962.9 24.848 -993.3 18.937 -1019.4 15.215
120 z -1019.4 15.215 -1044.4 13.355 -1066.2 12.588
c
c channel 2 outer boundary
125 z -261.2 112.36 -476.3 110.88 -685.4 107.61
126 z -685.4 107.61 -810.9 100.74 -841.3 92.253
127 z -841.3 92.253 -871.7 86.277 -902.1 74.661
128 z -902.1 74.661 -932.5 60.933 -962.9 50.372
129 z -962.9 50.372 -993.3 39.495 -1019.4 31.892
130 z -1019.4 31.892 -1044.4 24.711 -1066.2 19.536
c
c channel 3 outer boundary
135 z -261.2 136.61 -476.3 135.90 -685.4 133.85
136 z -685.4 133.85 -810.9 128.63 -841.3 124.54
137 z -841.3 124.54 -871.7 117.89 -902.1 107.35
138 z -902.1 107.35 -932.5 92.405 -962.9 75.213
139 z -962.9 75.213 -993.3 61.706 -1019.4 50.245
140 z -1019.4 50.245 -1044.4 39.397 -1066.2 22.922
c
c channel 4 outer boundary/channel 5 inner boundary
145 z -261.2 156.98 -476.3 156.98 -685.4 155.56
146 z -685.4 155.56 -810.9 153.54 -841.3 150.81
147 z -841.3 150.81 -871.7 144.02 -902.1 137.65
148 z -902.1 137.65 -932.5 125.00 -962.9 111.13
149 z -962.9 111.13 -993.3 92.609 -1019.4 72.973
150 z -1019.4 72.973 -1044.4 50.909 -1066.2 26.214
c
155 pz -685.4
156 pz -841.3
157 pz -902.1
158 pz -962.9
159 pz -1019.4
c
c fuel element
c
c .. fuel region
201 so 2.5
c
c unit cell boundaries in core
c
205 px -3.5921477 $ [-1 0 0]
206 px 3.5921477 $ [ 1 0 0]
207 py 3.5921477 $ [ 0 1 0]
208 py -3.5921477 $ [ 0 -1 0]
209 pz 3.5921477 $ [ 0 0 1]
210 pz -3.5921477 $ [ 0 0 -1]
c
c balls in unit bcc cell
c
211 so 3.0
212 s 3.5921477 3.5921477 3.5921477 3.0
213 s 3.5921477 3.5921477 -3.5921477 3.0
214 s 3.5921477 -3.5921477 -3.5921477 3.0
215 s 3.5921477 -3.5921477 3.5921477 3.0
216 s -3.5921477 3.5921477 3.5921477 3.0
217 s -3.5921477 3.5921477 -3.5921477 3.0

```

```

218 s      -3.5921477 -3.5921477 -3.5921477 3.0
219 s      -3.5921477 -3.5921477 3.5921477 3.0
c
c   coated fuel particle (cfp)
c
220 so      0.025                               $ UO2 kernel
221 so      0.034                               $ 1st PyC layer
222 so      0.038                               $ 2nd PyC layer
223 so      0.0415                             $ SiC layer
224 so      0.0455                             $ 3rd PyC layer
c
c   unit sc cell for cfp lattice in graphite matrix
c
225 px      0.0852133
226 px      -0.0852133
227 py      0.0852133
228 py      -0.0852133
229 pz      0.0852133
230 pz      -0.0852133
c
c   shutdown sites
c
c   .. KL1
271 81  px      3.0
272 81  px      -3.0
273 81  py      5.0
274 81  py      -5.0
275 81  c/z     0.0  5.0  3.0
276 81  c/z     0.0 -5.0  3.0
c
c   .. KL2
277 82  px      3.0
278 82  px      -3.0
279 82  py      5.0
280 82  py      -5.0
281 82  c/z     0.0  5.0  3.0
282 82  c/z     0.0 -5.0  3.0
c
c   .. KL3
283 83  px      3.0
284 83  px      -3.0
285 83  py      5.0
286 83  py      -5.0
287 83  c/z     0.0  5.0  3.0
288 83  c/z     0.0 -5.0  3.0
c
c   .. KL4
289 84  px      3.0
290 84  px      -3.0
291 84  py      5.0
292 84  py      -5.0
293 84  c/z     0.0  5.0  3.0
294 84  c/z     0.0 -5.0  3.0
c
c   .. KL5
295 85  px      3.0
296 85  px      -3.0

```

```

297 85  py      5.0
298 85  py     -5.0
299 85  c/z     0.0   5.0   3.0
300 85  c/z     0.0  -5.0   3.0
c
c .. KL6
301 86  px      3.0
302 86  px     -3.0
303 86  py      5.0
304 86  py     -5.0
305 86  c/z     0.0   5.0   3.0
306 86  c/z     0.0  -5.0   3.0
c
c .. KL7
307 87  px      3.0
308 87  px     -3.0
309 87  py      5.0
310 87  py     -5.0
311 87  c/z     0.0   5.0   3.0
312 87  c/z     0.0  -5.0   3.0
c
c .. KL8
313 88  px      3.0
314 88  px     -3.0
315 88  py      5.0
316 88  py     -5.0
317 88  c/z     0.0   5.0   3.0
318 88  c/z     0.0  -5.0   3.0
c
c .. KL9
319 89  px      3.0
320 89  px     -3.0
321 89  py      5.0
322 89  py     -5.0
323 89  c/z     0.0   5.0   3.0
324 89  c/z     0.0  -5.0   3.0
c
c .. KL10
325 90  px      3.0
326 90  px     -3.0
327 90  py      5.0
328 90  py     -5.0
329 90  c/z     0.0   5.0   3.0
330 90  c/z     0.0  -5.0   3.0
c
c .. KL11
331 91  px      3.0
332 91  px     -3.0
333 91  py      5.0
334 91  py     -5.0
335 91  c/z     0.0   5.0   3.0
336 91  c/z     0.0  -5.0   3.0
c
c .. KL12
337 92  px      3.0
338 92  px     -3.0
339 92  py      5.0

```

```

340 92  py   -5.0
341 92  c/z    0.0  5.0  3.0
342 92  c/z    0.0 -5.0  3.0
c
c .. KL13
343 93  px    3.0
344 93  px   -3.0
345 93  py    5.0
346 93  py   -5.0
347 93  c/z    0.0  5.0  3.0
348 93  c/z    0.0 -5.0  3.0
c
c .. KL14
349 94  px    3.0
350 94  px   -3.0
351 94  py    5.0
352 94  py   -5.0
353 94  c/z    0.0  5.0  3.0
354 94  c/z    0.0 -5.0  3.0
c
c .. KL15
355 95  px    3.0
356 95  px   -3.0
357 95  py    5.0
358 95  py   -5.0
359 95  c/z    0.0  5.0  3.0
360 95  c/z    0.0 -5.0  3.0
c
c .. KL16
361 96  px    3.0
362 96  px   -3.0
363 96  py    5.0
364 96  py   -5.0
365 96  c/z    0.0  5.0  3.0
366 96  c/z    0.0 -5.0  3.0
c
c .. KL17
367 97  px    3.0
368 97  px   -3.0
369 97  py    5.0
370 97  py   -5.0
371 97  c/z    0.0  5.0  3.0
372 97  c/z    0.0 -5.0  3.0
c
c helium channels in reflector
c
375  c/z  230.000   0.000  4.0
376  c/z  226.506  39.940  4.0
377  c/z  216.129  78.660  4.0
378  c/z  199.186 115.000  4.0
379  c/z  176.190 147.840  4.0
380  c/z  147.841 176.190  4.0
381  c/z  115.000 199.190  4.0
382  c/z   78.665 216.130  4.0
383  c/z   39.939 226.510  4.0
384  c/z    0.000 230.000  4.0
385  c/z  -39.939 226.510  4.0

```

```

386    c/z   -78.665  216.130  4.0
387    c/z   -115.000  199.190  4.0
388    c/z   -147.841  176.190  4.0
389    c/z   -176.190  147.840  4.0
390    c/z   -199.186  115.000  4.0
391    c/z   -216.129   78.660  4.0
392    c/z   -226.506   39.940  4.0
393    c/z   -230.000    0.000  4.0
394    c/z   -226.506  -39.940  4.0
395    c/z   -216.129  -78.660  4.0
396    c/z   -199.186  -115.000 4.0
397    c/z   -176.190  -147.840 4.0
398    c/z   -147.841  -176.190 4.0
399    c/z   -115.000  -199.190 4.0
400    c/z   -78.665  -216.130 4.0
401    c/z   -39.939  -226.510 4.0
402    c/z    0.000  -230.000 4.0
403    c/z   39.939  -226.510 4.0
404    c/z   78.665  -216.130 4.0
405    c/z  115.000  -199.190 4.0
406    c/z  147.841  -176.190 4.0
407    c/z  176.190  -147.840 4.0
408    c/z  199.186  -115.000 4.0
409    c/z  216.129  -78.660 4.0
410    c/z  226.506  -39.940 4.0

c
c      control sites
c
c      .. CR1
440  61  px  6.1
441  61  px -6.1
442  61  py  6.1
443  61  py -6.1
c
c      .. CR2
444  62  px  6.1
445  62  px -6.1
446  62  py  6.1
447  62  py -6.1
c
c      .. CR3
448  63  px  6.1
449  63  px -6.1
450  63  py  6.1
451  63  py -6.1
c
c      .. CR4
452  64  px  6.1
453  64  px -6.1
454  64  py  6.1
455  64  py -6.1
c
c      .. CR5
456  65  px  6.1
457  65  px -6.1
458  65  py  6.1
459  65  py -6.1

```

c
c .. CR6
460 66 px 6.1
461 66 px -6.1
462 66 py 6.1
463 66 py -6.1
c
c .. CR7
464 67 px 6.1
465 67 px -6.1
466 67 py 6.1
467 67 py -6.1
c
c .. CR8
468 68 px 6.1
469 68 px -6.1
470 68 py 6.1
471 68 py -6.1
c
c .. CR9
472 69 px 6.1
473 69 px -6.1
474 69 py 6.1
475 69 py -6.1
c
c .. CR10
476 70 px 6.1
477 70 px -6.1
478 70 py 6.1
479 70 py -6.1
c
c .. CR11
480 71 px 6.1
481 71 px -6.1
482 71 py 6.1
483 71 py -6.1
c
c .. CR12
484 72 px 6.1
485 72 px -6.1
486 72 py 6.1
487 72 py -6.1
c
c .. CR13
488 73 px 6.1
489 73 px -6.1
490 73 py 6.1
491 73 py -6.1
c
c .. CR14
492 74 px 6.1
493 74 px -6.1
494 74 py 6.1
495 74 py -6.1
c
c .. CR15
496 75 px 6.1

```

497 75 px -6.1
498 75 py 6.1
499 75 py -6.1
c
c .. CR16
500 76 px 6.1
501 76 px -6.1
502 76 py 6.1
503 76 py -6.1
c
c .. CR17
504 77 px 6.1
505 77 px -6.1
506 77 py 6.1
507 77 py -6.1
c
c .. CR18
508 78 px 6.1
509 78 px -6.1
510 78 py 6.1
511 78 py -6.1
c
c control rods
c
520 pz -462.45 $ bottom of rod (1/4 inserted)
c 520 pz -663.7 $ bottom of rod (1/2 inserted)
c
c .. lattice boundaries
523 px 6.0
524 px -6.0
525 py 6.0
526 py -6.0
c
c .. absorber unit cell
530 pz 26.6 $ top of joint (1/2 height)
531 pz 24.35 $ top of absorber section
532 pz -24.35 $ bottom of absorber section
533 pz -26.6 $ bottom of joint (1/2 height)
534 cz 2.75 $ inner surface of s/s sleeve
535 cz 3.0 $ inner surface of absorber
536 cz 5.25 $ outer surface of absorber
537 cz 5.5 $ outer surface of s/s sleeve
538 cz 5.7 $ inner surface of graphite
sleeve
c
c surfaces for tallies
c
551 pz -341.0
552 pz -420.8
553 pz -500.6
554 pz -580.4
555 pz -660.2
556 pz -740.0
557 pz -819.8
558 pz -899.6
c
c .. radial zones

```



```

1 10r 1 10r
1 10r 1 10r 1 10r 1 10r 1 10r      $ layers 43 - 57
1 10r 1 10r 1 10r 1 10r 1 10r
1 10r 1 10r 1 10r 1 10r 1 10r
1 10r                                         $ discharge pipe

c
c   transformations
c   channel 1
c
tr1    0      0   -280.176
tr2    0      0   -344.832
tr3    0      0   -409.488
tr4    0      0   -474.144
tr5    0      0   -538.800
tr6    0      0   -610.640
tr7    0      0   -675.296
tr8    0      0   -747.136
tr9    0      0   -818.976
c
c   channel 2
c
tr10   93.392  0   -280.176
tr11   93.392  0   -344.832
tr12   93.392  0   -409.488
tr13   93.392  0   -474.144
tr14   93.392  0   -538.800
tr15   86.208  0   -610.640
tr16   79.024  0   -675.296
tr17   79.024  0   -739.952
tr18   57.472  0   -811.792
tr19   21.552  0   -890.816
c
c   channel 3
c
tr20   122.128 0   -280.176
tr21   122.128 0   -344.832
tr22   122.128 0   -409.488
tr23   122.128 0   -481.328
tr24   122.128 0   -545.984
tr25   114.944 0   -610.640
tr26   114.944 0   -675.296
tr27   114.944 0   -739.952
tr28   114.944 0   -804.608
tr29   100.576 0   -862.08
tr30   79.024  0   -926.736
c
c   channel 4
c
tr31   143.68  0.0   -280.176
tr32   143.68  0.0   -344.832
tr33   143.68  0.0   -409.488
tr34   143.68  0.0   -474.144
tr35   143.68  0.0   -538.800
tr36   143.68  0.0   -610.640
tr37   143.68  0.0   -675.296
tr38   136.496 0.0   -739.952
tr39   136.496 0.0   -797.424

```

```

tr40 129.312 0.0 -854.896
tr41 114.944 0.0 -912.368
tr42 71.840 0.0 -969.84
c
c   channel 5
c
tr43 165.232 0.0 -280.176
tr44 165.232 0.0 -344.832
tr45 165.232 0.0 -416.672
tr46 165.232 0.0 -481.328
tr47 165.232 0.0 -553.168
tr48 165.232 0.0 -617.824
tr49 165.232 0.0 -682.480
tr50 158.048 0.0 -747.136
tr51 158.048 0.0 -811.792
tr52 158.048 0.0 -862.080
tr53 150.864 0.0 -905.184
tr54 143.680 0.0 -941.104
tr55 136.496 0.0 -969.840
tr56 122.128 0.0 -991.392
tr57 93.392 0.0 -1012.944
c
c   discharge pipe
c
tr58 0 0 -1084.784
c
c   control sites
c
*tr61 184.651 32.559 0.0 10 80 90 100 10 90 90 90 90 0 $ CR1
*tr62 162.380 93.750 0.0 30 60 90 120 30 90 90 90 90 0 $ CR2
*tr63 120.523 143.633 0.0 50 40 90 140 50 90 90 90 90 0 $ CR3
*tr64 64.129 176.192 0.0 70 20 90 160 70 90 90 90 90 0 $ CR4
*tr65 0.000 187.500 0.0 90 0 90 180 90 90 90 90 90 0 $ CR5
*tr66 -64.129 176.192 0.0 110 20 90 -160 110 90 90 90 90 0 $ CR6
*tr67 -120.523 143.633 0.0 130 40 90 -140 130 90 90 90 90 0 $ CR7
*tr68 -162.380 93.750 0.0 150 60 90 -120 150 90 90 90 90 0 $ CR8
*tr69 -184.651 32.559 0.0 170 80 90 -100 170 90 90 90 90 0 $ CR9
*tr70 -184.651 -32.559 0.0 -170 100 90 -80 -170 90 90 90 90 0 $ CR10
*tr71 -162.380 -93.750 0.0 -150 120 90 -60 -150 90 90 90 90 0 $ CR11
*tr72 -120.523 -143.633 0.0 -130 140 90 -40 -130 90 90 90 90 0 $ CR12
*tr73 -64.129 -176.192 0.0 -110 160 90 -20 -110 90 90 90 90 0 $ CR13
*tr74 0.000 -187.500 0.0 -90 180 90 0 -90 90 90 90 90 0 $ CR14
*tr75 64.129 -176.192 0.0 -70 -160 90 20 -70 90 90 90 90 0 $ CR15
*tr76 120.523 -143.633 0.0 -50 -140 90 40 -50 90 90 90 90 0 $ CR16
*tr77 162.380 -93.750 0.0 -30 -120 90 60 -30 90 90 90 90 0 $ CR17
*tr78 184.651 -32.559 0.0 -10 -100 90 80 -10 90 90 90 90 0 $ CR18
c
c   shutdown sites
c
*tr81 176.192 64.129 0.0 20 70 90 110 20 90 90 90 90 0 $ KL1
*tr82 143.633 120.523 0.0 40 50 90 130 40 90 90 90 90 0 $ KL2
*tr83 93.750 162.380 0.0 60 30 90 150 60 90 90 90 90 0 $ KL3
*tr84 32.559 184.651 0.0 80 10 90 170 80 90 90 90 90 0 $ KL4
*tr85 -32.559 184.651 0.0 100 10 90 -170 100 90 90 90 90 0 $ KL5
*tr86 -93.750 162.380 0.0 120 30 90 -150 120 90 90 90 90 0 $ KL6
*tr87 -143.633 120.523 0.0 140 50 90 -130 140 90 90 90 90 0 $ KL7
*tr88 -176.192 64.129 0.0 160 70 90 -110 160 90 90 90 90 0 $ KL8

```

```

*tr89 -187.500    0.000  0.0   180   90   90  -90   180   90   90  90  90  0  $ KL9
*tr90 -176.192   -64.129  0.0  -160  110   90  -70  -160  90   90  90  90  0  $ KL10
*tr91 -143.633  -120.523  0.0  -140  130   90  -50  -140  90   90  90  90  0  $ KL11
*tr92  -93.750  -162.380  0.0  -120  150   90  -30  -120  90   90  90  90  0  $ KL12
*tr93  -32.559  -184.651  0.0  -100  170   90  -10  -100  90   90  90  90  0  $ KL13
*tr94   32.559  -184.651  0.0   -80  -170   90   10  -80  90   90  90  90  0  $ KL14
*tr95   93.750  -162.380  0.0   -60  -150   90   30  -60  90   90  90  90  0  $ KL15
*tr96  143.633  -120.523  0.0   -40  -130   90   50  -40  90   90  90  90  0  $ KL16
*tr97  176.192   -64.129  0.0   -20  -110   90   70  -20  90   90  90  90  0  $ KL17
c
c      tally specifications - from model with homogenized layers
c
fc7   fission source for normalization (per unit mass)
core
f7:n  300
sd7   1
c
fc17  average fission power in inner reflector zone
      R-Z geometry, 9 x 80.5 cm regions top to bottom
      R1 = 73 cm
f17:n 300
fs17  561  551 552 553 554 555 556 557 558 559
sd17  1 10r
c
fc27  average prompt fission power in mixed mod/fuel zone
      R-Z geometry, 9 x 80.5 cm regions top to bottom
      R1 = 73 cm, R2 = 107.08 cm
f27:n 300
fs27  -561 562 551 552 553 554 555 556 557 558 559
sd27  1 11r
c
fc37  average prompt fission power in inner fuel zone
      R-Z geometry, 9 x 80.5 cm regions top to bottom
      R2 = 107.95 cm, R3 = 134.08 cm
f37:n 300
fs37  -562 563 551 552 553 554 555 556 557 558 559
sd37  1 11r
c
fc47  average prompt fission power in middle fuel zone
      R-Z geometry, 9 x 80.5 cm regions top to bottom
      R3 = 134.08 cm, R4 = 155.89 cm
f47:n 300
fs47  -563 564 551 552 553 554 555 556 557 558 559
sd47  1 11r
c
fc57  average prompt fission power in outer fuel zone
      R-Z geometry, 9 x 80.5 cm regions top to bottom
      R4 = 155.89 cm, R5 = 175 cm
f57:n 300
fs57  -564 34 551 552 553 554 555 556 557 558 559
sd57  1 11r
c
fc14  average neutron flux in inner reflector zone
      R-Z geometry, 9 x 80.5 cm regions top to bottom
      R1 = 73 cm
f14:n 300
fs14  561 551 552 553 554 555 556 557 558 559

```

```

sd14  1  1347694.55  9r
e14  1.86e-06  20
c
fc24  average neutron flux in mixed mod/fuel zone
      R-Z geometry, 9 x 80.5 cm regions top to bottom
      R1 = 73 cm, R2 = 107.09 cm
f24:n 300
fs24 -561  562  551  552  553  554  555  556  557  558  559
sd24  1  1  1599328.16  9r
e24  1.86e-06  20
c
fc34  average neutron flux in inner fuel zone
      R-Z geometry, 9 x 79.8 cm regions top to bottom
      R2 = 107.09 cm, R3 = 134.08 cm
f34:n 300
fs34 -562  563  551  552  553  554  555  556  557  558  559
sd34  1  1  1599328.70  9r
e34  1.86e-06  20
c
fc44  average neutron flux in middle fuel zone
      R-Z geometry, 9 x 79.8 cm regions top to bottom
      R3 = 134.08 cm, R4 = 155.89 cm
f44:n 300
fs44 -563  564  551  552  553  554  555  556  557  558  559
sd44  1  1  1599327.94  9r
e44  1.86e-06  20
c
fc54  average neutron flux in outer fuel zone
      R-Z geometry, 9 x 79.8 cm regions top to bottom
      R4 = 155.89 cm, R5 = 175 cm
f54:n 300
fs54 -564  34   551  552  553  554  555  556  557  558  559
sd54  1  1  1599328.28  9r
e54  1.86e-06  20
c
c      material specifications
c
c      structural materials
m1  5010.50c 2.97186e-03  5011.50c 2.00039e-02  6000.50c 8.52341e-02
mt1 grph.06t
m2  5010.50c 2.95398e-03  5011.50c 1.98835e-02  6000.50c 8.47225e-02
mt2 grph.06t
m3  5010.50c 2.64317e-03  5011.50c 1.77914e-02  6000.50c 7.58082e-02
mt3 grph.06t
m6  5010.50c 3.14663e-03  5011.50c 2.11803e-02  6000.50c 9.02479e-02
m7  5010.50c 2.91662e-03  5011.50c 1.96320e-02  6000.50c 8.36508e-02
mt6 grph.06t
m8  5010.50c 2.30612e-03  5011.50c 1.55227e-02  6000.50c 6.61415e-02
mt7 grph.06t
m40 5010.50c 2.17453e-03  5011.50c 1.46370e-02  6000.50c 6.23664e-02
mt40 grph.06t
m49 26000.50c 4.08572e-02  6000.50c 9.02479e-04
mt49 grph.06t
m50 5010.50c 2.77718e-03  5011.50c 1.85604e-02  6000.50c 7.82771e-02
mt50 grph.06t
m51 5010.50c 5.70121e-02  5011.50c 2.00242e-02  6000.50c 8.44504e-02
mt51 grph.06t

```

c
 c helium (4.814e-3 g/cc at 300K)
 m60 2003.60c 0.00000137 2004.60c 0.99999863
 c
 c stainless steel
 m61 24000.50c -0.190 25055.50c -0.020 26000.50c -0.685
 28000.50c -0.095 14000.50c -0.010
 c
 c boron carbide (B4C)
 m62 6000.50c -0.2174 5010.50c -0.1557 5011.50c -0.6269
 c
 c fuel corresponding to equilibrium burnup
 c VSOP cycle 261; layer 1; total N = 1.1655800E-01
 M100 92235.50c 4.07262E-08 92236.50c 6.58900E-09 92238.50c 1.07094E-06
 93239.60c 7.50066E-11 94239.50c 3.63122E-09 94240.50c 2.10990E-09
 94241.50c 1.08681E-09 94242.50c 5.42479E-10 93237.50c 2.30932E-10
 54135.50c 5.84360E-13 36083.50c 1.70197E-10 42095.50c 2.10732E-09
 43099.50c 2.56441E-09 44101.50c 2.29166E-09 44103.50c 2.26484E-10
 45103.50c 1.15521E-09 45105.50c 4.14982E-12 46105.50c 8.38610E-10
 46108.50c 2.84020E-10 47109.50c 1.53964E-10 48000.50c 1.83462E-13
 54131.50c 1.10083E-09 55133.50c 2.75069E-09 55134.60c 1.52320E-10
 59141.50c 2.50604E-09 60143.50c 1.80634E-09 60145.50c 1.55532E-09
 61147.50c 5.84537E-10 61148.50c 3.77982E-12 62147.50c 1.17966E-10
 61149.50c 4.16566E-12 62149.50c 4.97450E-12 62150.50c 5.66122E-10
 62151.50c 2.87247E-11 62152.50c 2.78273E-10 63153.50c 1.80856E-10
 63154.50c 3.36616E-11 63155.50c 1.10601E-11 64155.50c 1.49528E-13
 64156.50c 6.06263E-11 64157.50c 7.28950E-14 5010.50c 3.28991E-09
 14000.50c 2.62384E-06 6000.50c 8.77334E-02 8016.50c 2.34059E-06
 C VSOP cycle 261; layer 2; total N = 1.1655800E-01
 M101 92235.50c 3.98109E-08 92236.50c 6.72954E-09 92238.50c 1.07071E-06
 93239.60c 1.10818E-10 94239.50c 3.48284E-09 94240.50c 2.17671E-09
 94241.50c 1.05883E-09 94242.50c 5.62895E-10 93237.50c 2.32825E-10
 54135.50c 6.21233E-13 36083.50c 1.73786E-10 42095.50c 2.14275E-09
 43099.50c 2.62577E-09 44101.50c 2.34657E-09 44103.50c 2.41965E-10
 45103.50c 1.17273E-09 45105.50c 6.94228E-12 46105.50c 8.56632E-10
 46108.50c 2.91700E-10 47109.50c 1.58068E-10 48000.50c 1.74153E-13
 54131.50c 1.11721E-09 55133.50c 2.79548E-09 55134.60c 1.54946E-10
 59141.50c 2.56493E-09 60143.50c 1.82278E-09 60145.50c 1.59184E-09
 61147.50c 5.99805E-10 61148.50c 4.04966E-12 62147.50c 1.20406E-10
 61149.50c 6.77844E-12 62149.50c 4.09333E-12 62150.50c 5.76979E-10
 62151.50c 2.71804E-11 62152.50c 2.87516E-10 63153.50c 1.84517E-10
 63154.50c 3.44658E-11 63155.50c 1.11875E-11 64155.50c 9.73063E-14
 64156.50c 6.28466E-11 64157.50c 6.80328E-14 5010.50c 5.12410E-09
 14000.50c 2.62384E-06 6000.50c 8.77334E-02 8016.50c 2.34059E-06
 C VSOP cycle 261; layer 3; total N = 1.1655800E-01
 M102 92235.50c 3.85522E-08 92236.50c 6.92302E-09 92238.50c 1.07039E-06
 93239.60c 1.58675E-10 94239.50c 3.28932E-09 94240.50c 2.26442E-09
 94241.50c 1.02490E-09 94242.50c 5.91133E-10 93237.50c 2.35537E-10
 54135.50c 6.26026E-13 36083.50c 1.78637E-10 42095.50c 2.18010E-09
 43099.50c 2.70995E-09 44101.50c 2.42206E-09 44103.50c 2.70728E-10
 45103.50c 1.18871E-09 45105.50c 9.29268E-12 46105.50c 8.81808E-10
 46108.50c 3.02266E-10 47109.50c 1.63675E-10 48000.50c 1.66918E-13
 54131.50c 1.13895E-09 55133.50c 2.85951E-09 55134.60c 1.59086E-10
 59141.50c 2.64583E-09 60143.50c 1.83993E-09 60145.50c 1.64190E-09
 61147.50c 6.21381E-10 61148.50c 4.88820E-12 62147.50c 1.22772E-10
 61149.50c 9.50137E-12 62149.50c 4.13281E-12 62150.50c 5.91321E-10
 62151.50c 2.58933E-11 62152.50c 2.99540E-10 63153.50c 1.89705E-10

	63154.50c 3.56328E-11	63155.50c 1.13643E-11	64155.50c 6.12524E-14
	64156.50c 6.59242E-11	64157.50c 6.72216E-14	5010.50c 6.91338E-09
	14000.50c 2.62384E-06	6000.50c 8.77334E-02	8016.50c 2.34059E-06
C	VSOP cycle 261; layer 4; total N = 1.1655800E-01		
M103	92235.50c 3.70386E-08	92236.50c 7.15576E-09	92238.50c 1.06998E-06
	93239.60c 2.02213E-10	94239.50c 3.08514E-09	94240.50c 2.36288E-09
	94241.50c 9.90698E-10	94242.50c 6.25492E-10	93237.50c 2.39004E-10
	54135.50c 6.17953E-13	36083.50c 1.84329E-10	42095.50c 2.22063E-09
	43099.50c 2.81086E-09	44101.50c 2.51284E-09	44103.50c 3.07426E-10
	45103.50c 1.20480E-09	45105.50c 1.09310E-11	46105.50c 9.12214E-10
	46108.50c 3.15006E-10	47109.50c 1.70373E-10	48000.50c 1.59703E-13
	54131.50c 1.16749E-09	55133.50c 2.94368E-09	55134.60c 1.64601E-10
	59141.50c 2.74303E-09	60143.50c 1.86155E-09	60145.50c 1.70182E-09
	61147.50c 6.47138E-10	61148.50c 5.77646E-12	62147.50c 1.25106E-10
	61149.50c 1.18185E-11	62149.50c 4.20694E-12	62150.50c 6.09694E-10
	62151.50c 2.50505E-11	62152.50c 3.13328E-10	63153.50c 1.96196E-10
	63154.50c 3.71304E-11	63155.50c 1.15600E-11	64155.50c 4.51662E-14
	64156.50c 6.97323E-11	64157.50c 6.64257E-14	5010.50c 8.84364E-09
	14000.50c 2.62384E-06	6000.50c 8.77334E-02	8016.50c 2.34059E-06
C	VSOP cycle 261; layer 5; total N = 1.1655800E-01		
M104	92235.50c 3.54456E-08	92236.50c 7.40067E-09	92238.50c 1.06954E-06
	93239.60c 2.26988E-10	94239.50c 2.90579E-09	94240.50c 2.45858E-09
	94241.50c 9.61991E-10	94242.50c 6.62376E-10	93237.50c 2.42901E-10
	54135.50c 6.03558E-13	36083.50c 1.90147E-10	42095.50c 2.26508E-09
	43099.50c 2.91688E-09	44101.50c 2.60858E-09	44103.50c 3.43702E-10
	45103.50c 1.22298E-09	45105.50c 1.14781E-11	46105.50c 9.44908E-10
	46108.50c 3.28536E-10	47109.50c 1.77412E-10	48000.50c 1.53246E-13
	54131.50c 1.20228E-09	55133.50c 3.04293E-09	55134.60c 1.70928E-10
	59141.50c 2.84537E-09	60143.50c 1.89051E-09	60145.50c 1.76465E-09
	61147.50c 6.73503E-10	61148.50c 6.40090E-12	62147.50c 1.27483E-10
	61149.50c 1.29811E-11	62149.50c 4.28340E-12	62150.50c 6.30673E-10
	62151.50c 2.46821E-11	62152.50c 3.27412E-10	63153.50c 2.03347E-10
	63154.50c 3.88211E-11	63155.50c 1.17468E-11	64155.50c 4.04374E-14
	64156.50c 7.39185E-11	64157.50c 6.58863E-14	5010.50c 1.13633E-08
	14000.50c 2.62384E-06	6000.50c 8.77334E-02	8016.50c 2.34059E-06
C	VSOP cycle 261; layer 6; total N = 1.1655800E-01		
M105	92235.50c 3.38890E-08	92236.50c 7.63976E-09	92238.50c 1.06909E-06
	93239.60c 2.35738E-10	94239.50c 2.75935E-09	94240.50c 2.54463E-09
	94241.50c 9.40618E-10	94242.50c 6.99365E-10	93237.50c 2.46988E-10
	54135.50c 5.86958E-13	36083.50c 1.95653E-10	42095.50c 2.31346E-09
	43099.50c 3.02039E-09	44101.50c 2.70245E-09	44103.50c 3.74714E-10
	45103.50c 1.24412E-09	45105.50c 1.13402E-11	46105.50c 9.77584E-10
	46108.50c 3.41946E-10	47109.50c 1.84315E-10	48000.50c 1.47843E-13
	54131.50c 1.24110E-09	55133.50c 3.14927E-09	55134.60c 1.77630E-10
	59141.50c 2.94555E-09	60143.50c 1.92644E-09	60145.50c 1.82585E-09
	61147.50c 6.98281E-10	61148.50c 6.76533E-12	62147.50c 1.29950E-10
	61149.50c 1.32003E-11	62149.50c 4.32258E-12	62150.50c 6.52527E-10
	62151.50c 2.45635E-11	62152.50c 3.40953E-10	63153.50c 2.10678E-10
	63154.50c 4.05953E-11	63155.50c 1.19199E-11	64155.50c 4.01376E-14
	64156.50c 7.82159E-11	64157.50c 6.55200E-14	5010.50c 1.44400E-08
	14000.50c 2.62384E-06	6000.50c 8.77334E-02	8016.50c 2.34059E-06
C	VSOP cycle 261; layer 7; total N = 1.1655800E-01		
M106	92235.50c 3.24715E-08	92236.50c 7.85720E-09	92238.50c 1.06865E-06
	93239.60c 2.28293E-10	94239.50c 2.65173E-09	94240.50c 2.61727E-09
	94241.50c 9.26388E-10	94242.50c 7.34104E-10	93237.50c 2.50999E-10
	54135.50c 5.70051E-13	36083.50c 2.00509E-10	42095.50c 2.36533E-09
	43099.50c 3.11474E-09	44101.50c 2.78843E-09	44103.50c 3.96727E-10

	45103.50c	1.26874E-09	45105.50c	1.06042E-11	46105.50c	1.00848E-09
	46108.50c	3.54408E-10	47109.50c	1.90666E-10	48000.50c	1.43727E-13
	54131.50c	1.28144E-09	55133.50c	3.25505E-09	55134.60c	1.84188E-10
	59141.50c	3.03709E-09	60143.50c	1.96815E-09	60145.50c	1.88148E-09
	61147.50c	7.19756E-10	61148.50c	6.86570E-12	62147.50c	1.32548E-10
	61149.50c	1.25154E-11	62149.50c	4.36572E-12	62150.50c	6.73693E-10
	62151.50c	2.46026E-11	62152.50c	3.53205E-10	63153.50c	2.17690E-10
	63154.50c	4.23267E-11	63155.50c	1.20772E-11	64155.50c	4.28534E-14
	64156.50c	8.23348E-11	64157.50c	6.54426E-14	5010.50c	1.85014E-08
	14000.50c	2.62384E-06	6000.50c	8.77334E-02	8016.50c	2.34059E-06
C	VSOP cycle 261; layer 8; total N = 1.1655800E-01					
M107	92235.50c	3.12458E-08	92236.50c	8.04485E-09	92238.50c	1.06825E-06
	93239.60c	2.13446E-10	94239.50c	2.58354E-09	94240.50c	2.67645E-09
	94241.50c	9.17762E-10	94242.50c	7.65039E-10	93237.50c	2.54983E-10
	54135.50c	5.54225E-13	36083.50c	2.04580E-10	42095.50c	2.41983E-09
	43099.50c	3.19640E-09	44101.50c	2.86327E-09	44103.50c	4.08417E-10
	45103.50c	1.29674E-09	45105.50c	9.50911E-12	46105.50c	1.03644E-09
	46108.50c	3.65438E-10	47109.50c	1.96225E-10	48000.50c	1.40931E-13
	54131.50c	1.32077E-09	55133.50c	3.35395E-09	55134.60c	1.90315E-10
	59141.50c	3.11661E-09	60143.50c	2.01353E-09	60145.50c	1.92952E-09
	61147.50c	7.37095E-10	61148.50c	6.81389E-12	62147.50c	1.35287E-10
	61149.50c	1.12484E-11	62149.50c	4.41911E-12	62150.50c	6.93006E-10
	62151.50c	2.47330E-11	62152.50c	3.63691E-10	63153.50c	2.24110E-10
	63154.50c	4.39448E-11	63155.50c	1.22216E-11	64155.50c	4.81663E-14
	64156.50c	8.60758E-11	64157.50c	6.58135E-14	5010.50c	2.38964E-08
	14000.50c	2.62384E-06	6000.50c	8.77334E-02	8016.50c	2.34059E-06
C	VSOP cycle 261; layer 9; total N = 1.1655810E-01					
M108	92235.50c	3.02662E-08	92236.50c	8.19319E-09	92238.50c	1.06787E-06
	93239.60c	1.96095E-10	94239.50c	2.60360E-09	94240.50c	2.71496E-09
	94241.50c	9.10929E-10	94242.50c	7.88761E-10	93237.50c	2.59726E-10
	54135.50c	5.07863E-13	36083.50c	2.07679E-10	42095.50c	2.47592E-09
	43099.50c	3.26022E-09	44101.50c	2.92219E-09	44103.50c	4.06959E-10
	45103.50c	1.32852E-09	45105.50c	7.62552E-12	46105.50c	1.05951E-09
	46108.50c	3.73910E-10	47109.50c	2.00359E-10	48000.50c	1.36512E-13
	54131.50c	1.35679E-09	55133.50c	3.44050E-09	55134.60c	1.95810E-10
	59141.50c	3.17939E-09	60143.50c	2.06095E-09	60145.50c	1.96715E-09
	61147.50c	7.48803E-10	61148.50c	6.92585E-12	62147.50c	1.38165E-10
	61149.50c	9.20910E-12	62149.50c	4.32926E-12	62150.50c	7.09414E-10
	62151.50c	2.45106E-11	62152.50c	3.72007E-10	63153.50c	2.29572E-10
	63154.50c	4.53945E-11	63155.50c	1.23787E-11	64155.50c	5.52293E-14
	64156.50c	8.91727E-11	64157.50c	5.95267E-14	5010.50c	3.23723E-08
	14000.50c	2.62384E-06	6000.50c	8.77334E-02	8016.50c	2.34059E-06
C	VSOP cycle 261; layer 10; total N = 4.2400759E-01					
M109	92235.50c	3.97186E-06	92236.50c	6.56084E-07	92238.50c	9.16269E-05
	93239.60c	7.77269E-09	94239.50c	3.68020E-07	94240.50c	2.09775E-07
	94241.50c	1.08987E-07	94242.50c	5.38576E-08	93237.50c	2.31650E-08
	54135.50c	5.49556E-11	36083.50c	1.69440E-08	42095.50c	2.10482E-07
	43099.50c	2.55182E-07	44101.50c	2.28071E-07	44103.50c	2.20106E-08
	45103.50c	1.15497E-07	45105.50c	3.12717E-10	46105.50c	8.35589E-08
	46108.50c	2.82556E-08	47109.50c	1.53131E-08	48000.50c	1.86710E-11
	54131.50c	1.09870E-07	55133.50c	2.74429E-07	55134.60c	1.52235E-08
	59141.50c	2.49434E-07	60143.50c	1.80601E-07	60145.50c	1.54786E-07
	61147.50c	5.80413E-08	61148.50c	4.09661E-10	62147.50c	1.17835E-08
	61149.50c	3.23060E-10	62149.50c	5.60605E-10	62150.50c	5.63833E-08
	62151.50c	2.91539E-09	62152.50c	2.76134E-08	63153.50c	1.80414E-08
	63154.50c	3.36243E-09	63155.50c	1.10358E-09	64155.50c	1.70292E-11
	64156.50c	6.02348E-09	64157.50c	7.98278E-12	5010.50c	1.17845E-07

	14000.50c 2.27413E-04	6000.50c 8.70008E-02	8016.50c 2.02884E-04
C	VSOP cycle 261; layer 11; total N = 4.2400819E-01		
M110	92235.50c 3.90697E-06	92236.50c 6.66130E-07	92238.50c 9.16021E-05
	93239.60c 1.20278E-08	94239.50c 3.63611E-07	94240.50c 2.14788E-07
	94241.50c 1.06880E-07	94242.50c 5.52571E-08	93237.50c 2.35540E-08
	54135.50c 6.04063E-11	36083.50c 1.71960E-08	42095.50c 2.13904E-07
	43099.50c 2.59453E-07	44101.50c 2.31956E-07	44103.50c 2.24784E-08
	45103.50c 1.17379E-07	45105.50c 5.13256E-10	46105.50c 8.48871E-08
	46108.50c 2.88058E-08	47109.50c 1.55978E-08	48000.50c 1.79641E-11
	54131.50c 1.11161E-07	55133.50c 2.77821E-07	55134.60c 1.55057E-08
	59141.50c 2.53618E-07	60143.50c 1.82351E-07	60145.50c 1.57342E-07
	61147.50c 5.89074E-08	61148.50c 4.59501E-10	62147.50c 1.20237E-08
	61149.50c 5.07604E-10	62149.50c 4.39833E-10	62150.50c 5.72498E-08
	62151.50c 2.81105E-09	62152.50c 2.82025E-08	63153.50c 1.83624E-08
	63154.50c 3.44325E-09	63155.50c 1.11527E-09	64155.50c 1.32659E-11
	64156.50c 6.18399E-09	64157.50c 7.32931E-12	5010.50c 7.44660E-08
	14000.50c 2.27413E-04	6000.50c 8.70008E-02	8016.50c 2.02884E-04
C	VSOP cycle 261; layer 12; total N = 4.2400879E-01		
M111	92235.50c 3.81547E-06	92236.50c 6.80299E-07	92238.50c 9.15662E-05
	93239.60c 1.75943E-08	94239.50c 3.57697E-07	94240.50c 2.22020E-07
	94241.50c 1.04161E-07	94242.50c 5.72354E-08	93237.50c 2.41186E-08
	54135.50c 6.26583E-11	36083.50c 1.75489E-08	42095.50c 2.17389E-07
	43099.50c 2.65494E-07	44101.50c 2.37464E-07	44103.50c 2.41027E-08
	45103.50c 1.19074E-07	45105.50c 7.21220E-10	46105.50c 8.68038E-08
	46108.50c 2.95948E-08	47109.50c 1.60049E-08	48000.50c 1.75525E-11
	54131.50c 1.12706E-07	55133.50c 2.82407E-07	55134.60c 1.59544E-08
	59141.50c 2.59545E-07	60143.50c 1.83970E-07	60145.50c 1.60953E-07
	61147.50c 6.02242E-08	61148.50c 5.54805E-10	62147.50c 1.22518E-08
	61149.50c 7.37100E-10	62149.50c 4.40201E-10	62150.50c 5.83444E-08
	62151.50c 2.71549E-09	62152.50c 2.89938E-08	63153.50c 1.88276E-08
	63154.50c 3.56218E-09	63155.50c 1.13461E-09	64155.50c 9.18740E-12
	64156.50c 6.41165E-09	64157.50c 7.40653E-12	5010.50c 5.86142E-08
	14000.50c 2.27413E-04	6000.50c 8.70008E-02	8016.50c 2.02884E-04
C	VSOP cycle 261; layer 13; total N = 4.2400929E-01		
M112	92235.50c 3.70312E-06	92236.50c 6.97692E-07	92238.50c 9.15208E-05
	93239.60c 2.27314E-08	94239.50c 3.51920E-07	94240.50c 2.31101E-07
	94241.50c 1.01226E-07	94242.50c 5.96801E-08	93237.50c 2.48408E-08
	54135.50c 6.34184E-11	36083.50c 1.79774E-08	42095.50c 2.21045E-07
	43099.50c 2.72947E-07	44101.50c 2.44283E-07	44103.50c 2.65368E-08
	45103.50c 1.20724E-07	45105.50c 8.88688E-10	46105.50c 8.92281E-08
	46108.50c 3.05865E-08	47109.50c 1.65149E-08	48000.50c 1.72417E-11
	54131.50c 1.14694E-07	55133.50c 2.88476E-07	55134.60c 1.65527E-08
	59141.50c 2.66870E-07	60143.50c 1.85822E-07	60145.50c 1.65399E-07
	61147.50c 6.18732E-08	61148.50c 6.52729E-10	62147.50c 1.24714E-08
	61149.50c 9.45401E-10	62149.50c 4.58897E-10	62150.50c 5.97816E-08
	62151.50c 2.65306E-09	62152.50c 2.99241E-08	63153.50c 1.94201E-08
	63154.50c 3.71591E-09	63155.50c 1.15990E-09	64155.50c 6.69552E-12
	64156.50c 6.69770E-09	64157.50c 7.54381E-12	5010.50c 5.37807E-08
	14000.50c 2.27413E-04	6000.50c 8.70008E-02	8016.50c 2.02884E-04
C	VSOP cycle 261; layer 14; total N = 4.2401019E-01		
M113	92235.50c 3.58224E-06	92236.50c 7.16378E-07	92238.50c 9.14703E-05
	93239.60c 2.57167E-08	94239.50c 3.47467E-07	94240.50c 2.41113E-07
	94241.50c 9.85758E-08	94242.50c 6.23414E-08	93237.50c 2.56466E-08
	54135.50c 6.33040E-11	36083.50c 1.84324E-08	42095.50c 2.24951E-07
	43099.50c 2.81021E-07	44101.50c 2.51700E-07	44103.50c 2.91745E-08
	45103.50c 1.22494E-07	45105.50c 9.73939E-10	46105.50c 9.19546E-08
	46108.50c 3.16866E-08	47109.50c 1.70785E-08	48000.50c 1.69892E-11

	54131.50c	1.17167E-07	55133.50c	2.95809E-07	55134.60c	1.72369E-08
	59141.50c	2.74819E-07	60143.50c	1.88195E-07	60145.50c	1.70203E-07
	61147.50c	6.36328E-08	61148.50c	7.20646E-10	62147.50c	1.26903E-08
	61149.50c	1.06723E-09	62149.50c	4.76917E-10	62150.50c	6.14806E-08
	62151.50c	2.63221E-09	62152.50c	3.08998E-08	63153.50c	2.00835E-08
	63154.50c	3.89019E-09	63155.50c	1.18778E-09	64155.50c	5.73156E-12
	64156.50c	7.01808E-09	64157.50c	7.69998E-12	5010.50c	5.60492E-08
	14000.50c	2.27413E-04	6000.50c	8.70008E-02	8016.50c	2.02884E-04
C	VSOP cycle	261; layer	15; total N =	4.2401099E-01		
M114	92235.50c	3.46218E-06	92236.50c	7.34897E-07	92238.50c	9.14186E-05
	93239.60c	2.67557E-08	94239.50c	3.44153E-07	94240.50c	2.51281E-07
	94241.50c	9.64714E-08	94242.50c	6.50255E-08	93237.50c	2.64794E-08
	54135.50c	6.27405E-11	36083.50c	1.88775E-08	42095.50c	2.29131E-07
	43099.50c	2.89099E-07	44101.50c	2.59156E-07	44103.50c	3.15829E-08
	45103.50c	1.24481E-07	45105.50c	9.94387E-10	46105.50c	9.47838E-08
	46108.50c	3.28163E-08	47109.50c	1.76550E-08	48000.50c	1.67887E-11
	54131.50c	1.20011E-07	55133.50c	3.03881E-07	55134.60c	1.79553E-08
	59141.50c	2.82790E-07	60143.50c	1.91132E-07	60145.50c	1.74998E-07
	61147.50c	6.53392E-08	61148.50c	7.57905E-10	62147.50c	1.29141E-08
	61149.50c	1.10671E-09	62149.50c	4.89569E-10	62150.50c	6.33018E-08
	62151.50c	2.63839E-09	62152.50c	3.18585E-08	63153.50c	2.07704E-08
	63154.50c	4.07294E-09	63155.50c	1.21606E-09	64155.50c	5.55936E-12
	64156.50c	7.35220E-09	64157.50c	7.85537E-12	5010.50c	6.24007E-08
	14000.50c	2.27413E-04	6000.50c	8.70008E-02	8016.50c	2.02884E-04
C	VSOP cycle	261; layer	16; total N =	4.2401180E-01		
M115	92235.50c	3.35198E-06	92236.50c	7.51854E-07	92238.50c	9.13691E-05
	93239.60c	2.58797E-08	94239.50c	3.42508E-07	94240.50c	2.60814E-07
	94241.50c	9.50020E-08	94242.50c	6.75344E-08	93237.50c	2.72828E-08
	54135.50c	6.18879E-11	36083.50c	1.92799E-08	42095.50c	2.33566E-07
	43099.50c	2.96572E-07	44101.50c	2.66086E-07	44103.50c	3.33666E-08
	45103.50c	1.26748E-07	45105.50c	9.47973E-10	46105.50c	9.75280E-08
	46108.50c	3.38894E-08	47109.50c	1.82006E-08	48000.50c	1.66595E-11
	54131.50c	1.23055E-07	55133.50c	3.12099E-07	55134.60c	1.86489E-08
	59141.50c	2.90181E-07	60143.50c	1.94590E-07	60145.50c	1.79421E-07
	61147.50c	6.68409E-08	61148.50c	7.64716E-10	62147.50c	1.31482E-08
	61149.50c	1.05898E-09	62149.50c	5.02277E-10	62150.50c	6.50966E-08
	62151.50c	2.66277E-09	62152.50c	3.27368E-08	63153.50c	2.14283E-08
	63154.50c	4.25043E-09	63155.50c	1.24263E-09	64155.50c	5.90809E-12
	64156.50c	7.67492E-09	64157.50c	8.02495E-12	5010.50c	7.37780E-08
	14000.50c	2.27413E-04	6000.50c	8.70008E-02	8016.50c	2.02884E-04
C	VSOP cycle	261; layer	17; total N =	4.2401239E-01		
M116	92235.50c	3.25703E-06	92236.50c	7.66422E-07	92238.50c	9.13237E-05
	93239.60c	2.39147E-08	94239.50c	3.43015E-07	94240.50c	2.69205E-07
	94241.50c	9.40886E-08	94242.50c	6.97298E-08	93237.50c	2.80368E-08
	54135.50c	6.08801E-11	36083.50c	1.96214E-08	42095.50c	2.38198E-07
	43099.50c	3.03050E-07	44101.50c	2.72127E-07	44103.50c	3.43177E-08
	45103.50c	1.29299E-07	45105.50c	8.53030E-10	46105.50c	1.00037E-07
	46108.50c	3.48443E-08	47109.50c	1.86839E-08	48000.50c	1.66162E-11
	54131.50c	1.26095E-07	55133.50c	3.19898E-07	55134.60c	1.92819E-08
	59141.50c	2.96611E-07	60143.50c	1.98414E-07	60145.50c	1.83245E-07
	61147.50c	6.80446E-08	61148.50c	7.51893E-10	62147.50c	1.33947E-08
	61149.50c	9.48003E-10	62149.50c	5.16133E-10	62150.50c	6.67420E-08
	62151.50c	2.69728E-09	62152.50c	3.34875E-08	63153.50c	2.20241E-08
	63154.50c	4.41407E-09	63155.50c	1.26645E-09	64155.50c	6.69059E-12
	64156.50c	7.96669E-09	64157.50c	8.23365E-12	5010.50c	9.13299E-08
	14000.50c	2.27413E-04	6000.50c	8.70008E-02	8016.50c	2.02884E-04
C	VSOP cycle	261; layer	18; total N =	4.2401290E-01		

M117	92235.50c	3.18168E-06	92236.50c	7.78013E-07	92238.50c	9.12843E-05
	93239.60c	2.09997E-08	94239.50c	3.44249E-07	94240.50c	2.73802E-07
	94241.50c	9.65338E-08	94242.50c	7.15905E-08	93237.50c	2.86601E-08
	54135.50c	6.31163E-11	36083.50c	1.98928E-08	42095.50c	2.42958E-07
	43099.50c	3.08306E-07	44101.50c	2.77065E-07	44103.50c	3.43923E-08
	45103.50c	1.31913E-07	45105.50c	7.33931E-10	46105.50c	1.02227E-07
	46108.50c	3.56668E-08	47109.50c	1.90996E-08	48000.50c	1.71947E-11
	54131.50c	1.28947E-07	55133.50c	3.26863E-07	55134.60c	1.98140E-08
	59141.50c	3.01845E-07	60143.50c	2.02456E-07	60145.50c	1.86338E-07
	61147.50c	6.89202E-08	61148.50c	6.91410E-10	62147.50c	1.36565E-08
	61149.50c	8.05996E-10	62149.50c	5.69800E-10	62150.50c	6.81381E-08
	62151.50c	2.77326E-09	62152.50c	3.40548E-08	63153.50c	2.25379E-08
	63154.50c	4.54699E-09	63155.50c	1.29282E-09	64155.50c	8.35935E-12
	64156.50c	8.21211E-09	64157.50c	9.38945E-12	5010.50c	1.19684E-07
	14000.50c	2.27413E-04	6000.50c	8.70008E-02	8016.50c	2.02884E-04
C	VSOP cycle	261; layer	19; total N =	4.2401350E-01		
M118	92235.50c	3.11759E-06	92236.50c	7.87701E-07	92238.50c	9.12513E-05
	93239.60c	1.76288E-08	94239.50c	3.49643E-07	94240.50c	2.78881E-07
	94241.50c	9.58725E-08	94242.50c	7.30738E-08	93237.50c	2.92690E-08
	54135.50c	5.42900E-11	36083.50c	2.01124E-08	42095.50c	2.47749E-07
	43099.50c	3.12619E-07	44101.50c	2.81124E-07	44103.50c	3.37334E-08
	45103.50c	1.34862E-07	45105.50c	5.92464E-10	46105.50c	1.04030E-07
	46108.50c	3.63065E-08	47109.50c	1.94156E-08	48000.50c	1.63757E-11
	54131.50c	1.31494E-07	55133.50c	3.32803E-07	55134.60c	2.02639E-08
	59141.50c	3.06168E-07	60143.50c	2.06293E-07	60145.50c	1.88884E-07
	61147.50c	6.95387E-08	61148.50c	6.80266E-10	62147.50c	1.39293E-08
	61149.50c	6.53429E-10	62149.50c	5.09383E-10	62150.50c	6.93824E-08
	62151.50c	2.75217E-09	62152.50c	3.45894E-08	63153.50c	2.29625E-08
	63154.50c	4.66922E-09	63155.50c	1.30953E-09	64155.50c	9.21065E-12
	64156.50c	8.42520E-09	64157.50c	7.57218E-12	5010.50c	1.47687E-07
	14000.50c	2.27413E-04	6000.50c	8.70008E-02	8016.50c	2.02884E-04
C	VSOP cycle	261; layer	20; total N =	7.3386878E-01		
M119	92235.50c	7.95072E-06	92236.50c	1.29511E-06	92238.50c	1.81968E-04
	93239.60c	1.43936E-08	94239.50c	7.37664E-07	94240.50c	4.10737E-07
	94241.50c	2.19564E-07	94242.50c	1.05179E-07	93237.50c	4.56119E-08
	54135.50c	1.05204E-10	36083.50c	3.34547E-08	42095.50c	4.15745E-07
	43099.50c	5.02976E-07	44101.50c	4.49383E-07	44103.50c	4.26355E-08
	45103.50c	2.28318E-07	45105.50c	4.30118E-10	46105.50c	1.64553E-07
	46108.50c	5.54821E-08	47109.50c	3.00841E-08	48000.50c	3.85076E-11
	54131.50c	2.17275E-07	55133.50c	5.42250E-07	55134.60c	2.98958E-08
	59141.50c	4.91624E-07	60143.50c	3.58006E-07	60145.50c	3.05170E-07
	61147.50c	1.14551E-07	61148.50c	7.97393E-10	62147.50c	2.32287E-08
	61149.50c	4.62327E-10	62149.50c	1.36386E-09	62150.50c	1.10991E-07
	62151.50c	5.90405E-09	62152.50c	5.42800E-08	63153.50c	3.54931E-08
	63154.50c	6.58361E-09	63155.50c	2.18005E-09	64155.50c	3.92018E-11
	64156.50c	1.17790E-08	64157.50c	1.97876E-11	5010.50c	5.03683E-07
	14000.50c	4.51608E-04	6000.50c	8.62698E-02	8016.50c	4.02897E-04
C	VSOP cycle	261; layer	21; total N =	7.3386961E-01		
M120	92235.50c	7.86961E-06	92236.50c	1.30795E-06	92238.50c	1.81922E-04
	93239.60c	2.25011E-08	94239.50c	7.41727E-07	94240.50c	4.12554E-07
	94241.50c	2.22274E-07	94242.50c	1.06954E-07	93237.50c	4.63581E-08
	54135.50c	1.23677E-10	36083.50c	3.37715E-08	42095.50c	4.22386E-07
	43099.50c	5.08284E-07	44101.50c	4.54287E-07	44103.50c	4.16756E-08
	45103.50c	2.31883E-07	45105.50c	6.81811E-10	46105.50c	1.66330E-07
	46108.50c	5.62083E-08	47109.50c	3.04531E-08	48000.50c	3.83995E-11
	54131.50c	2.19331E-07	55133.50c	5.47205E-07	55134.60c	3.03358E-08
	59141.50c	4.96924E-07	60143.50c	3.61757E-07	60145.50c	3.08360E-07

	61147.50c 1.15299E-07	61148.50c 8.75434E-10	62147.50c 2.37131E-08
	61149.50c 6.71210E-10	62149.50c 1.08824E-09	62150.50c 1.12278E-07
	62151.50c 5.85034E-09	62152.50c 5.48826E-08	63153.50c 3.59779E-08
	63154.50c 6.69977E-09	63155.50c 2.20916E-09	64155.50c 3.82194E-11
	64156.50c 1.19811E-08	64157.50c 1.88527E-11	5010.50c 3.11355E-07
	14000.50c 4.51608E-04	6000.50c 8.62698E-02	8016.50c 4.02897E-04
C	VSOP cycle 261; layer 22; total N = 7.3387039E-01		
M121	92235.50c 7.75469E-06	92236.50c 1.32620E-06	92238.50c 1.81854E-04
	93239.60c 3.32958E-08	94239.50c 7.47395E-07	94240.50c 4.15754E-07
	94241.50c 2.26271E-07	94242.50c 1.09588E-07	93237.50c 4.74317E-08
	54135.50c 1.36034E-10	36083.50c 3.42234E-08	42095.50c 4.28936E-07
	43099.50c 5.15910E-07	44101.50c 4.61348E-07	44103.50c 4.24788E-08
	45103.50c 2.34844E-07	45105.50c 9.93955E-10	46105.50c 1.68943E-07
	46108.50c 5.72873E-08	47109.50c 3.10039E-08	48000.50c 3.88587E-11
	54131.50c 2.21414E-07	55133.50c 5.53211E-07	55134.60c 3.10501E-08
	59141.50c 5.04535E-07	60143.50c 3.64980E-07	60145.50c 3.12931E-07
	61147.50c 1.16602E-07	61148.50c 1.02198E-09	62147.50c 2.41740E-08
	61149.50c 9.95580E-10	62149.50c 1.03881E-09	62150.50c 1.13799E-07
	62151.50c 5.82719E-09	62152.50c 5.57120E-08	63153.50c 3.66839E-08
	63154.50c 6.87023E-09	63155.50c 2.25815E-09	64155.50c 3.30662E-11
	64156.50c 1.22724E-08	64157.50c 1.98204E-11	5010.50c 2.27025E-07
	14000.50c 4.51608E-04	6000.50c 8.62698E-02	8016.50c 4.02897E-04
C	VSOP cycle 261; layer 23; total N = 7.3387140E-01		
M122	92235.50c 7.61049E-06	92236.50c 1.34912E-06	92238.50c 1.81765E-04
	93239.60c 4.38786E-08	94239.50c 7.55627E-07	94240.50c 4.20562E-07
	94241.50c 2.31607E-07	94242.50c 1.13098E-07	93237.50c 4.87981E-08
	54135.50c 1.45254E-10	36083.50c 3.47938E-08	42095.50c 4.35554E-07
	43099.50c 5.25646E-07	44101.50c 4.70393E-07	44103.50c 4.47606E-08
	45103.50c 2.37393E-07	45105.50c 1.29214E-09	46105.50c 1.72411E-07
	46108.50c 5.87232E-08	47109.50c 3.17411E-08	48000.50c 3.97908E-11
	54131.50c 2.23916E-07	55133.50c 5.61031E-07	55134.60c 3.20195E-08
	59141.50c 5.14248E-07	60143.50c 3.68262E-07	60145.50c 3.18748E-07
	61147.50c 1.18396E-07	61148.50c 1.16396E-09	62147.50c 2.46152E-08
	61149.50c 1.32872E-09	62149.50c 1.11393E-09	62150.50c 1.15756E-07
	62151.50c 5.86378E-09	62152.50c 5.67334E-08	63153.50c 3.75995E-08
	63154.50c 7.09158E-09	63155.50c 2.32576E-09	64155.50c 2.74284E-11
	64156.50c 1.26482E-08	64157.50c 2.14518E-11	5010.50c 1.89435E-07
	14000.50c 4.51608E-04	6000.50c 8.62698E-02	8016.50c 4.02897E-04
C	VSOP cycle 261; layer 24; total N = 7.3387212E-01		
M123	92235.50c 7.45706E-06	92236.50c 1.37352E-06	92238.50c 1.81668E-04
	93239.60c 4.96643E-08	94239.50c 7.68056E-07	94240.50c 4.26548E-07
	94241.50c 2.37663E-07	94242.50c 1.17079E-07	93237.50c 5.02924E-08
	54135.50c 1.51179E-10	36083.50c 3.54035E-08	42095.50c 4.42377E-07
	43099.50c 5.36202E-07	44101.50c 4.80240E-07	44103.50c 4.74859E-08
	45103.50c 2.39936E-07	45105.50c 1.44297E-09	46105.50c 1.76422E-07
	46108.50c 6.03505E-08	47109.50c 3.25803E-08	48000.50c 4.09757E-11
	54131.50c 2.27033E-07	55133.50c 5.70574E-07	55134.60c 3.31077E-08
	59141.50c 5.24783E-07	60143.50c 3.72188E-07	60145.50c 3.25032E-07
	61147.50c 1.20348E-07	61148.50c 1.24776E-09	62147.50c 2.50523E-08
	61149.50c 1.50827E-09	62149.50c 1.22452E-09	62150.50c 1.18100E-07
	62151.50c 5.97424E-09	62152.50c 5.78127E-08	63153.50c 3.86146E-08
	63154.50c 7.33723E-09	63155.50c 2.40181E-09	64155.50c 2.43773E-11
	64156.50c 1.30644E-08	64157.50c 2.32701E-11	5010.50c 1.87163E-07
	14000.50c 4.51608E-04	6000.50c 8.62698E-02	8016.50c 4.02897E-04
C	VSOP cycle 261; layer 25; total N = 7.3387319E-01		
M124	92235.50c 7.30502E-06	92236.50c 1.39768E-06	92238.50c 1.81567E-04
	93239.60c 5.17432E-08	94239.50c 7.81923E-07	94240.50c 4.33275E-07

	94241.50c 2.44086E-07	94242.50c 1.21277E-07	93237.50c 5.18116E-08
	54135.50c 1.55356E-10	36083.50c 3.60103E-08	42095.50c 4.49448E-07
	43099.50c 5.46867E-07	44101.50c 4.90231E-07	44103.50c 5.01044E-08
	45103.50c 2.42670E-07	45105.50c 1.50259E-09	46105.50c 1.80675E-07
	46108.50c 6.20657E-08	47109.50c 3.34680E-08	48000.50c 4.22262E-11
	54131.50c 2.30654E-07	55133.50c 5.81171E-07	55134.60c 3.42328E-08
	59141.50c 5.35431E-07	60143.50c 3.76832E-07	60145.50c 3.31359E-07
	61147.50c 1.22286E-07	61148.50c 1.28531E-09	62147.50c 2.54942E-08
	61149.50c 1.57151E-09	62149.50c 1.31254E-09	62150.50c 1.20659E-07
	62151.50c 6.12453E-09	62152.50c 5.88924E-08	63153.50c 3.96618E-08
	63154.50c 7.59077E-09	63155.50c 2.48035E-09	64155.50c 2.35388E-11
	64156.50c 1.34968E-08	64157.50c 2.50492E-11	5010.50c 1.98107E-07
	14000.50c 4.51608E-04	6000.50c 8.62698E-02	8016.50c 4.02897E-04
C	VSOP cycle 261; layer 26;	total N = 7.3387408E-01	
M125	92235.50c 7.16216E-06	92236.50c 1.42033E-06	92238.50c 1.81471E-04
	93239.60c 5.04060E-08	94239.50c 7.95376E-07	94240.50c 4.40116E-07
	94241.50c 2.50649E-07	94242.50c 1.25466E-07	93237.50c 5.32558E-08
	54135.50c 1.57764E-10	36083.50c 3.65826E-08	42095.50c 4.56765E-07
	43099.50c 5.57082E-07	44101.50c 4.99838E-07	44103.50c 5.22096E-08
	45103.50c 2.45706E-07	45105.50c 1.48395E-09	46105.50c 1.84940E-07
	46108.50c 6.37734E-08	47109.50c 3.43538E-08	48000.50c 4.34203E-11
	54131.50c 2.34599E-07	55133.50c 5.92147E-07	55134.60c 3.53183E-08
	59141.50c 5.45629E-07	60143.50c 3.82100E-07	60145.50c 3.37397E-07
	61147.50c 1.24085E-07	61148.50c 1.28396E-09	62147.50c 2.59484E-08
	61149.50c 1.53772E-09	62149.50c 1.38410E-09	62150.50c 1.23249E-07
	62151.50c 6.29082E-09	62152.50c 5.99308E-08	63153.50c 4.06815E-08
	63154.50c 7.83642E-09	63155.50c 2.55623E-09	64155.50c 2.43285E-11
	64156.50c 1.39243E-08	64157.50c 2.66539E-11	5010.50c 2.19848E-07
	14000.50c 4.51608E-04	6000.50c 8.62698E-02	8016.50c 4.02897E-04
C	VSOP cycle 261; layer 27;	total N = 7.3387527E-01	
M126	92235.50c 7.03337E-06	92236.50c 1.44069E-06	92238.50c 1.81381E-04
	93239.60c 4.71475E-08	94239.50c 8.07961E-07	94240.50c 4.46604E-07
	94241.50c 2.57020E-07	94242.50c 1.29447E-07	93237.50c 5.45896E-08
	54135.50c 1.58511E-10	36083.50c 3.70995E-08	42095.50c 4.64279E-07
	43099.50c 5.66441E-07	44101.50c 5.08675E-07	44103.50c 5.35403E-08
	45103.50c 2.49091E-07	45105.50c 1.40195E-09	46105.50c 1.89026E-07
	46108.50c 6.53920E-08	47109.50c 3.51936E-08	48000.50c 4.45192E-11
	54131.50c 2.38650E-07	55133.50c 6.02901E-07	55134.60c 3.63214E-08
	59141.50c 5.54980E-07	60143.50c 3.87797E-07	60145.50c 3.42914E-07
	61147.50c 1.25648E-07	61148.50c 1.26342E-09	62147.50c 2.64188E-08
	61149.50c 1.43137E-09	62149.50c 1.44446E-09	62150.50c 1.25719E-07
	62151.50c 6.45777E-09	62152.50c 6.08851E-08	63153.50c 4.16353E-08
	63154.50c 8.06583E-09	63155.50c 2.62593E-09	64155.50c 2.63789E-11
	64156.50c 1.43287E-08	64157.50c 2.81046E-11	5010.50c 2.53002E-07
	14000.50c 4.51608E-04	6000.50c 8.62698E-02	8016.50c 4.02897E-04
C	VSOP cycle 261; layer 28;	total N = 7.3387587E-01	
M127	92235.50c 6.92228E-06	92236.50c 1.45821E-06	92238.50c 1.81300E-04
	93239.60c 4.28177E-08	94239.50c 8.20965E-07	94240.50c 4.52414E-07
	94241.50c 2.62798E-07	94242.50c 1.33023E-07	93237.50c 5.58087E-08
	54135.50c 1.57136E-10	36083.50c 3.75452E-08	42095.50c 4.71920E-07
	43099.50c 5.74606E-07	44101.50c 5.16423E-07	44103.50c 5.39082E-08
	45103.50c 2.52842E-07	45105.50c 1.26208E-09	46105.50c 1.92764E-07
	46108.50c 6.68451E-08	47109.50c 3.59458E-08	48000.50c 4.54940E-11
	54131.50c 2.42603E-07	55133.50c 6.12940E-07	55134.60c 3.72130E-08
	59141.50c 5.63159E-07	60143.50c 3.93713E-07	60145.50c 3.47718E-07
	61147.50c 1.26888E-07	61148.50c 1.23619E-09	62147.50c 2.69067E-08
	61149.50c 1.26772E-09	62149.50c 1.50098E-09	62150.50c 1.27950E-07

	62151.50c 6.61658E-09	62152.50c 6.17111E-08	63153.50c 4.24936E-08
	63154.50c 8.27412E-09	63155.50c 2.68674E-09	64155.50c 2.96326E-11
	64156.50c 1.46931E-08	64157.50c 2.93847E-11	5010.50c 3.03030E-07
	14000.50c 4.51603E-04	6000.50c 8.62698E-02	8016.50c 4.02897E-04
C	VSOP cycle 261; layer	29; total N = 7.3387688E-01	
M128	92235.50c 6.82638E-06	92236.50c 1.47328E-06	92238.50c 1.81227E-04
	93239.60c 3.83949E-08	94239.50c 8.34114E-07	94240.50c 4.57764E-07
	94241.50c 2.67497E-07	94242.50c 1.36187E-07	93237.50c 5.69345E-08
	54135.50c 1.52139E-10	36083.50c 3.79278E-08	42095.50c 4.79601E-07
	43099.50c 5.81687E-07	44101.50c 5.23170E-07	44103.50c 5.34617E-08
	45103.50c 2.56877E-07	45105.50c 1.11900E-09	46105.50c 1.96101E-07
	46108.50c 6.81285E-08	47109.50c 3.66072E-08	48000.50c 4.60232E-11
	54131.50c 2.46288E-07	55133.50c 6.21971E-07	55134.60c 3.79983E-08
	59141.50c 5.70276E-07	60143.50c 3.99548E-07	60145.50c 3.51881E-07
	61147.50c 1.27840E-07	61148.50c 1.20939E-09	62147.50c 2.74100E-08
	61149.50c 1.10509E-09	62149.50c 1.51442E-09	62150.50c 1.29942E-07
	62151.50c 6.74413E-09	62152.50c 6.24315E-08	63153.50c 4.32592E-08
	63154.50c 8.46390E-09	63155.50c 2.73814E-09	64155.50c 3.34629E-11
	64156.50c 1.50193E-08	64157.50c 2.97751E-11	5010.50c 3.61695E-07
	14000.50c 4.51608E-04	6000.50c 8.62698E-02	8016.50c 4.02897E-04
C	VSOP cycle 261; layer	30; total N = 7.3387718E-01	
M129	92235.50c 6.74810E-06	92236.50c 1.48553E-06	92238.50c 1.81169E-04
	93239.60c 3.11881E-08	94239.50c 8.45678E-07	94240.50c 4.62299E-07
	94241.50c 2.71325E-07	94242.50c 1.38858E-07	93237.50c 5.78279E-08
	54135.50c 1.45442E-10	36083.50c 3.82399E-08	42095.50c 4.87267E-07
	43099.50c 5.87538E-07	44101.50c 5.28753E-07	44103.50c 5.21475E-08
	45103.50c 2.61147E-07	45105.50c 9.42580E-10	46105.50c 1.98972E-07
	46108.50c 6.92075E-08	47109.50c 3.71637E-08	48000.50c 4.64230E-11
	54131.50c 2.49675E-07	55133.50c 6.29912E-07	55134.60c 3.85977E-08
	59141.50c 5.76148E-07	60143.50c 4.05190E-07	60145.50c 3.55313E-07
	61147.50c 1.28525E-07	61148.50c 1.13185E-09	62147.50c 2.79356E-08
	61149.50c 9.11300E-10	62149.50c 1.53931E-09	62150.50c 1.31623E-07
	62151.50c 6.84761E-09	62152.50c 6.30500E-08	63153.50c 4.38884E-08
	63154.50c 8.61767E-09	63155.50c 2.77722E-09	64155.50c 3.84686E-11
	64156.50c 1.52960E-08	64157.50c 2.99803E-11	5010.50c 4.52713E-07
	14000.50c 4.51608E-04	6000.50c 8.62698E-02	8016.50c 4.02897E-04
C	VSOP cycle 261; layer	31; total N = 7.3386890E-01	
M130	92235.50c 7.95784E-06	92236.50c 1.29400E-06	92238.50c 1.81972E-04
	93239.60c 1.30156E-08	94239.50c 7.38860E-07	94240.50c 4.10613E-07
	94241.50c 2.19301E-07	94242.50c 1.05022E-07	93237.50c 4.55680E-08
	54135.50c 9.95483E-11	36083.50c 3.34266E-08	42095.50c 4.15744E-07
	43099.50c 5.02505E-07	44101.50c 4.48954E-07	44103.50c 4.23158E-08
	45103.50c 2.28409E-07	45105.50c 3.72010E-10	46105.50c 1.64438E-07
	46108.50c 5.54194E-08	47109.50c 3.00518E-08	48000.50c 3.86044E-11
	54131.50c 2.17270E-07	55133.50c 5.42119E-07	55134.60c 2.98526E-08
	59141.50c 4.91161E-07	60143.50c 3.58091E-07	60145.50c 3.04888E-07
	61147.50c 1.14426E-07	61148.50c 7.79751E-10	62147.50c 2.32328E-08
	61149.50c 4.07308E-10	62149.50c 1.42529E-09	62150.50c 1.10877E-07
	62151.50c 5.91914E-09	62152.50c 5.42189E-08	63153.50c 3.54559E-08
	63154.50c 6.57526E-09	63155.50c 2.17664E-09	64155.50c 4.04506E-11
	64156.50c 1.17617E-08	64157.50c 2.02350E-11	5010.50c 1.02196E-06
	14000.50c 4.51608E-04	6000.50c 8.62699E-02	8016.50c 4.02898E-04
C	VSOP cycle 261; layer	32; total N = 7.3386949E-01	
M131	92235.50c 7.89054E-06	92236.50c 1.30466E-06	92238.50c 1.81932E-04
	93239.60c 1.94107E-08	94239.50c 7.44059E-07	94240.50c 4.12145E-07
	94241.50c 2.21497E-07	94242.50c 1.06481E-07	93237.50c 4.62194E-08
	54135.50c 1.18389E-10	36083.50c 3.36888E-08	42095.50c 4.22352E-07

	43099.50c 5.06893E-07	44101.50c 4.53014E-07	44103.50c 4.07592E-08
	45103.50c 2.32123E-07	45105.50c 5.66357E-10	46105.50c 1.65934E-07
	46108.50c 5.60195E-08	47109.50c 3.03559E-08	48000.50c 3.85240E-11
	54131.50c 2.19236E-07	55133.50c 5.46605E-07	55134.60c 3.02034E-08
	59141.50c 4.95554E-07	60143.50c 3.61904E-07	60145.50c 3.07526E-07
	61147.50c 1.14936E-07	61148.50c 8.31214E-10	62147.50c 2.37249E-08
	61149.50c 5.54093E-10	62149.50c 1.14758E-09	62150.50c 1.12013E-07
	62151.50c 5.87844E-09	62152.50c 5.47091E-08	63153.50c 3.58648E-08
	63154.50c 6.67396E-09	63155.50c 2.19894E-09	64155.50c 4.14735E-11
	64156.50c 1.19296E-08	64157.50c 1.91623E-11	5010.50c 6.38926E-07
	14000.50c 4.51608E-04	6000.50c 8.62699E-02	8016.50c 4.02898E-04
C	VSOP cycle 261; layer 33; total N = 7.3387033E-01		
M132	92235.50c 7.79111E-06	92236.50c 1.32046E-06	92238.50c 1.81872E-04
	93239.60c 2.91607E-08	94239.50c 7.49575E-07	94240.50c 4.14962E-07
	94241.50c 2.24926E-07	94242.50c 1.08736E-07	93237.50c 4.71663E-08
	54135.50c 1.32890E-10	36083.50c 3.40799E-08	42095.50c 4.28812E-07
	43099.50c 5.13478E-07	44101.50c 4.59113E-07	44103.50c 4.09344E-08
	45103.50c 2.35202E-07	45105.50c 8.61470E-10	46105.50c 1.68184E-07
	46108.50c 5.69485E-08	47109.50c 3.08304E-08	48000.50c 3.89208E-11
	54131.50c 2.21113E-07	55133.50c 5.51817E-07	55134.60c 3.08054E-08
	59141.50c 5.02132E-07	60143.50c 3.65034E-07	60145.50c 3.11475E-07
	61147.50c 1.15983E-07	61148.50c 9.61226E-10	62147.50c 2.41946E-08
	61149.50c 8.48215E-10	62149.50c 1.04086E-09	62150.50c 1.13365E-07
	62151.50c 5.85293E-09	62152.50c 5.54238E-08	63153.50c 3.64771E-08
	63154.50c 6.82219E-09	63155.50c 2.24005E-09	64155.50c 3.72441E-11
	64156.50c 1.21817E-08	64157.50c 1.98974E-11	5010.50c 4.34333E-07
	14000.50c 4.51608E-04	6000.50c 8.62699E-02	8016.50c 4.02898E-04
C	VSOP cycle 261; layer 34; total N = 7.3387110E-01		
M133	92235.50c 7.66166E-06	92236.50c 1.34106E-06	92238.50c 1.81793E-04
	93239.60c 3.91538E-08	94239.50c 7.56543E-07	94240.50c 4.19329E-07
	94241.50c 2.29716E-07	94242.50c 1.11850E-07	93237.50c 4.83831E-08
	54135.50c 1.43384E-10	36083.50c 3.45929E-08	42095.50c 4.35279E-07
	43099.50c 5.22211E-07	44101.50c 4.67216E-07	44103.50c 4.26626E-08
	45103.50c 2.37806E-07	45105.50c 1.16131E-09	46105.50c 1.71282E-07
	46108.50c 5.82290E-08	47109.50c 3.14900E-08	48000.50c 3.97754E-11
	54131.50c 2.23329E-07	55133.50c 5.58679E-07	55134.60c 3.16503E-08
	59141.50c 5.10838E-07	60143.50c 3.68069E-07	60145.50c 3.16692E-07
	61147.50c 1.17549E-07	61148.50c 1.09568E-09	62147.50c 2.46446E-08
	61149.50c 1.17169E-09	62149.50c 1.09395E-09	62150.50c 1.15087E-07
	62151.50c 5.87688E-09	62152.50c 5.63468E-08	63153.50c 3.72914E-08
	63154.50c 7.01851E-09	63155.50c 2.29979E-09	64155.50c 3.12483E-11
	64156.50c 1.25176E-08	64157.50c 2.14284E-11	5010.50c 3.38636E-07
	14000.50c 4.51608E-04	6000.50c 8.62699E-02	8016.50c 4.02898E-04
C	VSOP cycle 261; layer 35; total N = 7.3387200E-01		
M134	92235.50c 7.52227E-06	92236.50c 1.36325E-06	92238.50c 1.81705E-04
	93239.60c 4.47900E-08	94239.50c 7.67610E-07	94240.50c 4.24787E-07
	94241.50c 2.35221E-07	94242.50c 1.15409E-07	93237.50c 4.97251E-08
	54135.50c 1.49654E-10	36083.50c 3.51483E-08	42095.50c 4.41895E-07
	43099.50c 5.31783E-07	44101.50c 4.76133E-07	44103.50c 4.48916E-08
	45103.50c 2.40352E-07	45105.50c 1.31023E-09	46105.50c 1.74923E-07
	46108.50c 5.96923E-08	47109.50c 3.22469E-08	48000.50c 4.08998E-11
	54131.50c 2.26111E-07	55133.50c 5.67208E-07	55134.60c 3.26105E-08
	59141.50c 5.20384E-07	60143.50c 3.71645E-07	60145.50c 3.22392E-07
	61147.50c 1.19288E-07	61148.50c 1.17972E-09	62147.50c 2.50896E-08
	61149.50c 1.34606E-09	62149.50c 1.20655E-09	62150.50c 1.17159E-07
	62151.50c 5.97319E-09	62152.50c 5.73313E-08	63153.50c 3.82027E-08
	63154.50c 7.23820E-09	63155.50c 2.36798E-09	64155.50c 2.75784E-11

	64156.50c 1.28919E-08	64157.50c 2.32032E-11	5010.50c 3.21087E-07
	14000.50c 4.51608E-04	6000.50c 8.62699E-02	8016.50c 4.02898E-04
C	VSOP cycle 261; layer	36; total N = 7.3387271E-01	
M135	92235.50c 7.38410E-06	92236.50c 1.38524E-06	92238.50c 1.81613E-04
	93239.60c 4.68565E-08	94239.50c 7.80760E-07	94240.50c 4.30895E-07
	94241.50c 2.41050E-07	94242.50c 1.19145E-07	93237.50c 5.10959E-08
	54135.50c 1.53859E-10	36083.50c 3.57012E-08	42095.50c 4.48707E-07
	43099.50c 5.41441E-07	44101.50c 4.85166E-07	44103.50c 4.70362E-08
	45103.50c 2.43051E-07	45105.50c 1.36187E-09	46105.50c 1.78787E-07
	46108.50c 6.12289E-08	47109.50c 3.30441E-08	48000.50c 4.21095E-11
	54131.50c 2.29371E-07	55133.50c 5.76763E-07	55134.60c 3.36046E-08
	59141.50c 5.30021E-07	60143.50c 3.75883E-07	60145.50c 3.28123E-07
	61147.50c 1.21010E-07	61148.50c 1.21974E-09	62147.50c 2.55386E-08
	61149.50c 1.40255E-09	62149.50c 1.30066E-09	62150.50c 1.19433E-07
	62151.50c 6.11060E-09	62152.50c 5.83096E-08	63153.50c 3.91428E-08
	63154.50c 7.46509E-09	63155.50c 2.43846E-09	64155.50c 2.63211E-11
	64156.50c 1.32786E-08	64157.50c 2.49625E-11	5010.50c 3.30937E-07
	14000.50c 4.51608E-04	6000.50c 8.62699E-02	8016.50c 4.02898E-04
C	VSOP cycle 261; layer	37; total N = 7.3387378E-01	
M136	92235.50c 7.25620E-06	92236.50c 1.40557E-06	92238.50c 1.81526E-04
	93239.60c 4.55264E-08	94239.50c 7.94893E-07	94240.50c 4.37026E-07
	94241.50c 2.46886E-07	94242.50c 1.22791E-07	93237.50c 5.24010E-08
	54135.50c 1.55966E-10	36083.50c 3.62147E-08	42095.50c 4.55712E-07
	43099.50c 5.50532E-07	44101.50c 4.93704E-07	44103.50c 4.86235E-08
	45103.50c 2.46038E-07	45105.50c 1.32320E-09	46105.50c 1.82616E-07
	46108.50c 6.27291E-08	47109.50c 3.38241E-08	48000.50c 4.32978E-11
	54131.50c 2.32927E-07	55133.50c 5.86642E-07	55134.60c 3.45529E-08
	59141.50c 5.39099E-07	60143.50c 3.80720E-07	60145.50c 3.33502E-07
	61147.50c 1.22561E-07	61148.50c 1.22122E-09	62147.50c 2.59994E-08
	61149.50c 1.35257E-09	62149.50c 1.38240E-09	62150.50c 1.21712E-07
	62151.50c 6.26729E-09	62152.50c 5.92256E-08	63153.50c 4.00467E-08
	63154.50c 7.68310E-09	63155.50c 2.50558E-09	64155.50c 2.70821E-11
	64156.50c 1.36529E-08	64157.50c 2.66039E-11	5010.50c 3.64676E-07
	14000.50c 4.51608E-04	6000.50c 8.62699E-02	8016.50c 4.02898E-04
C	VSOP cycle 261; layer	38; total N = 7.3387462E-01	
M137	92235.50c 7.14163E-06	92236.50c 1.42374E-06	92238.50c 1.81445E-04
	93239.60c 4.23959E-08	94239.50c 8.08409E-07	94240.50c 4.42846E-07
	94241.50c 2.52502E-07	94242.50c 1.26216E-07	93237.50c 5.36013E-08
	54135.50c 1.56410E-10	36083.50c 3.66759E-08	42095.50c 4.62861E-07
	43099.50c 5.58802E-07	44101.50c 5.01499E-07	44103.50c 4.95057E-08
	45103.50c 2.49325E-07	45105.50c 1.23902E-09	46105.50c 1.86245E-07
	46108.50c 6.41381E-08	47109.50c 3.45577E-08	48000.50c 4.43995E-11
	54131.50c 2.36561E-07	55133.50c 5.96250E-07	55134.60c 3.54192E-08
	59141.50c 5.47363E-07	60143.50c 3.85928E-07	60145.50c 3.38382E-07
	61147.50c 1.23890E-07	61148.50c 1.20010E-09	62147.50c 2.64749E-08
	61149.50c 1.24750E-09	62149.50c 1.44430E-09	62150.50c 1.23871E-07
	62151.50c 6.42279E-09	62152.50c 6.00591E-08	63153.50c 4.08850E-08
	63154.50c 7.88508E-09	63155.50c 2.56677E-09	64155.50c 2.92424E-11
	64156.50c 1.40032E-08	64157.50c 2.80712E-11	5010.50c 4.14416E-07
	14000.50c 4.51608E-04	6000.50c 8.62699E-02	8016.50c 4.02898E-04
C	VSOP cycle 261; layer	39; total N = 7.3387557E-01	
M138	92235.50c 7.04327E-06	92236.50c 1.43931E-06	92238.50c 1.81372E-04
	93239.60c 3.87064E-08	94239.50c 8.22685E-07	94240.50c 4.48072E-07
	94241.50c 2.57546E-07	94242.50c 1.29254E-07	93237.50c 5.47132E-08
	54135.50c 1.54663E-10	36083.50c 3.70716E-08	42095.50c 4.70087E-07
	43099.50c 5.65964E-07	44101.50c 5.08287E-07	44103.50c 4.95328E-08
	45103.50c 2.52919E-07	45105.50c 1.10611E-09	46105.50c 1.89538E-07

	46108.50c 6.53921E-08	47109.50c 3.52084E-08	48000.50c 4.53997E-11
	54131.50c 2.40078E-07	55133.50c 6.05149E-07	55134.60c 3.61897E-08
	59141.50c 5.54548E-07	60143.50c 3.91304E-07	60145.50c 3.42602E-07
	61147.50c 1.24912E-07	61148.50c 1.17793E-09	62147.50c 2.69654E-08
	61149.50c 1.09673E-09	62149.50c 1.50319E-09	62150.50c 1.25805E-07
	62151.50c 6.57235E-09	62152.50c 6.07670E-08	63153.50c 4.16385E-08
	63154.50c 8.06911E-09	63155.50c 2.61998E-09	64155.50c 3.27166E-11
	64156.50c 1.43158E-08	64157.50c 2.94118E-11	5010.50c 4.91822E-07
	14000.50c 4.51608E-04	6000.50c 8.62699E-02	8016.50c 4.02898E-04
C	VSOP cycle 261; layer 40;	total N = 7.3387623E-01	
M139	92235.50c 6.95690E-06	92236.50c 1.45294E-06	92238.50c 1.81304E-04
	93239.60c 3.57331E-08	94239.50c 8.37367E-07	94240.50c 4.52993E-07
	94241.50c 2.617110E-07	94242.50c 1.31964E-07	93237.50c 5.57827E-08
	54135.50c 1.50142E-10	36083.50c 3.74170E-08	42095.50c 4.77309E-07
	43099.50c 5.72263E-07	44101.50c 5.14287E-07	44103.50c 4.89498E-08
	45103.50c 2.56708E-07	45105.50c 9.92255E-10	46105.50c 1.92492E-07
	46108.50c 6.65142E-08	47109.50c 3.57871E-08	48000.50c 4.60065E-11
	54131.50c 2.43322E-07	55133.50c 6.13124E-07	55134.60c 3.68918E-08
	59141.50c 5.60897E-07	60143.50c 3.96552E-07	60145.50c 3.46313E-07
	61147.50c 1.25691E-07	61148.50c 1.16711E-09	62147.50c 2.74667E-08
	61149.50c 9.69282E-10	62149.50c 1.51357E-09	62150.50c 1.27546E-07
	62151.50c 6.69464E-09	62152.50c 6.13822E-08	63153.50c 4.23271E-08
	63154.50c 8.24200E-09	63155.50c 2.66629E-09	64155.50c 3.66254E-11
	64156.50c 1.45990E-08	64157.50c 2.99384E-11	5010.50c 5.70871E-07
	14000.50c 4.51608E-04	6000.50c 8.62699E-02	8016.50c 4.02898E-04
C	VSOP cycle 261; layer 41;	total N = 7.3387641E-01	
M140	92235.50c 6.88377E-06	92236.50c 1.46445E-06	92238.50c 1.81243E-04
	93239.60c 3.20549E-08	94239.50c 8.53041E-07	94240.50c 4.57359E-07
	94241.50c 2.65177E-07	94242.50c 1.34287E-07	93237.50c 5.67680E-08
	54135.50c 1.44873E-10	36083.50c 3.77081E-08	42095.50c 4.84479E-07
	43099.50c 5.77605E-07	44101.50c 5.19405E-07	44103.50c 4.77422E-08
	45103.50c 2.60648E-07	45105.50c 8.60436E-10	46105.50c 1.95088E-07
	46108.50c 6.74834E-08	47109.50c 3.62835E-08	48000.50c 4.65875E-11
	54131.50c 2.46260E-07	55133.50c 6.20159E-07	55134.60c 3.74986E-08
	59141.50c 5.66312E-07	60143.50c 4.01590E-07	60145.50c 3.49462E-07
	61147.50c 1.26219E-07	61148.50c 1.14553E-09	62147.50c 2.79805E-08
	61149.50c 8.30193E-10	62149.50c 1.53931E-09	62150.50c 1.29042E-07
	62151.50c 6.80391E-09	62152.50c 6.18917E-08	63153.50c 4.29347E-08
	63154.50c 8.39758E-09	63155.50c 2.70497E-09	64155.50c 4.14543E-11
	64156.50c 1.48462E-08	64157.50c 3.05374E-11	5010.50c 6.86703E-07
	14000.50c 4.51608E-04	6000.50c 8.62699E-02	8016.50c 4.02898E-04
C	VSOP cycle 261; layer 42;	total N = 7.3387688E-01	
M141	92235.50c 6.81897E-06	92236.50c 1.47460E-06	92238.50c 1.81193E-04
	93239.60c 2.67857E-08	94239.50c 8.64018E-07	94240.50c 4.61407E-07
	94241.50c 2.68296E-07	94242.50c 1.36432E-07	93237.50c 5.75571E-08
	54135.50c 1.40026E-10	36083.50c 3.79672E-08	42095.50c 4.91555E-07
	43099.50c 5.82431E-07	44101.50c 5.24012E-07	44103.50c 4.62658E-08
	45103.50c 2.64576E-07	45105.50c 7.79061E-10	46105.50c 1.97421E-07
	46108.50c 6.83703E-08	47109.50c 3.67423E-08	48000.50c 4.69727E-11
	54131.50c 2.48920E-07	55133.50c 6.26377E-07	55134.60c 3.79784E-08
	59141.50c 5.71167E-07	60143.50c 4.06231E-07	60145.50c 3.52294E-07
	61147.50c 1.26675E-07	61148.50c 1.07283E-09	62147.50c 2.85089E-08
	61149.50c 7.32365E-10	62149.50c 1.52444E-09	62150.50c 1.30394E-07
	62151.50c 6.88161E-09	62152.50c 6.23904E-08	63153.50c 4.34604E-08
	63154.50c 8.52799E-09	63155.50c 2.73681E-09	64155.50c 4.64021E-11
	64156.50c 1.50734E-08	64157.50c 3.06447E-11	5010.50c 7.80534E-07
	14000.50c 4.51608E-04	6000.50c 8.62699E-02	8016.50c 4.02898E-04

C	VSOP cycle 261; layer 43; total N =	7.3386949E-01	
M142	92235.50c 7.96081E-06	92236.50c 1.29351E-06	92238.50c 1.81976E-04
	93239.60c 1.14867E-08	94239.50c 7.38087E-07	94240.50c 4.10558E-07
	94241.50c 2.19214E-07	94242.50c 1.04974E-07	93237.50c 4.55050E-08
	54135.50c 9.64301E-11	36083.50c 3.34155E-08	42095.50c 4.15753E-07
	43099.50c 5.02334E-07	44101.50c 4.48790E-07	44103.50c 4.21914E-08
	45103.50c 2.28444E-07	45105.50c 3.49003E-10	46105.50c 1.64395E-07
	46108.50c 5.53974E-08	47109.50c 3.00415E-08	48000.50c 3.85692E-11
	54131.50c 2.17288E-07	55133.50c 5.42090E-07	55134.60c 2.98148E-08
	59141.50c 4.90979E-07	60143.50c 3.58125E-07	60145.50c 3.04782E-07
	61147.50c 1.14399E-07	61148.50c 7.54282E-10	62147.50c 2.32366E-08
	61149.50c 3.84678E-10	62149.50c 1.44707E-09	62150.50c 1.10837E-07
	62151.50c 5.92073E-09	62152.50c 5.42101E-08	63153.50c 3.54320E-08
	63154.50c 6.56764E-09	63155.50c 2.17456E-09	64155.50c 4.09186E-11
	64156.50c 1.17553E-08	64157.50c 2.02249E-11	5010.50c 1.52667E-06
	14000.50c 4.51609E-04	6000.50c 8.62701E-02	8016.50c 4.02899E-04
C	VSOP cycle 261; layer 44; total N =	7.3387003E-01	
M143	92235.50c 7.89734E-06	92236.50c 1.30352E-06	92238.50c 1.81942E-04
	93239.60c 1.63352E-08	94239.50c 7.39970E-07	94240.50c 4.11974E-07
	94241.50c 2.21316E-07	94242.50c 1.06382E-07	93237.50c 4.60328E-08
	54135.50c 1.15787E-10	36083.50c 3.36639E-08	42095.50c 4.22364E-07
	43099.50c 5.06516E-07	44101.50c 4.52643E-07	44103.50c 4.04887E-08
	45103.50c 2.32187E-07	45105.50c 5.35559E-10	46105.50c 1.65815E-07
	46108.50c 5.59695E-08	47109.50c 3.03336E-08	48000.50c 3.83648E-11
	54131.50c 2.19261E-07	55133.50c 5.46469E-07	55134.60c 3.00971E-08
	59141.50c 4.95135E-07	60143.50c 3.61934E-07	60145.50c 3.07292E-07
	61147.50c 1.14898E-07	61148.50c 7.71997E-10	62147.50c 2.37356E-08
	61149.50c 5.17855E-10	62149.50c 1.15402E-09	62150.50c 1.11945E-07
	62151.50c 5.87271E-09	62152.50c 5.47042E-08	63153.50c 3.58006E-08
	63154.50c 6.65241E-09	63155.50c 2.19342E-09	64155.50c 4.23714E-11
	64156.50c 1.19153E-08	64157.50c 1.88690E-11	5010.50c 9.31666E-07
	14000.50c 4.51609E-04	6000.50c 8.62701E-02	8016.50c 4.02899E-04
C	VSOP cycle 261; layer 45; total N =	7.3387092E-01	
M144	92235.50c 7.79701E-06	92236.50c 1.31937E-06	92238.50c 1.81890E-04
	93239.60c 2.51573E-08	94239.50c 7.38146E-07	94240.50c 4.14655E-07
	94241.50c 2.24865E-07	94242.50c 1.08722E-07	93237.50c 4.68062E-08
	54135.50c 1.31730E-10	36083.50c 3.40606E-08	42095.50c 4.28823E-07
	43099.50c 5.13242E-07	44101.50c 4.58833E-07	44103.50c 4.07508E-08
	45103.50c 2.35210E-07	45105.50c 8.67029E-10	46105.50c 1.68062E-07
	46108.50c 5.69152E-08	47109.50c 3.08220E-08	48000.50c 3.85391E-11
	54131.50c 2.21156E-07	55133.50c 5.51640E-07	55134.60c 3.06236E-08
	59141.50c 5.01790E-07	60143.50c 3.64956E-07	60145.50c 3.11313E-07
	61147.50c 1.16060E-07	61148.50c 8.77266E-10	62147.50c 2.42129E-08
	61149.50c 8.37070E-10	62149.50c 1.00759E-09	62150.50c 1.13309E-07
	62151.50c 5.82328E-09	62152.50c 5.54892E-08	63153.50c 3.63802E-08
	63154.50c 6.78475E-09	63155.50c 2.23189E-09	64155.50c 3.74280E-11
	64156.50c 1.21717E-08	64157.50c 1.93149E-11	5010.50c 5.84666E-07
	14000.50c 4.51609E-04	6000.50c 8.62701E-02	8016.50c 4.02899E-04
C	VSOP cycle 261; layer 46; total N =	7.3387158E-01	
M145	92235.50c 7.66426E-06	92236.50c 1.34039E-06	92238.50c 1.81821E-04
	93239.60c 3.38866E-08	94239.50c 7.35074E-07	94240.50c 4.18650E-07
	94241.50c 2.29895E-07	94242.50c 1.12018E-07	93237.50c 4.77867E-08
	54135.50c 1.41762E-10	36083.50c 3.45886E-08	42095.50c 4.35309E-07
	43099.50c 5.22293E-07	44101.50c 4.67174E-07	44103.50c 4.26552E-08
	45103.50c 2.37723E-07	45105.50c 1.18108E-09	46105.50c 1.71220E-07
	46108.50c 5.82322E-08	47109.50c 3.15073E-08	48000.50c 3.91103E-11
	54131.50c 2.23462E-07	55133.50c 5.58657E-07	55134.60c 3.13734E-08

	59141.50c 5.10724E-07	60143.50c 3.67885E-07	60145.50c 3.16706E-07
	61147.50c 1.17819E-07	61148.50c 9.91194E-10	62147.50c 2.46732E-08
	61149.50c 1.17000E-09	62149.50c 1.05104E-09	62150.50c 1.15043E-07
	62151.50c 5.82256E-09	62152.50c 5.65228E-08	63153.50c 3.71585E-08
	63154.50c 6.96068E-09	63155.50c 2.28802E-09	64155.50c 3.06776E-11
	64156.50c 1.25181E-08	64157.50c 2.06128E-11	5010.50c 4.43221E-07
	14000.50c 4.51609E-04	6000.50c 8.62701E-02	8016.50c 4.02899E-04
C	VSOP cycle 261; layer 47; total N = 7.3387271E-01		
M146	92235.50c 7.52146E-06	92236.50c 1.36301E-06	92238.50c 1.81745E-04
	93239.60c 3.85415E-08	94239.50c 7.34906E-07	94240.50c 4.23337E-07
	94241.50c 2.35631E-07	94242.50c 1.15793E-07	93237.50c 4.88547E-08
	54135.50c 1.47182E-10	36083.50c 3.51579E-08	42095.50c 4.41964E-07
	43099.50c 5.32177E-07	44101.50c 4.76313E-07	44103.50c 4.50151E-08
	45103.50c 2.40185E-07	45105.50c 1.32196E-09	46105.50c 1.74918E-07
	46108.50c 5.97241E-08	47109.50c 3.22856E-08	48000.50c 3.99087E-11
	54131.50c 2.26394E-07	55133.50c 5.67470E-07	55134.60c 3.22229E-08
	59141.50c 5.20479E-07	60143.50c 3.71410E-07	60145.50c 3.22578E-07
	61147.50c 1.19759E-07	61148.50c 1.06137E-09	62147.50c 2.51312E-08
	61149.50c 1.33691E-09	62149.50c 1.15469E-09	62150.50c 1.17124E-07
	62151.50c 5.89569E-09	62152.50c 5.76233E-08	63153.50c 3.80262E-08
	63154.50c 7.15630E-09	63155.50c 2.35070E-09	64155.50c 2.66673E-11
	64156.50c 1.29024E-08	64157.50c 2.21267E-11	5010.50c 4.15580E-07
	14000.50c 4.51609E-04	6000.50c 8.62701E-02	8016.50c 4.02899E-04
C	VSOP cycle 261; layer 48; total N = 7.3387343E-01		
M147	92235.50c 7.38139E-06	92236.50c 1.38519E-06	92238.50c 1.81668E-04
	93239.60c 3.97078E-08	94239.50c 7.36829E-07	94240.50c 4.28232E-07
	94241.50c 2.41582E-07	94242.50c 1.19722E-07	93237.50c 4.99223E-08
	54135.50c 1.50345E-10	36083.50c 3.57167E-08	42095.50c 4.48833E-07
	43099.50c 5.42011E-07	44101.50c 4.85439E-07	44103.50c 4.71642E-08
	45103.50c 2.42830E-07	45105.50c 1.35072E-09	46105.50c 1.78786E-07
	46108.50c 6.12616E-08	47109.50c 3.30887E-08	48000.50c 4.07647E-11
	54131.50c 2.29828E-07	55133.50c 5.77318E-07	55134.60c 3.30882E-08
	59141.50c 5.30190E-07	60143.50c 3.75653E-07	60145.50c 3.28403E-07
	61147.50c 1.21650E-07	61148.50c 1.08923E-09	62147.50c 2.55960E-08
	61149.50c 1.37303E-09	62149.50c 1.23973E-09	62150.50c 1.19381E-07
	62151.50c 6.00942E-09	62152.50c 5.87039E-08	63153.50c 3.89097E-08
	63154.50c 7.35503E-09	63155.50c 2.41332E-09	64155.50c 2.53709E-11
	64156.50c 1.32941E-08	64157.50c 2.35903E-11	5010.50c 4.27688E-07
	14000.50c 4.51609E-04	6000.50c 8.62701E-02	8016.50c 4.02899E-04
C	VSOP cycle 261; layer 49; total N = 7.3387438E-01		
M148	92235.50c 7.25217E-06	92236.50c 1.40563E-06	92238.50c 1.81595E-04
	93239.60c 3.81437E-08	94239.50c 7.39978E-07	94240.50c 4.32847E-07
	94241.50c 2.47460E-07	94242.50c 1.23552E-07	93237.50c 5.09222E-08
	54135.50c 1.51614E-10	36083.50c 3.62321E-08	42095.50c 4.55897E-07
	43099.50c 5.51209E-07	44101.50c 4.94002E-07	44103.50c 4.86941E-08
	45103.50c 2.45770E-07	45105.50c 1.29832E-09	46105.50c 1.82571E-07
	46108.50c 6.27458E-08	47109.50c 3.38645E-08	48000.50c 4.15953E-11
	54131.50c 2.33540E-07	55133.50c 5.87420E-07	55134.60c 3.39048E-08
	59141.50c 5.39275E-07	60143.50c 3.80499E-07	60145.50c 3.33837E-07
	61147.50c 1.23349E-07	61148.50c 1.08361E-09	62147.50c 2.60738E-08
	61149.50c 1.31261E-09	62149.50c 1.30810E-09	62150.50c 1.21621E-07
	62151.50c 6.13956E-09	62152.50c 5.97106E-08	63153.50c 3.97532E-08
	63154.50c 7.54396E-09	63155.50c 2.47147E-09	64155.50c 2.60899E-11
	64156.50c 1.36706E-08	64157.50c 2.49215E-11	5010.50c 4.67602E-07
	14000.50c 4.51609E-04	6000.50c 8.62701E-02	8016.50c 4.02899E-04
C	VSOP cycle 261; layer 50; total N = 7.3387527E-01		
M149	92235.50c 7.13774E-06	92236.50c 1.42370E-06	92238.50c 1.81528E-04

	93239.60c 3.49554E-08	94239.50c 7.43677E-07	94240.50c 4.36945E-07
	94241.50c 2.52983E-07	94242.50c 1.27113E-07	93237.50c 5.18231E-08
	54135.50c 1.51129E-10	36083.50c 3.66882E-08	42095.50c 4.63105E-07
	43099.50c 5.59451E-07	44101.50c 5.01702E-07	44103.50c 4.94245E-08
	45103.50c 2.49026E-07	45105.50c 1.19470E-09	46105.50c 1.86103E-07
	46108.50c 6.41132E-08	47109.50c 3.45792E-08	48000.50c 4.23551E-11
	54131.50c 2.37299E-07	55133.50c 5.97156E-07	55134.60c 3.46357E-08
	59141.50c 5.47423E-07	60143.50c 3.85721E-07	60145.50c 3.38695E-07
	61147.50c 1.24781E-07	61148.50c 1.05705E-09	62147.50c 2.65674E-08
	61149.50c 1.19278E-09	62149.50c 1.36247E-09	62150.50c 1.23712E-07
	62151.50c 6.26929E-09	62152.50c 6.06131E-08	63153.50c 4.05243E-08
	63154.50c 7.71596E-09	63155.50c 2.52269E-09	64155.50c 2.82716E-11
	64156.50c 1.40178E-08	64157.50c 2.60893E-11	5010.50c 5.32385E-07
	14000.50c 4.51609E-04	6000.50c 8.62701E-02	8016.50c 4.02899E-04
C	VSOP cycle 261; layer 51; total N = 7.3387629E-01		
M150	92235.50c 7.03939E-06	92236.50c 1.43921E-06	92238.50c 1.81470E-04
	93239.60c 3.10435E-08	94239.50c 7.47811E-07	94240.50c 4.40451E-07
	94241.50c 2.57921E-07	94242.50c 1.30297E-07	93237.50c 5.26207E-08
	54135.50c 1.48693E-10	36083.50c 3.70794E-08	42095.50c 4.70382E-07
	43099.50c 5.66601E-07	44101.50c 5.08403E-07	44103.50c 4.93224E-08
	45103.50c 2.52569E-07	45105.50c 1.06164E-09	46105.50c 1.89283E-07
	46108.50c 6.53269E-08	47109.50c 3.52128E-08	48000.50c 4.29961E-11
	54131.50c 2.40914E-07	55133.50c 6.06113E-07	55134.60c 3.52642E-08
	59141.50c 5.54499E-07	60143.50c 3.91070E-07	60145.50c 3.42901E-07
	61147.50c 1.25917E-07	61148.50c 1.01970E-09	62147.50c 2.70772E-08
	61149.50c 1.04296E-09	62149.50c 1.40404E-09	62150.50c 1.25580E-07
	62151.50c 6.38841E-09	62152.50c 6.13967E-08	63153.50c 4.12073E-08
	63154.50c 7.86836E-09	63155.50c 2.56583E-09	64155.50c 3.16065E-11
	64156.50c 1.43276E-08	64157.50c 2.70362E-11	5010.50c 6.24542E-07
	14000.50c 4.51609E-04	6000.50c 8.62701E-02	8016.50c 4.02899E-04
C	VSOP cycle 261; layer 52; total N = 7.3387671E-01		
M151	92235.50c 6.95456E-06	92236.50c 1.45255E-06	92238.50c 1.81415E-04
	93239.60c 2.83670E-08	94239.50c 7.53622E-07	94240.50c 4.43623E-07
	94241.50c 2.61858E-07	94242.50c 1.33087E-07	93237.50c 5.33958E-08
	54135.50c 1.43343E-10	36083.50c 3.74137E-08	42095.50c 4.77644E-07
	43099.50c 5.72756E-07	44101.50c 5.14198E-07	44103.50c 4.85318E-08
	45103.50c 2.56327E-07	45105.50c 9.30825E-10	46105.50c 1.92088E-07
	46108.50c 6.63855E-08	47109.50c 3.57620E-08	48000.50c 4.33112E-11
	54131.50c 2.44225E-07	55133.50c 6.14070E-07	55134.60c 3.58255E-08
	59141.50c 5.60621E-07	60143.50c 3.96292E-07	60145.50c 3.46522E-07
	61147.50c 1.26763E-07	61148.50c 1.00213E-09	62147.50c 2.75981E-08
	61149.50c 9.02556E-10	62149.50c 1.41248E-09	62150.50c 1.27226E-07
	62151.50c 6.48545E-09	62152.50c 6.20629E-08	63153.50c 4.18207E-08
	63154.50c 8.00994E-09	63155.50c 2.60175E-09	64155.50c 3.55335E-11
	64156.50c 1.46022E-08	64157.50c 2.73529E-11	5010.50c 7.33437E-07
	14000.50c 4.51609E-04	6000.50c 8.62701E-02	8016.50c 4.02899E-04
C	VSOP cycle 261; layer 53; total N = 7.3387688E-01		
M152	92235.50c 6.88152E-06	92236.50c 1.46400E-06	92238.50c 1.81366E-04
	93239.60c 2.56954E-08	94239.50c 7.60770E-07	94240.50c 4.46416E-07
	94241.50c 2.65162E-07	94242.50c 1.35526E-07	93237.50c 5.41220E-08
	54135.50c 1.38415E-10	36083.50c 3.76996E-08	42095.50c 4.84834E-07
	43099.50c 5.78060E-07	44101.50c 5.19213E-07	44103.50c 4.72231E-08
	45103.50c 2.60189E-07	45105.50c 8.14958E-10	46105.50c 1.94550E-07
	46108.50c 6.73105E-08	47109.50c 3.62394E-08	48000.50c 4.36265E-11
	54131.50c 2.47190E-07	55133.50c 6.21035E-07	55134.60c 3.63142E-08
	59141.50c 5.65917E-07	60143.50c 4.01237E-07	60145.50c 3.49642E-07
	61147.50c 1.27374E-07	61148.50c 9.81107E-10	62147.50c 2.81295E-08

	61149.50c 7.79917E-10	62149.50c 1.41852E-09	62150.50c 1.28651E-07
	62151.50c 6.56722E-09	62152.50c 6.26291E-08	63153.50c 4.23673E-08
	63154.50c 8.13865E-09	63155.50c 2.63173E-09	64155.50c 4.00645E-11
	64156.50c 1.48451E-08	64157.50c 2.77366E-11	5010.50c 8.61623E-07
	14000.50c 4.51609E-04	6000.50c 8.62701E-02	8016.50c 4.02899E-04
C	VSOP cycle 261; layer 54; total N = 7.3387748E-01		
M153	92235.50c 6.81504E-06	92236.50c 1.47441E-06	92238.50c 1.81320E-04
	93239.60c 2.39410E-08	94239.50c 7.67331E-07	94240.50c 4.49030E-07
	94241.50c 2.68122E-07	94242.50c 1.37782E-07	93237.50c 5.48161E-08
	54135.50c 1.35115E-10	36083.50c 3.79588E-08	42095.50c 4.91901E-07
	43099.50c 5.82902E-07	44101.50c 5.23805E-07	44103.50c 4.57309E-08
	45103.50c 2.64007E-07	45105.50c 7.50433E-10	46105.50c 1.96788E-07
	46108.50c 6.81658E-08	47109.50c 3.66798E-08	48000.50c 4.39253E-11
	54131.50c 2.49808E-07	55133.50c 6.27161E-07	55134.60c 3.67612E-08
	59141.50c 5.70763E-07	60143.50c 4.05756E-07	60145.50c 3.52489E-07
	61147.50c 1.27860E-07	61148.50c 9.64024E-10	62147.50c 2.86672E-08
	61149.50c 7.06732E-10	62149.50c 1.40105E-09	62150.50c 1.29937E-07
	62151.50c 6.63193E-09	62152.50c 6.31439E-08	63153.50c 4.28767E-08
	63154.50c 8.26005E-09	63155.50c 2.65861E-09	64155.50c 4.45016E-11
	64156.50c 1.50720E-08	64157.50c 2.80756E-11	5010.50c 9.54749E-07
	14000.50c 4.51609E-04	6000.50c 8.62701E-02	8016.50c 4.02899E-04
C	VSOP cycle 261; layer 55; total N = 7.3387808E-01		
M154	92235.50c 6.75430E-06	92236.50c 1.48389E-06	92238.50c 1.81278E-04
	93239.60c 2.18885E-08	94239.50c 7.73157E-07	94240.50c 4.51476E-07
	94241.50c 2.70798E-07	94242.50c 1.39885E-07	93237.50c 5.54506E-08
	54135.50c 1.31652E-10	36083.50c 3.81949E-08	42095.50c 4.98829E-07
	43099.50c 5.87352E-07	44101.50c 5.28028E-07	44103.50c 4.41148E-08
	45103.50c 2.67750E-07	45105.50c 6.94569E-10	46105.50c 1.98862E-07
	46108.50c 6.89601E-08	47109.50c 3.70892E-08	48000.50c 4.41749E-11
	54131.50c 2.52157E-07	55133.50c 6.32674E-07	55134.60c 3.71557E-08
	59141.50c 5.75216E-07	60143.50c 4.09878E-07	60145.50c 3.55101E-07
	61147.50c 1.28254E-07	61148.50c 9.36760E-10	62147.50c 2.92117E-08
	61149.50c 6.45505E-10	62149.50c 1.38943E-09	62150.50c 1.31107E-07
	62151.50c 6.68684E-09	62152.50c 6.36236E-08	63153.50c 4.33458E-08
	63154.50c 8.37175E-09	63155.50c 2.68226E-09	64155.50c 4.89214E-11
	64156.50c 1.52845E-08	64157.50c 2.82975E-11	5010.50c 1.05245E-06
	14000.50c 4.51609E-04	6000.50c 8.62701E-02	8016.50c 4.02899E-04
C	VSOP cycle 261; layer 56; total N = 7.3387849E-01		
M155	92235.50c 6.69424E-06	92236.50c 1.49324E-06	92238.50c 1.81238E-04
	93239.60c 2.05724E-08	94239.50c 7.75782E-07	94240.50c 4.53927E-07
	94241.50c 2.73467E-07	94242.50c 1.42022E-07	93237.50c 5.60373E-08
	54135.50c 1.30861E-10	36083.50c 3.84285E-08	42095.50c 5.05603E-07
	43099.50c 5.91796E-07	44101.50c 5.32244E-07	44103.50c 4.26710E-08
	45103.50c 2.71303E-07	45105.50c 6.93267E-10	46105.50c 2.00891E-07
	46108.50c 6.97617E-08	47109.50c 3.75033E-08	48000.50c 4.43319E-11
	54131.50c 2.54290E-07	55133.50c 6.37792E-07	55134.60c 3.75290E-08
	59141.50c 5.79649E-07	60143.50c 4.13554E-07	60145.50c 3.57705E-07
	61147.50c 1.28661E-07	61148.50c 9.10116E-10	62147.50c 2.97598E-08
	61149.50c 6.32685E-10	62149.50c 1.35046E-09	62150.50c 1.32248E-07
	62151.50c 6.72497E-09	62152.50c 6.41203E-08	63153.50c 4.38057E-08
	63154.50c 8.47923E-09	63155.50c 2.70533E-09	64155.50c 5.23584E-11
	64156.50c 1.55002E-08	64157.50c 2.82965E-11	5010.50c 1.06496E-06
	14000.50c 4.51609E-04	6000.50c 8.62701E-02	8016.50c 4.02899E-04
C	VSOP cycle 261; layer 57; total N = 7.3387891E-01		
M156	92235.50c 6.63336E-06	92236.50c 1.50270E-06	92238.50c 1.81202E-04
	93239.60c 1.86646E-08	94239.50c 7.73968E-07	94240.50c 4.56387E-07
	94241.50c 2.76235E-07	94242.50c 1.44278E-07	93237.50c 5.65301E-08

54135.50c	1.30543E-10	36083.50c	3.86661E-08	42095.50c	5.12241E-07
43099.50c	5.96377E-07	44101.50c	5.36573E-07	44103.50c	4.14733E-08
45103.50c	2.74645E-07	45105.50c	7.11743E-10	46105.50c	2.02962E-07
46108.50c	7.05948E-08	47109.50c	3.79364E-08	48000.50c	4.43235E-11
54131.50c	2.56327E-07	55133.50c	6.42798E-07	55134.60c	3.78682E-08
59141.50c	5.84181E-07	60143.50c	4.16866E-07	60145.50c	3.60380E-07
61147.50c	1.29141E-07	61148.50c	8.66630E-10	62147.50c	3.03130E-08
61149.50c	6.38835E-10	62149.50c	1.30926E-09	62150.50c	1.33393E-07
62151.50c	6.74863E-09	62152.50c	6.46678E-08	63153.50c	4.42558E-08
63154.50c	8.57925E-09	63155.50c	2.72768E-09	64155.50c	5.46181E-11
64156.50c	1.57250E-08	64157.50c	2.79526E-11	5010.50c	1.04494E-06
14000.50c	4.51609E-04	6000.50c	8.62701E-02	8016.50c	4.02899E-04

c
c thermal s(alpha,beta) cross sections for graphite at 1200K
c

mt100 grph.06t
mt101 grph.06t
mt102 grph.06t
mt103 grph.06t
mt104 grph.06t
mt105 grph.06t
mt106 grph.06t
mt107 grph.06t
mt108 grph.06t
mt109 grph.06t
mt110 grph.06t
mt111 grph.06t
mt112 grph.06t
mt113 grph.06t
mt114 grph.06t
mt115 grph.06t
mt116 grph.06t
mt117 grph.06t
mt118 grph.06t
mt119 grph.06t
mt120 grph.06t
mt121 grph.06t
mt122 grph.06t
mt123 grph.06t
mt124 grph.06t
mt125 grph.06t
mt126 grph.06t
mt127 grph.06t
mt128 grph.06t
mt129 grph.06t
mt130 grph.06t
mt131 grph.06t
mt132 grph.06t
mt133 grph.06t
mt134 grph.06t
mt135 grph.06t
mt136 grph.06t
mt137 grph.06t
mt138 grph.06t
mt139 grph.06t
mt140 grph.06t
mt141 grph.06t

mt142 grph.06t
mt143 grph.06t
mt144 grph.06t
mt145 grph.06t
mt146 grph.06t
mt147 grph.06t
mt148 grph.06t
mt149 grph.06t
mt150 grph.06t
mt151 grph.06t
mt152 grph.06t
mt153 grph.06t
mt154 grph.06t
mt155 grph.06t
mt156 grph.06t

APPENDIX D.3: Modified subroutine VORSHU

```

SUBROUTINE VORSHU(NPRINT, IN1, MRY, NKEEP, DECAF, ICONPO, BU, VOLREG, VOL,
1                  DEN, DENIOD, HM, THBURN, FADOS3, NOPOW, HMETAL, TCHG2,
2                  KRESHZ, LRZN, TCHG1, N240, NALT, NTYP1, TEMZUT, TCELS,
3                  VERA, IHZ, VOLIHZ, VOLWEG, HMETAV, DAV, DA2, SCELS,
4                  SEMZUT, IREG, JAD11, IBOX, RVCB, HPOS,
5                  ABSIG, LAO, NHOT, SS, RPHIAV)

C
C
C      F U M A N    MANAGES FUELLING OPERATIONS
C
C      VORSHU MEANS: BEFORE SHUFFLING
C      -----
C
C      Subroutine VORSHU was modified (J.R. Lehenhaft, MIT, January 2000) to
C      write layer-averaged atom densities and reaction rates to files FORT.98
C      and FORT.99.
C
C      PARAMETER (NMC = 95)
C
C      COMMONS
C
COMMON / BLOCK1 /
1      IPRIN(15)      ,JTPE1      ,JTPE2
2,     JTPE3         ,JTPE4      ,JTPE5
3,     JTPE6         ,JTPE7      ,JTPE8
4,     JTPE9         ,JTPE10     ,NXS
5,     N26           ,KMAT       ,JN
6,     N200          ,NDR        ,NO
7,     NLUM          ,NC         ,POWER
8,     JSER          ,NXE        ,NRSTRT
9,     KINIT         ,MUHU(30)   ,K96
X,     K42           ,IRR9       ,KFR
COMMON / BLOCK1 /
1      MMAF          ,NLB        ,PI
2,     N20           ,KROT      ,NEND33
3,     MBOX          ,IAVC      ,JD11
4,     RINN          ,IBUCK     ,NVSOP
EQUIVALENCE(JTPE2,NS)
1,     (JTPE3,NT)

C
COMMON / BLOCK3 /
1      JNN           ,IRSUB     ,KREG
2,     N71           ,CRT       ,DELDAY
3,     DELSEC        ,NK        ,NL
4,     XYZ           ,ZF1       ,ZF2
5,     ZF3           ,ZF4       ,ZJNUM
6,     VOLUME        ,FIWATT    ,DIRAC(49,5)
7,     YIELD1(49)    ,YIELD2(49) ,YIELD3(49)
8,     YIELD4(49)    ,NP237    ,XNORM
9,     N27           ,N28       ,N29
X,     N31           ,N41(20)   ,SERCON
COMMON / BLOCK3 /
1      CORE          ,RADR(20)  ,NTYPE
2,     REACT(2)      ,XPPNEW(95),YPPNEW(95)
3,     LSER          ,ZKFIND    ,AWT(13)

```

4,	GS (13)	, GM (13)	, HCORE
5,	JS	, JSS	, KSS
6,	KSIM	, LSIM	, JSIM
7,	LBUMP	, NBUMP	, NQUIT
8,	JSMAX	, JSSMAX	, JSPEC
9,	SPECK (192)	, TIME (192)	, STORE (7, 96)
X,	NSTO (96)	, NSWIT	, JNUM
COMMON / BLOCK3 /			
1	JNSTOP	, NLT	, JNSP
2,	ISPEKT (20)	, FIFA	, HMTOT
3,	HMANFG	, REALNN (10)	, YMNEW
4,	XMNEW	, FITOT1	, XPNEW1
5,	YPNEW1	, LAYER (20)	, FF (4)
6,	NBOX		, IVSP (30)
7,	XVSP (3)	, IDIFF (20)	, CO1S
8,	CO2S	, ZPPNEW (95)	, ZMNEW

C

COMMON / BLOCKR /			
1	NRESHZ	, MAKEUP	, NSPALT
2,	XSPALT	, AAAA	, IDFISS (13)
3,	FICOMP (13)	, NNNN	, NWRITE
4,	NKT	, JEEP	, TDOWN
5,	TSTORE	, TREPRO	, TFAB
6,	BRUCH	, KUGL	, JTYP
7,	KLASSE (10)	, FIMAKL (20)	, NOPILE
8,	MREP	, MARX (10)	, NAJB (10)
9,	FOJB (10)	, NFUL (10)	, NBTOT
X,	NB0	, NCY	

C

COMMON / DABLCK /			
1	NDA10	, NXT10	, JSUM10
2,	NDA11	, NXT11	, JSUM11
3,	JAD10 (150)		, NXT30
4,	NXT40	, NDA8	, NXT8
5,	JSUM8	, JAD8 (20)	, NDA9
6,	NXT9	, JSUM9	, JAD9 (20)
7,	K10	, K08	
8,	NDA29	, NXT29	, N33
9,	NXT13	, N13	, NDA13
X,	ND13	, N14	, NXT28

COMMON / DABLCK /			
1	L8	, L9	, L10
2,	L11	, L13	, L28
3,	L29	, L30	, L40
4,	IWRITE	, IREAD	, JSUM13

C

COMMON / PROZ / INZWX, INZWXX, INZW (10), PRO (300)			
1,	FABC (10), REPC (10),		NN, LISTEQ
2,	DMAT (14, 4, 4), NTIK		

C

COMMON / ORIGEN /			
1	LOB	, NOR	
2,	VOR (50)	, NTO (50)	

C

COMMON / GRENZE/ NURTHM			
1,	THERGR, IDGAM, IDZUT, IDTHER, NGAM, IDESIN, JJGM, MSTU,		
1	MGHUS, NNOBG,		, NZT (10, 2),

```

2           IZUT(10,2,10),SIRA(68),NIRPI,NID,NDA30
3,           NKER,ITEMP(20)

C           COMMON /SPECTI/ IP1K(10)

C           COMMON /QVAR/ IVAR,ENDKEF,QVOLLL,QREDUZ,QREMAX,EPQ,EPC
1,           DQDDC,DELc,DCN,SBu,TE(4,99),TA(99),N61,URZ
2,           ZLEKA,ABXEN,TI(99),DQCMax,PSPALT,JRESTW,JRESTR
3,           JREST,TAU,Q0,QMI,QMA,QRAT,DMOD,DAEM

C           COMMON /OPT/ KENN,IOPUT,NIFKO,DZT,KONIN

C           COMMON /MPUNKT/ IMPU,KMPU,EMPU,TTTEIN,TTTAUS

C           COMMON /ANISO/ JH,IZONE(5),DU(5),KK,M1(6,4)

C           COMMON /IFA/ FA0,FA1,FA2,IEND,N44

C           COMMON /UI/ DUM(155),EM9                                25.8.94
C           COMMON /DECAYT/ DECY(17)                                25.8.94

C           COMMON /MCNP/ IPCYC                                11.6.00

C           DIMENSION BU(6,KMAT),VOLREG(NDR),VOL(N200)
1,           DEN(KMAT,N200),DENIOD(N200),HM(N200)
2,           THBURN(N200),FADOS3(N200),NOPOW(N200)
3,           HMETAL(N200),TCHG2(N200),KRESHZ(N200)
4,           LRZN(N200),TCHG1(N240),NALT(N240)
5,           NTYP1(N240),TEMZUT(NXS),TCELS(5,NXS)
6,           VERA(N200),IHZ(NDR),VOLIHZ(NDR)
7,           VOLWEG(NDR),HMETAV(N200),DAV(KMAT)
8,           DA2(KMAT),SCELS(NXS),SEMZUT(NXS)
9,           IREG(NDR),JAD11(JD11),IBOX(MBOX)
X,           RVCB(MBOX)

C           DIMENSION ABSIG(LA0),NHOT(N200),SS(N26,N200),RPHIAV(N26,NDR)

C           DIMENSION ADEN(KMAT),JP(KMAT),ABSRAT(KMAT)

C           F O R M A T E

C           5 FORMAT (2I3,5E12.5,I6)
11 FORMAT (24I3)
12 FORMAT (18I4)
114 FORMAT ('// FOR THE NEXT CYCLE THE TEMPERATURES OF THE RESONANCE A
           1BSORBERS AND SCATTERING NUCLIDES HAVE BEEN CHANGED: ')
115 FORMAT (6E12.5)
116 FORMAT ('// REPROCESSING MIXTURE:',I10,9I8)
117 FORMAT (' FRACTIONS OF JUMBLE BOXES:',F6.2,9F8.2)
500 FORMAT ('0' // 5('.'),' FOR OUT-OF-PILE BATCHES DECAY IS CALCULAT
           1ED FOR OUT-OF-PILE STORAGE TIME   TSTORE '
           2,G12.5,5('.')) // )
501 FORMAT (I3,9X,I2,8X,E12.5,4(3X,E12.5))
502 FORMAT ('0' // 5('.'),' FOR THE IN-PILE BATCHES DECAY IS CALCULAT
           1ED FOR THE DOWNTIME FOR REFUELING TDOWN '

```

```

2,G12.5,5('.' ) ///
504 FORMAT (/ ' MATERIAL',18X,'CONCENTRATION')
505 FORMAT ('0*****'*****'*****'*****'*****'*****'*****'*****'*****'
1*****'*****'*****'*****'*****'*****'*****'*****'*****'*****'
2 /30X,           ' END OF OPERATING CYCLE',I4,5X,' RELOAD NO', I4,
1 IS EXECUTED ' /1X,121('*') //)
506 FORMAT (// ' OPTIONS FOR NEXT CYCLE :'
1/' IPRIN(1)=' ,I3,' ,IPRIN(2)=' ,I3,' ,IPRIN(3)=' ,I3,' ,IPRIN(4)=' ,I3,
2',JNSTOP=' ,I3,' ,LIB=' ,I3,' ,NPRT=' ,I3,' ,IBUCK=' ,I3,' ,MUHU(3)=' ,I3
3,' ,XE-EXPL.=' ,I3/' NXE=' ,I3,' ,DELDAY=' ,E12.5,' ,POWER=' ,E12.5,' ,ZKF
4IND=' ,E12.5,' ,TDOWN=' ,E12.5//)
507 FORMAT (4I3,3E12.5,4E6.0)
510 FORMAT (I5,6X,G12.5,8X,G12.5)
511 FORMAT ('1','BATCHES BEFORE RELOAD NO ',I3//' BATCH    TOT.VOLUME (
1CCM) HEAVY METAL (GR)      FIMA      FUEL TYPE   BURNUP CLASS
2 IRRADIATION AGE      FDOSE//)
512 FORMAT (1H ,6A4,E12.5)
513 FORMAT ('+',45X,E12.5,6X,I2,12X,I2,9X,E12.5,5X,E12.5)
599 FORMAT ('1')
C 601 FORMAT (// ' AUF DIRECT-ACCESS-EINHEIT',I3,' WURDEN',I4,' SAETZE MITML 12.94
C 1 KONZENTRATIONEN VERBUCHT.'//)                                     ML 12.94
601 FORMAT (// ' ON DIRECT-ACCESS UNIT',I3,' - ',I4,' SETS WITH CONCENTRML 12.94
1ATIONS ARE WRITTEN.'//)                                         ML 12.94
603 FORMAT (18I4)
604 FORMAT (12I6)
700 FORMAT (////' OUT OF PILE BATCHES BEFORE RELOAD NO.',I5//' TYP     B
1URNUP CLASS          VOLUME      AVG.AGE      AVG.BURNUP      AVG.F
2-DOSE      HM-GRAM//)
C 710 FORMAT (/// ***VORSICHT: DIE ZWISCHENBOX',I4,' MIT VOL. =',E12.5,'ML 12.94
C 1 WIRD GELOESCHT.'/14X,'SIE WIRD AUCH IN DER KOSTENRECHNUNG NICHT BML 12.94
C 2ERUECKSICHTIGT.***'//)                                         ML 12.94
710 FORMAT (/// ***CAUTION: THE INTERMEDIATE BOX',I4,' WITH VOL. =', ML 12.94
1E12.5,' WILL BE DELETED.'/14X,'NO CONSIDERATION OF THIS BOX IN CALML 12.94
2CULATION OF COSTS.***'//)                                         ML 12.94
720 FORMAT (////' FROM RELOAD NO.',I5,' THE FOLLOWING STORAGE BOXES AR
1E PREPARED.'// THEY ARE AVAILABLE AT THIS RELOAD NO.',I5,' (DECAY
2TIME IS NOT APPLIED).///' BOX      TYPE      BURNUP CLASS      VOLUME
3   AVG.IRR.TIME      AVG.BURNUP      AVG.F-DOSE      TOT.HEAVY METAL (G
4R)'//)
721 FORMAT (I3,I7,9X,I2,8X,E12.5,3(3X,E12.5),6X,E12.5)
C
C
IF (TSTORE .LT. 0.0)      TSTORE=-TIME(1)/AAAA
TST=ABS(TSTORE)
DELSTO = DELDAY * JNSTOP
C
C
NEW OPTIONS FOR NEXT CYCLE
C
DO 29 I=1,3
IVSP(I+24)= 0
XVSP(I)    = 0.
29 CONTINUE
XTDOWN = 0.
IVSP(28) = 0
KONIN = 0
JREST = 0
IF(ITIK(1) .GT. 0) GO TO 3

```

```

ITIK(10) = 0
ITIK(9) = 0
IT10 = 0
IVAR = 0
URZ = 0.
JRESTW = 0
JRESTR = 0
EPQ = 0.
DMOD = 0.5
EM9 = 1.E-09
DQCMAX = 0.
3 CONTINUE
IF(IVSP(1) .GE. 1) GO TO 21
C
C CARD R9
C
READ (NS,11) (IVSP(I), I=1,6),(IVSP(I), I=8,14),IVOID,(IVSP(I), I=
115,17),(IVSP(I), I=19,24),MUHU(8)
C
N44 = IVSP(12)
IF(IVOID .LE. 0) GO TO 6
C
C CARD R10
C
READ (NS,12) JH,(IZONE(I),M1(I,1),M1(I,2), I=1,JH)
C
KK = JH + 1
M1(KK,1) = 0
IVOID = 0
6 CONTINUE
IF(IVSP(20) .LT. 100) GO TO 4
KONIN = IVSP(20) / 100
IVSP(20) = IVSP(20) - 100 * KONIN
4 CONTINUE
IF(IVSP(20) .LT. 10) GO TO 1
IT10 = IVSP(20) / 10
IF(IT10 .NE. 6) GO TO 9
ITIK(1) = 0
ITIK(9) = 0
IT10 = 5
IVSP(20) = 51
9 CONTINUE
IVSP(20) = IVSP(20) - 10 * IT10
IF(IT10 .EQ. 0) GO TO 1
ITIK(10) = 1
IF(IT10 .EQ. 1) GO TO 1
IF(IT10 .LE. 4) GO TO 2
IVAR = IT10 - 4
IT10 = IT10 - 3
C
C CARD R11
C
READ (NS,115) ENDK,QVOLLL,QREMAX,EPR,EPC,URZ
C
IF(EPR .NE. 0.) EPQ = EPR
IF((ITIK(1) .EQ. 0) .OR. (ENDK .NE. 0)) ENDKEF = ENDK
C

```

```

C CARD R12
C
C READ (NS,115) DQDDG,DELC,DCM,DQCMAZ,PSPALT,DMOT
C
C IMPU = 0
IF(DQDDG .NE. 0.) DQDDC = DQDDG
IF(DQCMAZ .NE. 0.) DQCMAX = DQCMAZ
IF(DMOT .NE. 0.) DMOD = DMOT
IF(DCM .NE. 0.) DCN = DCM
C
C CARD R13
C
C IF(ITIK(1) .EQ. 0) READ (NS,5) JRESTW,JRESTR,Q0,QMI,QMA,QRAT,DAEM
C
C IF(ITIK(1) .EQ. 0) EMPU = 0.
IF(QMI .NE. QMA) GO TO 2
QMI = EPQ
QMA = EPQ
2 CONTINUE
IF(QRAT .EQ. 0.) QRAT = 1.
ITIK(10) = 2
IF(ITIK(9) .GT. 0) GO TO 1
ITIK(9) = IT10 - 5
1 CONTINUE
MUHU(29)=0
IF (IVSP(3).LT.10) GOTO 22
MUHU(29)=IVSP(3)/10
IVSP(3)=IVSP(3)-10
22 CONTINUE
MUHU(1) = IVSP(23)
21 CONTINUE
N61 = 6
IF(URZ .LT. 0.) N61 = 4
NT=6
IVSP(1) = IVSP(1) - 1
ITIK(4) = IVSP(8)
IPRIN(1) = IVSP(2)
IPRIN(2) = IVSP(3)
IPRIN(3) = IVSP(4)
IPRIN(4) = IVSP(10)
LIB = IVSP(21)
NPRINT = IVSP(5)
NTIK = IVSP(20)
ITIK(6) = NTIK
IF((NTIK .EQ. 3) .OR. (NTIK .EQ. 1)) ITIK(1) = 0
NCYC = IVSP(14)
NTYPE=0
IF (IVSP(11).EQ.2) NTYPE=2
IVSP(14) = 0
IN2 = IVSP(9)
NKEEP = IVSP(13)
ISTORN = 0
NKP = NKEEP - 10 * (NKEEP/10)
IF(NKP .EQ. 2) ISTORN = 1
IVSP(13) = 0
LOB =-IVSP(22)
PU = POWER

```

```

HNUC = 0.
CONPOI = 0.
HPOS = 0.

C
C CARD R14
C
IF(IVSP(15) .EQ. 1) READ (NS,507) (IVSP(I), I=25,28), (XVSP(I), I=
11,3), HNUC, HPOS, XTDOWN, CONPOI

C
IF(IVSP(28) .GT. 0) NXE = 1
IF(CONPOI .LT. 0.) JSER = 1
ICONPO = IFIX(CONPOI)
IF(HNUC .GT. 0.) IVSP(29) = IFIX(HNUC)
HNUC = 0.
IF(XTDOWN .GT. 0.) TDOWN = XTDOWN
IF(XTDOWN .LT. 0.) TDOWN = 0.
IF(XVSP(1) .NE. 0.) DELDAY = XVSP(1)
IF(XVSP(2) .NE. 0.) POWER = XVSP(2)
IF(XVSP(3) .NE. 0.) ZKFIN = XVSP(3)
IF(IVSP(25).NE. 0 ) JNSTOP = IVSP(25)
IF(IVSP(26).NE. 0 ) JNUM = IVSP(26)
IF(IVSP(24) .GT. 0) JNSTOP = -JNSTOP
IVSP(24) = 0
IVSP(15) = 0
XVSP(2) = PU
IF(IVSP(27) .GT. 0) MUHU(3) = IVSP(27)
IF(NCYC .LE. 0) GO TO 42
IF(NCY .EQ. 0) NCYC = -NCYC
NCY = NCYC

C
C CARD R15
C
READ (NS,115) (FOJB(I), I=1,MREP)

C
WRITE (NT,116) (      I , I=1,MREP)
WRITE (NT,117) (FOJB(I), I=1,MREP)
42 CONTINUE
IF(IVSP(16) .LE. 0) GO TO 43
IVSP(16) = 0

C
C CARD R16
C
READ (NS,603) (ISPEKT(I), I=1,18)

C
ISPEKT(20) = 0
DO 47 I=1,18
IF(ISPEKT(I) .NE. 0) ISPEKT(20) = I
47 CONTINUE
43 CONTINUE
IF(IVSP(17) .LE. 0) GO TO 49
IVSP(17) = 0

C
C CARD R17
C
READ (NS,603) (IDIFF(I), I=1,18)

C
IDIFF(20) = 0

```

```

DO 48 I=1,18
IF(IDIFF(I) .NE. 0) IDIFF(20) = I
48 CONTINUE
49 CONTINUE
IF(ITIK(6) .EQ. 5) GO TO 41
IF((NTIK .LT. 1) .OR. (NTIK .GT. 2)) GO TO 58
C
C      CARD R18
C
41 READ (NS,603) (ITEMP(I), I=1,18)
C
ITEMP(20) = 0
DO 59 I=1,18
IF(ITEMP(I) .NE. 0) ITEMP(20) = I
59 CONTINUE
58 CONTINUE
IF(IVSP(19) .EQ. 0) GO TO 54
IF(IVSP(19) .EQ. 2) GO TO 60
C
C      CARD R19
C
READ (NS,115) (SEMZUT(I), I=1,NXS)
C
DO 56 I=1,NXS
56 IF(SEMZUT(I) .GT. 0.) TEMZUT(I) = SEMZUT(I)
      WRITE (NT,114)
      WRITE (NT,115) (TEMZUT(I), I=1,NXS)
      DO 53 J=1,NKER
C
C      CARD R20
C
READ (NS,115) (SCELS(I), I=1,NXS)
C
DO 57 I=1,NXS
57 IF(SCELS(I) .GT. 0.) TCELS(J,I) = SCELS(I)
      WRITE (NT,115) (TCELS(J,I), I=1,NXS)
53 CONTINUE
IF(IVSP(19) .EQ. 1) GO TO 54
60 CONTINUE
DO 61 I=1,IDESIN
      DO 61 J=1,2
C
C      CARD R21
C
READ (NS,604)NZ,(IZUT(I,J,M), M=1,NZ)
C
      WRITE (NT,604) NZ,(IZUT(I,J,M), M=1,NZ)
      NZT(I,J) = NZ
61 CONTINUE
54 CONTINUE
IVSP(19) = 0
IF(IPRIN(3) .EQ. -2) NT = 4
INZW(1) = IN2
IF(NPRINT.GE.0) WRITE (NT,599)
IN1=IPRIN(15)+1
INZW(3) = IN1
      WRITE ( 6,505) IN1,IPRIN(15)

```

```

      WRITE ( 6,506) (IPRIN(I),I=1,4),JNSTOP,LIB,NPRINT,IBUCK,MUHU(3),IV
      1SP(28),NXE,DELDAY,POWER,ZKFIND,TDOWN

C      CALCULATE AVERAGE BATCH PROPERTIES BEFORE RELOAD

      IF (NPRINT.GE.1) WRITE (NT,511) IPRIN(15)
      NCX2 = 0
      MRY = 0
      DECAF = 0.
      NDA28 = 28
      NXT28 = 1
      IL = 0

C      repeat for each batch
      DO 191 IR=1,NRESHZ
      -----
C      for fuel cycle ipcyc
      -----
      IF (IPRIN(15).EQ.IPCYC) THEN
          write cycle and batch number to file
          WRITE (96,*) 'CYCLE = ',IPCYC,' BATCH = ',IR
          WRITE (97,*) IR
          c      check if new layer
          IF (MOD(IR,11).EQ.1) THEN
              IF ((IL.GE.1).AND.(IL.LE.57)) THEN
                  print data on previous layer
                  WRITE (96,*) 'VOL OF LAYER ',IL,' = ',VOLAY
                  WRITE (98,*) IPCYC,IL,ADENT,VOLAY,FF(1)
                  WRITE (99,*) IL
                  DO 13 I=1,KMAT,5
                      KMAX = MIN(I+4,KMAT)
                      WRITE (98,*) (ADEN(K),K=I,KMAX)
                      WRITE (99,*) (ABSRAT(K),K=I,KMAX)
13            CONTINUE
              END IF
              increment layer counter
              IL = IL+1
              c      initialize variables
              DO 19 I=1,KMAT
                  ADEN(I) = 0.
                  ABSRAT(I) = 0.
19            CONTINUE
                  ADENT = 0.
                  VOLAY = 0.
              END IF
          END IF
          -----
          NCX1 = NCX2+1
          NCX2 = KRESHZ(IR)
          IF ((IR.GT.1).AND.(NPRINT.EQ.2)) WRITE (NT,599)
          NALT(IR) = 1
          DO 55 M=1,KMAT
55        DAV(M) = 0.0
          PARVOL=0.0
          HMETAV(IR) = 0.0
          HMGRM =0.0
          BURNRX = 0.0

```

```

DOSNRX = 0.0
MRZ = 0
IR1=NCX1
51 CONTINUE
  NCX = LRLZN(IR1)
  DO 50 M=1,KMAT
50 DAV(M) = DAV(M) + DEN(M,NCX) * VOL(NCX)
  HMETAV(IR) = HMETAV(IR) + HMETAL(NCX)*VOL(NCX)
  HMGRM =HMGRM+HM(NCX)
  BURNRX=BURNRX+THBURN(NCX)*VOL(NCX)
  DOSNRX=DOSNRX+FADOS3(NCX)*VOL(NCX)
  PARVOL=PARVOL+VOL(NCX)
  MRZ = MRZ + 1
  IR1 = IR1 + 1
  IF(IR1 .LE. NCX2) GO TO 51
  MRY = MAX0(MRY,MRZ)
  VERA(IR)=PARVOL
  HMETAV(IR) = HMETAV(IR) / PARVOL
  HMDEN =HMETAV(IR)
  BURNRX=BURNRX/PARVOL
  DOSNRX=DOSNRX/PARVOL
  TCHG1(IR)=TCHG2(IR)+TIME(1)
  IF (NPRINT.GE.1) WRITE (NT,510) IR,PARVOL,HMGRM
  IF (NPRINT .EQ. 2) WRITE(NT,504)
  HMEND = 0.
  DAVT = 0.
  IF (IPRIN(15).EQ.IPCYC) THEN
    WRITE (96,*) 'VOLUME OF BATCH ',IR,' = ',PARVOL
    VOLAY = VOLAY + PARVOL
  END IF
  DO 52 M=1,KMAT
  DAV(M) = DAV(M)/PARVOL
  -----
C   prepare layer averaged data for output if chosen cycle
C   -----
  IF (IPRIN(15).EQ.IPCYC) THEN
    print number of atoms of material M in batch
    WRITE (96,*) M,DAV(M)*PARVOL
    WRITE (97,*) DAV(M)
    number of atoms of material M in layer
    ADEN(M) = ADEN(M) + DAV(M)*PARVOL
    total number of atoms in layer
    AIDENT = AIDENT + ADEN(M)
    set up pointers into sigma and flux arrays
    IF (IR.EQ.1) THEN
      LA = (NHOT(IR)-1)*KMAT
      DO 24 I=1,KMAT
        JP(I) = (LA+I-1)*N26
24    CONTINUE
    ELSE IF (NHOT(IR).NE.NHOT(IR-1)) THEN
      LA = (NHOT(IR)-1)*KMAT
      DO 25 I=1,KMAT
        JP(I) = (LA+I-1)*N26
25    CONTINUE
    END IF
C   prepare total absorption rate for material M in the batch
C   using effective macroscopic cross section

```

```

      DO 26 IG=1,N26                               11.6.00
      SSFAC = SS(IG,IR)*RPHIAV(IG,IL)           11.6.00
      ABSRAT(M) = ABSRAT(M) + ABSIG(JP(M)+IG)*SSFAC 11.6.00
26    CONTINUE                                     11.6.00
      END IF                                       11.6.00
C -----
C   IF (M .LE. 13) HMEND = HMEND + DAV(M)       11.6.00
C   IF (NPRINT .NE. 2) GO TO 52
C   WRITE (NT,512)(BU(N,M),N=1,6),DAV(M)
52    CONTINUE                                     11.6.00
      IF (TDOWN .EQ. 0.0)      GO TO 190
C
C   DECRY DURING RESHUFFLE PERIOD
C
      DAV(2) = 0.
      DAV(3) = 0.
      DAV(8) = 0.
      DAV(9) = 0.
      DAV(11) = 0.                                25.8.94
      IF (NXE .LE. 0)
1DAV(14) = 0.
      TDOWM = TDOWN
      IF (TDOWM .LT. 0.) TDOWM = ABS(TDOWN) * DELSTO
      TT = TDOWM*3600.*24.
      IR1=NCX1
160   CONTINUE
      NX = LRZN(IR1)
      IF (NXE .GT. 0)      GO TO 155
      DEC = EXP(-2.87E-05*TT)
      DEN(14,NX) = (DEN(14,NX)-3.72727*DENO(DNX)*(EXP(-0.77E-05*TT)
1          -1.0))*EXP(-2.1E-05*TT)
      DENO(DNX) = DENO(DNX)*DEC
155   CONTINUE
      DEC = EXP(-TT*DECY(2))                         25.8.94
      DC = DEN(2,NX) * (1.0-DEC)
      DEN(3,NX) = DEN(3,NX)+DC
      DEN(2,NX) = DEN(2,NX)*DEC
      DECAF = DECAF + DC * VOL(NX)
      DEC = EXP(-TT*DECY(8))                         25.8.94
      DC = DEN(8,NX) * (1.0-DEC)
      DEN(9,NX) = DEN(9,NX)+DC
      DEN(8,NX) = DEN(8,NX)*DEC
      DECAF = DECAF + DC * VOL(NX)
      DEC = EXP(-TT*DECY(11))                         25.8.94
      DEN(11,NX) = DEN(11,NX)*DEC
      DAV(2) = DAV(2) + DEN(2,NX) * VOL(NX)         25.8.94
      DAV(3) = DAV(3) + DEN(3,NX) * VOL(NX)
      DAV(8) = DAV(8) + DEN(8,NX) * VOL(NX)
      DAV(9) = DAV(9) + DEN(9,NX) * VOL(NX)
      DAV(11) = DAV(11) + DEN(11,NX) * VOL(NX)        25.8.94
      IF (NXE .LE. 0)
1DAV(14) = DAV(14) + DEN(14,NX) * VOL(NX)
      IR1 = IR1 + 1
      IF (IR1 .LE. NCX2) GO TO 160
      DAV(2) = DAV(2)/PARVOL
      DAV(3) = DAV(3)/PARVOL
      DAV(8) = DAV(8)/PARVOL

```

25.8.94

```
DAV(9) = DAV(9)/PARVOL
DAV(11) = DAV(11)/PARVOL
IF (NXE .LE. 0)
1DAV(14) = DAV(14)/PARVOL
190 CONTINUE
C
C      FIND BURNUP (FIMA-VALUE) FOR THIS REGION
C
IF (NOPOW(IR).EQ.0) GOTO 182
FIMA=0.
GOTO 183
182 CONTINUE
FIMA = (HMETAV(IR)-HMEND)/HMETAV(IR)
IF(FIMA .LE. 0.) FIMA = EM9
183 CONTINUE
NTP = NTYP1(IR)
NTP1 = NTP-1
KL = 0
IF (NTP1 .LE. 0) GO TO 175
DO 170 I=1,NTP1
KL = KL+KLASSE(I)
170 CONTINUE
175 CONTINUE
IF(NOPOW(IR) .GT. 0) GO TO 184
KLZ = KLASSE(NTP)
DO 180 I=1,KLZ
IKLASS = I
IF (FIMA .LT. FIMAKL(KL+I)) GO TO 181
180 CONTINUE
184 CONTINUE
IKLASS = 0
181 CONTINUE
IF(NPRINT.GE.1)
1WRITE(NT,513) FIMA,NTP,IKLASS,TCHG1(IR),DOSNRX
WRITE (97,*) PARVOL,FIMA
JSATZ = 2+IR
IF (JAD11(JSATZ) .EQ. 0) JAD11(JSATZ)=JSUM11
NXT11 = JAD11(JSATZ)
WRITE (NDA11,REC=NXT11)(DAV(L),L=1,KMAT),PARVOL,TCHG1(IR),NTP
1,           IKLASS,BURNRX,DOSNRX,HMGRM,HMDEN
NXT11 = NXT11 + 1
IF (JSUM11 .LT. NXT11) JSUM11=NXT11
IF(IVSP(21) .GE. 0) GO TO 191
NTYP = NTP * 100 + 1
WRITE (NDA28,REC=NXT28) NTYP
NXT28 = NXT28 + 1
CALL WRDA(IWRITE,NDA28,NXT28,L28,DAV,KMAT)
191 CONTINUE
IF(IVSP(21) .GE. 0) GO TO 600
IVSP(21) = 0
NRS = NXT28 - 1
WRITE (6,601) NDA28,NRS
600 CONTINUE
IF (NPRINT .GT. 0)
1WRITE (NT,502) TDOWN
IF (KUGL .LE. 0) GO TO 199
```

C

```

C IHZ(KR) = NUMBER OF BATCHES / LAYER
C VOLIHZ(KR) = VOL. OF ONE LAYER
C
C IRRE1 = 0
DO 192 KR=1,NDR
IRRE2 = IREG(KR)
IHZ(KR) = IRRE2-IRRE1
VOLIHZ(KR) = VOLREG(KR)
VOLWEG(KR) = 0.0
IRRE1 = IRRE2
192 CONTINUE
IF(MBOX .LE. NBOX) GO TO 31
C
C FILLING OF THE STORAGE BOXES FROM INTERMEDIATE BOXES
C
DO 132 I=1,MBOX
132 RVCB(I) = 0.
K2 = KMAT + 8
ANUL = 0.
NB1 = NBOX + 1
DO 33 I=NB1,MBOX
RVCB(I) = 1.
JSATZ = NRESHZ + 2 + I
IF (JAD11(JSATZ) .EQ. 0) JAD11(JSATZ)=JSUM11
NXT11 = JAD11(JSATZ)
WRITE (NDA11,REC=NXT11) (ANUL, J=1,K2)
NXT11 = NXT11 + 1
IF (JSUM11 .LT. NXT11) JSUM11=NXT11
33 CONTINUE
IF(MBOX .EQ. 1) GO TO 31
IF(ISTORN .EQ. 1) GO TO 31
DO 34 I=1,NBOX
JSATZ = NRESHZ + 2 + I
JS2 = JSATZ
NXT11 = JAD11(JSATZ)
IF(NXT11 .EQ. 0) GO TO 34
READ (NDA11,REC=NXT11) (DAV(L), L=1,KMAT),PARVOL,XCHNRX,NTPNRX,
1 IKLNRX,BURNRX,DOSNRX,HMGRM,HMDEN
NXT11 = NXT11 + 1
IF(IBOX(I) .EQ. 0) GO TO 32
JSATZ = NRESHZ + 2 + IBOX(I)
NXT11 = JAD11(JSATZ)
READ (NDA11,REC=NXT11) (DA2(L), L=1,KMAT),PARVO2,XCHNR2,NTPNR2,
1 IKLNR2,BURNR2,DOSNR2,HMGR2,HMDE2
NXT11 = NXT11 + 1
PV = PARVOL + PARVO2
PV1 = PARVOL / PV
PV2 = PARVO2 / PV
DO 35 L=1,KMAT
35 DA2(L) = DAV(L) * PV1 + DA2(L) * PV2
PARVO2 = PV
XCHNR2 = XCHNRX * PV1 + XCHNR2 * PV2
NTPNR2 = NTPNRX
HMGR2 = HMGRM + HMGR2
HMDE2 = HMDEN * PV1 + HMDE2 * PV2
BURNR2 = BURNRX * PV1 + BURNR2 * PV2
DOSNR2 = DOSNRX * PV1 + DOSNR2 * PV2

```

```

DN2 = 0.
DO 36 L=1,13
36 DN2 = DN2 + DA2(L)
FIMA = (HMDE2-DN2) / HMDE2
IF(FIMA .LE. 0.) FIMA = EM9
NTP1 = NTPNR2 - 1
KL = 0
IF(NTP1 .LE. 0) GO TO 39
DO 20 L=1,NTP1
KL = KL + KLASSE(L)
20 CONTINUE
39 CONTINUE
KLZ = KLASSE(NTPNR2)
DO 37 L=1,KLZ
IKLNR2 = L
IF(FIMA .LT. FIMAKL(KL+L)) GO TO 38
37 CONTINUE
IKLNR2 = 0
38 CONTINUE
NXT11 = JAD11(JSATZ)
WRITE(NDA11,REC=NXT11) (DA2(L), L=1,KMAT),PARVO2,XCHNR2,NTPNR2,
1 IKLNR2,BURNR2,DOSNR2,HMGR2,HMDE2
NXT11 = NXT11 + 1
32 CONTINUE
IF(IBOX(I) .EQ. 0 .AND. PARVOL .GT. 0.) WRITE (6,710) I,PARVOL
NXT11 = JAD11(JS2)
WRITE(NDA11,REC=NXT11) (ANUL, J=1,K2)
NXT11 = NXT11 + 1
IBOX(I) = 0
34 CONTINUE
IF(NPRINT .LT. 0 .OR. IPRIN(15) .EQ. 0) GO TO 40
IPRO = IFIX(PRO(299))
WRITE (NT,720) IPRO,IPRIN(15)
DO 30 I=NB1,MBOX
J = I - NBOX
JSATZ = NRESHZ + 2 + I
NXT11 = JAD11(JSATZ)
READ(NDA11,REC=NXT11) (DA2(L), L=1,KMAT),PARVO2,XCHNR2,NTPNR2,
1 IKLNR2,BURNR2,DOSNR2,HMGR2,HMDE2
NXT11 = NXT11 + 1
WRITE (NT,721) J,NTPNR2,IKLNR2,PARVO2,XCHNR2,BURNR2,DOSNR2,HMGR2
30 CONTINUE
40 CONTINUE
31 CONTINUE
C
C      DECAY OF OUT-OF-PILE BATCHES DURING LAST CYCLE AND RESHUFFLE
C
TT=TST*3600.*24.
IF(NPRINT .GE. 1) WRITE (NT,700) IPRIN(15)
DO 194 N=1,NOPILE
IR=NRESHZ+N
JSATZ=2+MBOX+IR
NXT11=JAD11(JSATZ)
READ (NDA11,REC=NXT11) (DAV(L),L=1,KMAT),PARVOL,TXCHG,NTP,IKLASS,
1 BURNRX,DOSNRX,HMGRM,HMDEN
NXT11 = NXT11 + 1
IF (IKLASS .LE. 1) GOTO 194

```

```

TXCHG=TXCHG+TST*AAAA
TCHG1 (IR)=TXCHG
IF (NXE .LE. 0)
1DAV(14)=0.
DEC=EXP (-TT*DECY(2))                                         25.8.94
DC = DAV(2) * (1.-DEC)
DAV(3)=DAV(3)+DC
DAV(2)=DAV(2)*DEC
DECAF = DECAF + DC * PARVOL
DEC=EXP (-TT*DECY(8))                                         25.8.94
DC = DAV(8) * (1.-DEC)
DAV(9)=DAV(9)+DC
DAV(8)=DAV(8)*DEC
DECAF = DECAF + DC * PARVOL
DEC=EXP (-TT*DECY(11))                                         25.8.94
DAV(11)=DAV(11)*DEC                                         25.8.94
NXT11=JAD11(JSATZ)
WRITE (NDA11,REC=NXT11) (DAV(L),L=1,KMAT),PARVOL,TXCHG,NTP,IKLASS,
1                                         BURNRX,DOSNRX,HMGRM,HMDEN
NXT11 = NXT11 + 1
IF (NPRINT .LT. 1)      GOTO 194
WRITE (NT,501) NTP,IKLASS,PARVOL,TXCHG,BURNRX,DOSNRX,HMGRM
IF (NPRINT .NE. 2)      GOTO 194
DO 193 L=1,KMAT
WRITE (NT,512) (BU(I,L),I=1,6),DAV(L)
193 CONTINUE
194 CONTINUE
IF (NPRINT .GT. 0)
1WRITE (NT,500) TST
199 CONTINUE
RETURN
END

```

APPENDIX D.4: Program MCARDS

```

program mcards
c
c   prepare mcnp material cards using vsop fuel compositions for
c   each layer. The compositions are homogenized over the volume
c   of a fuel sphere, with an adjustment to U238 composition.
c
c   parameter (niso = 51)
c   parameter (kmat = 65)
c   parameter (layers = 57)
c
c   real nvsop(kmat),rate(kmat),nmcnp(niso),vlay(layers)
c   integer hit(kmat),ipoint(niso)
c   character*9 zaid(niso)*9,matnam*4
c
c   mcnp material i.d.
c
c   data zaid /
1    '90232.50c','91233.50c','92233.50c','92234.50c','92235.50c',
2    '92236.50c','92238.50c','93239.60c','94239.50c','94240.50c',
3    '94241.50c','94242.50c','93237.50c','54135.50c','36083.50c',
4    '42095.50c','43099.50c','44101.50c','44103.50c','45103.50c',
5    '45105.50c','46105.50c','46108.50c','47109.50c','48000.50c',
6    '54131.50c','55133.50c','55134.60c','59141.50c','60143.50c',
7    '60145.50c','61147.50c','61148.50c','62147.50c','61149.50c',
8    '62149.50c','62150.50c','62151.50c','62152.50c','63153.50c',
9    '63154.50c','63155.50c','64155.50c','64156.50c','64157.50c',
x    '5010.50c','5011.50c','26000.50c','14000.50c','6000.50c',
y    '8016.50c' /
c
c   data pf/0.61/,rfs/3.0/,pi/3.141592654/,scale/1.0/
c
c   mapping between vsop and mcnp
c
c   data hit / 14*1,0,0,1,0,1,0,8*1,1,0,1,0,3*1,0,1,0,1,0,4*1,0,3*1,
1      0,11*1,0,1,0,1,1 /
c
c   initializations
c
c   .. zaid pointer and mcnp atom density arrays
do 5 iz=1,niso
    ipoint(iz) = 0
    nmcnp(iz) = 0.0
5 continue
c
c   .. vsop material atom densities and reaction rates
do 10 m=1,kmat
    nvsop(m) = 0.0
    rate(m) = 0.0
10 continue
c
c   .. total reaction rate for non-hits
rden = 0.0
c
c   volume of fuel sphere
c
vfs = (4.0/3.0)*pi*rfs**3
c

```

```

open (unit=98,file='fort.98',status='old')
open (unit=99,file='fort.99',status='old')
open (unit=100,file='mcards_new.dat',status='new')

c
c      start numbering mcnp material cards at m100
matnum = 99

c
c      for each layer ..
do 45 l=1, layers
    input vsop cycle, layer number and total atom density
    read (98,*) ipcyc,laynum1,vlay(1),pf
    read (99,*) laynum2
    if (laynum1 .ne. laynum2) then
        stop 'mcards error: layer number mismatch'
    end if
c      input atom density and reaction rate for each material
matnum = matnum + 1
do 15 m=1,kmat,5
    kmax = min(m+4,kmat)
    read (98,*) (nvsop(k),k=m,kmax)
    read (99,*) (rate(k),k=m,kmax)
15 continue
c      calculate number of fuel spheres in layer
vol = vlay(1)
nfs = int(pf*vol/vfs)

c
c      transfer atom densities to mcnp file if nuclides match
c      or sum up reaction rates otherwise
im = 0
iz = 0
do 20 m=1,kmat
    mcnp library exists and density not zero
    if ((hit(m).eq.1).and.(nvsop(m).ne.0.0)) then
        include Pm148g with Pm148m (m=42)
        if (m.eq.43) then
            nmcnp(im) = nmcnp(im) + nvsop(m)
        B10
        else if (m.eq.58) then
            im = im + 1
            iz = iz + 1
            nmcnp(im) = nvsop(m)
            ib10 = im
            ipoint(im) = iz
        c      correct [U238] for heterogeneity
        else if (m.eq.7) then
            im = im + 1
            iz = iz + 1
            nmcnp(im) = scale*nvsop(m)
            ipoint(im) = iz
        c      all other nuclides
        else
            im = im + 1
            iz = iz + 1
            nmcnp(im) = nvsop(m)
            ipoint(im) = iz
        end if
    mcnp library exists but density is zero

```

```

c           else if ((hit(m).eq.1).and.(nvsop(m).eq.0.0)) then
c               increment zaid array pointer
c               iz = iz + 1
c               if (m.eq.58) then
c                   im = im + 1
c                   nmcnp(im) = 0.0
c                   ib10 = im
c                   ipoint(im) = iz
c               end if
c               mcnp library does not exist
c               else
c                   rden = rden + nvsop(m)*rate(m)
c               end if
20             continue
c
c               nmax = im
c               B10 atom density chosen to conserve total reaction rate
c               nmcnp(ib10) = nmcnp(ib10) + rden/rate(58)
c
c               adjust atom densities to volume of spheres and calculate
c               total atom density in layer
c
c               totn = 0.0
c               do 22 i=1,niso
c                   nmcnp(i) = nmcnp(i)*vol/(nfs*vfs)
c                   totn = totn + nmcnp(i)
22             continue
c
c               prepare mcnp material card
c
c               write (100,25) ipcyc,laynum1,totn
25             format ('C      VSOP cycle ',i4,'; layer ',i3,
c                      '; total N = ',1pe14.7)
c               do 40 i=1,nmax,3
c                   jmax = min(i+2,nmax)
c                   if (i.eq.1) then
c                       numold = matnum
c                       call mchar(numold,matnam)
c                       write (100,30) matnam,((zaid(ipoint(j)),nmcnp(j)),
c                                         j=i,jmax)
c
30             format(a4,1x,3(a9,1pe12.5,2x))
c                   else
c                       write (100,35) ((zaid(ipoint(j)),nmcnp(j)),j=i,jmax)
c
35             format(5x,3(a9,1pe12.5,2x))
c                   end if
c
40             continue
c
45             continue
c               end for loop
c
c               close (unit=97)
c               close (unit=98)
c               close (unit=99)
c               stop
c               end

```

```
subroutine mchar(num,number)
c
c   prepare character string Mn
c
c   character*4 number
c   character*1 digit(10)
c   data digit /'0','1','2','3','4','5','6','7','8','9'/
c
c   number = 'M   '
c   i = 4
c   if (num .gt. 999) stop 'number > 999'
10  continue
      n = mod(num,10) + 1
      number(i:i) = digit(n)
      num = int(num/10)
      i = i - 1
      if (i .gt. 1) go to 10
c   write (6,15) number
c15  format(1x,'material =',a4)
      return
      end
```

APPENDIX E. Plutonium Production in a Modular Pebble Bed Reactor

Appendix E.1 contains the MCNP4B input file with added lines for a MOCUP burnup calculation, which uses a supercell model to calculate plutonium production in a special, depleted-uranium pebble. Details on this model and related analysis may be found in Chapter 8.

Appendix E.2 contains the Excel spreadsheets that were used to analyze the results of the VSOP94 fuel management for the preliminary PBMR core (see Appendix D.1). The nuclide densities of fuel spheres in the batches at the bottom of the core were extracted from the VSOP94 output file prior to reload number 261. The five sets of eleven batches correspond to the five pebble flow channels in the VSOP94 model. The mass of ^{239}Pu was determined from these nuclide densities.

APPENDIX E.1: MOCUP Supercell Model of Production Sphere

CRITICAL DRIVER LATTICE WITH PRODUCTION PEBBLE IN CENTER

```

c MCNP4B model of a critical spherical assembly consisting of:
c
c - solid outer reflector
c - lattice of driver fuel pebbles with nuclide compositions that
c   correspond to the average VSOP model of equilibrium fuel cycle
c - a production pebble in the center with depleted uranium core
c
c J.R. Leibhaft, MIT, July 2000 - MCNP4B model
c K.D. Weaver, INEEL - MOCUP additions
c
c -----
c cell cards
c -----
c
1 0           1                               $ outside world
2 64 8.67418e-02 -1  2                   $ graphite reflector
3 0           -2                           fill=1      $ pebble bed
c
c core
c
4 0           -12  11 -14  13  15 -16          fill=2  u=1  $ production cell
5 0           (12:-11: 14:-13:-15: 16)        fill=5  u=1  $ driver core
c
c -----
c universe 2: production cell
c
10 0           -30                          fill=6  u=2  $ production [ 0  0  0]
11 4  8.7424986e-02 -31                  u=2  $ 1/8 driver [ 1  1  1]
12 4  8.7424986e-02 -32                  u=2  $ 1/8 driver [ 1  1 -1]
13 4  8.7424986e-02 -33                  u=2  $ 1/8 driver [ 1 -1 -1]
14 4  8.7424986e-02 -34                  u=2  $ 1/8 driver [ 1 -1  1]
15 4  8.7424986e-02 -35                  u=2  $ 1/8 driver [-1  1  1]
16 4  8.7424986e-02 -36                  u=2  $ 1/8 driver [-1  1 -1]
17 4  8.7424986e-02 -37                  u=2  $ 1/8 driver [-1 -1 -1]
18 4  8.7424986e-02 -38                  u=2  $ 1/8 driver [-1 -1  1]
19 1  -3.429e-03           30  31  32  33  34
                                35  36  37  38             u=2  $ helium
c
c .. universe 6: contents of production ball
c
20 64 8.674180e-02    40                  u=6  $ graphite shell
21 3  7.02567e-02    -40                 u=6  $ target region
c
c -----
c universe 5: driver lattice
c
70 0           -12  11 -14  13  15
                -16          lat=1 fill=10  u=5  $ driver cell
c

```

```

c   .. universe 10: contents of driver cell
71  4   8.7424986e-02  -30                                u=10 $ 1   driver [ 0  0  0]
72  4   8.7424986e-02  -31                                u=10 $ 1/8  driver [ 1  1  1]
73  4   8.7424986e-02  -32                                u=10 $ 1/8  driver [ 1  1  -1]
74  4   8.7424986e-02  -33                                u=10 $ 1/8  driver [ 1  -1  -1]
75  4   8.7424986e-02  -34                                u=10 $ 1/8  driver [ 1  -1  1]
76  4   8.7424986e-02  -35                                u=10 $ 1/8  driver [-1  1  1]
77  4   8.7424986e-02  -36                                u=10 $ 1/8  driver [-1  1  -1]
78  4   8.7424986e-02  -37                                u=10 $ 1/8  driver [-1  -1  -1]
79  4   8.7424986e-02  -38                                u=10 $ 1/8  driver [-1  -1  1]
80  1   -3.429e-03          30  31  32  33  34
                                         35  36  37  38                                u=10 $ helium

c -----
c surface cards
c -----
c universe boundaries
c
1    so 250.0                                     $ outer reflector
2    so 200.0                                     $ driver region
c     1      so 350.0                                     $ outer reflector
c     2      so 258.7                                     $ driver region
c
c production cell boundaries
c
11   px  -3.592148
12   px  3.592148
13   py  -3.592148
14   py  3.592148
15   pz  -3.592148
16   pz  3.592148
c
c balls in unit bcc lattice
c
30   so   3.0
31   s    3.592148  3.592148  3.592148  3.0
32   s    3.592148  3.592148 -3.592148  3.0
33   s    3.592148 -3.592148 -3.592148  3.0
34   s    3.592148 -3.592148  3.592148  3.0
35   s   -3.592148  3.592148  3.592148  3.0
36   s   -3.592148  3.592148 -3.592148  3.0
37   s   -3.592148 -3.592148 -3.592148  3.0
38   s   -3.592148 -3.592148  3.592148  3.0
c
c production fuel
c
40   so   2.1                                     $ fueled region in ball
c -----
c run time cards
c -----
c
c material cards
c -----
c
c helium (1200 K)

```

m1	2003.50c	0.00000137	2004.50c	0.99999863		
c						
c	UO2 (U235/U = 0.002)					
m3	8016.60c	0.0468378				
	36083.50c	1.000E-24				
	40091.86c	1.000E-24	40093.86c	1.000E-24		
	42095.50c	1.000E-24	42097.60c	1.000E-24		
	42098.50c	1.000E-24	43099.60c	1.000E-24		
	44101.50c	1.000E-24	45103.86c	1.000E-24		
	45105.86c	1.000E-24	46105.50c	1.000E-24		
	46107.96c	1.000E-24	47109.86c	1.000E-24		
	48113.86c	1.000E-24	53129.86c	1.000E-24		
	54131.86c	1.000E-24	54133.86c	1.000E-24		
	55133.86c	1.000E-24	55134.86c	1.000E-24		
	54135.54c	1.000E-24	55135.86c	1.000E-24		
	57139.60c	1.000E-24	59141.50c	1.000E-24		
	60143.50c	1.000E-24	60144.96c	1.000E-24		
	60145.50c	1.000E-24	61147.50c	1.000E-24		
	62147.50c	1.000E-24	60148.50c	1.000E-24		
	61148.50c	1.000E-24	61148.91c	1.000E-24		
	61149.50c	1.000E-24	62149.50c	1.000E-24		
	62150.50c	1.000E-24	62151.50c	1.000E-24		
	63151.50c	1.000E-24	62152.50c	1.000E-24		
	63153.60c	1.000E-24	63154.50c	1.000E-24		
	63155.50c	1.000E-24	64157.86c	1.000E-24		
	90232.86c	1.000E-24				
	91231.60c	1.000E-24				
	91233.50c	1.000E-24				
	92232.60c	1.000E-24				
	92233.86c	1.000E-24				
	92234.86c	1.000E-24				
	92235.54c	4.680E-05				
	92236.86c	1.000E-24				
	92238.54c	2.33721E-02				
	93237.50c	1.000E-24				
	93238.35c	1.000E-24				
	93239.60c	1.000E-24				
	94238.86c	1.000E-24				
	94239.82c	1.000E-24				
	94240.82c	1.000E-24				
	94241.82c	1.000E-24				
	94242.82c	1.000E-24				
	95241.98c	1.000E-24				
	95242.92c	1.000E-24				
	95243.88c	1.000E-24				
	96244.98c	1.000E-24				
c						
c	VSOP cycle 261; layer average; total N = 8.7424986E-02					
c						
m4	92235.54c	7.26748E-06	92236.86c	7.90922E-07	92238.54c	1.38334E-04
	93239.60c	2.31130E-08	94239.82c	5.65635E-07	94240.82c	2.52409E-07
	94241.82c	1.22065E-07	94242.82c	3.42635E-08	93237.50c	1.99774E-08
	54135.54c	1.19503E-10	36083.50c	2.07351E-08	42095.50c	2.17681E-07
	43099.60c	2.87436E-07	44101.50c	2.51240E-07	44103.50c	3.27984E-08
	45103.86c	1.26674E-07	45105.86c	7.00813E-10	46105.50c	8.38273E-08
	46108.50c	2.51655E-08	47109.86c	1.40838E-08	48000.50c	2.99848E-11
	54131.86c	1.25169E-07	55133.86c	3.07103E-07	55134.86c	1.19076E-08

```

59141.50c 2.78676E-07 60143.50c 2.18084E-07 60145.50c 1.76511E-07
61147.50c 7.52556E-08 61148.50c 6.39397E-10 62147.50c 1.10404E-08
61149.50c 7.32471E-10 62149.50c 1.03964E-09 62150.50c 5.90797E-08
62151.50c 4.31815E-09 62152.50c 3.03251E-08 63153.60c 1.65125E-08
63154.50c 2.34477E-09 63155.50c 1.10775E-09 64155.50c 1.68288E-11
64156.50c 4.56568E-09 64157.86c 1.63416E-11 5010.50c 7.58592E-09
14000.50c 3.41384E-04 6000.50c 8.66292E-02 8016.60c 3.04562E-04

mt4 grph.06t
c
c graphite matrix in fuel pebble (N = 8.674180e-02)
c
m64 6000.50c 8.674169e-02      5011.50c 9.032424e-08
      5010.50c 2.244010e-08
mt64 grph.06t
c
c U238 for (n,gamma) reaction rate tally
c m5 92238.50c 1
c
c Tally Materials
c
m701 36083.50c 1.000
m702 40091.86c 1.000
m703 40093.86c 1.000
m704 42095.50c 1.000
m705 42097.60c 1.000
m706 42098.50c 1.000
m707 43099.60c 1.000
m708 44101.50c 1.000
m709 45103.86c 1.000
m710 45105.86c 1.000
m711 46105.50c 1.000
m712 46107.96c 1.000
m713 47109.86c 1.000
m714 48113.86c 1.000
m715 53129.86c 1.000
m716 54131.86c 1.000
m717 54133.86c 1.000
m718 55133.86c 1.000
m719 55134.86c 1.000
m720 54135.54c 1.000
m721 55135.86c 1.000
m722 57139.60c 1.000
m723 59141.50c 1.000
m724 60143.50c 1.000
m725 60144.96c 1.000
m726 60145.50c 1.000
m727 61147.50c 1.000
m728 62147.50c 1.000
m729 60148.50c 1.000
m730 61148.50c 1.000
m731 61148.91c 1.000
m732 61149.50c 1.000
m733 62149.50c 1.000
m734 62150.50c 1.000
m735 62151.50c 1.000
m736 63151.50c 1.000
m737 62152.50c 1.000

```

```

m738    63153.60c   1.000
m739    63154.50c   1.000
m740    63155.50c   1.000
m741    64157.86c   1.000
m801    90232.86c   1.000
m802    91231.60c   1.000
m803    91233.50c   1.000
m804    92232.60c   1.000
m805    92233.86c   1.000
m806    92234.86c   1.000
m807    92235.54c   1.000
m808    92236.86c   1.000
m809    92238.54c   1.000
m810    93237.50c   1.000
m811    93238.35c   1.000
m812    93239.60c   1.000
m813    94238.86c   1.000
m814    94239.82c   1.000
m815    94240.82c   1.000
m816    94241.82c   1.000
m817    94242.82c   1.000
m818    95241.98c   1.000
m819    95242.92c   1.000
m820    95243.88c   1.000
m821    96244.98c   1.000

c
c      sources
c
ksrc  3.2    3.2    3.2
      2.5    2.5    2.5
      -3.2   -3.2   3.2
      -2.5   -2.5   2.5
      3.2    -3.2   -3.2
      2.5    -2.5   -2.5
      -3.2   3.2    -3.2
      -2.5   2.5    -2.5

c
c -----
c      tally specifications
c -----
c
fq0    e f
c
c fc7    fission source for normalization (per unit mass)
c f7:n  3
c sd7   1
c
c fc4    average neutron flux in production cell
c f4:n  4
c sd4   370.811
c e4    1.86e-6 29e-6 100e-3 20
c
c fc14   average U238 absorption rate in production ball
c f14:n (21 < 10 < 4 < 3)
c      atom density of depleted UO2 (1/b-cm)
c fm14  2.31457e-02 5 102
c      volume of target (cm3)

```

```

c sd14 38.7924
c e14 1.86e-6 20
c
c fc24 average U238 absorption rate in driver ball
c f24:n ((11 12 13 14 15 16 17 18) < 4 < 3)
c atom density of U238 (1/b-cm) from m4 card
c fm24 1.11479e-04 5 102
c sd24 113.0973
c e24 1.86e-6 20
c
c -----
c
c      (total fuel volume = 38.79 cm*3)
fc54 Total Fissions      Total Fission Neutrons
fm54 (-38.79   3  (-6)  (-6 -7))
f54:n 21
c
c -----
c
c      begin_mocup_flux_tallies
c      time dependent flux
fc94 Cell-averaged neutron flux (neutrons/cm**2 per source neutron)
f94:n 21
c      end_mocup_flux_tallies
c
c -----
c
c      begin_mocup_reaction_rate_tallies
c      time dependent reaction rates
fc904 (n,x) reactions - fuel region
f904:n 21
fm904 (1.0 701) (102))
(1.0 702) (102))
(1.0 703) (102))
(1.0 704) (102))
(1.0 705) (102))
(1.0 706) (102))
(1.0 707) (102))
(1.0 708) (102))
(1.0 709) (102))
(1.0 710) (102))
(1.0 711) (102))
(1.0 712) (102))
(1.0 713) (102))
(1.0 714) (102))
(1.0 715) (102))
(1.0 716) (102))
(1.0 717) (102))
(1.0 718) (102))
(1.0 719) (102))
(1.0 720) (102))
(1.0 721) (102))
(1.0 722) (102))
(1.0 723) (102))
(1.0 724) (102))
(1.0 725) (102))
(1.0 726) (102))

```

```

(1.0 727          (102))
(1.0 728          (102))
(1.0 729          (102))
(1.0 730          (102))
(1.0 731          (102))
(1.0 732          (102))
(1.0 733          (102))
(1.0 734          (102))
(1.0 735          (102))
(1.0 736          (102))
(1.0 737          (102))
(1.0 738          (102))
(1.0 739          (102))
(1.0 740          (102))
(1.0 741          (102))
(1.0 801 (16) (17) (18)          (102))$
(1.0 802 (16) (17) (18)          (102))$
(1.0 803 (16) (17) (18)          (102))$
(1.0 804 (16) (17) (18)          (102))$
(1.0 805 (16) (17) (18)          (102))$
(1.0 806 (16) (17)          (19:20) (102))$
(1.0 807 (16) (17)          (19:20) (102))$
(1.0 808 (16) (17)          (19:20) (102))$
(1.0 809 (16) (17)          (19:20) (102))$
(1.0 810 (16) (17) (18)          (102))$
(1.0 811 (16) (17)          (19)          (102))$
(1.0 812 (16) (17) (18)          (102))$
(1.0 813 (16) (17)          (19:20) (102))$
(1.0 814 (16) (17) (18)          (102))$
(1.0 815 (16) (17)          (19:20) (102))$
(1.0 816 (16) (17) (18)          (102))$
(1.0 817 (16) (17) (18)          (102))$
(1.0 818 (16) (17) (18)          (102))$
(1.0 819 (16) (17)          (19:20) (102))$
(1.0 820 (16) (17)          (19:20) (102))$
(1.0 821 (16) (17)          (19:20) (102))$

c   end_mocup_reaction_rate_tallies
c
c -----
c
c   neutron importance
c
imp:n 0                      $ outside world
      1                      $ outer reflector
      1                      $ pebble bed
      1 1                     $ u=1: target, driver
core
      1 9r                    $ u=2: production cell
      1 1                     $ u=6: production ball
      1                      $ u=5: driver lattice
      1 9r                    $ u=10: unit driver fuel
cell
c
mode n
phys:p 1j 1
kcode 5000 1.0 10 210
prdmp 55 55 55

```

```
print -60 -85 -130 -140
```

APPENDIX E.2: Excel analysis of VSOP94 equilibrium core results

Data used in calculations:

Gram atomic weights

	U235	U236	U238	Pu239	Pu240	Pu241	Pu242	NP237
	235.0439	236.0456	238.0508	239.0522	240.0538	241.0568	242.0587	237.0482

Avogadro's number 6.02E+23

pebble volume 113.0973 cm³

packing fraction 0.61

Composition of used fuel balls in batches at bottom of core before removal:

discharge burnup 79677 MWd/l
 average enrichment 4.33 %
 passes through core 10
 avg. fuel residence time 198.5 days

batch	volume	atom density (1/b-cm)										
		HM	U-235	U-236	U-238	NP-239	PU-239	PU-240	PU-241	PU-242	NP-237	
1	89	636.42	30.893	7.12E-06	4.05E-07	1.13E-04	2.07E-08	1.76E-07	4.52E-08	4.49E-09	3.48E-10	1.70E-09
	90	637.96	30.968	5.95E-06	6.08E-07	1.12E-04	2.06E-08	2.58E-07	1.55E-07	2.80E-08	4.93E-09	5.00E-09
	91	638.86	31.012	4.96E-06	7.75E-07	1.12E-04	2.05E-08	2.91E-07	2.48E-07	5.90E-08	1.68E-08	1.04E-08
	92	639.76	31.056	4.13E-06	9.11E-07	1.11E-04	2.05E-08	3.03E-07	3.16E-07	9.00E-08	3.67E-08	1.73E-08
	93	640.67	31.099	3.44E-06	1.02E-06	1.11E-04	2.04E-08	3.07E-07	3.62E-07	1.17E-07	6.32E-08	2.51E-08
	94	641.57	31.143	2.86E-06	1.11E-06	1.10E-04	2.03E-08	3.07E-07	3.92E-07	1.37E-07	9.45E-08	3.35E-08
	95	642.47	31.187	2.37E-06	1.18E-06	1.10E-04	2.02E-08	3.07E-07	4.10E-07	1.52E-07	1.29E-07	4.22E-08
	96	643.38	31.231	1.96E-06	1.24E-06	1.09E-04	2.01E-08	3.06E-07	4.21E-07	1.63E-07	1.65E-07	5.09E-08
	97	644.29	31.275	1.62E-06	1.28E-06	1.09E-04	2.00E-08	3.05E-07	4.28E-07	1.70E-07	2.02E-07	5.95E-08
	98	645.2	31.319	1.33E-06	1.32E-06	1.08E-04	1.99E-08	3.03E-07	4.31E-07	1.74E-07	2.39E-07	6.77E-08
	99	1.27E+06	47.795	5.06E-10	2.88E-11	9.45E-08	1.74E-11	1.47E-10	3.78E-11	3.76E-12	2.91E-13	1.21E-13
2	199	63642	3089.3	7.55E-06	3.49E-07	1.13E-04	2.18E-08	2.80E-07	5.80E-08	5.22E-09	3.02E-10	2.23E-09
	200	63729	3093.6	6.30E-06	5.60E-07	1.12E-04	2.17E-08	3.88E-07	1.66E-07	2.68E-08	3.67E-09	6.62E-09
	201	63819	3097.9	5.26E-06	7.33E-07	1.12E-04	2.16E-08	4.30E-07	2.60E-07	5.88E-08	1.38E-08	1.30E-08
	202	63909	3102.3	4.38E-06	8.75E-07	1.11E-04	2.15E-08	4.45E-07	3.31E-07	9.24E-08	3.17E-08	2.07E-08
	203	63999	3106.7	3.65E-06	9.91E-07	1.11E-04	2.14E-08	4.50E-07	3.79E-07	1.22E-07	5.64E-08	2.92E-08
	204	64090	3111.1	3.03E-06	1.08E-06	1.10E-04	2.13E-08	4.51E-07	4.10E-07	1.46E-07	8.62E-08	3.83E-08
	205	64180	3115.4	2.51E-06	1.16E-06	1.10E-04	2.12E-08	4.50E-07	4.30E-07	1.63E-07	1.19E-07	4.75E-08
	206	64270	3119.8	2.08E-06	1.22E-06	1.09E-04	2.11E-08	4.49E-07	4.42E-07	1.75E-07	1.55E-07	5.66E-08
	207	64361	3124.2	1.71E-06	1.27E-06	1.09E-04	2.10E-08	4.47E-07	4.49E-07	1.83E-07	1.90E-07	6.56E-08
	208	64452	3128.6	1.40E-06	1.30E-06	1.08E-04	2.09E-08	4.45E-07	4.52E-07	1.88E-07	2.26E-07	7.42E-08
	209	6.32E+05	23.866	5.36E-10	2.48E-11	9.44E-08	1.82E-11	2.34E-10	4.86E-11	4.37E-12	2.53E-13	1.59E-13
3	320	1.27E+05	6178.6	8.19E-06	2.57E-07	1.13E-04	1.94E-08	3.30E-07	5.03E-08	7.29E-09	3.02E-10	1.66E-09
	321	1.27E+05	6187.4	6.84E-06	4.83E-07	1.12E-04	1.93E-08	4.69E-07	1.38E-07	3.86E-08	3.59E-09	6.23E-09
	322	1.28E+05	6196.1	5.71E-06	6.69E-07	1.12E-04	1.92E-08	5.24E-07	2.17E-07	8.53E-08	1.31E-08	1.27E-08
	323	1.28E+05	6204.8	4.75E-06	8.22E-07	1.11E-04	1.91E-08	5.44E-07	2.76E-07	1.34E-07	3.00E-08	2.06E-08
	324	1.28E+05	6213.6	3.96E-06	9.46E-07	1.11E-04	1.91E-08	5.51E-07	3.16E-07	1.76E-07	5.36E-08	2.93E-08
	325	1.28E+05	6222.3	3.29E-06	1.05E-06	1.10E-04	1.90E-08	5.52E-07	3.43E-07	2.08E-07	8.24E-08	3.84E-08
	326	1.28E+05	6231.1	2.72E-06	1.13E-06	1.10E-04	1.89E-08	5.51E-07	3.59E-07	2.33E-07	1.15E-07	4.77E-08
	327	1.29E+05	6239.9	2.25E-06	1.19E-06	1.09E-04	1.88E-08	5.49E-07	3.69E-07	2.49E-07	1.49E-07	5.70E-08
	328	1.29E+05	6248.7	1.85E-06	1.24E-06	1.09E-04	1.87E-08	5.46E-07	3.75E-07	2.60E-07	1.85E-07	6.60E-08
	329	1.21E+05	5862.9	1.52E-06	1.28E-06	1.08E-04	1.86E-08	5.44E-07	3.78E-07	2.67E-07	2.21E-07	7.47E-08
	330	1	3.77E-05	5.82E-10	1.82E-11	9.43E-08	1.62E-11	2.76E-10	4.21E-11	6.10E-12	2.53E-13	1.18E-13
4	452	1.27E+05	6178.6	8.28E-06	2.42E-07	1.13E-04	1.67E-08	3.31E-07	4.66E-08	6.31E-09	2.44E-10	1.54E-09
	453	1.27E+05	6187.4	6.91E-06	4.71E-07	1.12E-04	1.66E-08	4.77E-07	1.34E-07	3.62E-08	3.24E-09	6.04E-09
	454	1.28E+05	6196.1	5.77E-06	6.59E-07	1.12E-04	1.65E-08	5.35E-07	2.14E-07	8.23E-08	1.23E-08	1.25E-08
	455	1.28E+05	6204.8	4.80E-06	8.14E-07	1.11E-04	1.64E-08	5.57E-07	2.75E-07	1.31E-07	2.87E-08	2.03E-08
	456	1.28E+05	6213.6	4.00E-06	9.40E-07	1.11E-04	1.64E-08	5.64E-07	3.16E-07	1.73E-07	5.19E-08	2.90E-08
	457	1.28E+05	6222.3	3.32E-06	1.04E-06	1.10E-04	1.63E-08	5.65E-07	3.43E-07	2.06E-07	8.05E-08	3.82E-08
	458	1.28E+05	6231.1	2.75E-06	1.12E-06	1.10E-04	1.62E-08	5.64E-07	3.60E-07	2.31E-07	1.13E-07	4.75E-08
	459	1.29E+05	6239.9	2.27E-06	1.19E-06	1.09E-04	1.62E-08	5.62E-07	3.71E-07	2.48E-07	1.47E-07	5.68E-08
	460	1.29E+05	6248.7	1.87E-06	1.24E-06	1.09E-04	1.61E-08	5.60E-07	3.77E-07	2.59E-07	1.83E-07	6.59E-08
	461	1.21E+05	5863.1	1.54E-06	1.28E-06	1.08E-04	1.60E-08	5.57E-07	3.80E-07	2.66E-07	2.18E-07	7.46E-08
	462	1	3.77E-05	5.88E-10	1.72E-11	9.44E-08	1.39E-11	2.77E-10	3.90E-11	5.28E-12	2.04E-13	1.09E-13
5	617	1.27E+05	6178.6	8.06E-06	2.75E-07	1.13E-04	1.16E-08	3.05E-07	5.24E-08	8.48E-09	4.00E-10	1.68E-09
	618	1.27E+05	6187.4	6.73E-06	4.99E-07	1.12E-04	1.16E-08	4.30E-07	1.41E-07	4.26E-08	4.30E-09	6.03E-09
	619	1.28E+05	6196.1	5.61E-06	6.83E-07	1.12E-04	1.15E-08	4.79E-07	2.17E-07	9.04E-08	1.47E-08	1.23E-08
	620	1.28E+05	6204.8	4.68E-06	8.33E-07	1.11E-04	1.15E-08	4.97E-07	2.74E-07	1.39E-07	3.25E-08	2.00E-08
	621	1.28E+05	6213.6	3.89E-06	9.57E-07	1.11E-04	1.14E-08	5.03E-07	3.12E-07	1.80E-07	5.70E-08	2.85E-08
	622	1.28E+05	6222.3	3.23E-06	1.06E-06	1.10E-04	1.14E-08	5.04E-07	3.37E-07	2.12E-07	8.65E-08	3.75E-08
	623	1.28E+05	6231.1	2.67E-06	1.14E-06	1.10E-04	1.13E-08	5.03E-07	3.53E-07	2.35E-07	1.19E-07	4.66E-08
	624	1.29E+05	6239.9	2.21E-06	1.20E-06	1.09E-04	1.13E-08	5.01E-07	3.62E-07	2.51E-07	1.54E-07	5.58E-08
	625	1.29E+05	6248.7	1.82E-06	1.25E-06	1.09E-04	1.12E-08	4.99E-07	3.67E-07	2.62E-07	1.90E-07	6.47E-08
	626	1.21E+05	5863.1	1.49E-06	1.29E-06	1.08E-04	1.12E-08	4.97E-07	3.70E-07	2.68E-07	2.26E-07	7.33E-08
	627	1	3.77E-05	5.73E-10	1.95E-11	9.44E-08	9.72E-12	2.56E-10	4.39E-11	7.10E-12	3.35E-13	1.19E-13

discharge volume = 4.27E+05

Mass of uranium and plutonium in batches at bottom of core before removal:

channel	batch	mass (g)								total HM	Pu	compare	HM is the total heavy metal content reported by VSOP. <- first pass through core
		U-235	U-236	U-238	PU-239	PU-240	PU-241	PU-242	NP-237				
1	89	1.77E+00	1.01E+01	2.84E+01	4.43E-02	1.15E-02	1.14E-03	8.91E-05	4.26E-04	30.32	1.13E-01	30.693	30.693
	90	1.48E+00	1.52E+01	2.83E+01	6.54E-02	3.95E-02	7.18E-03	1.28E-03	1.26E-03	30.09	1.13E-01	30.968	3
	91	1.24E+00	1.94E+01	2.83E+01	7.37E-02	6.32E-02	1.51E-02	4.32E-03	2.82E-03	29.85	1.56E-01	31.012	3
	92	1.03E+00	2.28E+01	2.82E+01	7.69E-02	8.06E-02	2.30E-02	9.43E-03	4.39E-03	29.63	1.90E-01	31.056	3
	93	8.81E-01	2.57E+01	2.81E+01	7.80E-02	9.24E-02	2.99E-02	1.63E-02	8.34E-03	29.43	2.17E-01	31.099	3
	94	7.16E-01	2.79E+01	2.80E+01	7.83E-02	1.00E-01	3.52E-02	2.44E-02	8.47E-03	29.25	2.38E-01	31.143	3
	95	5.94E-01	2.98E+01	2.79E+01	7.83E-02	1.05E-01	3.91E-02	3.33E-02	1.07E-02	29.08	2.56E-01	31.187	3
	96	4.92E-01	3.13E+01	2.78E+01	7.81E-02	1.08E-01	4.19E-02	4.27E-02	1.29E-02	28.92	2.71E-01	31.231	3
	97	4.08E-01	3.24E+01	2.78E+01	7.79E-02	1.10E-01	4.37E-02	5.23E-02	1.51E-02	28.78	2.84E-01	31.275	3
	98	3.34E-01	3.33E+01	2.77E+01	7.77E-02	1.11E-01	4.49E-02	6.19E-02	1.72E-02	28.64	2.95E-01	31.319	3
	99	2.50E-01	4.13E-02	4.73E+01	7.39E-02	1.91E-02	1.90E-03	1.48E-04	6.02E-05	47.68	9.50E-02	47.795	6830
2	199	1.87E+02	8.71E+00	2.84E+03	7.07E+00	1.47E+00	1.33E-01	7.73E-03	5.59E-02	3040.87	3.26E+00	3089.3	3089.3
	200	1.57E+02	1.40E+01	2.83E+03	9.81E+00	4.21E+00	6.85E-01	9.41E-02	1.68E-01	3013.20	1.48E+01	3093.6	343
	201	1.31E+02	1.83E+01	2.82E+03	1.09E+01	6.62E+00	1.50E+00	3.54E-01	3.26E-01	2988.39	1.94E+01	3097.9	344
	202	1.09E+02	2.19E+01	2.81E+03	1.13E+01	8.42E+00	2.36E+00	8.15E-01	5.20E-01	2965.64	2.29E+01	3102.3	344
	203	9.11E+01	2.49E+01	2.80E+03	1.14E+01	9.86E+00	3.13E+00	1.45E+00	7.36E-01	2944.92	2.57E+01	3106.7	345
	204	7.58E+01	2.72E+01	2.79E+03	1.15E+01	1.05E-01	3.73E+00	2.22E+00	9.65E-01	2926.02	2.79E+01	3111.1	345
	205	6.29E+01	2.92E+01	2.79E+03	1.15E+01	1.10E+01	4.18E+00	3.08E+00	1.20E+00	2908.88	2.97E+01	3115.4	346
	206	5.21E+01	3.07E+01	2.78E+03	1.14E+01	1.13E+01	4.50E+00	3.99E+00	1.43E+00	2892.80	3.13E+01	3119.8	346
	207	4.30E+01	3.19E+01	2.77E+03	1.14E+01	1.15E+01	4.72E+00	4.93E+00	1.66E+00	2877.91	3.26E+01	3124.2	347
	208	3.53E+01	3.28E+01	2.76E+03	1.14E+01	1.16E+01	4.85E+00	5.88E+00	1.88E+00	2863.97	3.37E+01	3128.6	347
	209	1.32E-01	8.14E-03	2.36E+01	5.88E-02	1.22E-02	1.11E-03	6.43E-05	3.95E-05	23.80	7.22E-02	23.866	3410
3	320	4.07E+02	1.28E+01	5.67E+03	1.67E+01	2.55E+00	3.71E-01	1.54E-02	8.33E-02	6109.64	6.13E+00	6178.6	6178.6
	321	3.40E+02	2.41E+01	5.65E+03	2.37E+01	7.03E+00	1.97E+00	1.84E-01	3.12E-01	6051.17	3.29E+01	6187.4	687
	322	2.84E+02	3.35E+01	5.64E+03	2.65E+01	1.10E+01	4.36E+00	6.74E-01	6.40E-01	5997.82	4.26E+01	6196.1	688
	323	2.37E+02	4.12E+01	5.62E+03	2.76E+01	1.41E+01	6.84E+00	1.54E+00	1.04E+00	5949.98	5.00E+01	6204.8	689
	324	1.98E+02	4.75E+01	5.60E+03	2.80E+01	1.61E+01	8.99E+00	2.76E+00	1.47E+00	5906.14	5.59E+01	6213.6	690
	325	1.64E+02	5.28E+01	5.59E+03	2.81E+01	1.75E+01	1.07E+01	4.25E+00	1.94E+00	5868.21	6.05E+01	6222.3	691
	328	1.36E+02	5.68E+01	5.57E+03	2.81E+01	1.84E+01	1.19E+01	5.92E+00	2.41E+00	5829.88	6.43E+01	6231.1	692
	327	1.13E+02	6.01E+01	5.55E+03	2.80E+01	1.89E+01	1.28E+01	7.72E+00	2.88E+00	5796.99	6.75E+01	6239.9	693
	328	9.32E+01	6.28E+01	5.54E+03	2.79E+01	1.92E+01	1.34E+01	9.57E+00	3.35E+00	5765.32	7.01E+01	6248.7	694
	329	7.17E+01	6.07E+01	5.17E+03	2.81E+01	1.82E+01	1.29E+01	1.07E+01	3.55E+00	5374.50	6.79E+01	5862.9	5
	330	2.27E-07	7.14E-09	3.73E-05	1.10E-07	1.68E-09	2.44E-09	1.02E-10	4.65E-11	3.77E-05	1.29E-07	3.77E-05	0
4	452	4.11E+02	1.21E+01	5.67E+03	1.67E+01	2.37E+00	3.22E-01	1.25E-02	7.69E-02	6114.13	6.13E+00	6178.6	6178.6
	453	3.44E+02	2.35E+01	5.65E+03	2.42E+01	8.83E+00	1.85E+00	1.66E-01	3.03E-01	6055.33	3.30E+01	6187.4	687
	454	2.87E+02	3.30E+01	5.64E+03	2.71E+01	1.09E+01	2.41E+00	6.32E-01	6.29E-01	6001.62	4.29E+01	6196.1	688
	455	2.40E+02	4.08E+01	5.62E+03	2.82E+01	1.40E+01	6.89E+00	1.48E+00	1.02E+00	5952.96	5.04E+01	6204.8	689
	456	2.00E+02	4.72E+01	5.60E+03	2.86E+01	1.61E+01	8.87E+00	2.67E+00	1.46E+00	5908.83	5.63E+01	6213.6	690
	457	1.66E+02	5.24E+01	5.59E+03	2.87E+01	1.75E+01	1.06E+01	4.15E+00	1.93E+00	5869.15	6.10E+01	6222.3	691
	458	1.38E+02	5.88E+01	5.57E+03	2.87E+01	1.84E+01	1.19E+01	5.81E+00	2.40E+00	5832.39	6.48E+01	6231.1	692
	459	1.14E+02	6.00E+01	5.55E+03	2.87E+01	1.90E+01	1.28E+01	7.60E+00	2.88E+00	5799.02	6.80E+01	6239.9	693
	460	9.41E+01	6.28E+01	5.54E+03	2.86E+01	1.93E+01	1.34E+01	9.45E+00	3.34E+00	5767.69	7.07E+01	6248.7	694
	461	7.24E+01	6.08E+01	5.17E+03	2.67E+01	1.83E+01	1.29E+01	1.06E+01	3.55E+00	5376.59	6.85E+01	5863.1	5
	462	2.29E-07	7.65E-09	3.73E-05	1.01E-07	1.75E-08	2.84E-09	1.34E-10	4.69E-11	3.77E-05	1.22E-07	3.77E-05	0
5	617	4.01E+02	1.37E+01	5.67E+03	1.54E+01	2.66E+00	4.32E-01	2.04E-02	8.41E-02	6104.12	6.13E+00	6178.6	6178.6
	618	3.35E+02	2.49E+01	5.85E+03	2.18E+01	7.16E+00	2.17E+00	2.20E-01	3.02E-01	6045.96	3.13E+01	6187.4	687
	619	2.80E+02	3.41E+01	5.64E+03	2.43E+01	1.11E+01	4.62E+00	7.55E-01	6.20E-01	5993.49	4.07E+01	6196.1	688
	620	2.33E+02	4.18E+01	5.62E+03	2.52E+01	1.39E+01	7.09E+00	1.87E+00	1.01E+00	5945.53	4.79E+01	6204.8	689
	621	1.94E+02	4.80E+01	5.60E+03	2.58E+01	1.59E+01	9.21E+00	2.93E+00	1.44E+00	5932.02	5.36E+01	6213.6	690
	622	1.61E+02	5.31E+01	5.59E+03	2.57E+01	1.72E+01	1.09E+01	4.45E+00	1.89E+00	5862.41	5.82E+01	6222.3	691
	623	1.34E+02	5.80E+01	5.57E+03	2.56E+01	1.81E+01	1.21E+01	6.16E+00	2.36E+00	5826.13	6.19E+01	6231.1	692
	624	1.11E+02	6.05E+01	5.55E+03	2.56E+01	1.86E+01	1.29E+01	7.98E+00	2.82E+00	5793.18	6.50E+01	6239.9	693
	625	9.13E+01	6.31E+01	5.54E+03	2.55E+01	1.89E+01	1.35E+01	9.85E+00	3.28E+00	5762.23	6.77E+01	6248.7	694
	626	7.01E+01	6.10E+01	5.17E+03	2.38E+01	1.78E+01	1.30E+01	1.10E+01	3.48E+00	5371.75	6.56E+01	5863.1	5
	627	2.23E-07	7.65E-09	3.73E-05	1.01E-07	1.75E-08	2.84E-09	1.34E-10	4.69E-11	3.77E-05	1.22E-07	3.77E-05	0

Total plutonium in batch groups: 6,406 d burnup step

batch group	grams								gPu/FS	#FS / 8 kg	gPu239/FS	#FS/8kg
	total Pu	Pu239	% Pu239	# pebbles	time/peb	gPu/FS	#FS / 8 kg	gPu239/FS				
1	66.29	55.91	84.34%	2404	4 min	0.028	290137	0.028	257991			
2	112.14	79.54	70.93%	2407	4 min	0.047		0.033	181574			
3	145.70	88.88	61.00%	2411	4 min	0.060		0.037	162763			
4	171.47	92.45	53.92%	2414	4 min	0.071		0.038	156869			
5	191.71	93.70	48.88%	2418	4 min	0.079		0.039	154832			
6	207.89	94.02	45.23%	2421	4 min	0.086		0.039	154491			
7	221.07	93.98	42.51%	2425	4 min	0.091		0.039	154825			
8	232.07	93.79	40.41%	2428	4 min	0.096		0.039	155331			
9	241.43	93.53	38.74%	2432	4 min	0.099		0.038	156010			
10	235.98	88.09	37.33%	2303	4 min	0.102	78075	0.038	158853			

↳ normally discharged

Fractions of plutonium isotopes in batches at bottom of core before removal:

channel	batch	PU-239	PU-240	PU-241	PU-242	total
1	89	77.74%	20.09%	2.00%	0.16%	100.00%
	90	57.68%	34.89%	6.31%	1.11%	100.00%
	91	47.13%	40.46%	9.65%	2.76%	100.00%
	92	40.47%	42.43%	12.13%	4.96%	100.00%
	93	36.02%	42.67%	13.80%	7.51%	100.00%
	94	32.89%	42.07%	14.80%	10.24%	100.00%
	95	30.60%	41.07%	15.31%	13.02%	100.00%
	96	28.85%	39.91%	15.47%	15.78%	100.00%
	97	27.45%	38.70%	15.41%	18.44%	100.00%
	98					100.00%
2	99	77.74%	20.09%	2.00%	0.16%	100.00%
	199	81.42%	16.95%	1.53%	0.09%	100.00%
	200	66.30%	28.43%	4.63%	0.64%	100.00%
	201	56.22%	34.20%	7.75%	1.83%	100.00%
	202	49.34%	36.78%	10.32%	3.56%	100.00%
	203	44.55%	37.62%	12.17%	5.65%	100.00%
	204	41.13%	37.54%	13.37%	7.96%	100.00%
	205	38.58%	36.99%	14.07%	10.36%	100.00%
	206	36.62%	36.21%	14.40%	12.77%	100.00%
	207	35.06%	35.33%	14.48%	15.13%	100.00%
3	208					100.00%
	209	81.42%	16.95%	1.53%	0.09%	100.00%
	320	85.01%	13.02%	1.89%	0.08%	100.00%
	321	72.11%	21.35%	5.99%	0.56%	100.00%
	322	62.26%	25.93%	10.23%	1.58%	100.00%
	323	55.16%	28.10%	13.66%	3.08%	100.00%
	324	50.07%	28.89%	16.10%	4.94%	100.00%
	325	46.38%	28.93%	17.67%	7.01%	100.00%
	326	43.63%	28.59%	18.58%	9.21%	100.00%
	327	41.50%	28.05%	19.01%	11.44%	100.00%
4	328	39.81%	27.43%	19.12%	13.64%	100.00%
	329					100.00%
	330	85.01%	13.02%	1.89%	0.08%	100.00%
	452	86.08%	12.19%	1.66%	0.06%	100.00%
	453	73.21%	20.69%	5.60%	0.50%	100.00%
	454	63.25%	25.46%	9.81%	1.47%	100.00%
	455	56.03%	27.77%	13.27%	2.93%	100.00%
	456	50.86%	28.65%	15.75%	4.75%	100.00%
	457	47.10%	28.74%	17.36%	6.79%	100.00%
	458	44.30%	28.43%	18.30%	8.97%	100.00%
5	459	42.15%	27.92%	18.76%	11.18%	100.00%
	460	40.43%	27.32%	18.89%	13.37%	100.00%
	461					100.00%
	462	86.08%	12.19%	1.66%	0.06%	100.00%
	617	83.21%	14.35%	2.33%	0.11%	100.00%
	618	69.52%	22.85%	6.93%	0.70%	100.00%
	619	59.64%	27.17%	11.34%	1.85%	100.00%
	620	52.64%	29.09%	14.78%	3.49%	100.00%
	621	47.67%	29.69%	17.17%	5.46%	100.00%
	622	44.08%	29.59%	18.67%	7.65%	100.00%
average	623	41.40%	29.14%	19.51%	9.95%	100.00%
	624	39.34%	28.52%	19.87%	12.27%	100.00%
	625	37.69%	27.84%	19.92%	14.54%	100.00%
	626					100.00%
	627	83.21%	14.35%	2.33%	0.11%	100.00%
	1st pass	82.69%	15.32%	1.88%	0.10%	100.00%
	discharge					100.0%